



# **The Effects of Growth Hormone Receptor-associated ERK Activation on Adipocyte Differentiation and Function.**

Candidate

**Souad A. M. Moftah**

Supervisors

Dr Mark Lewis  
Prof Marian Ludgate

Submitted in partial fulfillment of the requirements for the degree of  
Doctor of Philosophy (PhD)

Institute of Molecular & Experimental Medicine

School of Medicine

Cardiff University

December 2012

**Declaration**

This work has not previously been accepted in substance for any degree and is not concurrently submitted in candidature for any degree.

Signed ..... (candidate) Date

**STATEMENT 1**

This thesis is being submitted in partial fulfillment of the requirements for the degree of Doctor of Philosophy (PhD)

Signed ..... (candidate) Date

**STATEMENT 2**

This thesis is the result of my own independent work/investigation, except where otherwise stated.

Other sources are acknowledged by explicit references.

Signed ..... (candidate) Date .....

**STATEMENT 3**

I hereby give consent for my thesis, if accepted, to be available for photocopying and for inter-library loan, and for the title and summary to be made available to outside organisations.

Signed ..... (candidate) Date .....

**STATEMENT 4: PREVIOUSLY APPROVED BAR ON ACCESS**

I hereby give consent for my thesis, if accepted, to be available for photocopying and for inter-library loans **after expiry of a bar on access previously approved by the Graduate Development Committee.**

Signed ..... (candidate) Date .....

## Abstract

Growth hormone (GH) modulates adipocyte function to promote lipolysis via a cell surface GH receptor (GHR) which activates multiple signalling cascades including STAT5 and p42/44 MAP kinase (MAPK) pathways. The growth promoting effects of GH are mediated primarily by STAT5 activation but little is known about pathways mediating the effects of GH on adipocyte function. We therefore studied the effect of GH on STAT5 and MAPK (ERK) activation in the 3T3-L1 mouse pre-adipocyte cell line during adipogenesis. Cells were plated, allowed to reach confluence and cultured in adipogenic medium containing the PPAR $\gamma$  agonist, pioglitazone. GH induced activation (10 minutes exposure) of STAT5 and MAPK was analysed on days 0, 2, 5 and 8 during adipogenesis by phospho-specific western blotting and densitometry.

During adipogenesis, GH progressively loses the ability to activate p42/44 MAPK despite elevated GHR and unaltered total ERK levels. In contrast, GH-stimulated STAT5 activation increases as 3T3-L1 differentiation proceeds. Subsequently we investigated possible explanations for the altered GHR signalling. The adapter protein p66<sup>Shc</sup> is thought to be necessary to link GHR activation to the ERK pathway. However levels of this protein, measured by western blotting and densitometry, did not decrease as 3T3-L1 cells underwent adipocyte differentiation. GHR levels increase with adipogenic differentiation of 3T3-L1 cells leading us to hypothesize that this may lead to preferential association with JAK2-STAT5. This was tested by overexpressing the GHR in 3T3-L1; similar GH-stimulated ERK pathway activation was obtained in cells transfected with the GHR vector and in those transfected with the empty vector. Finally, we have investigated whether changes in GHR signalling also occur during adipogenesis of primary pre-adipocytes from mice and various human depots. There was minimal GH-induced phosphorylation of ERK at all time points before and during differentiation (required up to 15 days in primary cells) and no depot, either murine or human, demonstrated a reduction in pERK, suggesting that this feature is unique to 3T3-L1. Furthermore, ERK phosphorylation may be the stimulus for mitotic clonal expansion which occurs in the cell line but not in human primaries. GH-stimulated STAT5 activation increases as human and mouse primary pre-adipocytes differentiation progresses, as in the 3T3-L1 cell-line, and may be the result of increased GHR transcript levels as differentiation proceeds. Future studies could investigate the mechanisms responsible for these similarities and differences.

**For my father**

# Acknowledgements

I would like to thank my supervisor Dr Mark Lewis for his help and support to me during these years.

And I want to express my sincere gratitude to my supervisor Prof Marian Ludgate for her outstanding mentorship, constructive attitude, encouragement and kindness throughout my studies and her patience in editing the many versions of my thesis and for giving me a chance to learn from her.

The help and encouragement received from my various friends and colleagues have been invaluable. I would like to mention in particular Dr Mohd Shazli Drawen, Dr Fiona Grennan-Jones and Mr Ameen Bakhsh for their assistance.

Finally, a big thank you to my parents and my brother Walid for their continued support and help throughout the whole of my studies.

## List of abbreviations

<b>Abbreviations</b>	<b>Name</b>
<b>ACC</b>	Acetyl CoA Carboxylase
<b>ACLP</b>	Aortic Carboxypeptidase-like Protein
<b>ADD1</b>	Adipocyte Determination and Differentiation factor 1
<b>AEBP1</b>	Adipocyte Enhancer-binding Protein 1
<b>AKT</b>	Protein Kinase B
<b>AMP</b>	Adenosine monophosphate
<b>AMPK</b>	Monophosphate-activated Protein Kinase
<b>APS</b>	Ammonium Persulfate
<b>ATCC</b>	American Type Culture Collection
<b>BAT</b>	Brown Adipose Tissue
<b>BMSCs</b>	Bone marrow Stem Cells
<b>BSA</b>	Bovine Serum Albumin
<b>C</b>	Cysteines
<b>cAMP</b>	Cyclic Adenosine Monophosphate
<b>C/EBP</b>	CCAAT-Enhancer-binding Proteins
<b>CIS</b>	Cytokine-Inducible SH2-containing Protein
<b>CLA</b>	Conjugated Linoleic Acid
<b>CM</b>	Caveolar Membrane Fraction
<b>CREB</b>	cAMP Response Element-binding protein
<b>Ct</b>	Threshold Cycle
<b>DA</b>	Daltons
<b>Dex</b>	Dexamethasone
<b>DHAP</b>	Dihydroxyacetone Phosphate
<b>DIk1</b>	Delta-like Protein 1
<b>DMEM</b>	Dulbecco's Modified Eagle's Medium
<b>DMSO</b>	Dimethylsulfoxide
<b>dNTP</b>	Deoxyribonucleotide Triphosphate
<b>15d-GJ2</b>	15-deoxy- $\Delta$ 12, 14-prostaglandin J2
<b>ECL</b>	Enhanced Chemiluminescence
<b>ECM</b>	Extracellular Matrix
<b>ERK</b>	Extracellular Signal-regulated Kinase

<b>ES cell</b>	Embryonic Stem Cell
<b>FACS</b>	Fluorescence-Activated Cell Sorting
<b>FAS</b>	Fatty Acid Synthase
<b>FBS</b>	Fetal Bovine Serum
<b>FCS</b>	Fetal Calf Serum
<b>Gab1</b>	Grb2-associated Binding Protein 1
<b>GATA</b>	Transcription Factors binding GATA
<b>GDP</b>	Guanosine DiPhosphate
<b>GH</b>	Growth Hormone
<b>GHBP</b>	Growth Hormone Binding Protein
<b>GHD</b>	Growth Hormone Deficiency
<b>GHR</b>	Growth Hormone Receptor
<b>GHRH</b>	Growth Hormone Releasing Hormone
<b>GnRH</b>	Gonadotropin Releasing Hormone
<b>GPDH</b>	Glycerol-3-phosphate Dehydrogenase
<b>Grb2</b>	Growth Factor Receptor-bound Protein 2
<b>GRF</b>	Growth hormone -Releasing Factor
<b>GSK3<math>\beta</math></b>	Glycogen Synthase Kinase 3 $\beta$
<b>GST</b>	Glutathione S-Transferase
<b>GTP</b>	Guanosine TriPhosphate
<b>HBSS</b>	Hank's Balanced Salt Solution
<b>hGH</b>	Human Growth Hormone
<b>HLH-LZ</b>	Helix-Loop-Helix Leucine Zipper
<b>HRP</b>	Horseradish Peroxidase
<b>HSL</b>	Hormone-Sensitive Lipase
<b>IBMX</b>	Methylisobutylxanthine
<b>IGF</b>	Insulin-like Growth Factor-1
<b>INS</b>	Insulin
<b>IRS</b>	Insulin Receptor Substrates
<b>JAK</b>	Janus Kinase
<b>JAK 2</b>	Janus Kinase 2
<b>JNK</b>	c-Jun N-terminal kinase
<b>Kbp</b>	Kilo Base Pair
<b>KDa</b>	Kilo Daltons
<b>KLF</b>	Krüppel-Like Factor

<b>LB</b>	Luria Broth
<b>LXRs</b>	Liver X Receptors
<b>MAPK</b>	Mitogen Activated Protein Kinase
<b>MAPKK</b>	MAP Kinase Kinase
<b>MAPKKK</b>	MAP Kinase Kinase Kinase
<b>MCE</b>	Mitotic clonal expansion
<b>MEK</b>	Mitogen Extracellular Signal-regulated Kinase Kinase
<b>MMLV RT</b>	Moloney Murine Leukemia Virus Reverse Transcriptase
<b>mRNA</b>	Messenger RNA
<b>MSC</b>	Mesenchymal Stem Cells
<b>NGF</b>	Neuron Growth Factor
<b>NTC</b>	No Template Control
<b>ODT</b>	Oligo Deoxythymidine Primer
<b>p38 MAPK</b>	p38 Mitogen Activated Protein Kinase
<b>PACAP</b>	Pituitary Adenylate Activating Polypeptide
<b>PBS</b>	Phosphate Buffered Saline
<b>PCR</b>	Polymerase Chain Reaction
<b>PDGF</b>	Platelet Derived Growth Factor
<b>pDNA</b>	Plasmid DNA
<b>PI3K</b>	Phosphatidylinositol-3 Phosphate Kinase
<b>PKA</b>	Protein Kinase A
<b>PKB</b>	Protein Kinase B
<b>PKC</b>	Protein Kinase C
<b>PMA</b>	Phorbol 12-Myristate-13-Acetate
<b>PPAR</b>	Peroxisome Proliferator-Activated Receptor
<b>PPREs</b>	PPAR Response Elements
<b>Pref-1</b>	Preadipocyte Factor 1
<b>PRL</b>	Prolactin Hormone
<b>PTB</b>	Phosphotyrosine-binding Domain
<b>PTPase</b>	PhosphoTyrosine Phosphatase
<b>PVDF</b>	Polyvinylidene Fluoride
<b>PY</b>	Phosphotyrosine
<b>QPCR</b>	Quantitative Real Time Polymerase Chain Reaction
<b>RT</b>	Reverse Transcriptase
<b>RTK</b>	Receptor Tyrosine Kinase

<b>RXR</b>	Retinoid X Receptor
<b>SDS</b>	Sodium Dodecyl Sulphate
<b>SDS PAGE</b>	Sodium Dodecyl Sulphate Polyacrylamide Gel
<b>SH-2</b>	Src Homology Domain 2
<b>Shc</b>	Src Homology Protein
<b>siRNA</b>	Small Interfering RNA
<b>SOCS</b>	Suppressors Of Cytokine Signalling
<b>SREBP</b>	Sterol Regulatory Element-Binding Protein
<b>SRIF</b>	Somatostatin Receptor Antagonist
<b>SS</b>	Somatostatin
<b>STAT</b>	Signal Transducers and Activators of Transcription
<b>T3</b>	Triiodothyronine
<b>TAD</b>	Trans Activation Domain
<b>TBS</b>	Tris Buffered Saline
<b>TEMED</b>	N,N,N',N'-tetramethylethylenediamine
<b>TGF<math>\beta</math></b>	Transforming Growth Factor $\beta$
<b>TNF<math>\alpha</math></b>	Tumor Necrosis Factor $\alpha$
<b>TRH</b>	Thyrotrophic Releasing Hormone
<b>TZD</b>	Thiazolidinediones
<b>UCP-1</b>	Uncoupling Protein 1
<b>V</b>	Voltage
<b>WAT</b>	White Adipose Tissue
<b>Y</b>	Tyrosine

## List of figures

Figure number	Title	Page number
<b>Figure 1.1</b>	Hypothalamic-pituitary axes	2
<b>Figure 1.2</b>	Regulation of the GH secretion	4
<b>Figure 1.3</b>	Three-dimensional structure of GH	5
<b>Figure 1.4</b>	Schematic representation of the GHR	8
<b>Figure 1.5</b>	Mechanism of GH binding to GHR	12
<b>Figure 1.6</b>	Tyrosine phosphorylation of the GHR cytoplasmic domain	13
<b>Figure 1.7</b>	GH/GHR signalling pathways	16
<b>Figure 1.8</b>	Stem cell through differentiation	20
<b>Figure 1.9</b>	PPARs/RXR heterodimers	24
<b>Figure 1.10</b>	lipogenesis/lipolysis	29
<b>Figure 2.1</b>	1% Agarose gel electrophoresis	38
<b>Figure 2.2</b>	Phase contrast photomicrograph stages of adipocyte differentiation	44
<b>Figure 2.3</b>	ARP QPCR product	45
<b>Figure 2.4</b>	QPCR analysis of ARP	46
<b>Figure 2.5</b>	ARP Amplification plot	47
<b>Figure 2.6</b>	PPAR $\gamma$ QPCR product	48
<b>Figure 2.7</b>	PPAR $\gamma$ QPCR analysis	49
<b>Figure 2.8</b>	GPDH QPCR product	50
<b>Figure 2.9</b>	GPDH QPCR analysis	51
<b>Figure 2.10</b>	PPAR $\gamma$ amplification curve	52

<b>Figure 2.11</b>	PPAR $\gamma$ expression during 3T3-L1 differentiation	53
<b>Figure 2.12</b>	GPDH amplification curve	54
<b>Figure 2.13</b>	GPDH expression during 3T3-L1 differentiation	54
<b>Figure 3.1</b>	GHR-associated JAK2	60
<b>Figure 3.2</b>	GHR cell signalling	61
<b>Figure 3.3</b>	Western blotting schematic	68
<b>Figure 3.4</b>	Basal ERK activation	70
<b>Figure 3.5</b>	Phosphorylation of ERK and STAT5	72
<b>Figure 3.6</b>	Densitometric analysis of ERK and STAT5	73
<b>Figure 3.7</b>	PMA-induced ERK phosphorylation	74
<b>Figure 3.8</b>	Densitometric analysis of 3T3-L1 cells with PMA	74
<b>Figure 3.9</b>	GHR QPCR product	75
<b>Figure 3.10</b>	GHR QPCR analyses	76
<b>Figure 3.11</b>	Amplification curve of GHR	77
<b>Figure 3.12</b>	GHR expression during 3T3-L1 differentiation	77
<b>Figure 4.1</b>	Shc signaling pathway	86
<b>Figure 4.2</b>	Shc expression in 3T3-L1 cells	96
<b>Figure 4.3</b>	66kDa form of Shc levels	97
<b>Figure 4.4</b>	3T3-L1 cells transfected with GFP using geneJammer	98
<b>Figure 4.5</b>	3T3-L1 cells transfected with GFP using electroporation	98
<b>Figure 4.6</b>	hGHR QPCR product	99
<b>Figure 4.7</b>	hGHR QPCR analyses	100
<b>Figure 4.8</b>	QPCR analysis of GHR expression in 3T3-L1 transfected	101
<b>Figure 4.9</b>	Phosphorylation of ERK and STAT5 following GH and PMA in transfected cells	102

<b>Figure 4.10</b>	Densitometric analysis of GH on ERK activation in cells transfected with hGHR	103
<b>Figure 4.11</b>	Densitometric analysis of GH on STAT5 activation in cells transfected with hGHR	103
<b>Figure 4.12</b>	Effect of hGHR dose on GH activation of ERK and STAT5	104
<b>Figure 4.13</b>	Effect of hGHR dose on GH activation of ERK and STAT5	105
<b>Figure 4.14</b>	Densitometric analysis of GH on ERK activation following transfection with hGHR	106
<b>Figure 4.15</b>	Densitometric analysis of GH on STAT5 activation following transfection hGHR	106
<b>Figure 4.16</b>	MKP-1 target members of the MAP kinases and inactivate their function in both the cytosol and the nucleus.	110
<b>Figure 5.1</b>	Mouse adipocyte differentiation	122
<b>Figure 5.2</b>	ARP amplification plot	123
<b>Figure 5.3</b>	PPAR $\gamma$ amplification curve	124
<b>Figure 5.4</b>	PPAR $\gamma$ expression during primary mouse pre-adipocytes differentiation	125
<b>Figure 5.5</b>	GPDH amplification curve	126
<b>Figure 5.6</b>	GPDH expression during primary mouse pre-adipocytes differentiation	127
<b>Figure 5.7</b>	Amplification curve of GHR	128
<b>Figure 5.8</b>	GHR expression during mouse pre-adipocytes differentiation	129
<b>Figure 5.9</b>	Basal P-ERK and total ERK levels	131

<b>Figure 5.10</b>	Phosphorylation of ERK and STAT5	133
<b>Figure 5.11</b>	Densitometric analysis of ERK and STAT5	134
<b>Figure 5.12</b>	Adipocyte differentiation	136
<b>Figure 5.13</b>	APRT Amplification plot	137
<b>Figure 5.14</b>	LPL amplification curve	138
<b>Figure 5.15</b>	LPL expression during primary human orbital cells differentiation	138
<b>Figure 5.16</b>	PPAR $\gamma$ expression	140
<b>Figure 5.17</b>	Amplification curve of GHR	141
<b>Figure 5.18</b>	GHR expression during human orbital pre-adipocytes differentiation	141
<b>Figure 5.19</b>	Basal ERK levels	143
<b>Figure 5.20</b>	Phosphorylation of ERK and STAT5	144
<b>Figure 5.21</b>	Densitometric analysis of ERK and STAT5	145
<b>Figure 5.22</b>	MCE in human orbital cells	146
<b>Figure 5.23</b>	MCE in 3T3-L1 cell line	147
<b>Figure 5.24</b>	Breast fat pre-adipocyte differentiation	149
<b>Figure 5.25</b>	PPAR $\gamma$ amplification curve	150
<b>Figure 5.26</b>	PPAR $\gamma$ expression during breast fat differentiation	150
<b>Figure 5.27</b>	LPL amplification curve	151
<b>Figure 5.28</b>	LPL expression during breast fat differentiation	152
<b>Figure 5.29</b>	Amplification curve of GHR	153
<b>Figure 5.30</b>	GHR expression during human breast fat differentiation	153
<b>Figure 5.31</b>	Phosphorylation of ERK and STAT5	155
<b>Figure 5.32</b>	Densitometric analysis of ERK and STAT5	156

## List of tables

Table number	Title	Page number
<b>Table 2.1</b>	Components of the differentiation medium	36
<b>Table 2.2</b>	QPCR primers	39
<b>Table 2.3</b>	Program used for sequencing	42
<b>Table 2.4</b>	ARP Ct values	47
<b>Table 2.5</b>	PPAR $\gamma$ Ct values	53
<b>Table 3.6</b>	GPDH Ct values	54
<b>Table 3.1</b>	Components of SDS-PAGE	65
<b>Table 3.2</b>	Primary and secondary antibodies	67
<b>Table 3.3</b>	Primers of GHR and ARP	69
<b>Table 3.4</b>	GHR and ARP QPCR assays	78
<b>Table 4.1</b>	Primers of the hGHR and ARP	95
<b>Table 5.1</b>	Components of the primary mouse pre-adipocytes differentiation medium	115
<b>Table 5.2</b>	QPCR primers along with amplicon size	118
<b>Table 5.3</b>	PPAR $\gamma$ Ct values	125
<b>Table 5.4</b>	QPCR for PPAR $\gamma$	125
<b>Table 5.5</b>	GPDH Ct values	127
<b>Table 5.6</b>	QPCR for GPDH	127
<b>Table 5.7</b>	GHR and ARP QPCR assays	129
<b>Table 5.8</b>	QPCR for GHR	129

<b>Table 5.9</b>	LPL CT values	139
<b>Table 5.10</b>	QPCR GPDH and LPL late marker for adipogenesis	139
<b>Table 5.11</b>	GHR and APRT QPCR assays	142
<b>Table 5.12</b>	QPCR for GHR	142
<b>Table 5.13</b>	PPAR $\gamma$ qPCR assays	151
<b>Table 5.14</b>	LPLQ PCR assays	152
<b>Table 5.15</b>	GHR Q PCR assays	154

# Table of Contents

Declaration.....	
Abstract.....	I
For my father .....	II
Acknowledgements.....	III
List of abbreviations .....	IV
List of Figures .....	VIII
List of Tables .....	XII
Table of Contents.....	XIV
<b>1. Chapter one (General Introduction)</b> .....	<b>1</b>
1.1 Endocrine system.....	1
1.2 Growth hormone .....	2
1.2.1 Historical background .....	2
1.2.2 Structure and secretion of GH .....	3
1.2.3 Growth hormone receptor and distribution.....	7
1.2.4 GHR signalling .....	10
1.2.5 Activation of multiple signalling pathways .....	14
1.2.6 Effects of GH.....	17
1.3 Adipocytes .....	18
1.3.1 Adipogenesis.....	21
1.3.2 Transcriptional regulation of adipogenesis.....	22
1.3.3 Effect of GH on adipocyte biology.....	27
1.4 Objectives .....	30
<b>2. Chapter Two</b> .....	<b>31</b>
2.1 Introduction .....	31
2.1.1 The 3T3-L1 cell line .....	31
2.1.2 The polymerase chain reaction.....	32
2.1.3 Oil Red O staining .....	34
2.1.4 Aims .....	34
2.2 Materials and Methods .....	35
2.2.1 Cell culture .....	35
2.2.1.1 3T3-L1 cell culture medium .....	35
2.2.1.2 Trypsinization of cell cultures.....	35
2.2.1.3 Freezing and thawing of cells .....	36
2.2.1.4 Differentiation of 3T3-L1 .....	36

2.2.1.5 Oil Red O staining .....	37
2.2.2 QPCR analysis of gene expression .....	37
2.2.2.1 Extraction RNA of 3T3-L1 cells.....	37
2.2.2.2 Reverse transcription.....	38
2.2.2.3 QPCR reaction .....	39
2.2.2.4 DNA Sequencing.....	41
2.2.3 Statistical analysis .....	42
2.3 Results .....	43
2.3.1 Morphology of 3T3-L1 during differentiation .....	43
2.3.2 Oil Red O of 3T3-L1 during differentiation .....	43
2.3.3 Validation of QPCR assays .....	44
2.3.3.1 Validation of the ARP assay .....	45
2.3.3.2 Validation of the PPAR $\gamma$ assay .....	48
2.3.3.3 Validation of the GPDH assay .....	50
2.3.3.4 PPAR $\gamma$ expression during 3T3-L1 cell differentiation.....	51
2.3.3.5 Expression GPDH during 3T3-L1 differentiation .....	53
2.4 Discussion.....	55
<b>3. Chapter Three.....</b>	<b>60</b>
3.1 Introduction .....	60
3.1.1 GH signalling.....	60
3.1.2 Western blotting .....	63
3.2 Materials and Methods .....	64
3.2.1 GH signalling during 3T3-L1 differentiation .....	64
3.2.2 SDS–PAGE and western blotting .....	64
3.2.2.1 Cellular protein quantitation .....	65
3.2.2.2 Gel preparation.....	65
3.2.2.3 Western blot analysis of protein.....	67
3.2.2.4 Detection of specific proteins by immunoblotting .....	67
3.2.2.6 Detection of antibody–antigen complex .....	68
3.2.2.7 Stripping and reprobing membrane.....	69
3.2.3 RNA extraction and QPCR .....	70
3.2.3.1 Agarose gel electrophoresis analysis of QPCR product.....	70
3.2.3.2 Sequencing .....	70
3.2.4 Statistical analysis .....	70
3.3 Results.....	71

3.3.1 Basal ERK activation during 3T3-L1 differentiation .....	71
3.3.2 GH stimulated ERK and STAT5 activation during 3T3-L1 differentiation..	72
3.3.3 Maximal ERK phosphorylation during 3T3-L1 differentiation.....	74
3.3.4 Validation of the GHR QPCR assay .....	76
3.3.5 GHR expression during differentiation .....	78
3.4 Discussion.....	79
<b>4. Chapter Four .....</b>	<b>84</b>
4.1 Introduction .....	84
4.1.1 Src Homology (Shc) protein.....	85
4.1.2 GHR expression in 3T3-L1 cells .....	87
4.1.3 Transfection.....	87
4.1.4 Aims .....	89
4.2 Material and methods.....	90
4.2.1 Detection of Shc in differentiating 3T3-L1 cells .....	90
4.2.2 Over expression of the GHR in 3T3-L1 cells.....	90
4.2.2.1 GHR expression vector.....	91
4.2.2.2 Transformation of E. coli with the plasmid vector. ....	91
4.2.2.3 Midi-prep of plasmid DNA.....	92
4.2.2.4 Transfection of 3T3-L1 with the GHR plasmid .....	93
4.2.2.5 Western blotting techniques .....	94
4.2.2.6 RNA extraction and QPCR analysis of human GHR expression .....	94
4.3 Results .....	96
4.3.1 Basal Shc activation during 3T3-L1 differentiation .....	96
4.3.2 Transfection efficiency .....	97
4.3.3 Validation of the hGHR QPCR assay.....	99
4.3.4 Effect of GHR expression on GH-induced ERK and STAT5 activation...	101
4.4 Discussion.....	107
<b>5. Chapter Five .....</b>	<b>111</b>
5.1 Introduction .....	111
5.1.1 Human primary pre-adipocyte model.....	112
5.1.2 Human orbital pre-adipocytes.....	113
5.1.3 Aims .....	114
5.2 Material and methods.....	115
5.2.1 Isolation and culture of primary mouse pre-adipocytes .....	115
5.2.1.1 Differentiation of primary mouse pre-adipocytes.....	115

5.2.2 Tissue specimen and preparation.....	116
5.2.2.1 Cell culture of primary human pre-adipocytes.....	116
5.2.2.2 Differentiation of primary human pre-adipocytes.....	116
5.2.3 Breast fat tissue extraction .....	117
5.2.4 Oil Red O staining .....	117
5.2.4.1 Cell proliferation studies .....	117
5.2.5 QPCR analysis of gene expression .....	118
5.2.5.1 Extraction RNA of primary mouse adipocytes cultures .....	118
5.2.5.2 Reverse transcription.....	118
5.2.6 Western blot analysis of protein.....	119
5.2.7 Statistical analysis .....	119
5.3 Results.....	120
5.3.1 Are the changes in GH signalling during adipogenesis unique to the 3T3-L1 cell line? .....	120
5.3.1.1 Morphology of primary mouse cells during differentiation .....	121
5.3.1.2 Oil Red O of primary mouse cells during differentiation .....	121
5.3.1.3 PPAR $\gamma$ expression during primary mouse cells differentiation.....	122
5.3.1.4 GPDH expression during primary mouse cells differentiation.....	126
5.3.1.5 GHR expression during primary mouse pre-adipocytes differentiation	128
5.3.1.6 Basal ERK activation during mouse primary pre-adipocytes differentiation	130
5.3.1.7 GH stimulated ERK and STAT5 activation during primary mouse pre-adipocytes differentiation.....	131
5.3.2 Are the changes in GH signalling during adipogenesis species dependent?135	
5.3.2.1 Morphology of primary human orbital cells during differentiation.....	135
5.3.2.2 Oil Red O of human orbital during differentiation .....	136
5.3.2.3 LPL expression during primary orbital cells differentiation .....	137
5.3.2.4 PPAR $\gamma$ expression during human orbital pre-adipocytes differentiation .....	138
5.3.2.5 GHR expression during human orbital pre-adipocytes differentiation..	140
5.3.2.6 Basal ERK activation during human orbital pre-adipocyte differentiation	142
5.3.2.7 GH stimulated ERK and STAT5 activation during orbital human pre-adipocytes differentiation.....	143
5.3.2.8 Mitotic clonal expansion (MCE) .....	145
5.3.3 Are there depot-specific differences in GH signalling during adipogenesis?148	
5.3.3.1 Morphology of primary human breast fat cells during differentiation....	148
5.3.3.2 Oil Red-O of human breast fat cells during differentiation.....	148

5.3.3.3 PPAR $\gamma$ expression during breast fat cells differentiation .....	149
5.3.3.4 LPL expression during breast fat cells differentiation .....	151
5.3.3.5 GHR expression during human breast fat differentiation.....	152
5.3.3.6 GH stimulated ERK and STAT5 activation during breast fat cells .....	154
5.5. Discussion.....	157
<b>6. Chapter Six</b> .....	<b>159</b>
6.1 Discussion.....	159
Appendix 1 .....	164
Appendix 2.....	168
References .....	173

# **Chapter One**

## **General Introduction**

# 1. Chapter one (General Introduction)

## 1.1 Endocrine system

The nervous system works together with the endocrine system to maintain homeostasis and long-term control of the organism using chemical signals known as hormones that regulate body processes. The principal glands that make up the human endocrine system include the hypothalamus and pituitary which together form the hypothalamic-pituitary axis, which is the basis of the link between the nervous system and the endocrine system. The hypothalamus secretes hormones into the blood which travel through the hypophyseal portal vessel to the secondary capillary plexus in the pituitary gland. The hypothalamic releasing hormones stimulate pituitary cells to release their hormones into the secondary plexus. The pituitary gland consists of two lobes known as the anterior pituitary or 'adenohypophysis' and the posterior pituitary or 'neurohypophysis'. The posterior pituitary is not a separate organ, but instead is a physical extension of the hypothalamus that is primarily composed of the axons of hypothalamic neurons which extend downward forming a large bundle behind the anterior pituitary. The posterior pituitary releases the hormones vasopressin and oxytocin. The anterior pituitary is a gland composed chiefly of cells that secrete a variety of endorphins along with six different types of secretory cells. The anterior pituitary releases a number of hormones including growth hormone (GH) which plays a role in stimulating growth (Lloyd, 2004).

**“This image has been removed by the author for copyright reasons”.**

**Figure 1.1 Hypothalamic-pituitary axis.** To view image see <http://kcampbell.bio.umb.edu>

## **1.2 Growth hormone**

### **1.2.1 Historical background**

The first indication that the pituitary gland was involved in growth control came in 1886 when Pierre Marie observed that this gland was enlarged in one of his acromegalic patients (Marie, 1886; Brunori *et al.*, 1995). Later, in the first half of the 20<sup>th</sup> century, Evan and Long (1922), demonstrated the complexity of the pituitary gland's role in a study of the effects of a saline extract of bovine anterior pituitary gland on the growth of animals. Additional studies revealed that hypophysectomization (surgical removal of the pituitary gland) significantly altered the growth process. Hypophysectomy of young animals such as rats, frogs and dogs inhibited their growth. In older animals the procedure caused visceral atrophy and weight loss (Cole, 1938; Chawla *et al.*, 1983).

In 1927, Smith *et al.* demonstrated that hypophysectomized rats treated with pituitary extract regained their normal growth pattern. The extract contained substances from the anterior pituitary gland of mammals and it was thought to be responsible for promoting body growth. This work with hypophysectomized animals helped to clarify the role of the pituitary gland in development. By 1945, other research had successfully isolated specific growth hormone (GH) from anterior pituitary glands (Li *et al.*, 1945; Kopchick and Andry, 2000). Later, around 1950, human GH was isolated from the pituitary and was used to treat short stature patients suffering from dwarfism (Raben, 1958). This condition is the result of pituitary growth hormone deficiency (GHD).

### **1.2.2 Structure and secretion of GH**

GH is a member of the cytokine superfamily that also includes the hormones prolactin (PRL) and chorionic somatomammotropin, which share some structural homology with GH (Barsh *et al.*, 1983; Forsyth, 1986; Corbacho *et al.*, 2002; Jeay *et al.*, 2002; Anderson *et al.*, 2004; Le Tissier *et al.*, 2012). The human GH gene is part of a cluster of 5 related genes on chromosome 17q23 which contains the GH1 and GH2 genes, two chorionic somatomammotropin genes and a pseudogene (CSHPI) (Barsh *et al.*, 1983; Ohta, 1993; Procter *et al.*, 1998) and is believed to have arisen following gene duplication events. The genes differ in their 3' flanking regions, but are essentially homologous through their 5' flanking regions (Barsh *et al.*, 1983; Chen *et al.*, 1989; Procter *et al.*, 1998).

The term "growth hormone" refers to the hormone produced and released from somatotrophic cells in the anterior pituitary gland (Anderson *et al.*, 2004); it is also known as somatotrophin (Cole, 1938). GH affects the growth and differentiation of cartilage, bone and adipose cells through cell surface GH receptors (GHRs), which influence the metabolism of carbohydrates, proteins and lipids (Maharajan and Maharajan, 1993; Le Roith *et al.*, 2001; Liao and Zhu 2004; Wei *et al.*, 2009; Fuentes *et al.*, 2012). GH primarily promotes growth indirectly; it binds to GHR on liver cells and promotes the release of insulin-like growth

factor-1 (IGF-1). IGF-1 then travels via the circulation to act directly on muscle, long bones and fat cells via IGF-1 receptors (Berneis and Keller, 1996; Wei *et al.*, 2009) Figure 1.2.

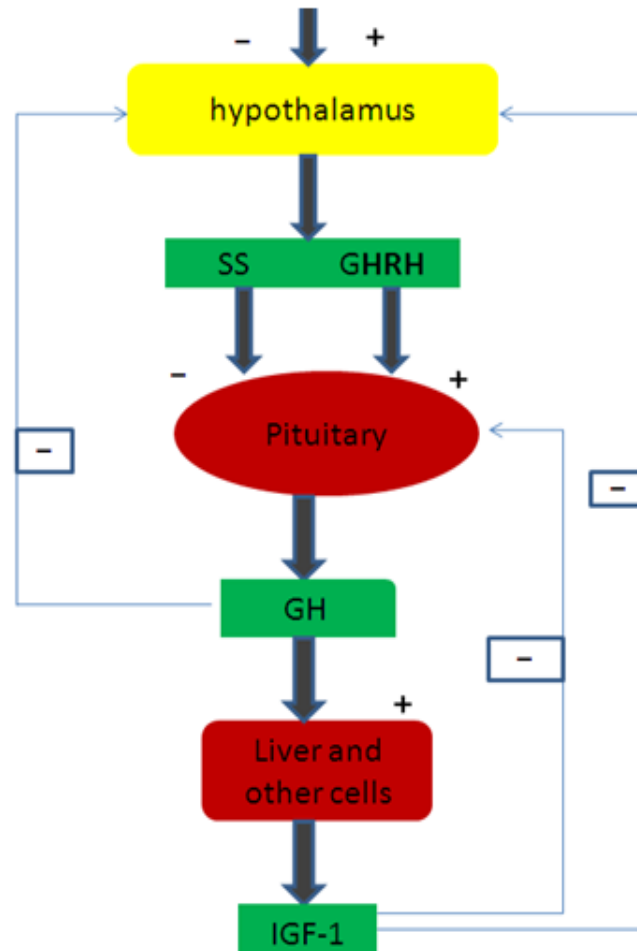


**Figure 1.2 Regulation of the GH secretion**

The hypothalamus regulates GH secretion through two hypothalamic peptides, a stimulating hormone called “growth hormone releasing hormone” (GHRH) and the inhibiting hormone “somatostatin” (SS). Regulation is via two pathways with the feed forward pathway affecting the liver/cells that secrete IGF-1. This hormone affects the hypothalamus and pituitary to inhibit further secretion GHRH and GH. GH then stimulates the hypothalamus to secrete SS which in turn prevents further secretion of GH. (Adapted from [www.elp.manchester.ac.uk](http://www.elp.manchester.ac.uk)).

The GH gene, is localized on the 17q22-24 region of the long arm of chromosome 17 is about 3 kb long and is composed of 5 exons and 4 introns, which encode a 217-amino-acid protein. Cleavage of the signal peptide forms a mature single-chain polypeptide of 191-amino-acid residues with a molecular weight of 22,124 Daltons (Da) (Niall *et al.*, 1971; Chawla *et al.*, 1983; Kopchick *et al.*, 2002).

**“This image has been removed by the author for copyright reasons”.**

### **Figure 1.3 Three-dimensional structure of GH**

The structure of GH was elucidated after being crystallized in complex with its receptor. GH consists of four anti-parallel-helical bundles symbolized here as helix rods (shown as cylinders) arranged in an up-up-down-down topology. To view image see Abdel-Meguid *et al.*, (1987) Proc. Natl. Acad. Sci. 84:6434–6437.

X-ray crystallography reveals the three dimensional structure of hGH as comprising two disulphide bridges linked to one large and one small peptide loop at residues 110 and 6 respectively. Antiparallel secondary and tertiary structures with four  $\alpha$ -helices are arranged with an unusual configuration comprising a left handed bundle with an up-up-down-down topology (Abdel-Meguid *et al.*, 1987; Watahiki *et al.*, 1989; de Vos *et al.*, 1992; Kopchick, *et al.*, 2000). Three shorter helices, that could cause conformational changes of hGH when binding to its receptor, reside in the loop connecting the major helices (Kopchick *et al.*, 2002) (Figure 1.3).

The level of GH secretion is controlled by a complex regulatory system (Figure 1.2). Many physiological factors influence GH secretion including age, gender, nutrition and hormones (Roemmich and Rogol, 1997; Trobec *et al.*, 2011). The primary control of this system is exerted by two hypothalamic neuroendocrine hormones: growth hormone releasing hormone (GHRH) that stimulates secretion of GH and somatostatin (SS) which inhibits its secretion (Muller, 1987; Butler and Le Roith, 2001; Anderson *et al.*, 2004). GH acts directly on the hypothalamus by a short loop mechanism to inhibit GHRH and stimulate production of SS to reduce secretion of GH. IGF-1 exerts indirect negative feedback via a long loop mechanism that inhibits secretion of GHRH (Colonna *et al.*, 1989). Additionally, other hypothalamic neuropeptides contribute both directly and indirectly in the regulation of GH secretion. The complexities surrounding the regulation of each of these neuropeptides are determined at both the physiological and molecular levels (Butler and Le Roith, 2001).

Additionally, free fatty acids act on the pituitary gland to inhibit GH production by forming a feedback loop while GH stimulates the mobilization of lipid (Butler and Le Roith, 2001). The action of leptin on rodents has been observed to stimulate the secretion of GH by acting on the hypothalamus to regulate GHRH and SS activity. Leptin stimulates GH release via its inhibition of the GH inhibitory peptide, neuropeptide Y. GH secretion is also regulated by other factors such as gonadotropin releasing hormone (GnRH), ghrelin, pituitary adenylate activating polypeptide (PACAP) and thyrotrophic releasing hormone (TRH) (Anderson *et al.*, 2004). Excess secretion of GH in young people causes gigantism and acromegaly in adults and deficiency of GH causes dwarfism (Zhou *et al.*, 1997; Stewart, 2000).

### 1.2.3 Growth hormone receptor and distribution

For understanding the regulation of growth and role of the GH in adipogenic differentiation, it is important to study the principles of GH action. At the molecular level the biological effect GH is initiated in the cell by binding on the cell surface growth hormone receptor (GHR). The GHR is a member of the Class I superfamily of transmembrane cytokine receptors, also known as the hematopoietic cytokine receptor family that comprises receptors for interleukins, interferon, colony-stimulating factors and tumour necrosis factors. These receptors share similar mechanisms of signal generation and transmission (Moutoussamy *et al.*, 1998; Kopchick *et al.*, 2002; Liongue and Ward, 2007).

The Class I cytokine receptor family is the main group of cytokine receptors comprising structurally homologous cell surface receptors which do not possess intrinsic tyrosine kinase activity (Gent *et al.*, 2002; Perret-Vivancos *et al.*, 2006; Waters *et al.*, 2006; Liongue and Ward, 2007; Deng *et al.*, 2007). The Class I cytokine superfamily receptor has several characteristics which include a single membrane-spanning domain, an extracellular domain of about 210 amino acids with significant sequence homology (14-44%), along with preserved pairs of cysteine residues present in the extracellular domain (seven cysteine residues, six are paired and one unpaired) and a preserved tryptophan residue next to the second cysteine in the N-terminal fibronectin domain. The intracellular region immediately proximal to the membrane spanning region contains an 8 amino acid proline-rich box 1 region and a box 2 region of approximately 15 hydrophobic amino acid residues and one or two positively charged amino acids which are located approximately 30 amino acids toward the c-terminal from box 1 in the GHR (Kopchick and Andry, 2000; Zhu *et al.*, 2001; Gent *et al.*, 2002). GHR lacks intrinsic tyrosine kinase activity therefore the activation of one or more members of the Janus kinase (JAK) family is required for the initiation of GH signal transduction upon ligand to the receptor.

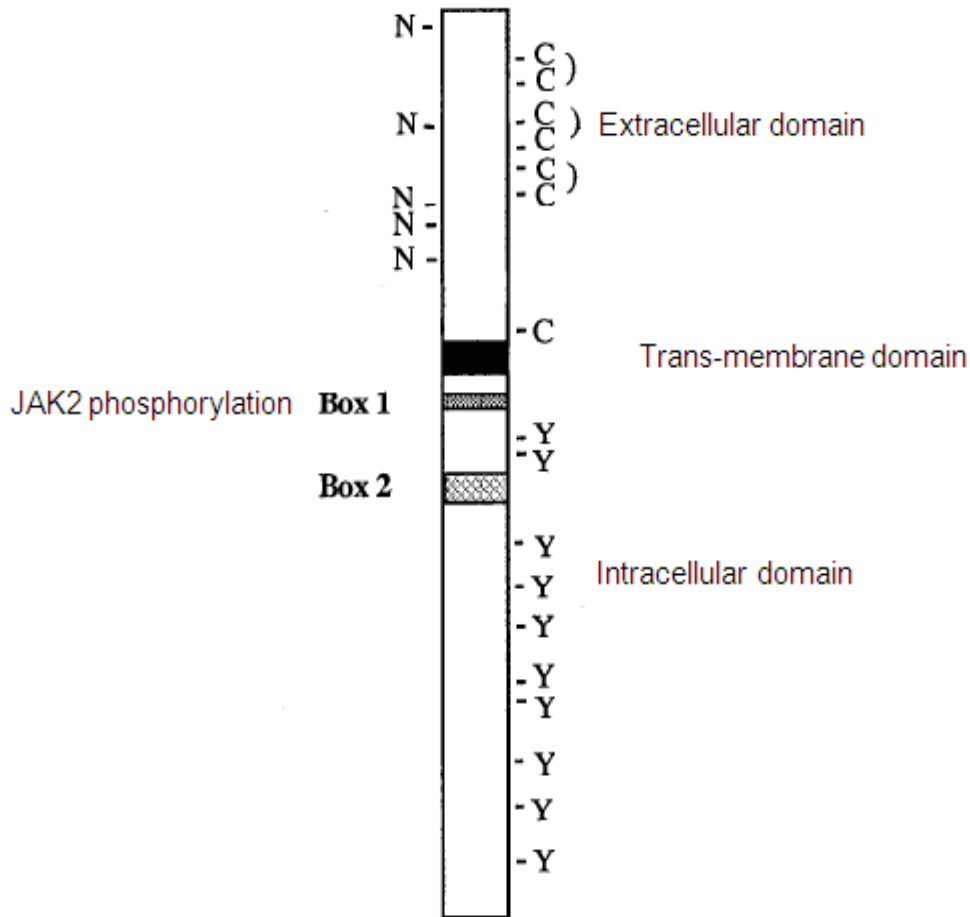


**Figure 1.4 Schematic representation of the GHR.**

A schematic diagram of the GHR in which N represents extracellular domain N-linked glycosylation site, C represents cysteine residues and Y the tyrosine residues. (Adapted from Kopchick and Andry, 2000, *Mol Genet Metab.* 71: 293–314).

The interaction of the box 1/box 2 regions and the N-terminal region of JAKs leads to alignment of the JAK causing dimerization and reconfiguration of the receptor resulting in phosphorylation of both the JAKs and the receptor following GH binding, (Figure 1.4) (Murakami *et al.*, 1991; Carter-Su *et al.*, 1996; Kopchick and Andry, 2000; Zhu *et al.*, 2001; Deng *et al.*, 2007). Both box 1 and box 2 deletions and mutations abrogate signalling in members of the cytokine receptors superfamily (Ihle *et al.*, 1995). In addition, mutation of the box 1 GHR region abrogates JAK2-STAT5 signalling *in vivo*, but preserves other signalling pathways (Barclay *et al.*, 2010).

The GHR can exist in one of two distinct forms: the membrane-bound full length receptor or a soluble form of GHR also known as GH binding protein (GHBP) which comprises the extracellular domain of the GHR. In humans the GHR cDNA encodes a 638-amino acid polypeptide that consists of both a mature full-length receptor of 620-amino acids and an 18-amino acid signal peptide. The mature GHR consists of an extracellular GH-binding domain of 246 amino acid residues, a transmembrane domain of 24 amino acid residues and a cytoplasmic domain of 350 amino acid residues (Postel-Vinay and Kelly, 1996; Edens and Talamantes, 1998; Moffat *et al.*, 1999; Kopchick *et al.*, 2002). The extracellular domain of the GHR includes two  $\beta$  sandwich subdomains (N-terminal 1-123 amino acids and C-terminal 128-238 amino acids) which include seven  $\beta$  strands in both subdomains. The two subdomains 1 and 2 are bound together with seven strands via six loops organized into two antiparalle  $\beta$  sheets, while two highly preserved disulphide bridges maintain the stability of subdomain 1 (Postel-Vinay and Kelly, 1996; Behncken and Waters, 1999; Frank, 2002). The predicted molecular weight of the GHR is 70 kDa, but the apparent molecular weight 109 kDa in human IM-9 lymphocyte and 124 kDa in human liver are due to post-translational modification, such as N-glycosylation (Kopchick and Andry, 2000).

Low levels of GHR mRNA are present at birth, but increase in the postnatal period in organs such as the liver, adipose tissue, kidney, heart and muscle. GH regulates GHR gene expression (Moffat *et al.*, 1999).

The hGHR gene is located on the short arm of chromosome 5 spanning about 87 kbp in the 5p13-p12 region. The hGHR gene encodes nine exons (exon 2-exon 10), exon 2 codes the signal peptide, exons 3-7 encode the extracellular domain, the transmembrane domain is encoded by exon 8, exons 9 and 10 encode the cytoplasmic domain (Amselem *et al.*, 1996; Moffat *et al.*, 1999; Blum *et al.*, 2006).

GH binding protein (GHBP) corresponds to the extracellular ligand binding domain of the GHR (Moffat *et al.*, 1999; Talamantes and Ortiz, 2002). In some species such as human and chickens, GHBP arises from the proteolytic cleavage of a membrane-spanning receptor, but in rats and mice the GHBP arises from an alternately spliced mRNA in which exons encoding the transmembrane and cytosolic domains of GHR are replaced with an exon that encodes a hydrophilic peptide (Frick *et al.*, 1998; Moffat *et al.*, 1999; Kopchick *et al.*, 2002).

The GHR is distributed in many tissues, including adipose tissue, hepatic tissue and immune tissue; it is also present in the eye, brain, heart, muscle, bone and kidney. GHR expression in adipose tissue is depot specific. For example, in the rat a high level of expression of the GHR is observed in the epididymal fat pad, while the retroperitoneal fat pad in contrast expresses a low level of GHR (Nam and Lobie 2000; Kopchick *et al.*, 2002).

#### **1.2.4 GHR signalling**

GH has two GHR-binding domains and thus initiates signalling by binding to the extracellular domain of two receptors (Zhu *et al.*, 2001). The GHR lack intrinsic tyrosine kinase activity and was the first cytokine receptor identified that induces signal transduction through receptor dimerization. Using X-ray crystallographic analysis of the molecular structure it was found that GH binds to two receptor molecules (Sundstrom *et al.*, 1996). A model was designed showing how hGH has two receptor-binding sites with distinctive binding faces on either side of the molecule. These interactions are responsible for the structure and stabilization of the GH/GHR complex (Behncken and Waters, 1999; Zhu *et al.*, 2001; Waters *et al.*, 2006).

Current models of receptor activation suggest that GH induces rotation of the receptor monomers within a pre-existing receptor dimer (see Figure 1.5), resulting in activation of Janus kinase 2 (JAK2), a cytoplasmic tyrosine kinase that is associated with box 1 domain of GHR. Upon ligand binding, JAK2 autophosphorylates and phosphorylates seven different tyrosine residues in the cytoplasmic domain of the hGHR. Adapter proteins contain multiple SH2 and/or PTB domains and can bind to other phosphotyrosine (PY) containing signalling proteins thus binding them to the cytoplasmic domain of the GHR and forming a multiprotein signalling complex (Zhu *et al.*, 1998). The GHR cytoplasmic domain phosphotyrosine residues then act as docking points for SH2 and PTB domain-containing proteins resulting in the formation of a multiprotein signalling complex centred around the focal adhesion kinase associated protein p130<sup>Cas</sup> and the adaptor protein CrkII (Zhu *et al.*, 1998).

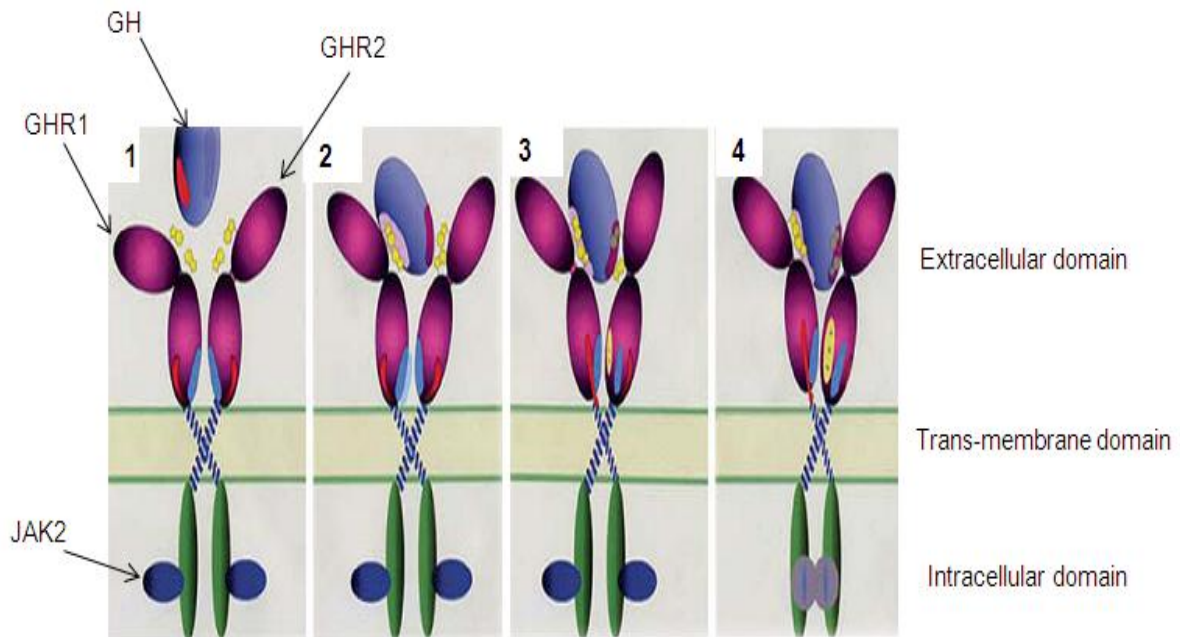


**Figure 1.5 Mechanism of GH binding to GHR**

GH binds first via its site 1 to receptor 1. Then binding to GH site 2 realigns the receptors such that receptor 1 is raised and rotated relative to receptor 2 because of the asymmetric placement of the receptor binding sites on the hormone. This relocation is transmitted through the transmembrane domain (TMD), aligning JAK2 kinases bound to box1 of the receptor, which facilitates their activation by transphosphorylation, so initiating the GH signaling cascades. (Adapted from Lichanska and Waters, 2008, *Horm Res.* 69: 138-145).

The complex comprises at least 15 different proteins including adaptor/scaffold proteins, cytoskeletal proteins and components of ERK and PI-3 kinase pathways and Src, thereby linking GHR activation to multiple downstream cell signalling pathways. The complex may be associated with the caveolae and lipid raft plasma membrane fraction and it is suggested that this localisation is necessary for coupling of the GHR to ERK pathway activation (Yang *et al.*, 2004). The pathways leading from the GHR to ERK and PI3-kinase activation are complex and much remains to be determined. GH activates the ERK pathway both in a JAK2-dependent manner via the well characterised SHC-Grb2-SOS-Ras-Raf-MEK route (Vanderkurr *et al.*, 1997) possibly involving Gab1 (Kim *et al.*, 2002) and in a JAK2 independent manner via Src (Zhu *et al.*, 2002). Negative regulators of cell signalling are also associated with the GHR and possibly form part of the signalling complex. The protein

tyrosine phosphatase, SHP2, binds to the GHR where it may serve to down regulate GHR-associated signalling and possibly to act as an adapter protein (Rowland *et al.*, 2005). The suppressor of cytokine signalling proteins (SOCS2, SOCS3 and CIS) bind GHR phosphotyrosine residues (Du *et al.*, 2003) and are believed to inhibit GH-induced transcription by competing with STAT5 (Figure 1.6).

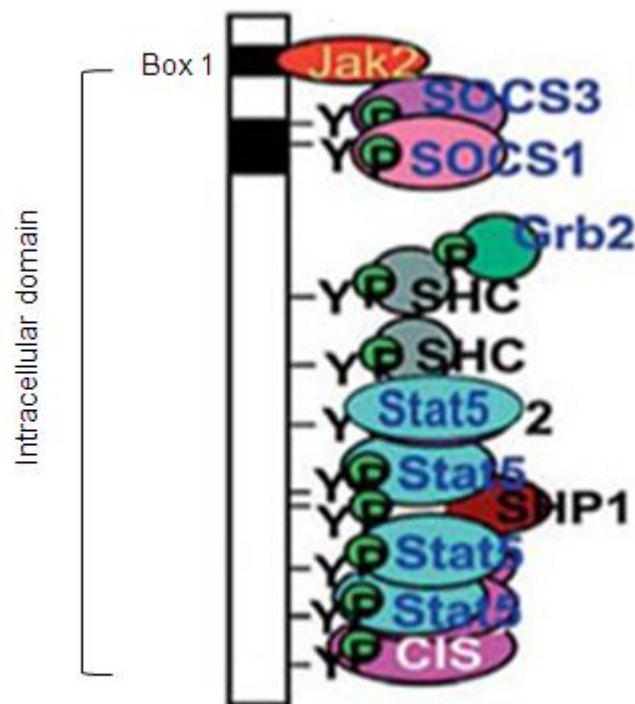


**Figure 1.6 Tyrosine phosphorylation of the GHR cytoplasmic domain**

GH binding results in multiple tyrosine phosphorylation of the GHR which then act as docking points for signalling proteins resulting in activation of multiple signalling pathways. (Adapted from Lichanska and Waters, 2008, *Horm Res.* 69: 138-145).

## 1.2.5 Activation of multiple signalling pathways

### STAT5

The signal transducer and activator of transcription (STAT) pathway is important in mediating the effects of GH. STATs are a family of latent transcription factors, including STAT1, 3, 5a and 5b, which are located in the cytoplasm of cells and are central regulators of the biological effects of GHR. Following GHR activation JAK2 phosphorylates the receptor cytoplasmic domain generating docking sites for specific signalling proteins, including STAT proteins (Ward *et al.*, 2000; Waxman and O'Connor, 2006). STATs then become tyrosine phosphorylated by JAK2. Phosphorylated STAT5 forms a homodimer through its phosphotyrosine residues and is then translocated to the nucleus where it acts as a transcription factor resulting in the increased expression of specific target genes. Activation of the JAK2-STAT5 pathway appears to be necessary for normal growth by regulating the expression of the target gene, IGF1 (Floyed *et al.*, 2007; Moller and Jorgensen, 2009) (Figure 1.7).

### ERK

Mitogen-activated protein kinases (MAPKs) are a family of signal transduction protein kinases which are activated by extracellular factors and produce downstream control of a variety of cellular actions. The MAPKs super-family is composed of three major sets of kinases: the extracellular signal regulated kinases (ERK 1-5) and two types of MAPK-related kinases; (c-Jun N-terminal kinases/stress-activated protein kinases (JNK1-3) and the p38 MAP Kinases (p38 alpha, p38 beta2, p38 gamma and p38 delta). The MAPKs are a group of serine/threonine protein kinases. The extracellular signal-regulated kinase pathway, also known as p42/44 MAPK cascade consists of the MAPKKKs A-Raf, B-Raf and Raf-1, the MAPKKs MEK1 and MEK2 and the MAPKs ERK1 and ERK2. ERK1 and ERK2 are expressed in all tissues and cells with ERK2 levels generally higher than ERK1 (Roux and Blenis, 2004). The ERK 1/2 cascade is activated by a variety of stimuli such as growth factors, GH, insulin and cytokines, and controls proliferation, differentiation, cell cycle

progression, survival and many other cellular processes (Chuderland and Seger, 2005, Matsushita *et al.*, 2009). The Ras/ERK pathway is activated by GH when JAK2 stimulates tyrosine phosphorylation of the Src homology-collagen adapter protein shc. This leads to activation of guanosine triphosphate (GTP)-binding proteins and Ras by inducing the exchange of GDP with GTP. This converts Ras into its active form (Horbinski and Chu, 2005, Vantaggiato *et al.*, 2006) enabling it to interact with a number of downstream effectors (Kolch, 2000). Activated Ras binds to Raf kinases at the cell membrane, which in turn activates MEK1 which then phosphorylate and activates ERK1 and ERK2 (Matsushita *et al.*, 2009). Activation of ERKs 1 and 2 by GH in 3T3-F442A pre-adipocytes leads to phosphorylation of the nuclear transcription factor CEBP $\beta$  and differentiation into adipocytes (Lanning and Carter-Su, 2006) (Figure 1.7).

### **PI3 kinase**

Phosphatidylinositol 3-kinase (PI3 kinase) plays an important role in regulating many cellular processes including cellular metabolism, glucose uptake, lipid deposition, adiponectin secretion from adipocytes, cell proliferation and survival. GH stimulates actin cytoskeletal reorganization and lipogenesis via activation of PI3 kinase (Zhu *et al.*, 2001, Del Rincon *et al.*, 2007). GH activation of PI3 kinase follows activation of the insulin receptor substrate (IRS) proteins that associate with p85 protein, leading to activation of the protein kinase Akt (Wang *et al.*, 2008; Moller and Jorgensen, 2009). Akt contributes to GH induction of ERK, p70 S6 kinase and phosphodiesterase activation, as well as engaging in antiapoptosis and proliferation (Wang *et al.*, 2008). Akt plays a role in cell survival via inhibition of the proapoptotic caspase-3 protein (Lanning and Carter-Su, 2006) (Figure 1.7).

**“This image has been removed by the author for copyright reasons”.**

**Figure 1.7 GH/GHR signalling pathways**

Diagram shows the various GH/GHR signalling pathways. To view image see Xu and Messina, (2009) *Vita & Horm* 80: 125–153.

### 1.2.6 Effects of GH

GH is involved in the control of several complex physiological processes, including growth and aspects of metabolism (Le Roith *et al.*, 2001; Kopchick *et al.*, 2002; Wei *et al.*, 2009). It plays an important role in regulation of many processes including differentiation of adipocytes, supports maintenance and development of the immune system, neurological and cardiac function (Kopchick *et al.*, 2002). An important concept in understanding GH activity is that it has two distinct types of effects: direct and indirect (Nam and Lobie, 2000). The direct effects of GH are via the GHR on target cells such as chondrocytes and osteoblasts. GH also affects adipocytes leading to stimulation of triglyceride breakdown and suppression of their ability to take up and accumulate circulating lipids (Davidson, 1987, Richelsen *et al.*, 1994; Moller and Jorgensen 2009). The principal function of GH in promoting body growth is an indirect effect caused by stimulating the liver and various other tissues to secrete IGF-I. IGF-I then acts on its target cells, for example by stimulating proliferation of chondrocytes, resulting in bone growth. IGF-1 also plays an important role in the regulation of 3T3-L1 adipocyte differentiation and lipid accumulation (Kloting *et al.*, 2008, Wei *et al.*, 2009). Stimulation of IGF1 synthesis by GH in peripheral tissue regulates many other processes such as insulin sensitivity (Clemmons, 2007). GH has important effects on protein and carbohydrate metabolism, both directly and indirectly via IGF-1. These functions vary from protein synthesis, leading to increased muscle mass to calcium retention and mineralization of bones, as well as stimulating the immune system to maintain functions such as homeostasis (Morikawa *et al.*, 1984).

## 1.3 Adipocytes

The balance between both lipogenesis and lipolysis is modulated by hormonal signals from the bloodstream, which provide an indication of the body's metabolic condition (Large *et al.*, 2004; Kim and Ntambi 1999). In addition, adipose tissue can be regarded as the largest endocrine organ in mammals acting as a secretory and endocrine organ that mediates physiological and pathological processes (Gregoire, 2001; Galic *et al.*, 2009; Li *et al.*, 2009). The adipocyte plays an essential role in energy balance and storage in the form of triglycerides (Gregoire *et al.*, 1998; Leonardsson *et al.*, 2004; Li *et al.*, 2009) which can be broken down into free fatty acids when energy is required. Adipose tissue growth involves an increase in adipocyte size and the development of new adipocytes from precursor cells (Gregoire *et al.*, 1998; Louveau and Gondret 2004). Hormones and proteins secreted by adipocytes include more than 50 types of adipokines (Goralski and Sinal 2007) and include leptin, adiponectin, resistin and tumor necrosis factor  $\alpha$  (TNF $\alpha$ ) (Maeda *et al.*, 2002; Fain and Gerald, 2006; Scherer, 2006).

The adipocyte develops from an embryonic stem cell precursor with the capacity to differentiate into the mesodermal cell types of adipocytes, chondrocytes, osteoblasts, and myocytes (Gregoire *et al.*, 1998). Several transcription factors regulate the differentiation of preadipocytes into mature adipocytes (Figure 1.8). Following growth arrest, at the G1/S phase, preadipocytes receiving appropriate mitogenic and adipogenic signals differentiate into mature adipocytes. Mitotic clonal expansion may be required for progression through subsequent steps in the differentiation program. Upregulation of the transcriptional regulators C/EBP $\alpha$  and PPAR $\gamma$  is essential for activation of adipocyte specific genes following addition of an adipogenic cocktail comprising insulin or IGF-1, a glucocorticoid and a mediator to enhance levels of cAMP (Figure 1.8) (Altjok *et al.*, 1997; Otto and Lane, 2005).

Two types of adipose tissue exist: white and brown (Tiraby and Langin, 2003). White adipose tissue (WAT) stores energy when food intake exceeds energy expenditure. WAT development takes place quickly after birth as a consequence of enlarged adipocyte cell size and an increase in adipocyte cell number (Kozak *et al.*, 1988). Brown adipose tissue (BAT) stores less lipid and has more mitochondria than WAT (Kozak *et al.*, 1988; Klaus, 2004). The inner mitochondrial membrane of BAT cells expresses the uncoupling protein 1 (UCP-1) which renders the inner mitochondrial membrane leaky. Thus energy utilization is uncoupled from ATP generation, instead producing heat in a process called adaptive thermogenesis (Klaus, 2004).

A variety of cell culture models, including preadipocyte cell lines and primary cultures, have been used to understand the molecular and cellular activities that take place during the adipocyte differentiation process (Gregoire *et al.*, 1998). The most commonly utilized cells for the study of adipocyte differentiation are the 3T3-L1 and 3T3-F442A preadipocyte cell lines (Watt, 1991; Salazar-Olive *et al.*, 1995).

These were clonally isolated from Swiss 3T3 fibroblast cells derived from disaggregated 17-19-day old mouse embryos (Green and Kehinde; 1974; Green and Meuth, 1974; Green and Kehinde, 1975). Adipocyte differentiation of 3T3-L1 and 3T3-F442A cells occurs spontaneously after growth arrest in confluent cultures and cells develop characteristics of mature adipocytes. The phenotype changes to a rounded cell shape characteristic of adipocytes with accumulating lipid droplets.

**“This image has been removed by the author for copyright reasons”.**

**Figure 1.8 The adipocyte differentiation pathway**

Pluripotent stem cell precursors give rise to a mesenchymal precursor cell with the potential to differentiate into myoblast, chondroblast, osteoblast and adipoblast. Adipoblast conversion into mature adipocytes occurs at the terminal differentiation stage. To view image see Gregoire *et al.*, 1998 *Physiol Rev* 78:783-809.

### 1.3.1 Adipogenesis

Obesity is a major health problem, especially in the developed world. It is a risk factor for a number of pathological disorders such as cardiovascular disease, hypertension, insulin resistance, Type 2 diabetes, certain cancers, and atherosclerosis (Caprio, *et al.*, 1995; Ntambi and Young-Cheul, 2000; Hossain *et al.*, 2007; Knai *et al.*, 2007). Obesity is a result of increased food intake and low energy expenditure leading to increased tissue mass. Adipose tissue increases its' mass by increasing the size of adipocytes; known as hypertrophy, increase in cell number (hyperplasia) involves differentiation of preadipocytes (Otto and Lane, 2005).

Understanding adipogenesis is an important goal towards understanding the way to control obesity (Ntambi and Young-Cheul, 2000). Under growth arrest conditions, several cell lines such as 3T3-L1 can convert to adipocytes in response to hormones and growth factors (Smith *et al.*, 1988; Shang and Waters, 2003). In cell culture, the adipogenic process can be initiated by adipogenic hormonal cocktails, which can include insulin, glucocorticoids and fetal calf serum (FCS), dexamethasone (Dex), methylisobutylxanthine (IBMX) and triiodothyronine (T3) (Smith *et al.*, 1988; Salazar-Olive *et al.*, 1995 Farmer, 2006). Differentiated cells then display adipocyte morphology with increased accumulation of triglycerides and high expression of lipogenic enzymes (Smith *et al.*, 1988). Insulin also affects adipogenesis in the early stages by acting through the insulin-like growth factor 1 (IGF-1) receptor. IGF-1 promotes proliferation in preadipocyte and enhances cell differentiation in cell lines and primary cultures (Kamai *et al.*, 1996; Gerfault *et al.*, 1999). Dex is a synthetic glucocorticoid agonist that stimulates the glucocorticoid receptor pathway (Wang *et al.*, 2012). IBMX is a cAMP-phosphodiesterase inhibitor that stimulates the cAMP-dependent protein kinase pathway. Glucocorticoids may also lead to an increase in cAMP (Green and Kehinde, 1974; Green and Kehinde 1975; Green and Meuth, 1974; Morrison and Farmer, 1999; Ntambi and Young-CheulKim, 2000; Morrison and Farmer, 2000).

Glucocorticoids and cAMP signalling are required during adipogenesis to induce the transcription of CEBP $\alpha$  and CEBP $\beta$  (Cao *et al.*, 1991; Zhang *et al.*, 2004). T3 appears to function as a positive modulator of PPAR $\gamma$  activity (Obregon, 2008). Pref-1 is expressed in pre-adipocytes and down regulation is required for cells to progress along the adipogenic pathway. Pref-1 is present in 3T3-L1 preadipocytes, but absent in mature adipocytes and plays an important role in inhibiting of adipocyte differentiation (Sul *et al.*, 2000).

### 1.3.2 Transcriptional regulation of adipogenesis

#### PPAR $\gamma$

PPAR $\gamma$  is a member of the nuclear hormone receptor family (Adams *et al.*, 1997; Fajas *et al.*, 2001; Viswakarma *et al.*, 2010; Shen *et al.*, 2012) which plays an important role in control of various biological processes (Koeffler, 2003; Shen *et al.*, 2012). The three major types that have been identified are: PPAR $\alpha$ , PPAR $\beta$  and PPAR $\gamma$ . PPAR $\gamma$  is expressed in two isoforms, PPAR $\gamma$ 1 and PPAR $\gamma$ 2. PPAR $\gamma$ 2 is mainly expressed in adipocyte cells while PPAR $\gamma$ 1 is also expressed in liver and breast. PPAR $\gamma$  is a master key for regulation and stimulation of adipogenesis (Tontonoz *et al.*, 1994; Viswakarma *et al.*, 2010; Cipolletta *et al.*, 2012). C/EBP $\alpha$  interacts with PPAR $\gamma$  gene (Fajas *et al.*, 2001; Rosen *et al.*, 2002; Miard and Fajas, 2005) regulating numerous genes leading to adipogenesis (Kletzien *et al.*, 1992; Sandouk *et al.*, 1993; Tontonoz *et al.*, 1994; Lehmann *et al.*, 1995; Chen *et al.*, 1998; Saladin *et al.*, 1999; Grimaldi, 2001; Fajas *et al.*, 2001; Viswakarma *et al.*, 2010).

The expression of PPAR $\gamma$  is both essential and sufficient for adipocyte differentiation *in vitro* and *in vivo* (Tamori *et al.*, 2002; Shang and Waters, 2003; He *et al.*, 2003; Matsuaue *et al.*, 2004; Imai *et al.*, 2004, Kim and Chen, 2004; Jones *et al.*, 2005). PPARs are activated by specific ligands which act to stimulate expression of specific target genes (Marx, 2002). PPAR $\gamma$  is activated by a number of endogenous activators including the eicosanoids 9 and

13-hydroxyoctadecadienoic acids (Willson *et al.*, 2000), prostaglandin D2 derivative 15-deoxy- $\Delta$  12, 14-prostaglandin J2 (15d-PGJ2) forms of oxidized linoleic acids (Touyz & Schiffrin, 2006) and conjugated linoleic acid (CLA) (Moya-Camarena *et al.*, 1999). PPAR activation lead to heterodimers with the retinoid X receptor (RXR) causing the heterodimerization and binding of PPAR response elements (PPREs) within the promoter target genes enhancing gene expression (Figure 1.9). Many factors such as protein kinase A (PKA) and PKC, ERK, 5' adenosine monophosphate-activated protein kinase (AMPK), medium and long-chain fatty acids and eicosanoids enhance the expression of PPARs (Escher and Wahli, 2000; Touyz and Schiffrin, 2006). Growth factors such as platelet derived growth factor (PDGF) phosphorylate PPARs through the ERK signalling pathways and decrease transcriptional activity of PPAR (Paoletti *et al.*, 2004). Once PPAR is ligand-activated the co-repressor complex begins to dissociate while a co-activator complex, containing histone acetylase activity is recruited by the PPAR/RXR heterodimer. These PPARs have been demonstrated to regulate gene expression by a number of transcriptional activities. First, PPARs bind to response elements thus the initiating of transcription; secondly, PPARs can negatively regulate the expression of gene in a ligand dependent manner (Ricote and Glass, 2007).

**“This image has been removed by the author for copyright reasons”.**

#### **Figure 1.9 PPARs/RXR heterodimers**

PPARs form heterodimers with RXR. The heterodimers bind to PPAR response elements (PPREs) stimulating gene expression. To view image see Marx (2002). *Curr Hypertens Rep* 4:71-77.

#### **C/EBP**

CCAAT/enhancer binding protein  $\alpha$  (C/EBP $\alpha$ ) is a member of the C/EBP family and was the first transcription factors recognized to play a major role in adipocyte differentiation (Freytag *et al.*, 1994). In the early stage of adipocyte differentiation treatment of the pre-adipocyte with factors and hormonal inducers of adipogenesis leads to increased expression of C/EBP $\beta$  and C/EBP $\gamma$  followed by an increase of expression of C/EBP $\alpha$  (Darlington, *et al.*, 1998; Rosen *et al.*, 2000; Tong *et al.*, 2005; Khanna-Gupta, 2008; Moller and Jorgensen, 2009; Rahman *et al.*, 2012). The main role of C/EBP $\alpha$  is to conserve PPAR $\gamma$  expression during adipogenesis and insulin sensitivity (Lazar, 2002; Lefterova *et al.*, 2008). Evidence from C/EBP $\alpha$  knockout mice supports the physiological function of C/EBP $\alpha$  in adipose tissue development, since C/EBP $\alpha$  null mice do not develop either WAT or BAT (Chen *et al.*, 2000). C/EBP $\beta$  and C/EBP $\gamma$  are essential factors for terminal differentiation of WAT and BAT adipocytes, but do not induce spontaneous differentiation without hormonal inducers

(Tanaka *et al.*, 1997; Darlington *et al.*, 1998). Knockout of C/EBP $\beta$  and C/EBP $\gamma$  genes in mice do not produce any effect on the levels of PPAR $\gamma$  or C/EBP $\alpha$ . In addition, they do not induce adipogenesis (Tanaka *et al.*, 1997). C/EBP $\alpha$  is involved in the regulation of 3T3-L1 adipocyte differentiation (Breed *et al.*, 1997, Tong *et al.*, 2005). C/EBP $\alpha$  binds and transactivates the promoters of several adipocyte genes that include aP2, stearoyl-CoA desaturase (SCD1), glucose transporter type 4 (GLUT-4), phosphoenolpyruvate carboxykinase (PEPCK), leptin and the insulin receptor (Darlington *et al.*, 1998).

## **KLFs**

Some kruppel-like zinc finger transcription factors (KLFs) act as promoters, but others act as transcriptional repressors. (Li *et al.*, 2005; Brey *et al.*, 2009). KLF2-7, KLF11 and KLF15 are key factors for controlling adipocyte differentiation (Brey *et al.*, 2009). Overexpression of KLF15 leads to increased PPAR $\gamma$  expression and adipogenesis (Mori *et al.*, 2005). However inhibition of KLF15 does not affect the expression of C/EBP $\beta$  (Mori *et al.*, 2005). Reduction of KLF4 blocks differentiation and represses C/EBP $\beta$  expression (Birsoy *et al.*, 2008). KLF5 regulates the transcription factor network that governs and promotes adipocyte differentiation at an early stage. Inhibition of KLF5 and KLF6 exhibit a decrease in differentiation (Oishi *et al.*, 2005; Li *et al.*, 2005; Brey *et al.*, 2009). KLF2 is present in pre-adipocytes and overexpression inhibits PPAR $\gamma$  and C/EBP $\alpha$  expression, but does not effect C/EBP $\beta$  and C/EBP $\gamma$  (Banerjee *et al.*, 2003; Brey *et al.*, 2009). Overexpression of KLF7 in pre-adipocyte represses differentiation (Kanazawa *et al.*, 2005; Brey *et al.*, 2009).

## Other transcription factors

Several molecules are expressed at different levels over the course of adipocyte differentiation. Overexpression of the zinc finger-containing transcription factor Krox20 promotes the early stage of differentiation through the transactivation of C/EBP $\beta$  (Chen *et al.*, 2005; Birsoy *et al.*, 2008). Adipocyte determination and differentiation factor 1/sterol regulatory element-binding protein (ADD1/SREBP) is a member of helix-loop-helix leucine zipper (HLH-LZ) family takes part in the differentiation by repressing differentiation (Kim *et al.*, 1998). ADD1/SREBP1c may stimulate pre-adipocyte differentiation through induction of the endogenous ligand of PPAR $\gamma$  (Kim and Spiegelman, 1996; Kim *et al.*, 1998). In addition, ADD1/SREBP1c mediates insulin stimulation of the fatty acid synthase (FAS) and leptin genes through transactivation promoters (Kim *et al.*, 1998). ADD1/SREBP1c knockout mice exhibit normal WAT development, but reduced fatty acid synthesis in the liver (Shimano *et al.*, 1997). However, a mouse model with adipose tissue specific overexpression of SREBP-1c driven by adipocyte-specific aP2 enhancer/promoter shows retarded WAT differentiation, fatty liver, insulin resistance and diabetes (Shimomura *et al.*, 1998).

Liver X receptors (LXRs) are nuclear hormone receptors. In liver and macrophages LXRs regulate cholesterol, fatty acid and glucose homeostasis. LXR $\alpha$  enhances lipogenesis and binds to the promoters of PPAR $\gamma$  and ADD1/SREBP1c to increase gene expression and enhance differentiation (Seo *et al.*, 2004). LXR $\beta$  is crucial for adipocyte size enlargement. In LXR $\beta$  deficient mice reduced lipid accumulation in adipose tissue and impaired glucose sensitivity leads to reduced insulin secretion (Gerin *et al.*, 2005).

### 1.3.3 Effect of GH on adipocyte biology

The differentiation of pre-adipocytes into adipocytes takes place following a specific sequence of events (Gregorie, 2001). GHR expression is present in both immature and mature adipocytes, but GHR numbers increase with differentiation (Zou *et al.*, 1997, Yu, 2000). GH plays an important role in the stimulation of the differentiation of pre-adipocytes to adipocytes both directly (Berneis and Keller, 1996; Zou *et al.*, 1997; Iida *et al.*, 2003; Flint *et al.*, 2006) and indirectly via IGF-1 (Daughaday and Rotwein, 1989; Zou *et al.*, 1997; Flint *et al.*, 2006). A stimulatory effect of GH on adipogenesis is seen in GHD patients who have an enlarged mean adipocyte volume with decreased numbers of adipocytes and regain normal levels of adipocytes following GH treatment (Bengtsson *et al.*, 1992; Rosenbaum *et al.*, 1989). GH has two opposite actions on adipose tissues: to induce an insulin-like effect that stimulates adipogenesis and an anti-insulin-like effect to induce lipolysis (Moller *et al.*, 1999). The regulation of adipocyte differentiation and function by GH mediated signalling involves PPAR $\gamma$  and C/EBP $\alpha$  (Richter *et al.*, 2003; Floyed *et al.* 2007). In young rodents the lack of STAT5 or GHR causes weight loss from the epididymal fat pads, while in the mature subject this affects accumulation of subcutaneous fat (Aubert *et al.*, 1999; Lichanska and Waters, 2008). In COS cells STAT5 plays a role in inhibition of PPAR $\alpha$  transcriptional activity stimulated by GH. Both STAT5 and PPAR $\gamma$  signalling cascade stimulation by GHR in preadipocytes induces differentiation into adipocytes (Aubert *et al.*, 1999).

The process of triglyceride breakdown into free fatty acids and glycerol along with the release of energy inside the adipocyte is known as lipolysis (Figure 1.10)(Langin, 2006). GH is an important stimulator of lipolysis (Sakharova *et al.*, 2008, Dietz and Schwartz, 1991) causing the breakdown of fat, thus reducing the mass of adipose tissue by the activation of hormone-sensitive lipase (HSL) (Dietz and Schwartz, 1991; Asada *et al.*, 2000).

GH acts together with adrenergic catecholamines (Kamel *et al.*, 2000) released from the hypothalamus to cause the phosphorylation of HSL, an effect mediated by cAMP-protein kinase A. Phosphorylated HSL is then translocated to the surface of lipid droplets which are then hydrolysed into FFAs and glycerol leading to increased fatty acid release to the blood (Vernon *et al.*, 1993; Yang *et al.*, 2004; Miyoshi *et al.*, 2008). Other factors play a critical role in regulating lipolysis, such as leptin, which is secreted by adipocytes and functions as an inhibitor of lipogenesis (Fruhbeck *et al.*, 1997; Ramsay, 2003) and adipokines, such as resistin, adiponectin and visfatin (Bouloumie *et al.*, 2005) that have the ability to regulate fat metabolism, energy balance and insulin sensitivity (Trayhurn *et al.*, 2006).

**“This image has been removed by the author for copyright reasons”.**

**Figure 1.10 Lipogenesis/lipolysis.**

The balance between lipogenesis and lipolysis. To view image see Kahn and Flier, 2000, J Clin Invest. 106: 473–481

## 1.4 Objectives

The primary objective of this study was to increase the understanding of those mechanisms which allow GH to regulate the function of adipocytes. Secondary objectives were to provide a unifying framework and to validate objective through experimentation. Therefore, the first part of this study was to determine if 3T3-L1 cells are a suitable model for this study of pre-adipocyte differentiation under this protocol. The second part of the study was to determine the level of GHR during differentiation and observe GH-activated cell signalling pathways at various time points as the 3T3-L1 cell line progresses along the differentiation pathway. Results from Chapter 3 show that ERK activation declined as 3T3-L1 cells underwent differentiation. Therefore, the third part of this study was to find possible explanations as to why ERK declined. As the effect of the GH on adipocyte function is poorly understood, the study was broadened to observe the GH signalling pathways on primary mouse and human cell as they undergo differentiation.

## **Chapter Two**

### **The 3T3-L1 cell line as a model for the study of adipocyte differentiation**

## 2. Chapter Two

### 2.1 Introduction

#### 2.1.1 The 3T3-L1 cell line

Although cell lines had been originally developed by the zoologist Harrison earlier in 1907 (Walker and Rapley, 2008), those cell lines in use during the 1960s were not evolved according to any protocol that would ensure defined properties (Todaro and Green, 1963). Therefore, in 1963 Todaro and Green decided to develop a new approach that would allow any researcher to control both the inoculation density and frequency of transfer, thereby allowing the cell density to be regulated. With their strict protocol they succeeded in deriving stable cell lines which include the now ubiquitous 3T3-L1 cell line. Green then went on to develop the 3T3-L1 cell line as a model for adipose differentiation (Green and Kehinde, 1975).

3T3-L1 cells exhibit a fibroblast-like morphology that under appropriate incubation conditions are able to differentiate into adipocyte-like phenotypes. Once confluent the medium is replaced with a cocktail comprised of hormones and growth factors. When the cell morphology begins to change an increase in enzyme activity related to the metabolism of fat can be observed (Grimaldi *et al.*, 1978). A critical regulator of the transcriptional cascade that leads to adipogenesis is PPAR $\gamma$  (Grimaldi, 2001). PPAR $\gamma$  is the main target for the class of drugs known as thiazolidinediones (TZD) that are used to treat Type 2 diabetes. In addition to their use in adipogenesis and increasing insulin sensitivity they increase glucose uptake to mediate glucose homeostasis. By including a PPAR $\gamma$  agonist such as pioglitazone in the medium, adipocyte differentiation can be improved which allows for an increase in the synthesis and accumulation of triglycerides. Also, PPAR $\gamma$  expression can be used as the marker of the differentiation of pre-adipocytes cells into adipocytes.

The 3T3-L1 pre-adipocyte cell line can be used as an *in vitro* model of adipogenesis through the inducement of differentiation. In turn, the encouragement of differentiation reveals morphological changes that are characteristic of adipogenesis such as the appearance of vacuoles occupied with lipid (Rose *et al.*, 2002; Stephens and Pekala, 1992). A combination of phase contrast microscopy, cell staining and quantitative real time polymerase chain reaction (QPCR) were valid procedures for investigating the effect that physiological mediators had upon pre-adipocyte differentiation using the 3T3-L1 cell line.

### **2.1.2 The polymerase chain reaction**

The polymerase chain reaction (PCR) was invented in 1983 by Kerry Mullis and is one of the most widespread methods of analysing DNA (Bartlett and Stirling, 2003). The sole purpose of PCR is to amplify specific regions of a section of DNA. PCR produces several million copies of a gene which allows a template for sequencing. The first of three steps in a PCR is denaturation where the double stranded the DNA split to form two single strands of DNA molecules. Next is annealing of the primers which takes place. Finally, the extension is an ideal working temperature for the polymerase. This technique was further refined by Higuchi *et al.*, (Higuchi, 1993) to allow the real-time analysis of PCR product accumulation. This technique is also known as quantitative PCR (QPCR). The main advantage of QPCR over conventional PCR is that QPCR allows for the determination of the starting template copy number with a high level of accuracy and sensitivity across a broad dynamic range. QPCR is based on the relationship between the amount of the initial template and the threshold cycle (CT) value obtained during amplification. Also, as the QPCR reactions are run and evaluated within a closed-tube system the possibility for contamination is significantly reduced. Finally, this method is fast, easily automated and allows for the use of SYBR green. Also, samples can be analysed with any pair of primers for the detection of any product without the need to specify specific probes. QPCR allows the DNA to be measured after each cycle through the use of one of several fluorescent markers.

Of the various QPCR techniques, the simplest uses the fluorescent dye, SYBR Green (Rasmussen *et al.*, 1998). When the dye binds to the double stranded (ds) DNA the fluorescent signal increases proportionally to the quantity of dsDNA present. The starting quantity of the amplified target DNA molecule is inversely proportional to the Ct which is the cycle at which the fluorescent signal of the sample has increased above background fluorescence level. Ct is measured during the exponential phase of PCR when the amount of amplicon doubles each cycle. In QPCR samples with a higher initial concentration of template take less time to accumulate a threshold concentration and have a lower Ct value than a template with a lower starting concentration.

Absolute and relative quantification are the two methods used to present quantitative gene expression. Absolute quantification calculates the copy number of the gene usually by relating the PCR signal to a standard curve; whereas relative gene expression presents the data of the gene relative to some calibration or internal control gene. The selection and optimization of the reference housekeeping gene is an extremely important step in the development of QPCR assay. For many genes, expression levels alter significantly from gene to gene or cell to cell. An internal control gene are the transcription of such genes should not be affected by experimental conditions. The housekeeping gene used as an internal standard and the transcription of such genes is used for the normalization of gene expression data. QPCR is used to look at expression levels of adipocyte differentiation markers in 3T3-L1 cells undergoing differentiation. The cytosolic enzyme glycerol-3-phosphate dehydrogenase (GPDH) catalyse the conversion of dihydroxyacetone phosphate (DHAP) to glycerol 3-phosphate as part of the process of triglyceride synthesis in adipose tissue. The level of this enzyme has been shown to increase in cells during the later stages of adipocyte differentiation (Wise and Green, 1979; Sottile and Seuwen, 2001) and as such is a useful late stage differentiation marker. Additionally, PPAR $\gamma$  expression is up-regulated in cells undergoing adipocyte differentiation (section 1.3.2) and can also be used as a differentiation marker.

### **2.1.3 Oil Red O staining**

Lipids within tissues are difficult to stain as they are un-reactive and possess only a limited number of sites where molecules from a stain can bind. Also, as lipids are leached out during routine procedures by those solvents for staining, their presence is inferred by the absence from tissue. Furthermore, most lipid stains do not form covalent, ionic or hydrogen bonds with lipid components, therefore stains such as Oil Red O depend upon the preferential solubility of some chemicals. However, the advantages of Oil Red O are that it is inexpensive, simple and useful stain for revealing the presence of fat in 3T3-L1 cells during differentiation. Oil Red O is a fat-soluble diazo dye used to stain neutral triglycerides and lipids that allows the differentiation changes to become visible under microscopic observation based on the identification of cytoplasmic lipid. Differentiation was evaluated by measuring the lipid content by Oil Red O staining and expression of adipocyte differentiation markers. Special stains for neutral fats are often helpful in establishing the lipid content of cytoplasmic vacuoles as well as a diagnostic tool for the differentiation of 3T3-L1.

### **2.1.4 Aims**

The principle aim was to validate a differentiation method that would maximize the differentiation of the 3T3-L1 pre-adipocyte cell line into adipocytes using a combination of QPCR, phase contrast microscopy and cell staining. In addition, I wished to study the effect that the GH/GHR complex had upon cell signalling during 3T3-L1 cell differentiation while becoming familiar with these methods.

## **2.2 Materials and Methods**

### **2.2.1 Cell culture**

Culture procedures were carried out within an aseptic environment maintained in a laminar flow hood. All culture media and components were obtained from Lonza (Lonza Group, Basle, Switzerland) and tissue culture plates from Nunc (Fisher Scientific UK Ltd., Loughborough, UK).

#### **2.2.1.1 3T3-L1 cell culture medium**

3T3-L1 cells were obtained from American Type Culture Collection (ATCC). The medium was Dulbecco's Modified Eagle Medium (DMEM) with 4.5 g/l glucose, L-glutamine without sodium pyruvate, supplemented with 10% calf serum and antibiotics with a final concentration of 100 µg/ml penicillin, 100 µg/ml streptomycin and 2.5 µg/ml fungizone. The cultures grew as a monolayer and were maintained in an incubator at 37°C in a humidified atmosphere of 5% CO<sub>2</sub> in air.

#### **2.2.1.2 Trypsinization of cell cultures**

3T3-L1 cultures were trypsinized at 70-80% confluence, to avoid spontaneous differentiation. Culture medium was aspirated and the monolayers washed twice with 5 ml Hank's Balanced Salt Solution (HBSS) with phenol red without Ca<sup>2+</sup> or Mg<sup>2+</sup>. Trypsin (0.05% w/v in HBSS), 5 ml per 75 cm<sup>2</sup> flask culture cell was added until they detached from the plate aided by manual agitation. Trypsin was removed and the flask washed with 5 ml complete medium (section 2.2.1.1) then added to 5 ml trypsin to remove the cells. The cell suspension was centrifuged at 1000 rpm (Sanyo, MSE, Fisons, UK) for 5 minutes at room temperature. The supernatant was removed and the cell pellet re-suspended in 5 ml of culture medium (section 2.2.1.1) pre-warmed to 37°C. Cells were counted using a haemocytometer (Weber Scientific International Ltd, Teddington, Middlesex, UK) and maintained by trypsinizing and plating at 1:5 dilution two times per week.

### 2.2.1.3 Freezing and thawing of cells

3T3-L1 cultures were trypsinized (section 2.2.1.2) then centrifuged for 5 minutes at 1000 rpm at room temperature. The supernatant was aspirated and the pellet was re-suspended at  $1 \times 10^6$  cells/ml in chilled 10% Dimethylsulfoxide (DMSO) in FCS then aliquot into 1 ml sterile cryo vials. Cells were cooled at a controlled rate to  $-85^{\circ}\text{C}$  using a Nalgene Cryo 1 C container. The following day cells were transferred into liquid nitrogen until required. Cells were quickly thawed under warm tap water and transferred to 10 ml culture medium, centrifuged at 1000 rpm for 5 minutes supernatant removed. Pellet was re-suspended in 5 ml of culture medium and cell suspension transferred to a  $25 \text{ cm}^2$  tissue culture flask. After 24 hours of incubation, the medium was removed by aspiration and replaced with 5 ml fresh culture medium. These cells were then trypsinized until 70-80% confluent.

### 2.2.1.4 Differentiation of 3T3-L1

In order to induce adipocyte differentiation the pre-adipocyte 3T3-L1 cells were changed to differentiation medium (Table 2.1) (Zhang *et al.*, 2006) when the cells became confluent. The differentiation medium comprised a 1:1 mix of DMEM and Ham's F12 supplemented with 5% FCS and a cocktail of supplements (Table 2.1).

**Table 2.1: Components of the differentiation medium**

Components	Final concentration
Biotin	33 $\mu\text{M}$
Pantothenic acid	17 $\mu\text{M}$
T3	1 nM
Hydrocortisone	1 $\mu\text{M}$
Pioglitazone	1 $\mu\text{M}$
Insulin	500 nM

### **2.2.1.5 Oil Red O staining**

The degree of adipocyte differentiation was calculated by staining the cells with Oil Red O (Sigma-Aldrich, Saint Louis, MO, USA). Prior to use, 3 ml Oil Red O solution was mixed with 2 ml distilled water and left at room temperature for 5-10 minutes, the solution was then filtered with Whatman filter paper (Whatman Ltd, Maidstone, Kent, UK) and used within one hour. The volumes stated below are for cells in a 12 well plate. Cells were carefully washed twice in 1 ml phosphate buffered saline (PBS) before fixing in 1 ml 60% isopropanol for 10 minutes, the cells were washed once with 1 ml PBS and 1 ml Oil Red O solution was added to the cells for 15 minutes, after which the background was cleared by rinsing in 1 ml 60% isopropanol and then 1 ml of water. A microscope was used to observe the lipid droplets which displayed a red colour.

## **2.2.2 QPCR analysis of gene expression**

### **2.2.2.1 Extraction RNA of 3T3-L1 cells**

Quality RNA is necessary for QPCR analysis as RNA is susceptible to degradation by RNAses. RNA was extracted using the Absolutely RNA RT-PCR Miniprep kit (Stratagene, La Jolla, CA, USA) according to the manufacture's instructions which included a DNase treatment step to eliminate genomic DNA contamination. RNA was quantified by spectrophotometric measurement (Gene Quant pro RNA/DNA calculator Biochrom Ltd, Cambridge, UK) at 260 and 280 nm. The quality of the RNA was assessed by the ratio of optical density 260/280 nm. Pure RNA solutions have 260/280 ratio of 2.0 whereas ratios less than this indicates contamination by protein or phenol. Electrophoresis in 1% agarose gel (Melford Laboratories Ltd., Ipswich, UK) in 1x TAE shows the spectrum of RNA sizes (Figure 2.1) including 28s and 18s ribosomal RNA, and illustrates the integrity of the RNA.

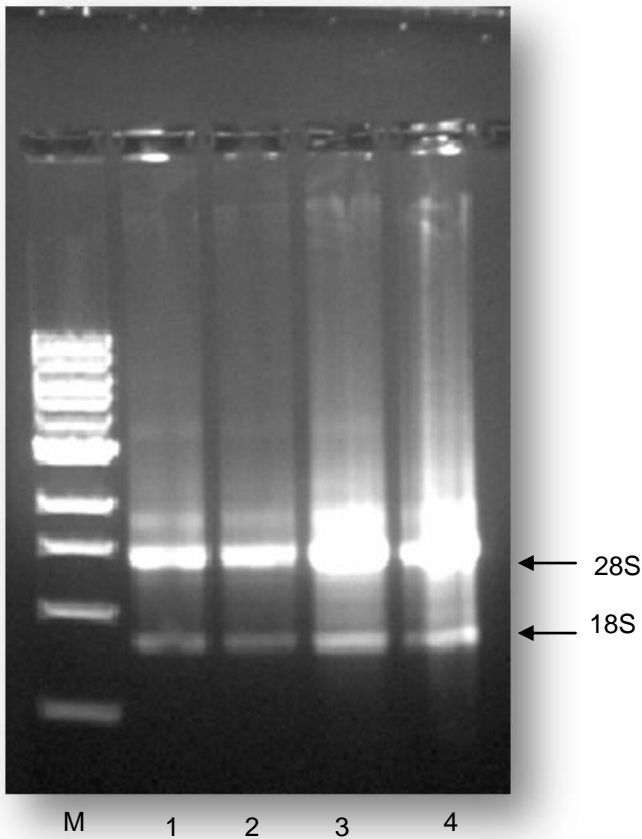


**Figure 2.1: 1% Agarose gel electrophoresis**

Agarose gel electrophoresis (1%) in 1 x TAE which shows the separation of the RNA sizes. Lane M: DNA 1Kb ladder, Lanes 1 through 4: which contains the RNA products, shows 28S and 18S RNA.

### 2.2.2.2 Reverse transcription

RNA was reverse transcribed to cDNA to provide a QPCR template. Prior to reverse transcription the RNA 1 µg/µl then 1 µl was added to 6.5 µl water and denatured by heating at 65°C for 10 minutes. RT requires primers for cDNA synthesis which binds to the poly A tail at the 3' terminus of mRNA forming the necessary double strand to initiate synthesis. 5 µl oligo deoxythymidine primer (ODT) 100 µg/ml (Promega, Madison, WI, USA), 1 µl RNase inhibitor 8 µg/µl (Promega), 5 µl deoxyribonucleotide triphosphate dNTP 10 mM (Promega), 2 µl Moloney Murine Leukemia Virus Reverse Transcriptase MMLV RT (Promega); 6 µl 5 x reverse transcriptase buffer (Promega) and 3.5 µl distilled water were added sequentially to the tube. To maintain a final reaction volume of 30 µl the ratio of RNA to water was inversely proportional, incubated at 37°C for 1 hour then heat treated to stop the reaction at 95°C for 10 minutes. The cDNA was stored at -20°C prior to QPCR analysis.

### 2.2.2.3 QPCR reaction

QPCR reaction was performed using Mx3000P™ (Stratagene Corp, La Jolla, CA, USA). The QPCR primers were designed using primer 3 software (<http://frodo.wi.mit.edu/primer3/>). Primers of 20 bases were chosen to ideally give a QPCR product in the 70-150bp range. The specificity of the resulting primers was checked against known DNA sequences using the Basic Local Alignment Search Tool (BLAST) (<http://blast.ncbi.nlm.nih.gov/Blast.cgi>). The primers were obtained from Invitrogen and used at a final concentration of 500 nM. The primers for the PPAR $\gamma$ , GPDH and acidic ribosomal phosphoprotein (ARP) (Zhang *et al.*, 2009) QPCR assays are detailed (Table 2.2).

**Table 2.2: QPCR primers**

QPCR primers PPAR $\gamma$ , GPDH and ARP along with amplicon size.

<b>PPAR<math>\gamma</math></b>		
Forward	Reverse	Amplicon size
TTTTCAAGGGTGCCAGTTTC Exon 6	AATCCTTGGCCCTCTGAGAT Exon 6	220bp
<b>ARP</b>		
Forward	Reverse	Amplicon size
GAGGAATCAGATGAGGATATGGGA Exon 7	AAGCAGGCTGACTTGGTTGC Exon 7	72bp
<b>GPDH</b>		
Forward	Reverse	Amplicon size
ATGCTCGCCACAGAATCCACAC Exon 8	AATCCTTGGCCCTCTGAGAT Exon 8	124bp

QPCR master mix for each reaction was a mixture of 9  $\mu$ l H<sub>2</sub>O, 12.5  $\mu$ l of master mix (Invitrogen Platinum SYBR Green QPCR super mix-UDG), 1.25  $\mu$ l of forward and 1.25  $\mu$ l of reverse primers that were combined in the order described above. The first well on the plate was filled only with distilled water which will act as a negative control, the second well on the plate was filled with 24  $\mu$ l master mix along with 1  $\mu$ l distilled water as no template control (NTC), while remaining wells were filled with 24  $\mu$ l of master mix and target gene 1  $\mu$ l cDNA. QPCR assay was heated to between 94-95°C 2 minutes to allow the cDNA to completely denature and then reduced temperature to allow the primers anneal to the template. Next a 40 cycle amplification phase at 95°C for 15 seconds then 60°C for 30 seconds and extension

primer at 72°C. The fluorescent signal was measured for each well at the end of each cycle followed by the melt curve analysis. Temperature was held at 95°C for one minute then 55°C for 30 seconds to allow PCR product to anneal. As the temperature increased toward 95°C the fluorescent signal was measured to determine at what point the PCR product melted. ARP was the housekeeping gene (Zhang *et al.*, 2009). PPAR $\gamma$  and GPDH gene expression levels were analysed by comparison with ARP gene expression using the MxPro software Mx3000 (Stratagene) and expressed relative to the appropriate control sample, usually day 0.

#### **2.2.2.3.1 Agarose gel electrophoresis analysis of QPCR product**

QPCR products were analysed in a 2% agarose gel containing 400 ng/ml ethidium bromide (Promega) was prepared in 1x TAE buffer, (50x TAE, 242 g Tris, 100 ml EDTA [50 mM, pH 8] and 57.1 ml glacial acetic acid, 1 M); the same concentration of ethidium bromide was maintained in TAE. The product containing 5  $\mu$ l PCR and 2  $\mu$ l loading buffer (Promega) loaded into each well while 5  $\mu$ l DNA ladder (Promega) and 2  $\mu$ l buffer were loaded into the first well. Each PCR product was compared against a 100bp DNA ladder to confirm the size of the amplicon.

#### **2.2.2.4 DNA Sequencing**

The QPCR product was sequenced to confirm the identity.

##### **2.2.2.4.1 DNA purification**

QPCR purity was achieved using Wizard SV gel and PCR clean-up system (Promega). QPCR products were purified using equal volumes of membrane binding solution to the reaction. Samples were transferred to SV Minicolumn placed on fresh 2 ml collection tube and incubated for 1 minute at room temperature. Tubes were centrifuged at 14,000 rpm for 1 minute and liquid discarded. SV Minicolumn was washed with 700  $\mu$ l ethanol centrifuged at 14,000 rpm for 1 minute. Column was washed a second time with 500  $\mu$ l then transferred to a new 1.5 ml tube. DNA was eluted in 20  $\mu$ l of Nuclease-free water then stored at 4°C.

##### **2.2.2.4.2 Agarose gel electrophoresis analysis of purified QPCR product**

QPCR purity was verified by agarose gel as described earlier (section 2.2.3 1).

##### **2.2.2.4.3 Sequencing**

Each sequence reaction contained 2  $\mu$ l Big Dye Terminator Cycle Sequencing Ready Reaction mix (Life Technologies, Grand Island, NY, USA), 1  $\mu$ l forward and reverse primers PPAR $\gamma$ , GPDH (10 pmol/ $\mu$ l) (Table 2.2), approximately 25 ng (typically 5  $\mu$ l) of purified QPCR product as quantified by comparison with 100bp DNA ladder on an agarose gel then made up to 10  $\mu$ l with H<sub>2</sub>O. Sequencing reactions were run on a Genius (Bibby Scientific Limited, Staffordshire, UK) PCR machine (Table 2.3).

**Table 2.3: Program used for Sequencing**

The number of cycles, temperature and times used in the program for PPAR $\gamma$  and GPDH.

Number of cycles	Temperature °C	Time
1	96	2 min
30	96	30 sec
	60	4 min

#### **2.2.2.4.4 Sodium acetate precipitation**

Prior to sequencing, the QPCR product was precipitated. 1  $\mu$ l of 3 M sodium acetate (pH 5.2) and 30  $\mu$ l of absolute ethanol was added to each 10  $\mu$ l sample to be sequenced then vortexed and incubated at room temperature for 10 minutes. Samples were centrifuged for 30 minutes at 13,000 rpm, the supernatant was discarded and the pellet washed with 500  $\mu$ l of 70% ethanol. The supernatant was discarded and samples were air dried before re-suspension and analysis on an ABI 3100 Genetic Analyser.

#### **2.2.3 Statistical analysis**

Data was expressed as the mean  $\pm$  SE. The ANOVA Statistical programme was used to examine differences between control and treated groups with post hoc analysis using the Student-Newman-Keuls test to examine differences among various groups.

## **2.3 Results**

### **2.3.1 Morphology of 3T3-L1 during differentiation**

During incubation in differentiation medium 3T3-L1 cells underwent morphological changes that are characteristic of conversion from a fibroblast to an adipocyte. Undifferentiated 3T3-L1 cells have the appearance of fibroblasts with an elongated shape (Figure 2.2 A+B). Whereas the cells cultured in differentiation medium (section 2.2.5) appear to have a morphology more typical of mature adipocyte cells at day 8 where they appear as very rounded and with extensive lipid droplet accumulation in approximately 80% of the 3T3-L1 cells (Figure 2.2 C+D).

### **2.3.2 Oil Red O of 3T3-L1 during differentiation**

3T3-L1 cells which underwent adipogenic differentiation were stained with Oil Red O to allow the visualization of the lipid droplets (see Figure 2.2). No Oil Red O staining was detected during day 0 (see Figure 2.2 B), however after 8 days in differentiation medium approximately 70-80% of the cells were observed to contain Oil Red O stained lipid droplets (Figure 2.2 D).

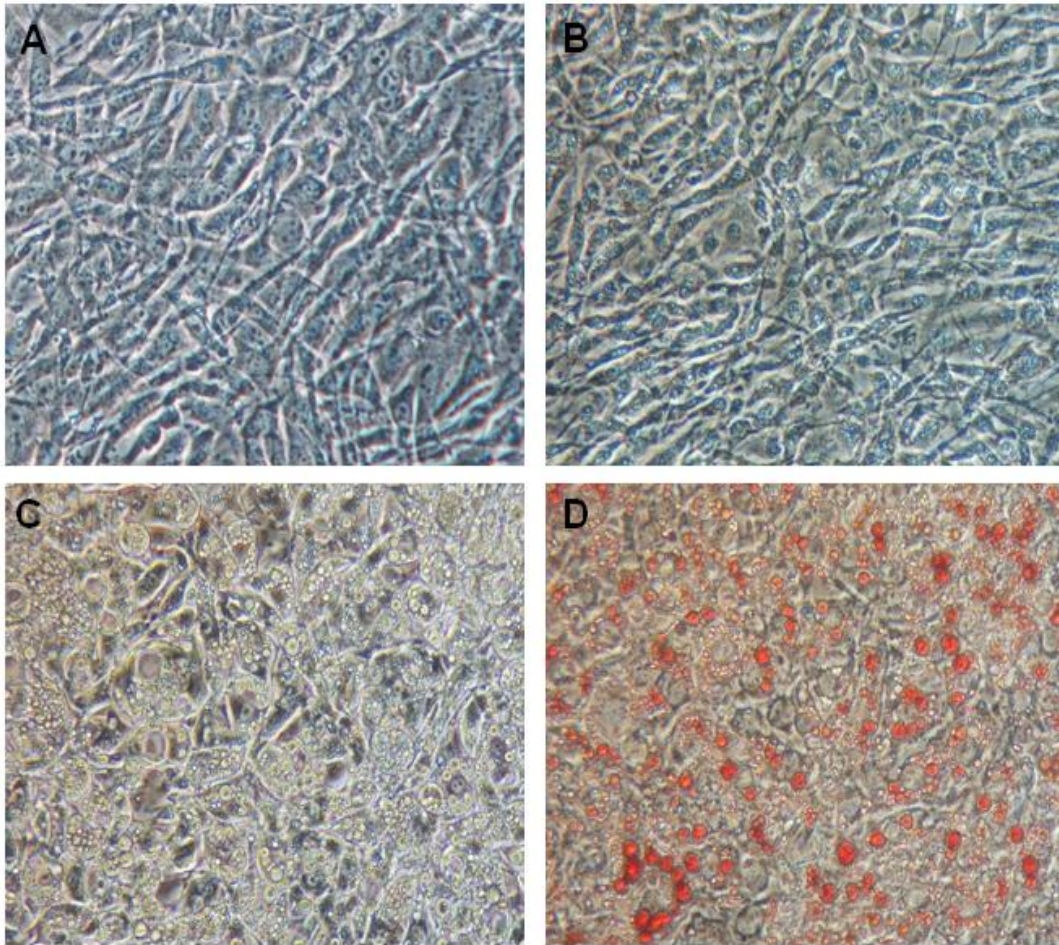


**Figure 2.2: Phase contrast photomicrograph stages of adipocyte differentiation**

(A) Undifferentiated cells day 0 (C) after 8 days in differentiation medium. (B) Undifferentiated Oil Red O stained cells day 0 (D) after 8 days in differentiation medium. After 8 days lipid droplet accumulation in differentiated cells is clearly visible in 70-80% of the cells. Magnification 100x.

### 2.3.3 Validation of QPCR assays

In order to confirm that the QPCR assay performed correctly the experimental data was validated by confirming that: (a) gel electrophoresis was a single product of the appropriate size, (b) there was a single peak for the melt curve, (c) the reaction efficiency through the analyse of serial 10 fold dilutions which contained pooled cDNA sample and (d) the identity of the DNA sequencing product.

### 2.3.3.1 Validation of the ARP assay

Agarose gel electrophoresis and melt curve analysis (Figures 2.3 and 2.4B) confirmed that the ARP assay produced a single PCR product of 71bp. Analysis of serial 10 fold dilutions of pooled cDNA (Figure 2.4A) determined the efficiency of the assay. This was calculated from the Ct slope plotted against the initial cDNA concentration where the undiluted pool was defined using the MxPro software (Stratagene). This technique determined the ARP efficiency to be 97.9%. As ARP was intended to be use as the housekeeping gene it must be expressed at relatively high levels and be unaltered through experimental procedures. ARP when amplified with Ct value in the range of cycle 15-16 thereby was unaltered by the state of the differentiation (Figure 2.5), which confirmed that ARP was a suitable housekeeping gene for studies which look at differentiation of 3T3-L1. The intra assay coefficient of variation for the APP QPCR assay was 3.2%. This was typical for all QPCR assays, none having an intra assay CV of greater than 5%.

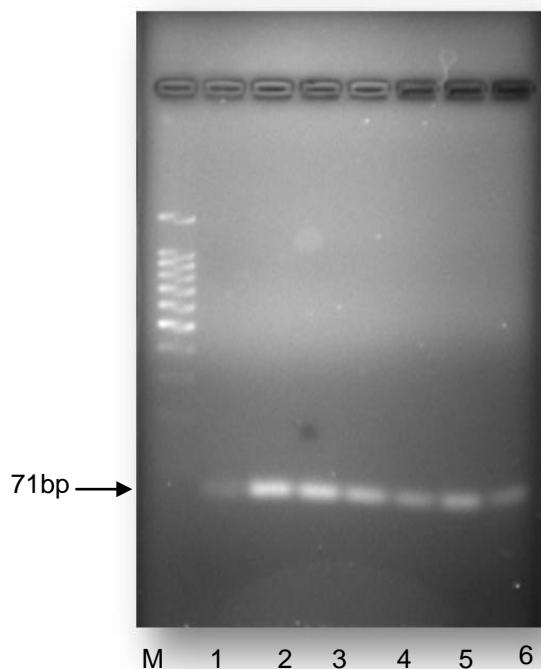


**Figure 2.3: ARP QPCR product**

Agarose gel (2%) electrophoresis in 1x TAE shows the ARP product. Lane M: DNA 100bp ladder, lane 1: no template control and lanes 2 through 6: These contain the ARP QPCR products. The size of amplicon was 71bp.

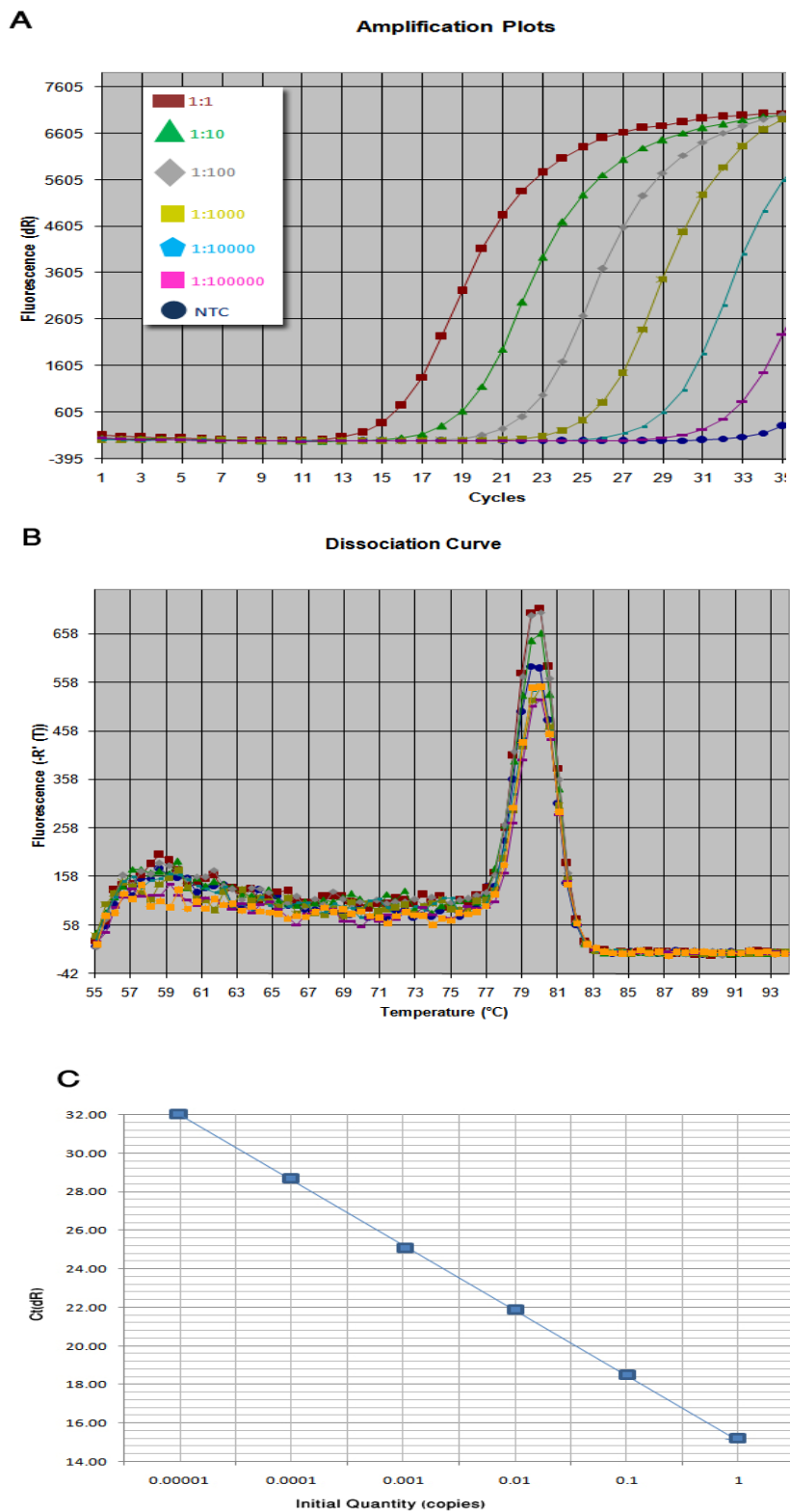


**Figure 2.4: QPCR analysis of ARP**

QPCR analysis of ARP which shows (A) amplification plots along with (B) the melt curve analysis which plots serial dilutions of pooled 3T3-L1 cDNA from 1:1 to 1:100,000 that were used to calculate a plot of Ct vs. initial starting dilution (C), the slope which gives the efficiency of the ARP QPCR assay of 97.9%.

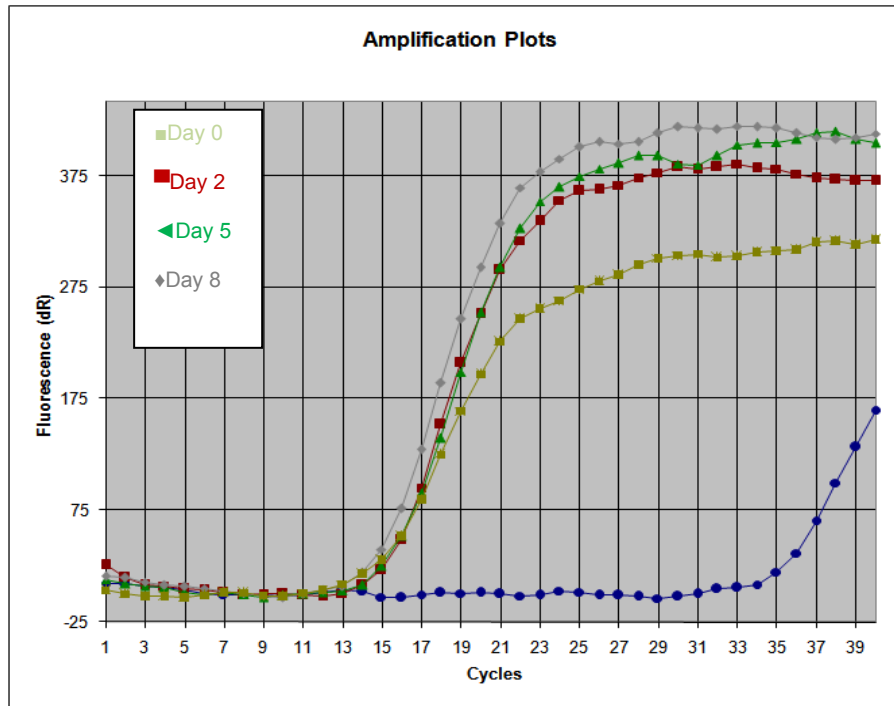


**Figure 2.5: ARP amplification plot**

Amplification plots show that ARP expression was unchanged during 3T3-L1 differentiation. Cells by length of time in differentiation medium (Table 2.4).

**Table 2.4: ARP Ct values**

Ct values for the ARP QPCR assays during 3T3-L1 adipogenic differentiation for days 0 to 8 show unaltered of Ct values.

	Ct value			
	0 days	2 days	5 days	8 days
<b>ARP</b>	16.7	16.61	16.25	16.80

### 2.3.3.2 Validation of the PPAR $\gamma$ assay

Agarose gel electrophoresis (Figure 2.6) along with melt curve analysis (Figure 2.7B) confirmed that the PPAR $\gamma$  assay produced a single PCR product of the correct size 220bp. Analysis of serial 10 fold dilutions of pooled cDNA (Figure 2.7A) was used to determine the efficiency of the assay. This can be calculated from the slope of the line of Ct value plotted against initial cDNA concentration where the undiluted pool was defined as one using the MxPro software (Stratagene, La Jolla, CA, USA). This technique was used to determine the value of the PPAR $\gamma$  assay to be 97.9% efficiency. PPAR $\gamma$  was intended to be used as a maker gene of 3T3-L1 differentiation as results confirmed that the QPCR assay was appropriate to be used as detector of PPAR $\gamma$  expression.

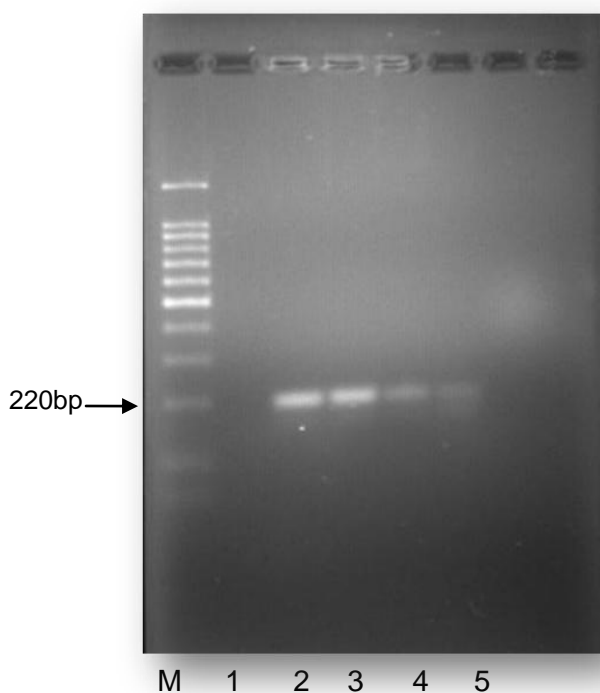


**Figure 2.6: PPAR $\gamma$  QPCR product**

Agarose gel electrophoresis (2%) in 1x TAE which shows confirmation of the sizes of the PPAR $\gamma$  QPCR product 220bp. Lane M: DNA 100bp ladder, lane 1: no template control and lanes: 2 through 5 which contain the amplified PCR products.

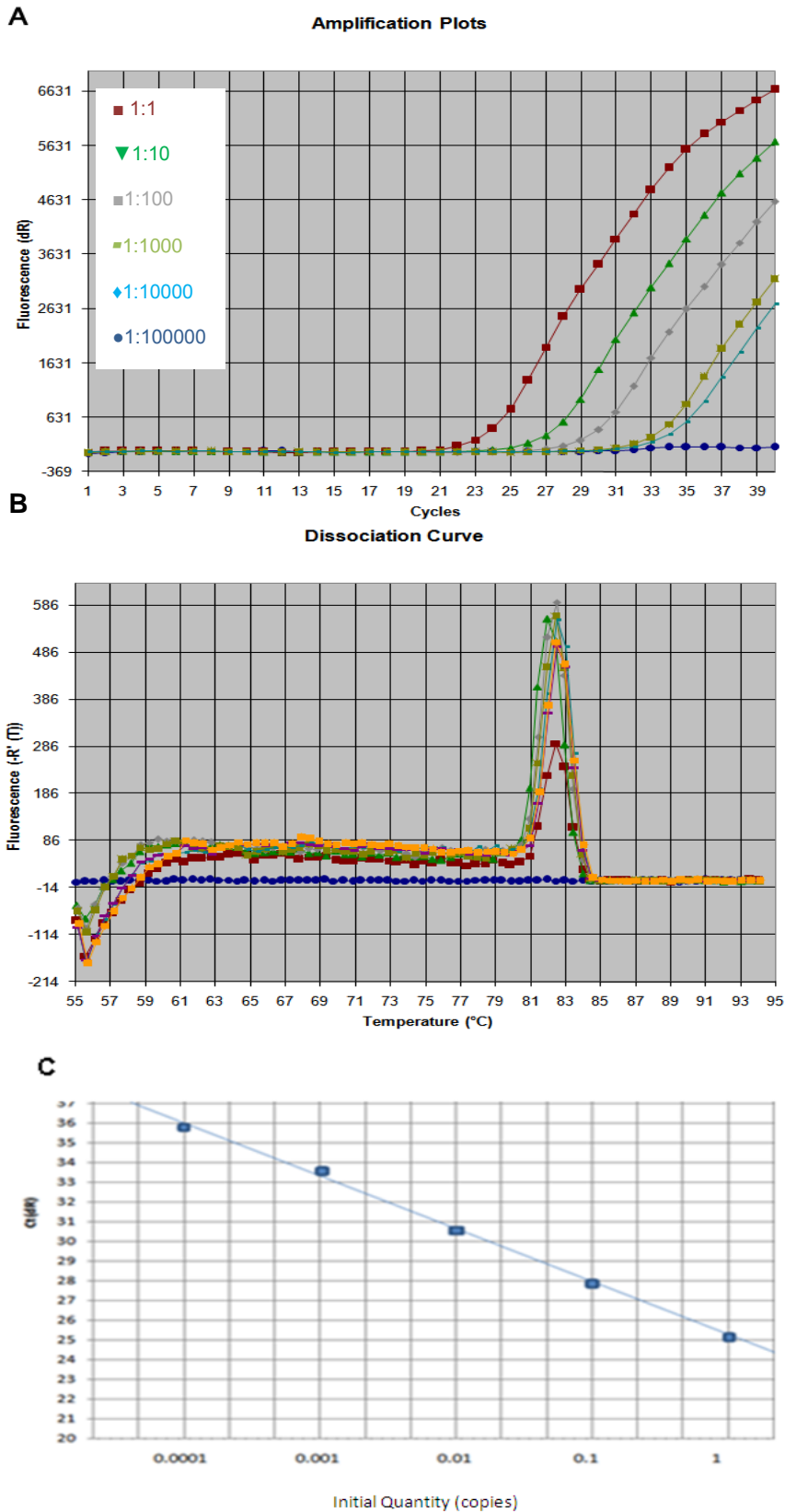


**Figure 2.7: PPAR $\gamma$  qPCR analysis**

Mention the results (A) cDNA from 1:1 to 1:10000 (B) which result in the melt peak curve analysis of the products and (C) the standard curve.

### 2.3.3.3 Validation of the GPDH assay

Agarose gel electrophoresis (Figure 2.8) along with melt curve analysis (Figure 2.9B) confirmed that the GPDH assay produced a single PCR product of the correct size 124bp. Analysis of serial 10 fold dilutions of pooled cDNA (see Figure 9A) was used to determine the efficiency of the assay which was found to be 105%. These results confirmed that the GPDH QPCR assay was an appropriate detector of GPDH expression.

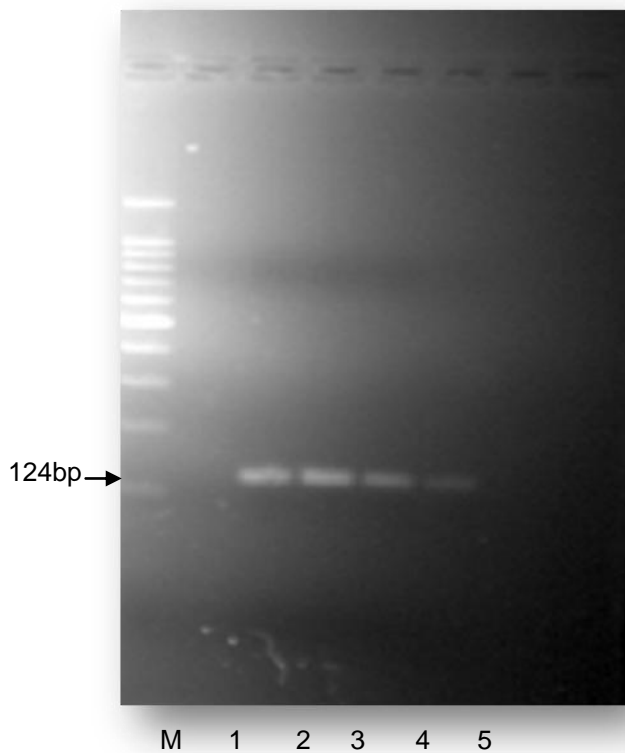


**Figure 2.8: GPDH QPCR product**

Agarose gel (2%) electrophoresis in 1x TAE which shows confirmation of the size of the GPDH QPCR product, 124bp. Lane M: DNA 100bp ladder, lane 1: no template control and lanes 2 through 5: contain the amplified PCR products.

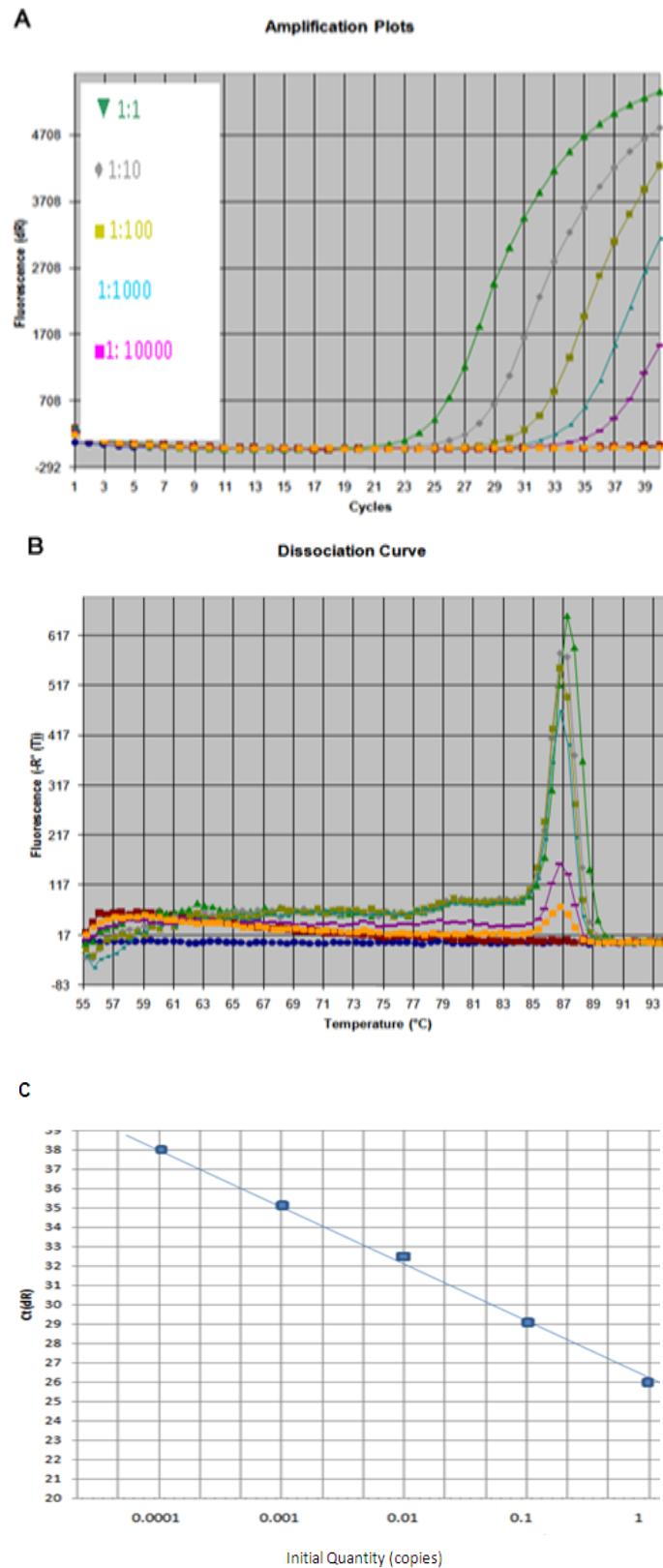


**Figure 2.9: GPDH QPCR analysis**

The results (A) cDNA from 1:1 to 1:10000 (B) which result in the melt peak curve analysis of the products and (C) the standard curve. QPCR products sequenced were matched.

### 2.3.3.4 PPAR $\gamma$ expression during 3T3-L1 cell differentiation

QPCR was used to determine PPAR $\gamma$  gene expression at 0, 2, 5 and 8 days after start of differentiation. PPAR $\gamma$  expression increased (Figure 2.10 and Table 2.5) with higher expression of PPAR $\gamma$  observed in differentiated cells at day 5 (mean  $\pm$  SE,  $7.68 \pm 1.346$   $P < 0.05$ ) and day 8 (mean  $\pm$  SE,  $11.73 \pm 3.11$   $P < 0.01$ ) compared to day 0, (mean  $\pm$  SE,  $n=4$  separate experiments). Analysis was way ANOVA post hoc test with Student-Newman-Keuls test (Figure 2.11).

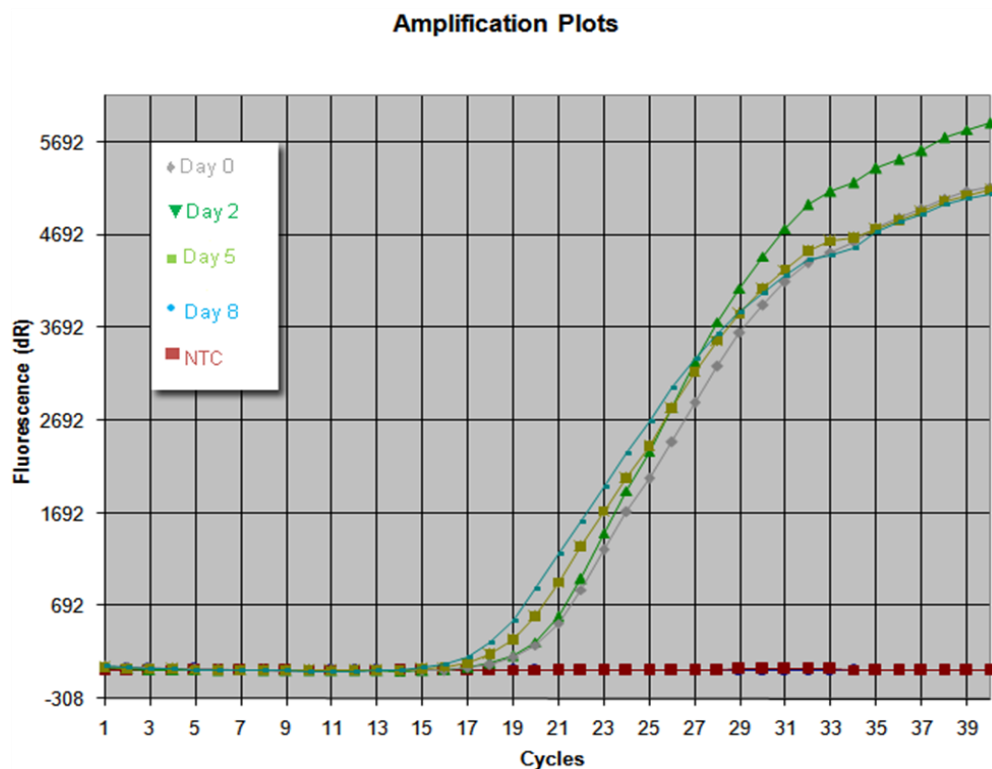


**Figure 2.10: PPAR $\gamma$  amplification curve**

PPAR $\gamma$  amplification curves at day 0, 2, 5 and 8 after the addition of differentiation medium. PPAR $\gamma$  expression increased during the 3T3-L1 differentiation.

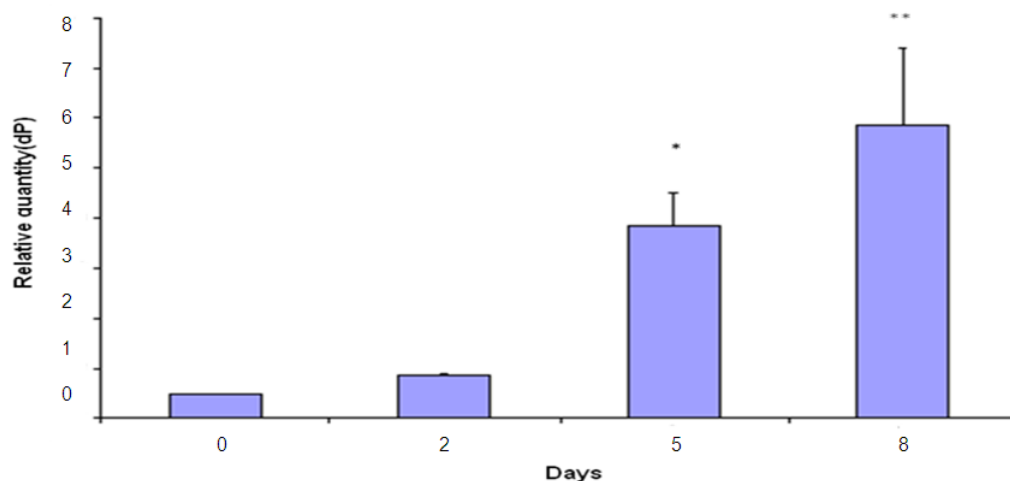


**Figure 2.11: PPAR $\gamma$  expression during 3T3-L1 differentiation**

QPCR analysis of PPAR $\gamma$  expression during 3T3-L1 differentiation shows increase of PPAR $\gamma$  at day 5 and day 8 with differentiation medium compared to control cultures day 0. \*  $P < 0.05$ , \*\*  $P < 0.01$  vs. control,  $n = 4$  separate experiments, ANOVA, post hoc analysis with Student-Newman-Keuls test.

**Table 2.5: PPAR $\gamma$  Ct values**

Ct values for PPAR $\gamma$  and ARP QPCR assays during 3T3-L1 adipogenic differentiation for days 0 to 8 shows increased the level of PPAR $\gamma$  expression, reduced the Ct value, minimum effect on ARP.

	Ct value			
	0 days	2 days	5 days	8 days
ARP	14.82	15.03	15.81	15.95
PPAR $\gamma$	21.74	21.76	20.23	19.99

### 2.3.3.5 Expression GPDH during 3T3-L1 differentiation

QPCR was used to determine GPDH gene expression at day 0, 2, 5 and 8 days after initiation of differentiation. GPDH expression was increased during the differentiation process (Figure 2.12 and Table 2.6) with significantly higher expression observed in differentiated cells at day 8,  $n = 4$  separate experiments.

### Amplification Plots

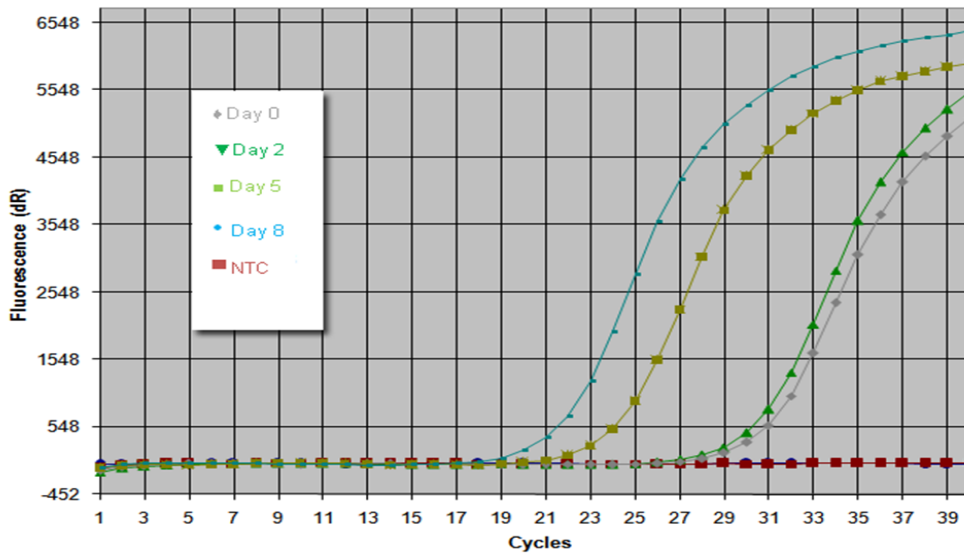


**Figure 2.12: GPDH amplification curve**

GPDH amplification curve shows at day 0, 2, 5 and 8. GPDH expression was increased during 3T3-L1 differentiation.

**Table 2.6: GPDH Ct values**

Ct values for the GPDH and ARP QPCR assays during 3T3-L1 adipogenic differentiation for days 0 to 8 shows differentiation increased level of GPDH which reduced Ct value, no effect on ARP.

	Ct value			
	0 days	2 days	5 days	8 days
<b>ARP</b>	14.82	15.03	15.81	15.95
<b>GPDH</b>	29.92	30.84	24.52	21.41

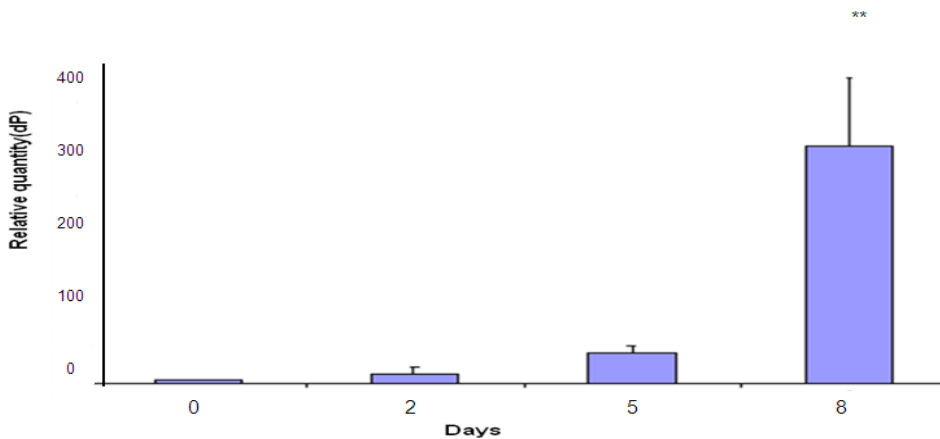


**Figure 2.13: GPDH expression during 3T3-L1 differentiation**

QPCR analysis of GPDH during 3T3-L1 differentiation shows significant increase of GPDH at day 8 compared to control day 0. \*\*  $P < 0.01$  vs. control cultures,  $n = 4$  separate experiments, ANOVA, post hoc analysis with Student-Newman-Keuls test.

### 2.3.3.6 Sequence of cDNA

The QPCR products sequenced were matched.

## 2.4 Discussion

Analysis of my results clearly demonstrates that I was able to validate a protocol that would maximize the differentiation of the 3T3-L1 pre-adipocyte cell line into adipocytes. This method was accomplished through a combination of phase contrast microscopy, cell staining and QPCR.

Since Todaro and Green's pioneering research in 1963 the 3T3-L1 cell line has played a central role in identifying specific transcriptional factors as well as numerous signal cascades that are responsible for the regulation of adipogenesis. Although the results from this chapter have built upon their work by demonstrating that the murine pre-adipocyte 3T3-L1 cell line can be induced to differentiate and is convenient for those studies, this is dependent upon the conditions of the cell culture. In addition, when the cell culture conditions are altered, the 3T3-L1 cell line can differentiate from fibroblast into an adipocyte which then acquires the ability to accumulate lipids (section 2.3.2).

Oil Red O was selected as this dye is generally fast and easy to use. However, this dye does require tissue fixation and more time to process (Listenberger and Brown 2007). Nevertheless, results clearly showed that after 8 days this dye was successfully absorbed by approximately 70-80% of the 3T3-L1 cells which allowed for the qualitative observation of lipid cells with a phase contrast microscope (section 2.3.2 and Figure 2.2D). The characteristic sign of Oil Red O staining and morphological changes of round cells with the manifestation of lipid droplets were detected during 3T3-L1 differentiation. Alternately, Nile Red dye could have been used. However, Nile Red dye ability to offer more quantitative results in difficult samples, its use where interaction with cellular membranes must be minimized or multiple labelling is required (Bonilla and Prelle, 1987).

Analysis of the QPCR confirmed that expression levels of adipocyte differentiation markers (Figure 2.4), PPAR $\gamma$  (Figure 2.10) and GPDH (Figure 2.12) increased when the cells were incubated in a differentiation medium. Also, GPDH as a marker of terminal differentiation appeared later than PPAR $\gamma$  with higher levels observed in differentiated cells only at day 8 while PPAR $\gamma$  showed significantly higher levels from day 5 (Figure 2.11). The combination of gel electrophoresis and analysis of melt curves when used together validated the QPCR assay (section 2.3.3.1.2). However, running a standard curve via serial-fold dilution of template DNA with SYBR Green fluorescent dye helped to verify the robustness of the QPCR assay.

Alternative markers to monitor adipocyte differentiation could include pref-1 for pre-adipocytes, LPL (Smas *et al.*, 1997; Smas *et al.*, 1998; Kim *et al.*, 2007), GLUT4 (Ferryhough *et al.*, 2007) and ALBP/aP2 (Marr *et al.*, 2006). Also, C/EBP  $\alpha$  and  $\beta$  also play early catalytic roles in the differentiation pathway and can be used as markers of the early phase of differentiation (Herrera *et al.*, 1989). Another alternative approach to measure adiponectin in culture medium using a commercial ELISA.

QPCR was used with SYBR green reporter to reveal the expression of differentiation markers and is identical in principle to PCR except that a fluorescent SYBR reporter molecule include in the reaction. Following the first use of SYBR Green for PCR in 1997, very little consideration has been given to the advancement of alternate dyes. The limitations of SYBR Green known such as limited dye stability, dye-dependent PCR inhibition and selective detection of amplicons. On the other hand, a distinct disadvantage of SYBR chemistry is its inherent non-specificity. SYBR dye will bind to all dsDNA molecules that is mean the fluorescent signal amplified non specific contaminating genomic DNA and primer dimmers. Alternately, EvaGreen dye is a green fluorescent nucleic acid dye with features that make the dye useful for QPCR. The DNA-bound dye has excitation and emission

spectra very close to those of SYBR Green, making the dye readily compatible with instruments equipped with the 488 nm argon laser or any visible light excitation with wavelength in the region. EvaGreen dye is extremely stable both thermally and hydrolytically, providing convenience during routine handling. EvaGreen dye is non-mutagenic and non-cytotoxic by being completely impermeable to cell membranes (Ohta *et al.*, 2001).

Absolute quantification expresses results as an absolute copy number where as relative quantification expresses results as a fold change relative to a reference point such as untreated cells with the advantage there is no need for a standard curve. However, the problem is that absolute quantification gives the concentration of transcript in terms of copy number by relating the QPCR signal to a standard curve, whereas the standard curve often uses a plasmid containing the sequence of the gene of interest. Therefore, sequence in cDNA and plasmid is not the same, while the proportion of a plasmid which contains the sequence of interest can increase the risk of contamination.

An optimized QPCR can be recognized as conforming to a linear standard curve, a high amplification efficiency and consistency across replicate reactions. To test whether or not the QPCR assay's were optimized serial dilutions of a template were run (section 2.3.3.1) and the results used to create a standard curve (Figure 2.4) that was plotted against the Ct value obtained during the amplification phase of each dilution. These graphs show an evenly spaced amplification curve with each amplification cycle almost doubling. In addition, the spacing of the fluorescence curves also show a linear progression. However, the simplicity of the QPCR method is that it is relatively easy to produce a result, effective quality control is necessary in order to create results which are dependable and meaningful. The principal variables regarding a QPCR reaction are contamination, amplification bias, poor efficiency and sensitivity.

An alternative technique for the analysis of protein marker expression would have been western blotting as this technique can identify specific proteins from a mixture or synthesized *in vitro* and can detect the size along with the expression of a protein. However, western blot is dependent on the quality of antibody that use to probe for protein of interest, and how specific it is for this protein. Western blotting is able to detect existence of a specific protein hiding amongst others, the state phosphorylation as well as measuring the PPAR $\gamma$  activation as a result of differentiation by using a high-quality antibody directed against the PPAR $\gamma$  protein (Zhang *et al.*, 2009). However, with respect to this study western blotting is slow in comparison to QPCR while the results are only semi quantitative. However, in this study agarose gel electrophoresis was used (section 2.3.3.1.3) which allowed the measurement amplicon size of PPAR $\gamma$  and GPDH as a result of differentiation (Figures 2.3, 2.6 and 2.8).

From these results it is clear that the murine pre-adipocyte 3T3-L1 cell line can be induced to differentiate and that induced differentiation is an appropriate model with which to study those changes in GHR signalling that are related to lineage specific differentiation.

## **Chapter Three**

**GH stimulated ERK and STAT5 activation  
during 3T3-L1 differentiation**

## 3. Chapter Three

### 3.1 Introduction

#### 3.1.1 GH signalling

GH has a variety of functions, including an important role in the regulation of adipose tissue biology (Nam and Lobie, 2000; Flint *et al.*, 2003; Ray *et al.*, 2012). The major isoform of human growth hormone is a peptide secreted from the pituitary gland of 191 amino acids with a molecular weight of 22kDa (Li *et al.*, 1969). The effects of GH on the tissues of the body are mediated via the cell surface growth hormone receptor (GHR).

Like GH, GHR is also a member of the cytokine receptor superfamily which as previously described (section 1.2.3) comprises an extracellular ligand-binding domain, a single transmembrane region and a cytosolic domain lacking intrinsic tyrosine kinase activity (Figure 3.1) (Uyttendaele *et al.*, 2007; Ma *et al.*, 2011). Each GH molecule has two receptor binding sites with the latest evidence suggesting that GH binding to the receptor induces a conformational change in a pre-existing receptor dimer (Lichanska and Waters, 2008). This causes the tyrosine kinase JAK2 that is associated with the each GHR cytoplasmic domain to come into close proximity to each other resulting in their trans-activation, leading to the phosphorylation of multiple tyrosine residues of the receptor cytoplasmic domain (Argetsinger *et al.*, 1993; Brown *et al.*, 2005). The resulting cytoplasmic domain phospho-tyrosines then act as docking points for proteins containing SH2 or PTB domains such as STAT5, Grb2, Sos and IRS-1 leading to the activation of multiple signalling pathways including p42/44 MAPK, also known as ERK and JAK2-STAT5 (Figure 3.2) and described in a review by Waters *et al.* (2006). These pathways regulate a variety of functions that result in the ability of GH to control growth and other metabolic processes.

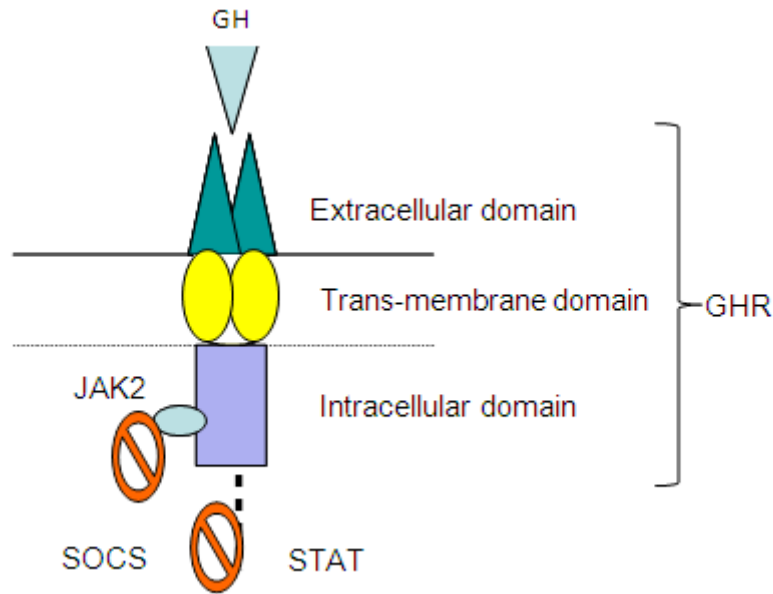


**Figure 3.1: GHR-associated JAK2**

This diagram shows the mechanism of GH. GH activates the GHR-associated JAK2 by phosphorylation (JAK2-P). This result in auto-phosphorylation and phosphorylation of the intracellular domain stimulating STAT. SCOS is also able to bind the GHR and may, therefore, block STAT5 and JAK2.

Of the GHR signalling pathways STAT5 is regarded as the most important mediator of the effects of GH. After GHR activation, STAT5 is phosphorylated by JAK2. Phosphorylated cytoplasmic STAT5 forms a homodimer via its phospho-tyrosine residues and translocates to the nucleus (Benekli *et al.*, 2003; Wang *et al.*, 2009). After nuclear translocation the STAT5 dimer binds to specific DNA sequences in the promoter region of its target genes where transcription starts. The most important of these in the case of longitudinal growth is the IGF-1 gene. STAT5 is implicated in the regulation of adipogenesis in other model systems (Richter *et al.*, 2003, Wang *et al.*, 2009; Stewart *et al.*, 2011). In differentiating 3T3-L1 cells STAT5 protein is directly regulated with both PPAR $\gamma$  and C/EBP $\alpha$  under a combination of different conditions (Stewart *et al.*, 2011).

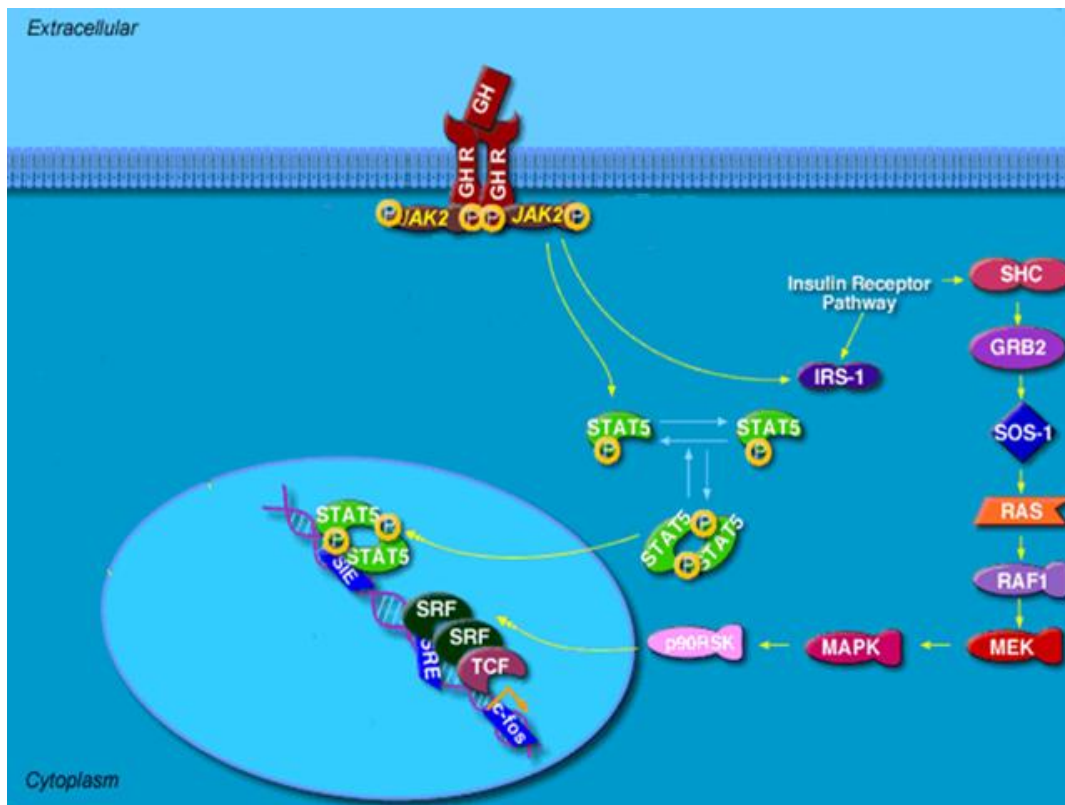


**Figure 3.2: GHR cell signalling**

Schematic drawing of cell Signalling via the GHR. (Adapted from [www.biocarta.com](http://www.biocarta.com)).

Activation of ERK via the GHR is regulated by a phosphorylation cascade from the cell membrane to the nucleus mediated through specific components such as Ras, Raf and MEK leading to ERK phosphorylation. ERK1 (p44) and ERK2 (p42) are widely expressed and involved in a range of functions (Johnson and Lapadat, 2002; Wang *et al.*, 2009). The role of ERK in the differentiation of adipocytes is complex and depends on many parameters (Bost *et al.*, 2005). ERK1 and ERK2 are essential for induction of mitotic clonal expansion that is an essential early step for the initiation of differentiation which is then followed by expression of genes that produce the adipocyte phenotype. Many contemporary studies argue that mitotic clonal expansion is not a required step for 3T3-L1 pre-adipocyte differentiation into adipocytes as inhibition of ERK1 and ERK2 activation abolishes mitotic clonal expansion, but does not prevent adipogenic differentiation (Qiu *et al.*, 2001, Tang *et al.*, 2003).

### 3.1.2 Western blotting

Western blot, also known as western immunoblotting or immunoblot, originated from Stanford University to visualise assay for antigens specific to monoclonal antibodies. Proteins exist in phosphorylated or non-phosphorylated states which distinguish between active and inactive forms allowing specific pathways to be located (Mandell, 2003). The proteins are separated depending on size using sodium dodecyl sulphate-polyacrylamide gel electrophoresis (SDS-PAGE). The protein is then transferred from the SDS-gel to a membrane, the blot, which is then incubated. A secondary antibody, such as horseradish peroxidase (HRP), is used to visualize the protein bands on the blot.

The 3T3-L1 cells were incubated with serum free DMEM medium at 37°C for 4 hours to ensure down regulation of the signalling pathways. Cells were treated with GH for 10 minutes as previous research by Lewis *et al.* determined that 10 minutes is the optimum time for GH regulated ERK and STAT5 (Lewis *et al.*, 2004). Additional research by Lewis *et al.*, examined the GHR-associated signalling pathways in mesenchymal stem cells (MSCs) derived from rat bone marrow stem cells (BMSCs) induced to differentiate (Lewis *et al.*, 2006). GH treatment activated STAT5 alone in undifferentiated BMSCs, but activated both STAT5 and the ERK pathway in adipocyte-differentiated stem cells. The level of GH induced ERK pathway activation increased in a time-dependent manner over a 7 day adipocyte differentiation period, therefore ERK activation may be particularly important in mediating the effects of GH on adipocyte function. Building upon the research by Lewis *et al.*, (2006) this study hypothesised that adipocyte differentiation modulates coupling of the GHR to activation of the ERK pathway. As Lewis *et al.* has argued that the profile of signal pathway activation differs with adipocyte differentiation this study will develop research by using the 3T3-L1 pre-adipocyte cell line.

## **3.2 Materials and Methods**

### **3.2.1 GH signalling during 3T3-L1 differentiation**

3T3-L1 cells were cultured as described previously (section 2.2.1.1), in 6 wells plates with 150,000 cell per well in 2 ml DMEM containing 10% calf serum. Once confluent, medium was changed (section 2.2.1.4) day 0 and cells were incubated for 2, 5 and 8 days. To study those pathways associated with the GHR at each time point, cells were treated with GH and studied using phospho-specific western blotting. The medium was removed and all cells were washed twice with 1 ml of PBS and 2 ml serum free DMEM was added. Cells were incubated for 2 hours at 37°C, the medium removed and 2 ml of serum free DMEM was added at 37°C for 2 hours. Recombinant human GH (50 nM, Genotropin, Pfizer, UK) was added to one well then incubated for 10 minutes at 37°C. The cells were then washed twice with 1 ml of ice cold PBS containing 1mM sodium orthovanadate (Sigma-Aldrich, Saint Louis, MO, USA) to preserve the phosphorylated proteins that inhibited endogenous phosphatases. Cells were lysed with 250 µl loading buffer without pyronin Y (Appendix 1) frozen in liquid nitrogen and stored at -20°C.

### **3.2.2 SDS–PAGE and western blotting**

The protein sample was heated with 2-mercaptoethanol reducing agent (Sigma-Aldrich, Sant Louis, Missouri, USA) and denatured with SDS (Fisher Scientific, Loughborough, UK). Proteins were separated by gel electrophoresis. The samples were loaded onto a polyacrylamide gel where 200v was applied causing smaller proteins to migrate more quickly as they were retarded less by the gel. After gel electrophoresis the bands were transferred onto a polyvinylidene fluoride membrane (PVDF, Hybond-P™) (GE Healthcare, Little Chalfont, Bucks, UK) for detection using specific antibodies and western blotting. The key processes are described below.

### **3.2.2.1 Cellular protein quantitation**

For the detection of differences in protein expression during the period of the cell differentiation to be meaningful, an equal amount of protein from each sample must be compared. The protein concentration of the cell lysates must be determined. The protein assay was performed with loading buffer without pyronin Y (Sigma, St Louis, MO, USA). To achieve this, samples were boiled for 5 minutes and centrifuged at 14,000 rpm for 5 minutes and 20  $\mu$ l of each cell lysate aliquotted into a 96 well microtitre plate. The standard curve of 1-20  $\mu$ g was prepared from a bovine serum albumin stock solution (Sigma) 1 mg/ml in loading buffer (Appendix 1) and the volume adjusted to 50  $\mu$ l with loading buffer. Subsequently 50  $\mu$ l of 60% trichloroacetic acid (Sigma-Aldrich, Saint Louis, MO, USA) was added to all of the wells and the plate incubated at room temperature for 30 minutes. This cocktail was measured by reading the absorbance at 630 nm in a plate reader (Dynex, Technologies Inc, Chantilly, VA, USA) and a standard curve was constructed allowing the protein concentrations for each cell sample to be calculated.

### **3.2.2.2 Gel preparation**

The mini-gel system from Bio Rad was used for all SDS-PAGE and electroblotting procedures. The running gel was prepared as described (Table 3.1). The acrylamide concentration, typically 8% or 10% was chosen according to the separation range required. The percentage of acrylamide to be used in the running gel depended on the size of the protein of interest. Gels of 10% were routinely used and have a useful separation range of 30-80 kDa. Proteins of greater than 80 kDa should be separated on an 8% or lower gel. A low percentage of acrylamide creates large pores that allowed for the separation of proteins that have a high molecular weight, whilst a higher percentage was used for gel having smaller sized pores suitable for the separation of the proteins that have a lower molecular weight.

Casting plates were washed with 100% ethanol and assembled on the casting stand. A running mixture of 7.0 ml for 1.5 mm gels was prepared (Table 3.1). Polymerization was initiated by ammonium persulfate in the presence of N,N,N',N'-tetramethylethylenediamine (TEMED) (Sigma-Aldrich), added to the mixture prior to pouring. Gel mix was poured into plates leaving space at the top for the stacking gel to be added. 1 ml water-saturated N-butanol was added on top of gel to exclude oxygen and allow polymerization of the acrylamide. When set, the N-butanol was removed by tipping the plates upside down then washed three times with water. Stacked gel mixture (Table 3.1) was added to the top of the running gel. Combs were placed, ensuring no air bubbles were under the comb fingers.

**Table 3.1: Components of SDS-PAGE**

SDS-PAGE running and stacking gel components. Volumes above are for 10 ml running gel and 10 ml stacking gel. \* APS is made up fresh and TEMED added immediately prior to use.

	10% running gel	8% running gel	Stacking gel 4%
30% acrylamide	3.3 ml	2.64 ml	1.3 ml
Water	2.92 ml	3.58 ml	6.1 ml
1M Tris (pH8.8)	3.75 ml	3,75 ml	-
0.5M Tris (pH 6.8)	-	-	2.5 ml
10% SDS	100 µl	100 µl	100 µl
10% ammonium persulfate (APS)*	100 µl	100 µl	100 µl
TEMED*	5 µl	5 µl	10 µl

The stacking gel allows the protein bands to concentrate prior to the running gel. Once set the combs were removed from the gels. If the samples were not already in loading buffer with pyronin Y, this would be added to the sample to final concentration of 0.2%. Samples were then boiled in water for 5 minutes then centrifuged for 5 minutes at 13,000 rpm. The molecular weight marker 10 µl pre-stained (7-175 kDa)(New England Biolabs, Ipswich, MA, USA) and samples which contained 20 µg protein were loaded into the wells and run through the gel at 200v for 30 minutes using a Tris-glycine running buffer (Appendix 1) until the tracking dye band had reached the bottom of the gel.

### **3.2.2.3 Western blot analysis of protein**

Protein transfer was achieved using Bio Rad Mini Transblot. PVDF membrane was cut to fit the gel 5 cm x 8 cm and pre-activated by briefly soaking in 100% methanol. After two rinses each lasting 5 minute in distilled H<sub>2</sub>O, the membrane and previously run SDS-PAGE gel were equilibrated in blotting buffer (Appendix 1) for 15 minutes by gently shaking. For each SDS-PAGE gel blot, two pieces of filter paper (5 cm x 8 cm) and two fibre pads were soaked in blotting buffer for 10 minutes to ensure no air was trapped in the fibre pad. The transfer sandwich comprised of a fibre pad on the black side of the transfer cassette, followed by filter paper, gel, membrane then filter paper. The stack was rolled to ensure good contact between gel and membrane and a fibre pad placed on top. The cassette was inserted into the tank containing pre-cooled blotting buffer and an ice pack to prevent overheating. Transfer was achieved by the application of a constant current of 350 mA for one hour while stirring.

### **3.2.2.4 Detection of specific proteins by immunoblotting**

All washes/incubations used an orbital shaker. After blotting the membrane was transferred and washed for 5 minutes in Tris buffered saline–tween (TBS-T). The membrane was blocked with 50 ml blocking buffer (Appendix 1) for 1 hour at room temperature then placed in a square Petri dish in 8 ml blocking buffer containing primary antibody at optimal dilution (Table 3.2). Membranes were incubated for 1 hour at room temperature or overnight at 4°C (Table 3.2). After incubation, primary antibody was removed and membrane washed three times for 5 minutes with 15 ml TBS-T. Secondary antibodies (GE Healthcare, Little Chalfont, Bucks, UK) were used at 1:5000 in 10 ml blocking buffer for 1 hour at room temperature. The membranes were then subjected to a series of washes with TBS-T these were: two brief 30 second washes, one 15 minute followed by three 5 minute washes.

**Table 3.2: Primary and secondary antibodies**

Antibodies for western blotting include primary anti-phospho-ERK, anti-phospho-STAT5, mix of anti-total ERK1/anti-total ERK2 and total anti-STAT5.

Antibodies ( Ab)	Species	Supplier	Dilution	Incubation
Primary anti-phospho-ERK	Mouse monoclonal	Cell Signalling Technology, Danvers, MA, USA	1:2000	4°C overnight (O/N)
Anti-phospho-STAT5	Mouse monoclonal	Millipore, Billerica, MA, USA	1:1000	4°C O/N
Mix of anti-total ERK1 and anti-total ERK2	Rabbit polyclonal	Santa Cruz, CA, USA	1:2000	1 hour at room temperature (RT)
Anti-STAT5	Rabbit polyclonal	Santa Cruz, CA, USA	1:500	1 RT

### 3.2.2.6 Detection of antibody–antigen complex

Immobilised protein labelled with HRP conjugate was detected via chemiluminescence (ECL Plus) (GE Healthcare, Little Chalfont, Bucks, UK) by exposing PVDF membrane with antigen–antibody to photographic film. After washing the membranes were removed from the TBS-T and any excess drained. ECL reagent was prepared (40:1 ratio of solution A: solution B) and 3 ml carefully pipetted onto the protein side of the membrane and incubated at room temperature for 5 minutes. Excess solution was drained before wrapping in Saran wrap (Dow Chemical Company) and placed into an autoradiography film cassette with the protein side up and developed in the darkroom. A sheet of film (Hyperflim™ ECL) (GE Healthcare, Little Chalfont, Bucks, UK) was placed on top of the membrane for 30 seconds to 10 minutes depending on signal strength. Exposed film was placed into the developer solution (Kodak D-19) (Kodak, Hemel Hempstead, Herts, UK) for 2 minutes, then briefly rinsed in water and placed in fixer (Kodak D-19) (Kodak, Hemel Hempstead, Herts, UK) for 5 minutes. Process was repeated with longer/shorter exposure times as needed. Developed film was washed with water for 15 minutes then dried. Film was aligned with blot and the position of the standards marked. The final films were analysed by imaging densitometry (Alpha Innotech Corp, San Leandro, CA, USA).

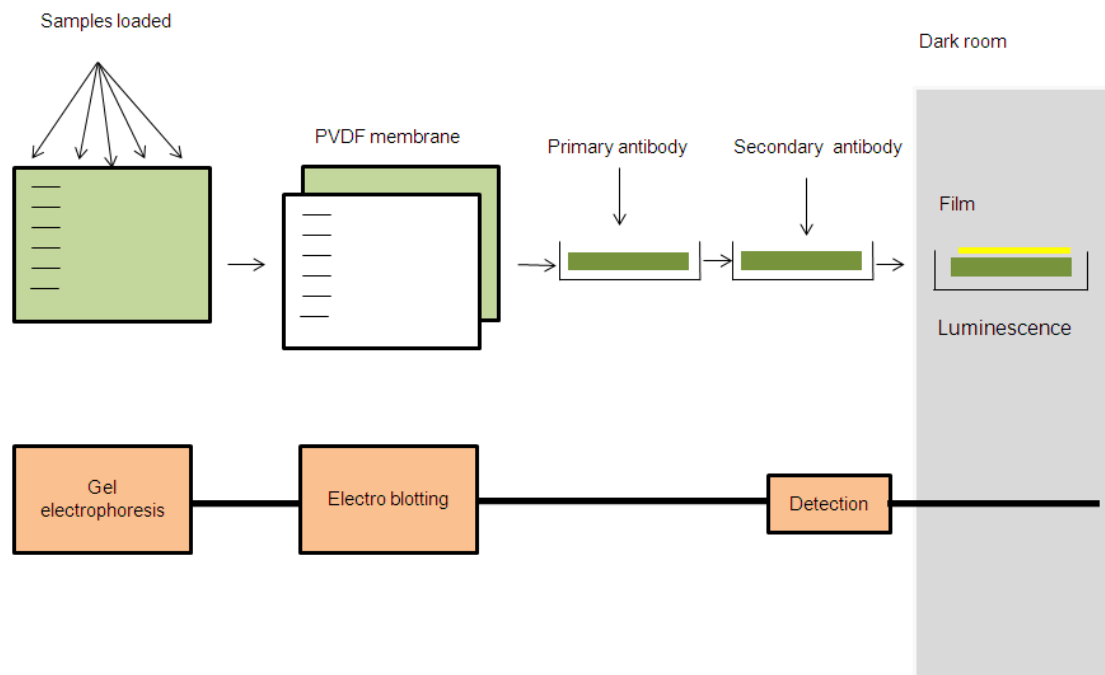


**Figure 3.3:** Western blotting schematic (Adapted from Rice, 2008).

### 3.2.2.7 Stripping and reprobing membrane

Membranes were reprobbed by stripping antibodies off the membrane which were then probed with a different antibody. If the blot dries out the membrane would be re-wetted with methanol for 30 seconds and washed three times 5 minutes with TBS-T, if still wet this step would be omitted. Blots were then incubated at 60°C with 50 ml pre-warmed stripping buffer for 30 minutes in a hybridization oven (GE Healthcare Life Sciences, Amersham Place, Little Chalfont, UK) with gentle mixing. After stripping, blots were washed three times for 10 minutes with 50 ml of TBS-T. These blots were blocked with blocking buffer for 1 hour at room temperature and were then ready for next primary antibody.

### 3.2.3 RNA extraction and QPCR

GHR expression was analysed using QPCR (section 2.2.6). RNA was extracted (section 2.2.6.2). Reverse transcribed mRNA (cDNA) provided the necessary DNA template for PCR amplification (section 2.2.6.3). The nuclear protein ARP was used as the housekeeping gene. Primers are detailed below (Table 3.2) were used at a final concentration of 500 nM. GHR expression was analysed by comparison with ARP expression using the MxPro software (Stratagene).

**Table 3.3: Primers of GHR and ARP**

Primers for QPCR analysis of GHR and ARP expression.

GHR		
Forward	Reverse	Amplicon size
CCATTCAAGCCACACAGCTA	CCTTGGGCTCTCACTTCTTG	103 bp
ARP		
Forward	Reverse	Amplicon size
GAGGAATCAGATGAGGATATGGGA	AAGCAGGCTGACTTGGTTGC	71 bp

#### 3.2.3.1 Agarose gel electrophoresis analysis of QPCR product

The QPCR product was verified by agarose gel electrophoresis as described earlier (section 2.2.6.3 1).

#### 3.2.3.2 Sequencing

Sequenced DNA was to confirm the identification of the QPCR product as described earlier (section 2.2.6.4) and primers which used (Table 3.3).

### 3.2.4 Statistical analysis

Statistical analysis was performed as described earlier (section 2.2.3).

## 3.3 Results

### 3.3.1 Basal ERK activation during 3T3-L1 differentiation

3T3-L1 cells were plated in 6 well plates at 150,000 cells/well (Nunc, Fisher Scientific, Bishop Meadow Road, Loughborough, UK) and once confluent were incubated with differentiation medium of day 0 until day 20. Medium was changed every two days. The 3T3-L1 cells were analysed over a time course when the medium was removed and cells were then washed twice with 1 ml of PBS. Cells were lysed with 250  $\mu$ l loading buffer and were rapidly frozen in liquid nitrogen before being stored at  $-20^{\circ}\text{C}$ . Basal ERK phosphorylation (activation) was detected by western blotting. The bands representing phospho-ERK1 (p44) and ERK2 (p42) are shown below (Figure 3.2). Basal ERK activation was influenced by the length of time in differentiation medium which observed high activation at day 0 and after that the level of activation of ERK declines rapidly with increased adipogenic differentiation to a level that is barely detectable by day 2. The appearance of the cells altered over the course of experiment changing from an elongated fibroblast shape into more rounded cells which can be seen from day 5. This is accompanied by an increase in lipid droplet accumulation, being seen in approximately 90% of the 3T3-L1 cells by day 8.

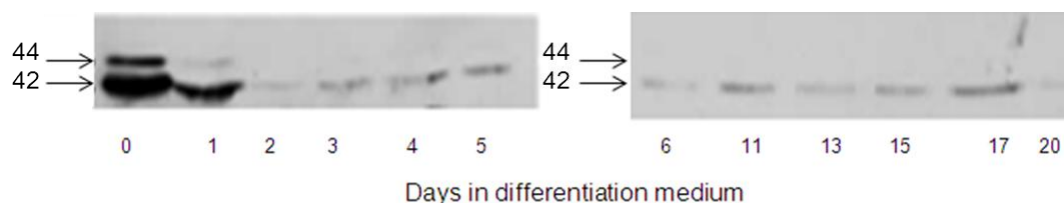


**Figure 3.4: Basal ERK activation**

Basal ERK activation during 3T3-L1 adipocyte differentiation.

### **3.3.2 GH stimulated ERK and STAT5 activation during 3T3-L1 differentiation**

3T3-L1 cells were plated and cultured (section 3.2.1). Those cells undergoing adipocyte differentiation from day 0 to day 8 were exposed to GH for 10 minutes at 50 nM then placed in loading buffer. ERK / STAT5 activation was detected by western blot with antibodies for phospho-ERK and STAT5 (Figure 3.3). GH-induced ERK activation in 3T3-L1 was high in undifferentiated cells, with high activation of ERK2 (p42) at day 0 after which the level of activation of ERK declines rapidly. In contrast, levels of total ERK1 (p44) and ERK2 (p42) show no change with increased adipogenic differentiation. In addition, GH-induced STAT5 activation increased during 3T3-L1 differentiation and total STAT5 increased with the time of differentiation. Densitometric analysis of the blots (Figure 3.4) confirmed that ERK activation by GH was maximal during the early days of differentiation, but was undetectable by day 8. Analysis of data revealed a significant reduction of GH-induced ERK activation at day 8 compared with day 0 of  $4.5\% \pm 1.7\%$  ( $p < 0.01$ ,  $n=4$ ) and that total ERK was unchanged. In contrast, GH-stimulated STAT5 phosphorylation was significantly increased in differentiated cells at day 8 compared with day 0 ( $734\% \pm 52\%$ ,  $p < 0.01$ ,  $n=4$ ), as was total STAT5  $4784\% \pm 1090\%$ ,  $p < 0.01$ ,  $n=4$ ).

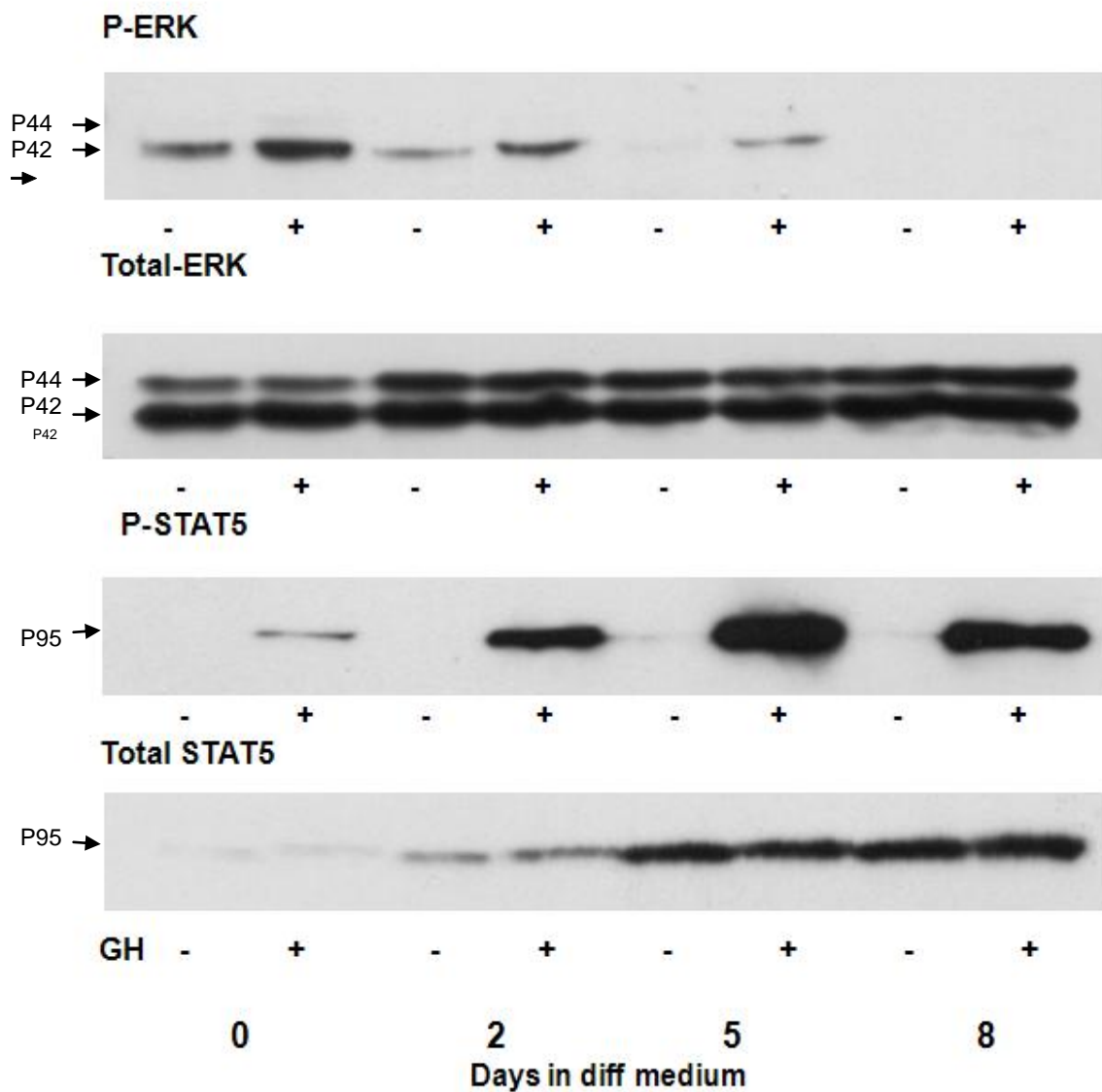


**Figure 3.5: Phosphorylation of ERK and STAT5**

A western blot which shows phosphorylation of ERK and STAT5 following GH stimulation (+) over a time course of 8 days in adipocyte differentiation medium. The level of GH-stimulated ERK phosphorylation declines with increasing time in differentiation medium. The total ERK blot has two bands upper is p44 and lower p42. Only p42 was visible for P-ERK. In contrast the level of total STAT5 and GH stimulated STAT5 phosphorylation increased with 3T3-L1 differentiation.

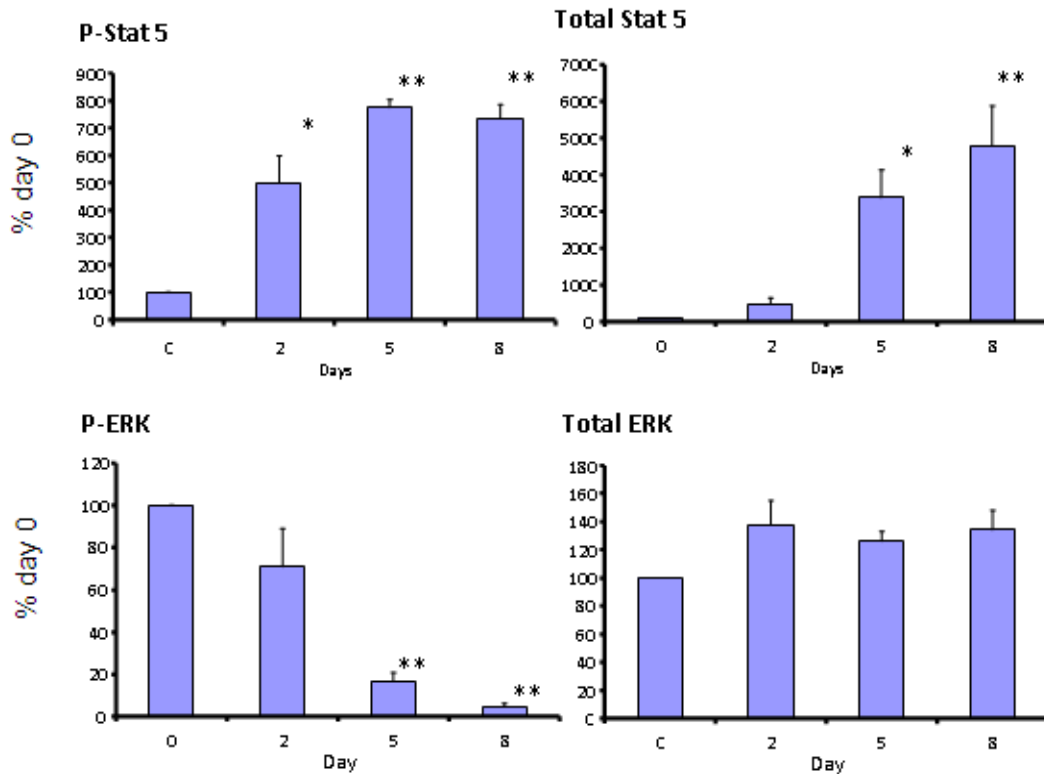


**Figure 3.6: Densitometric analysis of ERK and STAT5**

Densitometric analysis of western blots (Fig 3.3) expressed as % day 0 show increased total STAT5 and GH-stimulated STAT5 activation following differentiation, but reduced ERK activation despite same total ERK, \*  $p < 0.05$ , \*\* $p < 0.01$  vs. control cultures (day 0).  $n = 4$  separate experiments.

### 3.3.3 Maximal ERK phosphorylation during 3T3-L1 differentiation

In order to determine whether adipogenesis causes a non-specific reduction of ERK with the potential to be phosphorylated, 3T3-L1 cells undergoing differentiation were treated with phorbol 12-myristate 13-acetate (PMA, 1 $\mu$ M, Sigma, UK) for 10 minutes and the level of ERK phosphorylation analysed by western blotting. PMA was used as a positive control for ERK pathway activation as it directly activates protein kinase C thus causing non-receptor-mediated ERK activation and equivalent experiments were performed (section 3.2.1). PMA-induced ERK phosphorylation was unchanged by adipogenic differentiation which confirmed that the reduction in GH-induced ERK

phosphorylation seen in differentiated cells was specific and not due to a global reduction in ERK with the potential to be phosphorylated (Figures 3.7 and 3.8).

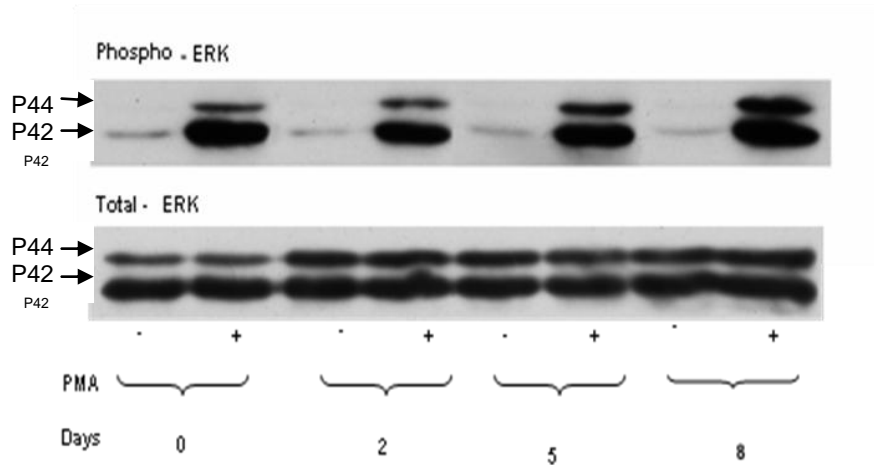


**Figure 3.7: PMA-induced ERK phosphorylation**

A western blot of 3T3-L1 cells treated with PMA shown levels of ERK activation were the same in differentiated cells and no significant difference in any of them.

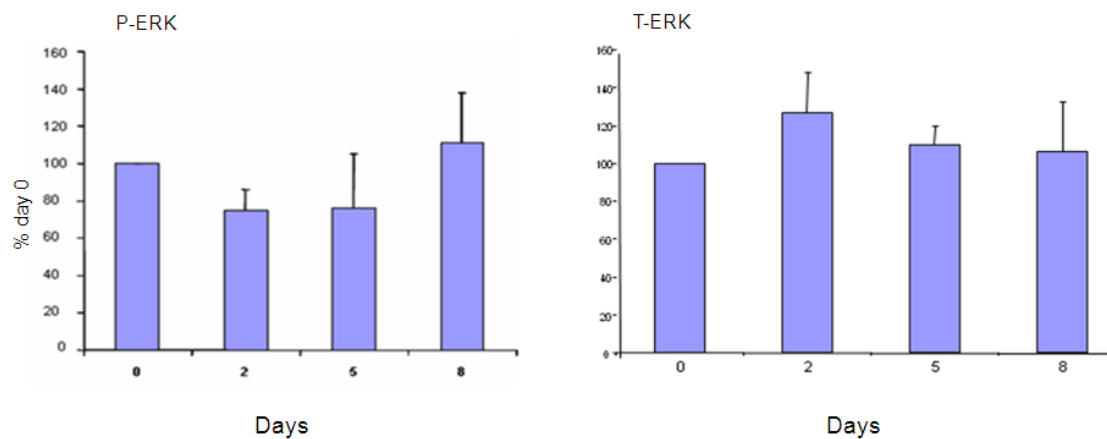


**Figure 3.8: Densitometric analysis of 3T3-L1 cells with PMA**

Densitometric analysis of western blots of 3T3-L1 cells treated with PMA shown highest levels of ERK activation in differentiated cells, n=3.

### 3.3.4 Validation of the GHR QPCR assay

Agarose gel electrophoresis along with melt curve analysis (Figures 3.7 and 3.8B) confirmed that the GHR QPCR assay produced a single product of the correct size (103 bp). Analysis of serial 10 fold dilutions of pooled cDNA (Figure 3.8A) was used to determine the efficiency of the assay. This can be calculated from the slope of the line of Ct value plotted against initial cDNA concentration where the undiluted pool is defined as one using the MxPro software (Stratagene). This technique allowed determination that the GHR assay had an efficiency of 98.8%. ARP amplified with a Ct value typically in the range of cycle 15-16 and this was unaltered by the differentiation state of the 3T3-L1 cells (section 2.3.3.1.1). ARP was confirmed as a suitable housekeeping gene for GHR analysis as it had a similar efficiency of 98.3% (determined as described in section 2.3.3.1) and its expression did not alter during 3T3-L1 cell differentiation (Table 2.4). Sequence analysis of the GHR QPCR product confirmed the sequence was that of the GHR using the BLAST sequence search tool. (<http://blast.ncbi.nlm.nih.gov/Blast.cgi>).

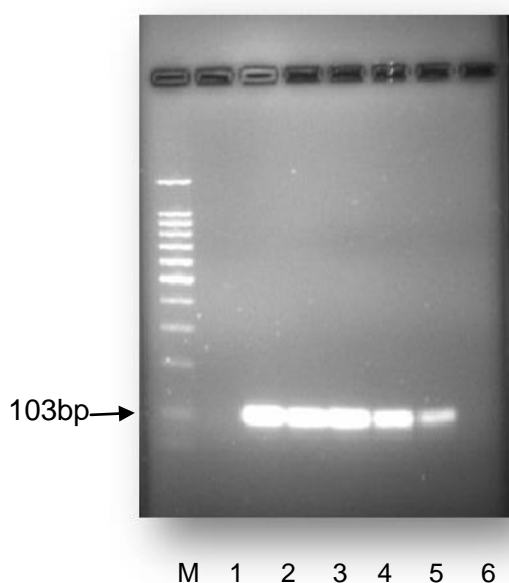


**Figure 3.9: GHR QPCR product**

Agarose gel electrophoresis of 2% in 1 x TAE confirmed the sizes of the GHR QPCR product, 103bp. M: DNA 100bp ladder, lane 1: no template control and lanes 2 through 6: contain the amplified PCR products.

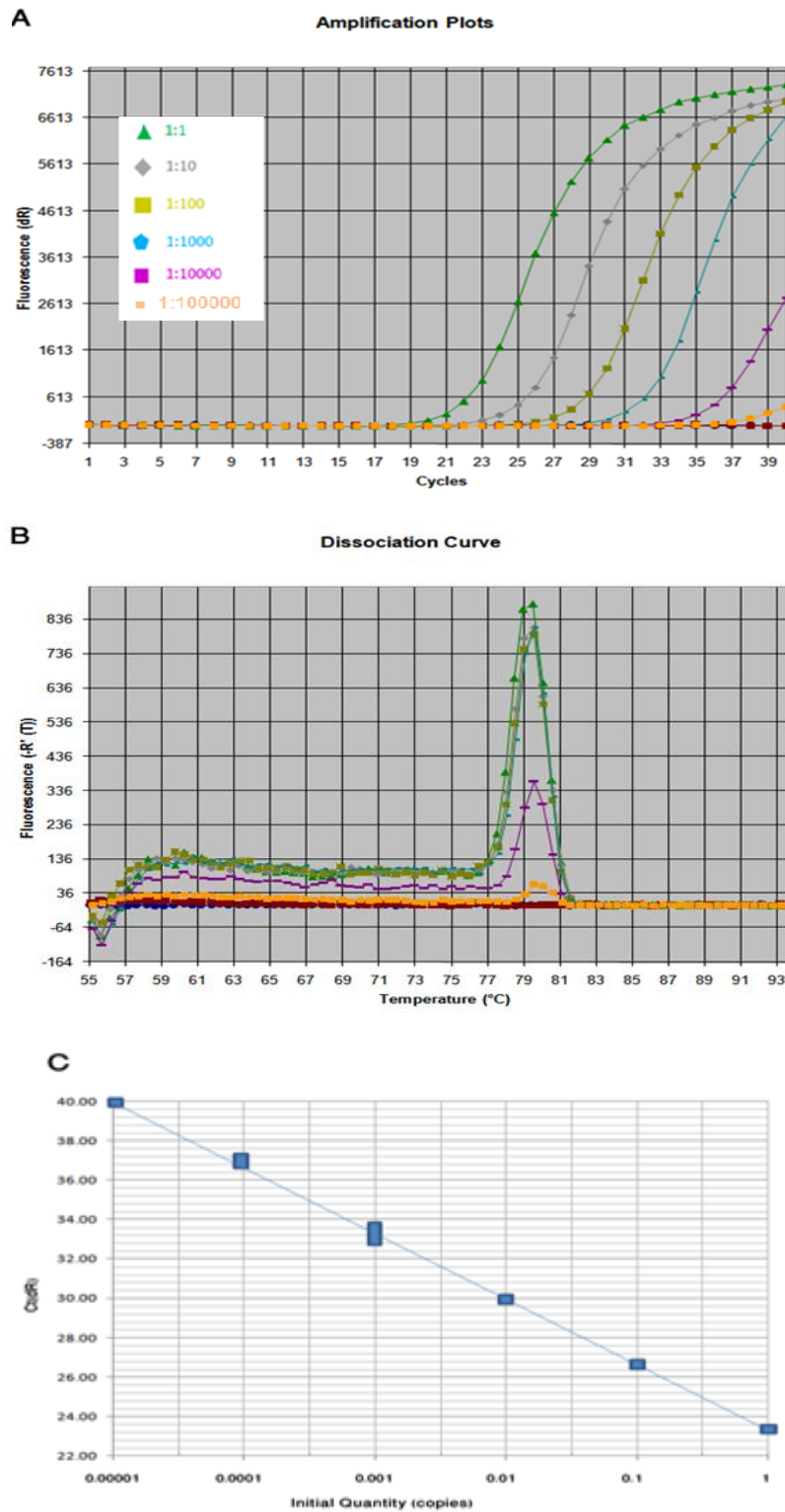


**Figure 3.10: GHR QPCR analyses**

Validation of GHR QPCR assay performed on (A) serial dilutions of cDNA from 1:1 to 1:100000 and NTC (B) resulting in the melting peak curve analysis of the resulting products and (C) the standard curve. The efficiency of the reaction was determined to be 98.8%.

### 3.3.5 GHR expression during differentiation

The level of GHR gene transcription during 3T3-L1 differentiation was analyzed using QPCR. GHR expression was increased during the differentiation process (Figure 3.9, 3.10 and Table 3.3) with significantly higher levels being observed in differentiated cells at day 8 ( $610\% \pm 71\%$  \*  $p < 0.05$ ,  $n=4$ ).

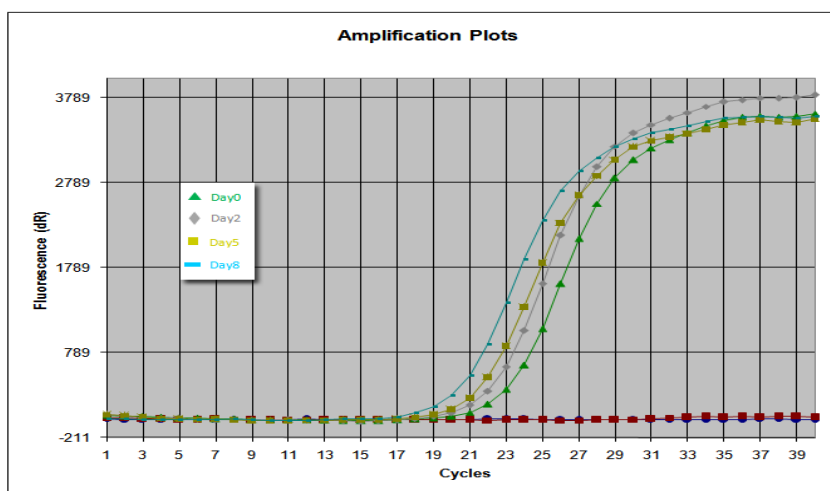


**Figure 3.11: Amplification curve of GHR**

GHR QPCR amplification curve day for 3T3-L1 cells in differentiation medium from day 0 to day 8. GHR expression was increased with the 3T3-L1 differentiation.

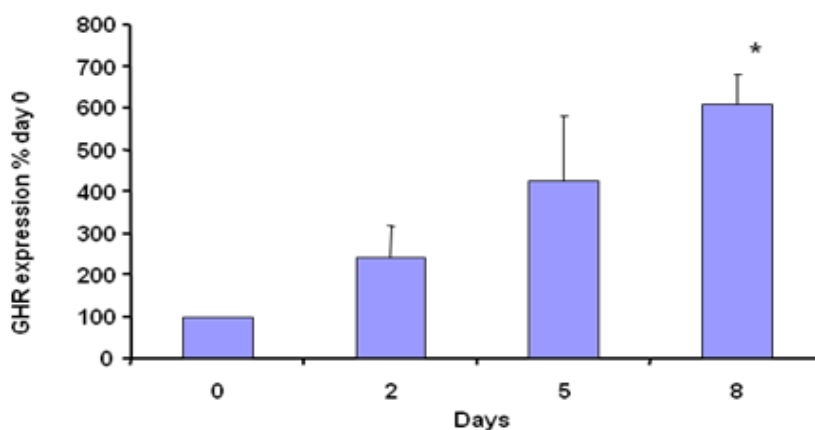


**Figure 3.12: GHR expression during 3T3-L1 differentiation**

QPCR analysis of GHR expression during 3T3-L1 differentiation shown a significant increase with cellular differentiation compared to control cultures, \*  $p < 0.05$  vs day 0 cultures,  $n=4$ .

**Table 3.4: GHR and ARP QPCR assays**

Ct values for GHR and ARP QPCR assays during differentiation from days 0-8 had no effect on ARP.

	Ct value			
	0 days	2 days	5 days	8 days
GHR	23.47	22.54	21.91	20.82
ARP	15.91	14.73	14.85	15.69

### 3.4 Discussion

GH modulates the function of adipocytes through the promotion of lipolysis by means of the GHR which activates multiple signalling cascades that include both STAT5 and MAPK (ERK) pathways. However, although the growth effects of GH are mediated primarily by STAT5, at present little is known about how GH effects adipocyte differentiation of fat cell precursors. Therefore, the effect of GH on STAT5 and ERK activation pathways on 3T3-L1 pre-adipocyte cell line during differentiation was observed.

The 3T3-L1 pre-adipocyte cell line was used as an *in vitro* model of adipogenesis as they can be induced to differentiate to adipocytes by modulating the culture conditions. After approximately 8 days in differentiation medium cells displayed morphological changes typical of adipocytes. Cultured samples were analysed for GHR expression using QPCR where increased expression of GHR was detected in differentiated cells.

Adipogenic differentiation was found to effect GHR-associated signalling pathways in two ways. GH-induced STAT5 activation increased in differentiated cells reflecting the increased levels of total STAT5 and GHR, while GH-induced ERK activation decreased in differentiated cells, total ERK was unaltered and high levels of PMA-induced ERK activation were observed. This inverse relationship between GH-induced ERK activation and GH-induced STAT5 activation/PMA-induced ERK activation demonstrates a level of ERK with the potential to be activated. There seems to be a specific uncoupling of GHR activation from the ERK pathway in adipocyte differentiated 3T3-L1 cells.

Results from this study are in general agreement with other studies that show the level of GHR expression increases during adipocyte differentiation (Zou *et al.*, 1997; Ji *et al.*, 2002, Flint *et al.*, 2006). GH binds to its receptor results in activation of STAT5 pathway in many cell types including adipocytes (Story and Stephens, 2006). Additionally, bind with the ERK pathway in bone marrow stem cell (BMSCs) and adipocytes (Winston and Bertics, 1992; Lewis *et al.*, 2006; Wang *et al.*, 2009).

A range of *in vitro* studies have shown that STAT5 expression and/or activity is related with human and murine adipogenesis (Stephens *et al.*, 1996; Harp *et al.*, 2001; Nanbu-Wakao *et al.*, 2002; Shang *et al.*, 2003; Stewart *et al.*, 2011). Previous research from Lewis *et al.*, (2006) confirmed that GH-induced STAT5 activation increased during differentiation of BMSCs into adipocytes (Lewis *et al.*, 2006). This study is in agreement, with my finding that 3T3-L1 differentiation results in increased GH-induced activation of STAT5 (Figure 3.3). GH-induced adipogenesis is mediated at least in part through STAT5 activation mediation via the transcription adipogenic factors C/EBP $\beta$ , C/EBP $\delta$  and PPAR $\gamma$  causing increased expression of lipogenic enzymes and in triglyceride accumulation in 3T3-F442A and 3T3-L1 cells (Yarwood *et al.*, 1999; Nanbu-Wakao *et al.*, 2002; Kawai *et al.*, 2007). The STAT5 pathway acts with other intercellular signalling to induce adipocyte differentiation (Aubert *et al.*, 1999, Stewart *et al.*, 2011).

Stimulation of the GHR in 3T3-F442A leads to ERK pathway activation (Winston and Bertics, 1992; Wang *et al.*, 2009). Other results from this study have demonstrated that GH-induced ERK activation decreases in differentiated adipocyte cells (Figure 3.3). This study is first to demonstrate a finding which contrasts those seen by Lewis *et al.*, which showed that adipocyte differentiation increased GH activation of ERK in BMSCs (Lewis *et al.*, 2004). However, BMSCs are a mixed population and therefore it may be possible that the increase in GH-stimulated ERK was due to cells other

than those which differentiated along the adipocyte lineage. Interestingly, other studies are in agreement with those results presented in this study which show that basal ERK activation pathway declines during differentiation of preadipocytes into adipocytes (Kim *et al.*, 2001; Sakaue *et al.*, 2002).

Studies in pre-adipocyte cell lines and embryonic stem cells confirm a critical role for the ERK pathway in the early phase of adipocyte differentiation (Sale *et al.*, 1995; Bost *et al.*, 2002). This plays a key role in mediating the early mitotic clonal expansion initiated by adipogenic stimuli, such as insulin that induce adipogenic gene expression program (Qiu *et al.*, 2001). Other studies have shown that in the early phase of adipogenesis ERK1/2 activation results in phosphorylation of C/EBP $\alpha$  and  $\beta$  (Prusty *et al.*, 2002; Lanning and Carter-Su, 2006) and stimulation of PPAR $\gamma$  expression leading to initiation of differentiation of fibroblasts into adipocytes (Aubert *et al.*, 1999; Horie *et al.*, 2004). The 3T3-L1 pre-adipocytes treated with dexamethasone (DEX), insulin (INS), isobutylmethylxanthine (IBMX) and fetal bovine serum (FBS) stimulate transient induction of the MEK/ERK pathway. This activation of the MEK/ERK pathway takes limited time before starting differentiation (Prusty *et al.*, 2002).

Pref-1 (also known as Delta-like protein 1, Dlk1) is a member of the Notch/Delta/Serrate family and is expressed in the cell membrane of pre-adipocyte (Wang *et al.*, 2006; Sul, 2009; Wang and Su, 2009; Armengol *et al.*, 2012). This expression declines with pre-adipocyte differentiation and is absent in mature adipocytes (Sul *et al.*, 2000; Gregoire, 2001; Kim *et al.*, 2007; Sul, 2009, Armengol *et al.*, 2012). Pref-1 is cleaved to release an extracellular 50 kDa active form by Notch ligand Delta TACE [TNF $\alpha$  (tumour necrosis factor  $\alpha$ )-converting enzyme] (Smas *et al.*, 1997; Wang and Sul 2009; Sul, 2009; Armengol *et al.*, 2012). These studies have established that pref-1 prevents adipogenesis and therefore believed that this is

mediated via the transcription factors Sox9 that suppresses C/EBP $\delta$  and C/EBP $\beta$  expression (Wang and Sul 2009; Sul, 2009). Also, Pref-1 causes the activation of ERK which in turn prevents down regulation of Sox9 thus inhibiting adipogenesis (Smas *et al.*, 1997; Kim *et al.*, 2007; Sul, 2009; Wang and Sul, 2009). Other studies suggest that Pref-1 could act on adipocyte differentiation during modulation of Notch pathways (Armengol *et al.*, 2012). Negative regulation of Pref-1 expression appears during adipogenesis in the cell treatment with combination of MIX/DEX, which promotes adipocyte differentiation (Sul *et al.*, 2000).

The advantages of western blotting are sensitivity to as little milligrams of protein and specificity amongst hundreds of thousands of alternate proteins. Enhanced chemiluminescence was used to detect immobilised proteins labelled with HRP. The advantages of this technique are sensitivity down to the photon level, speed, non hazardous reagents and simple procedures. The only disadvantage involves the very high sensitivity which requires secondary anti-bodies to be diluted several thousand times in order to avoid background noise (Kricka, 1991).

The advantages of reprobing membrane are the conservation of the sample, quick, inexpensive and easy to correct mistakes or anomalies in the blots. However, disadvantages are that stripping removes antibodies, but alters also the protein quantity on the membrane as they are not covalently fixed. Incomplete stripping may result in blocked epitopes by still bound antibodies which are disturbed when re-probed with another polyclonal antibody.

There are several possible explanations as to how GH-induced ERK activation declines during 3T3-L1 differentiation. The classic study of Love *et al.*, (1998) showed that GH is capable of activating the ERK pathway in 3T3-F442A cells, but not in IM-9 lymphocyte cells and that the 66 kDa form of the ERK pathway adapter protein Shc is only present in 3T3- F442A cells (Love *et al.*, 1998; Yang *et al.*, 2004; Wang *et al.*, 2009). Therefore, the possibility exists that the 66 kDa form of Shc is necessary to couple the GHR to ERK pathway activation. Determination of Shc levels during 3T3-L1 differentiation could explain the decline in GH-stimulated ERK activation; experiments will be performed to look at Shc levels in 3T3-L1 during differentiation (Chapter 4). Also, it is possible that the elevated GHR expression levels seen in differentiated 3T3-L1 may modulate the profile of signalling pathways associated with ERK pathway.

## **Chapter Four**

**Do the expression levels of p66<sup>Shc</sup> and the GHR modulate GH signalling during 3T3-L1 differentiation?**

## 4. Chapter Four

### 4.1 Introduction

Chapter 3 demonstrated that GH-stimulated ERK pathway activation declines as 3T3-L1 cells progress down the adipocyte differentiation pathway. In this chapter, two possible explanations for the decline in GH-stimulated ERK activation were explored.

Love *et al.* (1998) demonstrated that GH stimulates the tyrosine phosphorylation of JAK2, ERK1/2 and STAT5 in 3T3-F442A cells (another murine pre-adipocyte cell line), but failed to activate the ERK1/2 pathways in IM-9 (human B lymphoblastic cell line). The 66 kDa form of the ERK pathway adapter protein Shc p66<sup>Shc</sup> is present in 3T3-F442A, but absent in IM-9 cells. These observations lead Love *et al.* to suggest that p66<sup>Shc</sup> is necessary for GHR activation to link with the ERK pathway (Love *et al.*, 1998). Therefore, this study proposes that adipocyte differentiation of 3T3-L1 cells results in the decline of p66<sup>Shc</sup> levels resulting in the selective uncoupling of the GHR from the ERK pathway in 3T3-L1 cells. In order to determine whether the difference in the amount of basal p66<sup>Shc</sup> could explain the decline in GH-stimulated ERK activation and the selective uncoupling of the GHR from the ERK pathway, western blotting was used to analyse expression of p66<sup>Shc</sup> in 3T3-L1 cells as they undergo differentiation.

Findings from this study confirmed that expression of the GHR increases during 3T3-L1 differentiation from pre-adipocytes into adipocytes (section 3.4.5). In addition, previous studies have shown that GHR is expressed in both pre-adipocytes and mature adipocytes, but GHR expression increases with adipocyte differentiation (Zou *et al.*, 1997; Yu, 2000; Ji *et al.*, 2002; Flint *et al.*, 2006). An increase in GHR expression may possibly modulate the pattern of signalling pathways associated with

GHR activation. As such, elevated GHR levels may result in preferential association of the GHR with JAK2-STAT5 leading to reduced ERK activation. To test this hypothesis a technique was employed to over-express the GHR in undifferentiated 3T3-L1 cells in an attempt to mimic the effect of adipogenic differentiation on GHR numbers and GHR-associated cell signalling.

#### **4.1.1 Src Homology (Shc) protein**

Shc is an adapter protein and one of several proto-oncogene products which do not possess any intrinsic catalytic activity. The molecular structure of Shc is made up of at least three tyrosine phosphorylation sites each of which are located within the central collagen-homology domain along with two PTB domains, one SH2 domain located near the carboxyl terminus and another PTB domain located near the amino terminus. Based upon this molecular structure, many studies have demonstrated that this protein will function as an adaptor molecule that will assist in the mediation of phosphotyrosine-dependent signalling events that take place near cell surface receptors (Pelicci *et al.*, 1996; Zhang *et al.*, 2002). This is accomplished by binding tyrosine phosphorylated proteins via SH2 and PTB domains, thus acting as a bridge that links together proteins in a signalling pathway (Pelicci *et al.*, 1995; Song *et al.*, 2002).

The Shc protein exists as three isoforms of 46, 52, 66 kDa; p46<sup>Shc</sup>, p52<sup>Shc</sup> and p66<sup>Shc</sup>. These isoforms are produced from one gene through the process of alternative splicing (Almind *et al.*, 1999; Kisielow *et al.*, 2002; Purdom and Chen, 2003; Landry *et al.*, 2003). Receptors possess tyrosine phosphorylation sites that Shc can bind to, which is surprising as it was originally thought that Shc acted solely as an ERK pathway adapter protein linking receptor activation to ERK via its interaction with Grb2 forming a Shc-Grb2-Sos signalling complex (Figure 4.1) (Charlotte *et al.*, 1998;

Sasaoka and Kobayashi, 2000; Ravichandran, 2001, Wang *et al.*, 2009). This signalling complex then activates Ras, which in turn triggers the first kinase in a three-kinase cascade leading to ERK (MAPK) activation (Charlotte *et al.*, 1998). However, recent data suggests that the p66<sup>Shc</sup> is involved in mitochondrial reactive oxygen species generation and thus may play a central role in linking high levels of glucose with the adverse side effects of diabetes (Francia *et al.*, 2009).

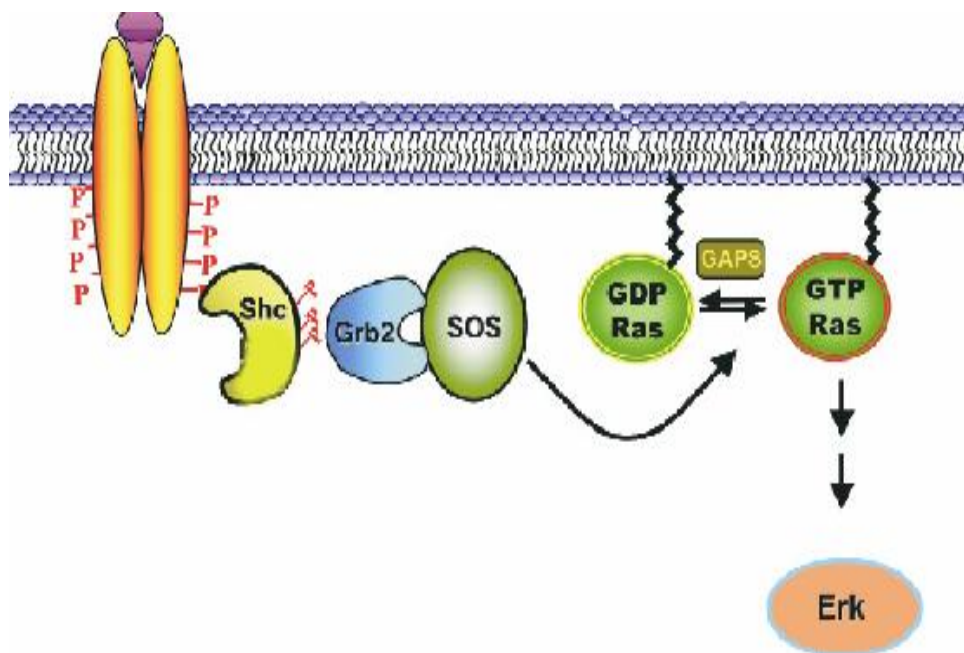


**Figure 4.1: Shc signaling pathway**

Shc mediate Ras activation downstream of receptor RTK. Shc binds to phosphorylated RTKs and recruits the Grb2/SOS complex which activates ERK pathway (adapted from Kleiner, 2005).

### **4.1.2 GHR expression in 3T3-L1 cells**

GHR levels increase with adipogenic differentiation of 3T3-L1 cells (section 3.3.3) which lead to the hypothesis that elevated expression of the GHR may be linked to the preferential association of the GHR with JAK2-STAT5 resulting in reduced ERK activation. This hypothesis was tested by transfecting 3T3-L1 cells with a GHR expression vector to induce over expression of the GHR and thus mimic the elevated GHR levels in differentiated 3T3-L1 cells. Studies then determined whether this had any effect on GHR associated cell signalling compared to cells transfected with the empty vector.

### **4.1.3 Transfection**

Transfection is the transient introduction of RNA or DNA into cultured cells, including mammalian, to study gene function, gene expression or protein production. Carrier molecules which enable gene delivery into primary cells include plasmid DNA (pDNA), messenger RNA (mRNA) and short interfering RNA (siRNA). No single method of delivery can be applied to all types of cells as transfection efficiencies depend on the reagent, protocol and cell type utilized. There are two types of transfection, transient when the introduced plasmid remains autonomous and is gradually diluted out at each cell division and stable in which the plasmid DNA becomes incorporated into the host genome and is thus transmitted to all daughter cells. Production of the cDNA-encoded protein continues only for a limited time in transiently transfected cells (plasmids replicate independently of the chromosomal DNA), while in stable transfection the exogenous DNA is integrated into the host genome allowing cells to continually produce the cDNA-encoded protein as long as the culture is maintained.

Liposome-mediated and electroporation are two methods of transfection developed to facilitate the introduction of DNA into cells. Liposome-mediated transfection is the most widely used. In this type of transfection the plasmid is complexed with cationic polymer (polyplex), cationic lipid (lipoplex) or a mixture of these called a lipopolyplex (Lechardeur *et al.*, 2002). The charged DNA complex is taken from the extracellular compartment by endocytosis and transferred into the nucleus. Advantages of using liposome-mediated transfection are its relatively high efficiency of gene transfer, the ability to transfect certain cell types that are resistant to calcium phosphate or DEAE-dextran, the successful delivery of DNA of all sizes including oligonucleotides (Felgner *et al.*, 1987), the ability to delivery RNA (Malone *et al.*, 1989), the delivery of proteins (Debs *et al.*, 1990) and the ability to generate transient and stable integration (Felgner *et al.*, 1995).

Electroporation is a mechanical transfection method that utilizes an electronic pulse to form momentary pores within cell membranes (Toneguzzo *et al.*, 1988) through which substances such as nucleic acids can pass (Chu *et al.*, 1987). Voltage is the critical parameter for electroporation as for a given capacitance/buffer there was an optimal voltage for transfection (Chu *et al.*, 1987). Electroporation is a simple process where both the target cells and specified molecules are suspended within an electrically conductive solution. An electric circuit is closed around the solution. This allows an electric pulse lasting between several microseconds to a millisecond and at an optimal voltage to be discharged through the target cells. This disrupts the phospholipid bilayer of the cell membrane by allowing temporary pores to appear. Concurrently, the electrical potential across the cellular membrane rises to allow the specified molecules, which are now charged, to be forced across the membrane through these temporary pores (Chu *et al.*, 1987). Cells can then divide to produce new cells that contained the introduced plasmids. This process is approximately ten times more effective than that of chemical transformation. However, both of these

liposome-mediated and electroporation techniques suffer from problems related with cellular toxicity, poor reproducibility, inconvenience or inefficiency of DNA delivery. Also, transfection efficiencies can vary noticeably depending on the transfection method, reagent, protocol or type of cells

#### **4.1.4 Aims**

The aim of this chapter was to explore possible mechanisms to explain why GH-stimulated ERK activation declines as 3T3-L1 cells undergo adipogenic differentiation. This was determined by measuring the amount of basal p66<sup>Shc</sup> in preadipocytes and at several time points during *in vitro* induced adipogenesis to test the hypothesis that limitation of this adaptor protein could explain the decline in GH-stimulated ERK activation and the selective uncoupling of the GHR from the ERK1/2 pathway. Western blotting was used to analyse p66<sup>Shc</sup> in 3T3-L1 cells as they undergo differentiation. Also, elevated GHR expression, as found in differentiated adipocytes, could explain the reduction in GH-stimulated ERK observed in differentiated 3T3-L1 cells. This was tested by transfecting 3T3-L1 cells pre-adipocyte with a GHR expression vector and observing GH induced activation of the ERK pathway.

## **4.2 Material and methods**

### **4.2.1 Detection of Shc in differentiating 3T3-L1 cells**

Western blotting techniques have been used to determine Shc expression levels during 3T3-L1 differentiation (section 3.2.2.4). 3T3-L1 cells (150,000cells/well) were plated in 6 well plates in DMEM containing 10% calf serum and once confluent designated day 0 were induced to differentiate along the adipogenic lineage by changing the culture medium to differentiation medium (section 2.2.4). Samples were then collected at day 0, 2, 5 and 8 when cells were washed 2 times in PBS and lysed in 250 µl loading buffer. Protein was measured (section 3.2.2.1) and 20 µg samples were run on SDS-PAGE using a 10% gel followed by the detection of Shc using western blotting. All SDS-PAGE and western blotting procedures were performed as described (section 3.2.2). Blots were blocked for 1 hour and then incubated in primary anti-total Shc antibody overnight at 4°C (Cell Signalling, Technology, Danvers, MA, USA) at 1:2000 dilution. Secondary antibody, anti-mouse IgG horseradish peroxidase (GE Healthcare, Little Chalfont, Bucks, UK), was used at a 1:5000 dilution for 1 hour. The blots were then visualised using ECL Plus (GE Healthcare, Little Chalfont, Bucks, UK) as described earlier (section 3.2.2.6).

### **4.2.2 Over expression of the GHR in 3T3-L1 cells**

The aim of this section was to transfect 3T3-L1 cells with a vector (pUB/Bsd) modified to contain the hGHR sequence under the control of the CMV promoter so that the cells over expressed the GHR.

#### 4.2.2.1 GHR expression vector

The hGHR vector was prepared by Dr David Millar of the Institute of Medical Genetics in Cardiff University. The GHR was PCR amplified from human cDNA using primers GHRNHE5, **GCTAGCC**ACCATGGATCTCTGGCAGCTGC, and GHRXBA3, **TCTAGACTA**AGGCATGATTTTGTTCAG. The fragment was cut with the restriction enzymes NheI and XbaI (sites in bold on primers) and cloned into pRLCMV cut with the same enzymes. Clone was sequenced. Second PCR was performed using primers GHRBSD5 **GTCGACTTTT**GCTCACATGGCTCGAC and GHRBSD3 **CTCGAGGCC**ACCTGGATCCTTATCG which PCR amplifies the CMV promoter, the GHR cDNA and the SV40 3'UTR. The fragment was cut with Sall and XhoI (sites in brown bold on primers) and cloned into the Sall site of pUBBsd. Again, clone was sequenced to confirm identity.

#### 4.2.2.2 Transformation of *E. coli* with the plasmid vector.

Transformation is the process by which bacterial cells take up plasmid DNA which allows the introduction of a foreign plasmid into bacteria to use the transformed bacteria to amplify the plasmid. When a plasmid is inserted into bacterial cells, they can be grown in large amounts to produce milligram quantities of the plasmid which can be used in subsequent experiments.

In this study Competent Topp<sup>10</sup> *E. coli* were transformed with the GHR plasmid expression vector. 1 µl of the plasmid at a concentration 10 ng/µl DNA was placed in the bottom of a microfuge tube. A second tube without plasmid containing 1 µl of sterile water was used as a negative control. The competent bacteria were thawed on ice, and then 25 µl of competent cells added to each tube. Both tubes were then kept on ice for 30 minutes. The competent cells were then heat shocked at 42°C for 30 seconds and then placed back on ice. One ml Luria Broth (LB) medium (Sigma,

St. Louis, MO, USA) containing 20 mM filter sterilised glucose was added to the cells and shaken at 37°C, 200rpm (Orbital shaker S 150, Stuart Scientific) for 1 hour. Following this incubation 100 µl of cells were spread onto a LB agar plate (Sigma, Gillingham, Dorset; UK) (Appendix 1) containing 100 µg/ml ampicillin (Sigma, UK) and incubated overnight. The remaining 900 µl was centrifuged and the resulting bacteria were resuspended in 100 µl LB broth and were plated on another plate. The presence of ampicillin resistant bacterial colonies following an overnight culture confirmed that the transfection had been successful.

#### **4.2.2.3 Midi-prep of plasmid DNA**

5 ml of LB broth with 100 µg/ml ampicillin were inoculated with a single colony of transformed *E. coli* and incubated overnight at 37°C in an orbital shaker at 200 rpm. Next day the culture medium was observed to be cloudy, 1 ml transferred to Erlenmeyer flask with 95 ml LB ampicillin then incubated via vigorous shaking orbital shaker at 37°C overnight and a further 1 ml used to prepare glycerol stock (Appendix 1). Next day the LB bacterial suspension was centrifuged for 50 minutes/4°C at 3600 rpm and plasmid extracted using Pure Yield™ Midiprep system (Promega, Madison, WI, USA) according to the manufacturer's instructions. Briefly the pellet was re-suspended in cell solution and lysed in cell lysis buffer. Plasmid DNA was precipitated and purified using a column based procedure according to the manufacturer's instructions. The purified plasmid DNA was eluted from the column with elution buffer and DNA concentration determined via spectrophotometer analysis at 260 nm then stored at -80°C.

#### **4.2.2.4 Transfection of 3T3-L1 with the GHR plasmid**

Transfection is the phenomenon of incorporation of exogenous nucleic acids through the cell membrane. 3T3-L1 cells were transfected with an expression vector containing the hGHR sequence using two different methods, a reagent liposomal based method and an electroporation method.

##### **4.2.2.4.1 Reagent-based transfected**

The reagent-based method uses a polycationic polyamine reagent, GeneJammer (Stratagene). GeneJammer has several positively charged amino groups, which bind to and neutralize the negatively charged DNA allowing the target cell to readily assimilate the DNA by endocytosis. For transient transfections, 150,000 3T3-L1 cells were plated in 6 well plates then cultured until confluent (section 2.2.1). Initially, cells were transfected with a green fluorescent protein plasmid GFP, (2 µg, pmax GFP) (Lonza, Basle, Switzerland) to determine transfection efficiency. The transfection mixture was prepared in 50 µl serum free medium with 3 µl GeneJammer and 1 µg plasmid, the mixture was then incubated for 15 minutes before being added drop wise to the cells in complete culture medium. Cells were cultured for 24 hours and examined for GFP expression using fluorescence microscopy. Transfection efficiency was determined by counting the GFP positive cells and comparing this against the total number of cells.

##### **4.2.2.4.2 Electroporation**

The hGHR expression vector and empty vector were also transfected into 3T3-L1 cells using a technique known as electroporation using a proprietary kit optimized for 3T3-L1 pre-adipocytes (Lonza). 3T3-L1 cells were subjected to electroporation with either buffer alone (control), empty vector, GHR expression vector (either 1 µg or 10 µg) and GFP vector (2 µg, pmax GFP) (Lonza). Cells were cultured before

electroporation in a 75 cm<sup>2</sup> flask culture cells in DMEM containing 10% calf serum. Once 80% confluent, the medium was removed and the cells trypsinized before being counted (section 2.2.1.2). The cells were centrifuged and the pellet resuspended in 100 µl nucleofector solution per 1x10<sup>6</sup> cells. The 100 µl cell suspension containing the plasmid DNA was then transferred to an Amaxa cuvette where the electroporation was performed using an Amaxa Nucleofector II electroporation apparatus (Lonza). The appropriate nucleofector program T-30 was selected and the cuvette inserted into the holder where the electroporation was then performed. The cuvette was removed then 500 µl of the pre-warmed culture medium added. The contents of the cuvette was transferred into one well of a 6 well plate which contain 2 ml complete medium then cultured. After 24 hours of incubation, the medium was removed and replaced with 1.5 ml fresh culture medium. Cells were grown for between 2 to 3 days until 80% confluent when a signalling experiment was carried out (section 3.2.1). Transfection efficiency was assessed by counting GFP positive cells against total number of cells after 24 hours had elapsed.

#### **4.2.2.5 Western blotting techniques**

Experiments were carried out as described previously (section 3.2.2.4).

#### **4.2.2.6 RNA extraction and QPCR analysis of human GHR expression**

To determine if transfection with the hGHR vector caused elevated GHR expression, RNA was extracted for QPCR analysis (sections 2.2.6, 2.2.6.2 and 2.2.6.3). The gene ARP was used as the housekeeping gene. Primers are detailed below (Table 4.1) and were used at a concentration of 500 nM. hGHR expression was compared with ARP using MxPro (MX3000P™, Stratagene).

**Table 4.1 Primers of the hGHR and ARP**

hGHR and ARP primers for QPCR analysis were used to detect hGHR expression.

<b>hGHR</b>		
Forward	Reverse	Amplicon size
GCCACTGGACAGATGAGGTT	TCAGGCCATTCTTTCCATTC	229bp
<b>ARP</b>		
Forward	Reverse	Amplicon size
GAGGAATCAGATGAGGATATGGGA	AAGCAGGCTGACTTGGTTGC	71bp

## 4.3 Results

### 4.3.1 Basal Shc activation during 3T3-L1 differentiation

The hypothesis proposed that down regulation of p66 Shc may cause the reduction in GH-stimulated ERK seen during 3T3-L1 differentiation. To gain an insight into whether the p66<sup>Shc</sup> level declines in 3T3-L1 cells undergoing adipocyte differentiation, Shc levels were analysed by western blotting. The bands representing Shc isoforms 46 kDa, 52 kDa and 66 kDa from two separate experiments are shown below (Figure 4.2). Western blots from ten separate experiments were analysed by imaging densitometry (Figure 4.3) and the mean level of p66<sup>Shc</sup> over the time course of differentiation showed a transient rise at days 2 to (310% ± 120 of the level at day 0) and at day 5 (360± 140 of the level at day 0) followed by a decline at day 8 to (270 % ± 100 of the level at day 0) but to a level greater than at day 0. None of the results were significantly different to the basal day 0 level (p=0.337). Shc level also were reanalysed and plotted as a scatter plot (Appendix 2).



**Figure 4.2 Shc expression in 3T3-L1 cells**

Western blot analysis of Shc expression in 3T3-L1 cells at day 0 and days 2, 5 and 8 in differentiation medium. These blots are two independent experiments.

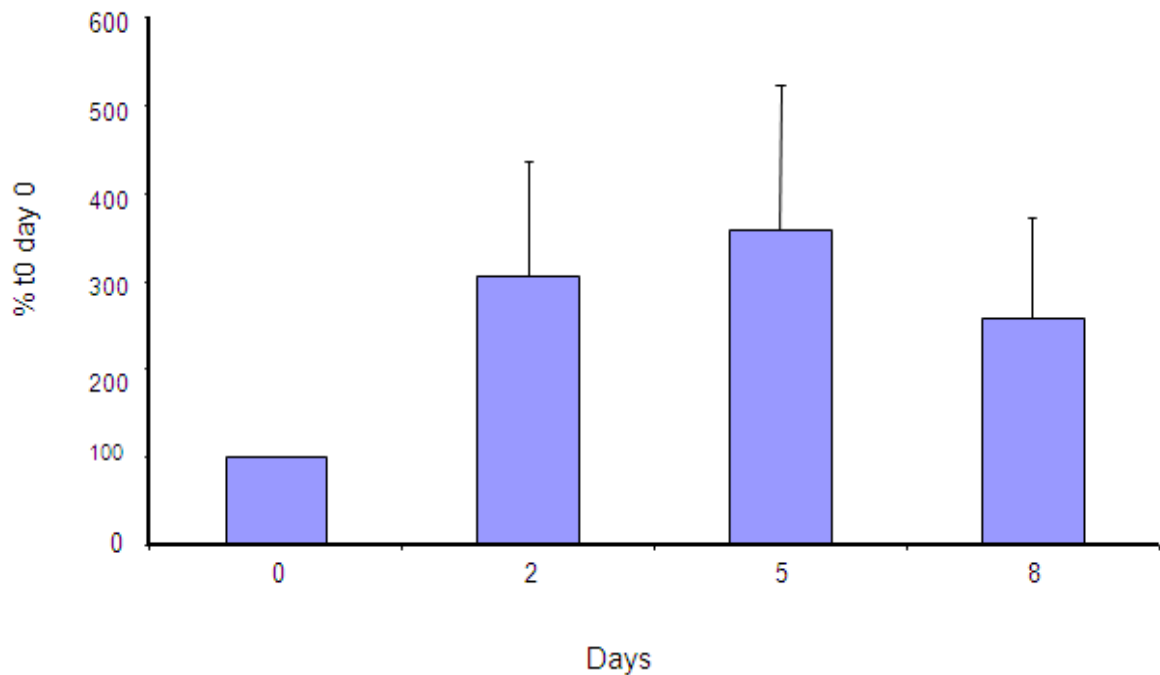


**Figure 4.3 66 kDa form of Shc levels**

Densitometric analysis of 66KDa form of Shc from western blot as 3T3-L1 undergoes differentiation. The results are expressed as % of day 0. The results demonstrated no significant difference of the level of Shc during 3T3-L1 differentiation ( $p=0.337$ ,  $n=10$ ). Shc level also were reanalysed and plotted as a scatter plot (Appendix 2).

### 4.3.2 Transfection efficiency

Transfection efficiency was assessed by counting the number of GFP positive cells 24 hours after transfection and expressing this as a percentage of the total cells in that field. Each result is the mean of four separate fields chosen at random in three separate experiments. The reagent-based method using GeneJammer had very low transfection efficiency (3-4%, Figure 4.4). In contrast, electroporation resulted in much better transfection efficiency (60-70%, Figure 4.5). Therefore, electroporation was used for all subsequent experiments.

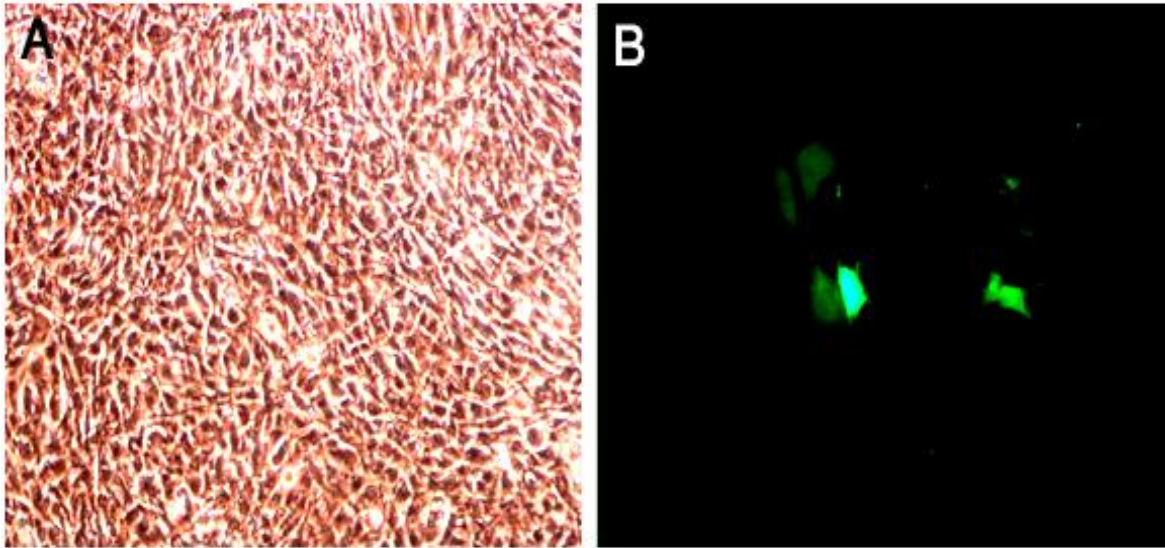


**Figure 4.4 3T3-L1 cells transfected with GFP using GeneJammer**

The 3T3-L1 cells were transfected with GFP using GeneJammer and were analyzed by fluorescence microscopy (B) to check transfection efficiency after 24-48 hours. The same field of view is shown with phase contrast (A) to show the total number of the cells. Transfection efficiency was 3-4%.

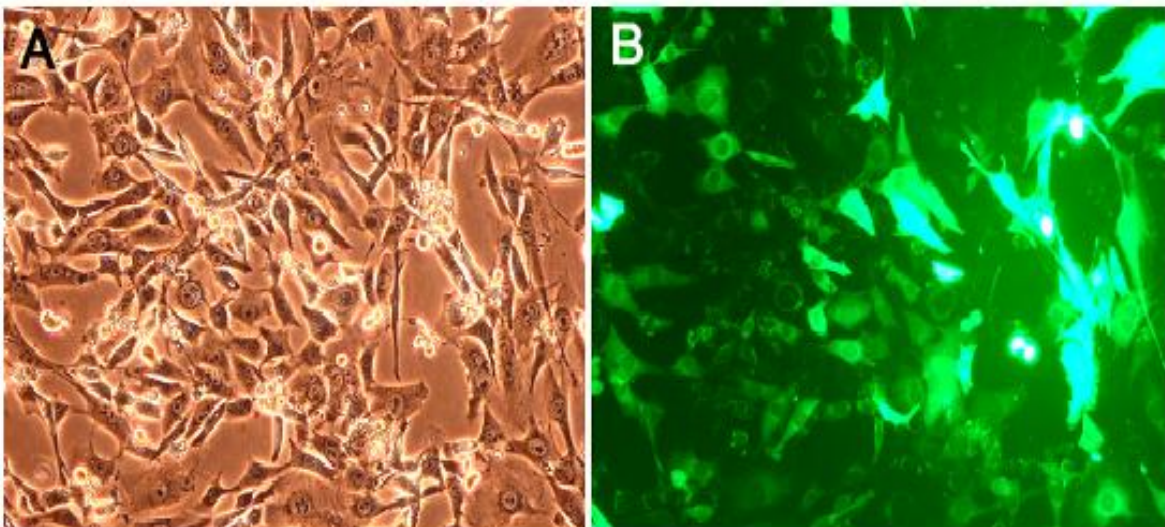


**Figure 4.5 3T3-L1 cells transfected with GFP using electroporation**

The 3T3-L1 cells were transfected with GFP using electroporation and were analyzed by fluorescence microscopy (B) to check transfection efficiency after 24 hour. The same field of view is also shown with phase contrast (A) to show the total number of the cells. Transfection efficiency was 60-70%.

### 4.3.3 Validation of the hGHR QPCR assay

Agarose gel electrophoresis and melt curve analysis (Figures 4.6 and 4.7B) confirmed that the hGHR QPCR assay produced a single product of the correct size which was 229bp. Analysis of serial dilutions of pooled cDNA (Figure 4.7A) was used to determine the efficiency of the assay. This can be calculated from the slope of the line of Ct value plotted against initial cDNA concentration where the undiluted pool was defined as one using the MxPro software (Stratagene). This technique was to determine that the hGHR assay had an efficiency of 100.5%.

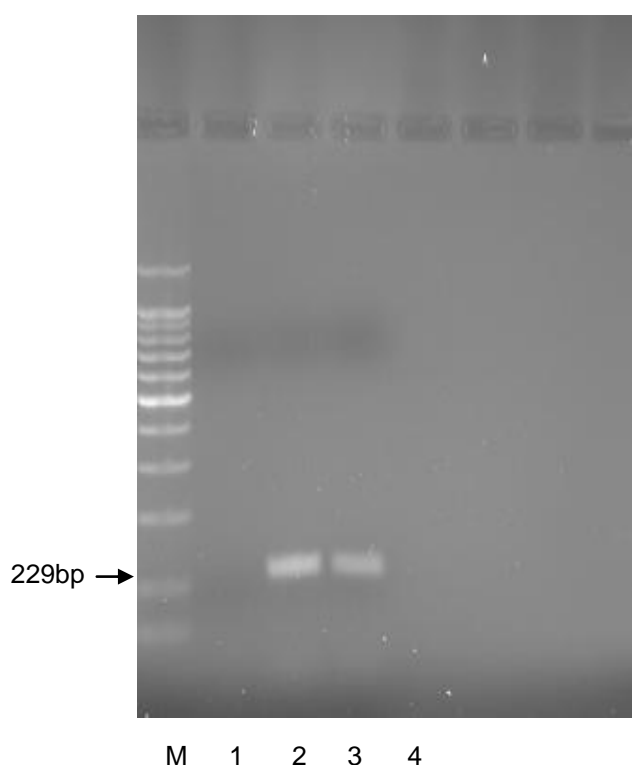


**Figure 4.6 hGHR QPCR product**

Agarose gel (2%) in 1xTAE confirmed the sizes of the hGHR QPCR product was 229bp. Lanes (M) DNA 100bp ladder, (1) empty vector transfected cells, sample from hGHR transfected cells (2-3) and no template control, (4).

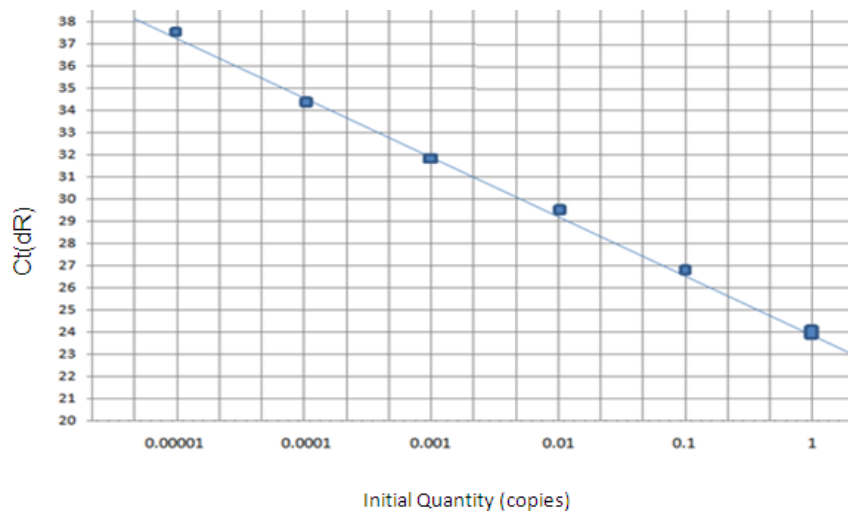
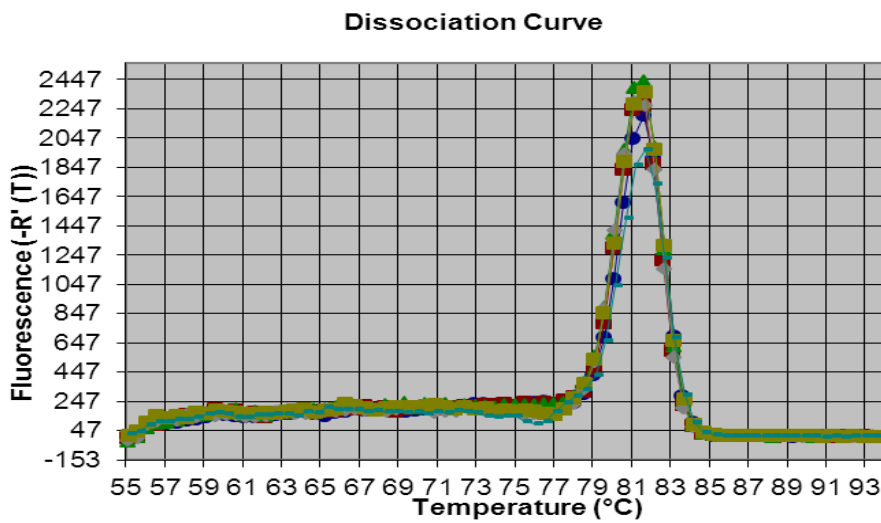
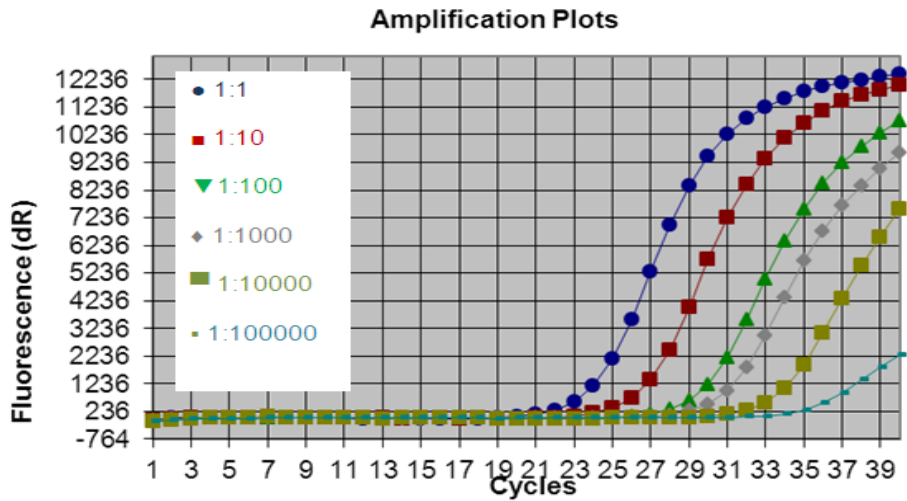


**Figure 4.7 hGHR qPCR analyses**

Validation of hGHR QPCR assay performed on (A) serial dilutions of cDNA from 1:1 to 1:1000 and NTC (B) which resulted in the melting peak curve analysis products (C) which result the standard curve.

#### 4.3.4 Effect of GHR expression on GH-induced ERK and STAT5 activation

The effect of elevated GHR expression on GH-induced ERK and STAT5 activation was analysed by phospho-specific western blotting (section 3.2.2) in cells treated for 10 minutes with GH (50 nM) and PMA (1  $\mu$ M) as a positive control for ERK. The level of GHR gene transcription in 3T3-L1 transfected with 1  $\mu$ g and 10  $\mu$ g of the hGHR vector was analyzed using QPCR. QPCR results confirmed high expression of the GHR transcript in 3T3-L1 transfected with the hGHR compared with empty vector in three separate experiments (Figure 4.8).

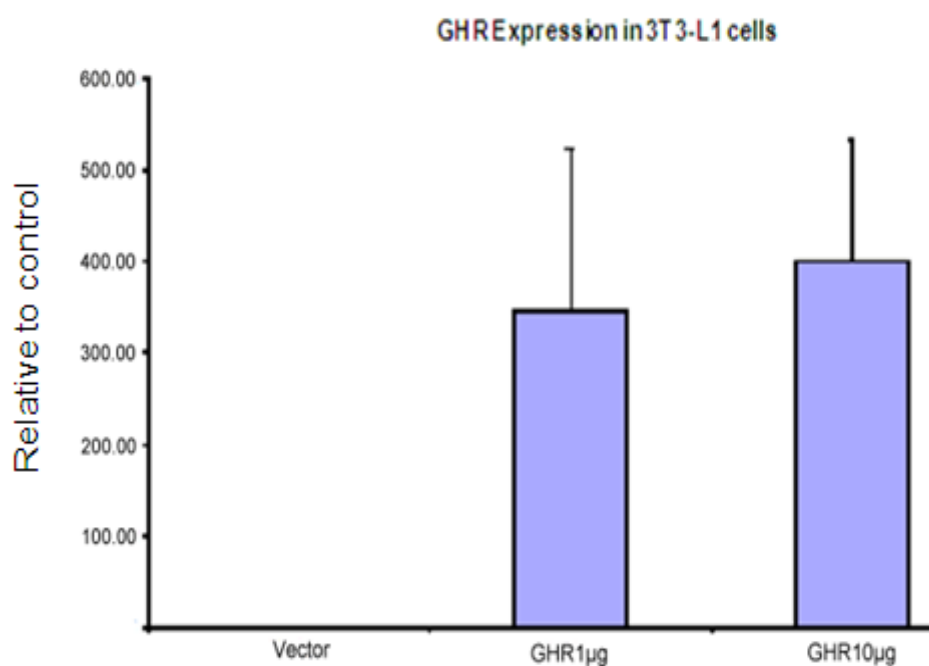


**Figure 4.8 QPCR analysis of GHR expression in 3T3-L1 transfected**

QPCR analysis of GHR expression in 3T3-L1 transfected which show a 350.00 fold increase in cells transfected with 1  $\mu$ g hGHR plasmid and 400.00 fold increase in cells transfected with 10  $\mu$ g hGHR plasmid relative to empty vector transfected cells, in three separate experiments, n=3.

Signalling experiments were performed in transfected cells for ERK and STAT5 activation, detected by western blotting with antibodies for phospho-ERK and phospho-STAT5 (Figure 4.9). Densitometric analysis of the data from multiple experiments (n=5, Figure 4.10) demonstrated no significant difference in the GH-stimulated ERK activation between 1 µg GHR and empty vector transfected cells (15.6%± 6.9 vs. 16.1% ± 4.4 compared to control respectively p=0.29). Total ERK levels did not differ between the two groups. In contrast STAT5 activation showed a significant increase in 1 µg GH transfected cells compared with empty vector (26058 ± 12338 and 7680 ± 900, n=5 separate experiments \*p<0.05). Maximal stimulation of ERK using PMA was unaltered in GHR transfected compared to empty vector transfected cells (Figure 4.9).

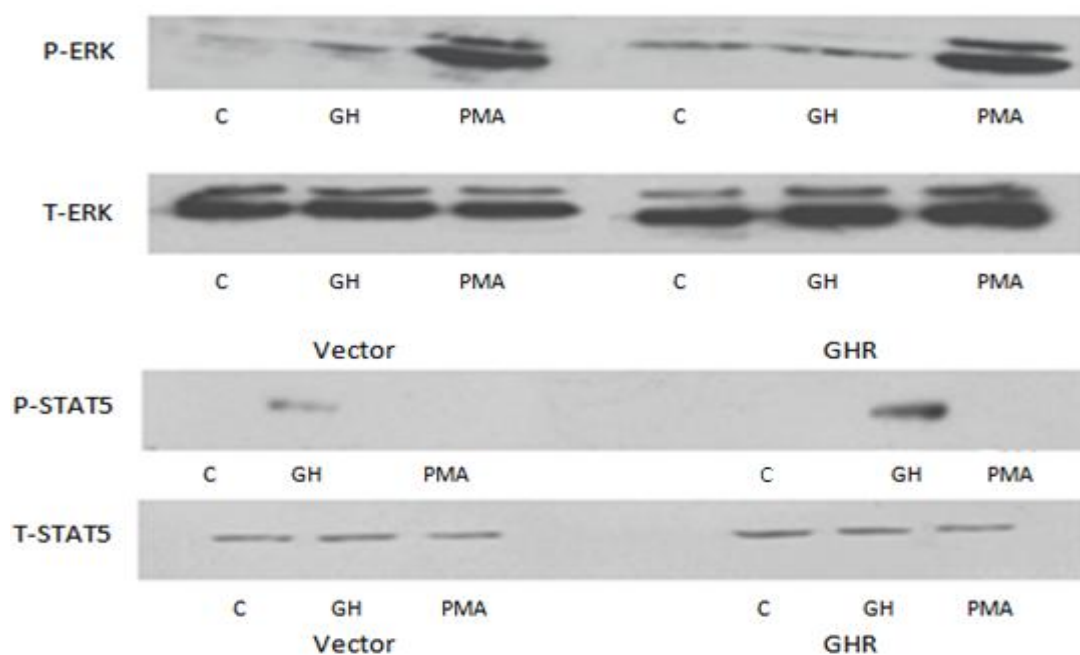


**Figure 4.9 Phosphorylation of ERK and STAT5 following GH and PMA in transfected cells**

Western blot reveals phosphorylation of ERK/STAT5 following GH/PMA treatment in cells transfected with empty vector (Vector) and GHR expression vector (GHR). Level of GH-stimulated ERK phosphorylation is unaltered in GHR transfected cells compared empty vector transfected cells; in contrast level of GH stimulated STAT5 phosphorylation increased in hGHR transfected cells.

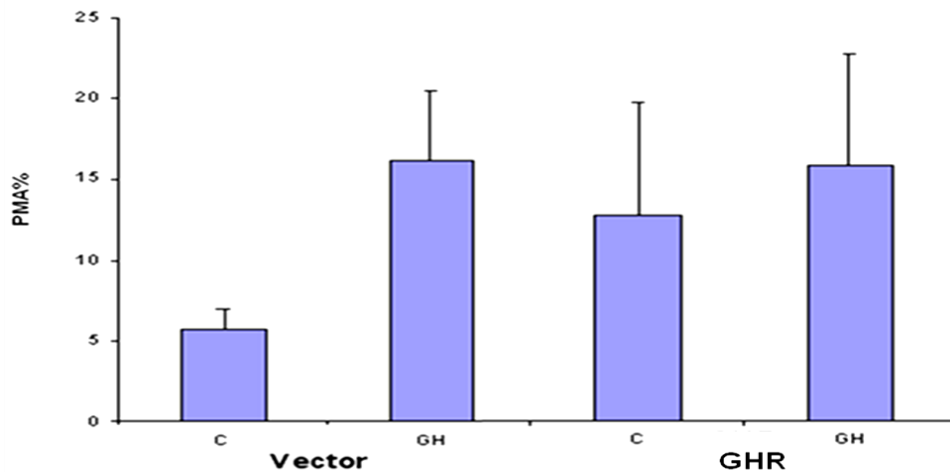


**Figure 4.10 Densitometric analysis of GH on ERK activation in cells transfected with hGHR.**

Densitometric analysis of western blots that look at the effect of GH on ERK activation following cells transfected with 1  $\mu$ g hGHR plasmid. The bands at day 0 observed different results therefore, the result is expressed as % PMA. The Each value is the % of the PMA band for that experiment (mean  $\pm$  SE, n=5). These results show no significant difference between the vector and GHR transfected cells.

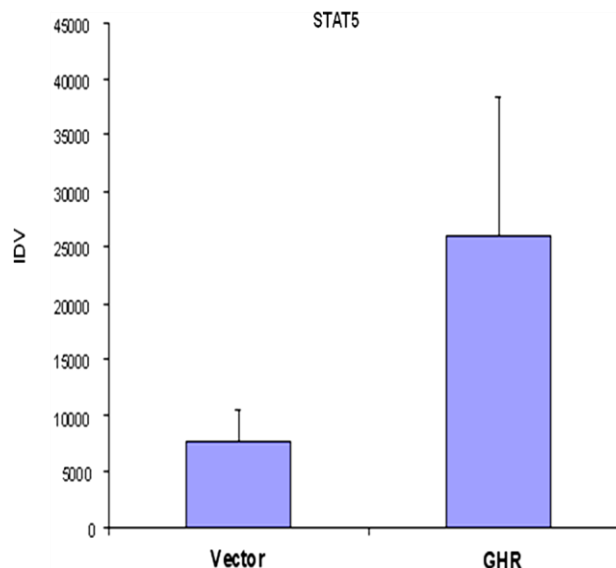


**Figure 4.11 Densitometric analysis of GH on STAT5 activation in cells transfected with hGHR.**

Densitometric analysis of the western blot shows in Figure 4.9. The results (integrated density value, IDV) show GH-stimulated STAT5 activation in transfected cells with hGHR plasmid and empty vector. The results display increased STAT5 activation in hGHR transfected cells.

The same experiment was performed using cells transfected with 10  $\mu$ g hGHR to test if greater over expression of the GHR modulated ERK activation. The results revealed no difference between the levels of activation ERK in cells transfected with 1  $\mu$ g or 10  $\mu$ g hGHR. In conclusion, over expression of the hGHR was shown to have no effect on GH stimulated ERK activation, but slightly increased the level of STAT5 activation.

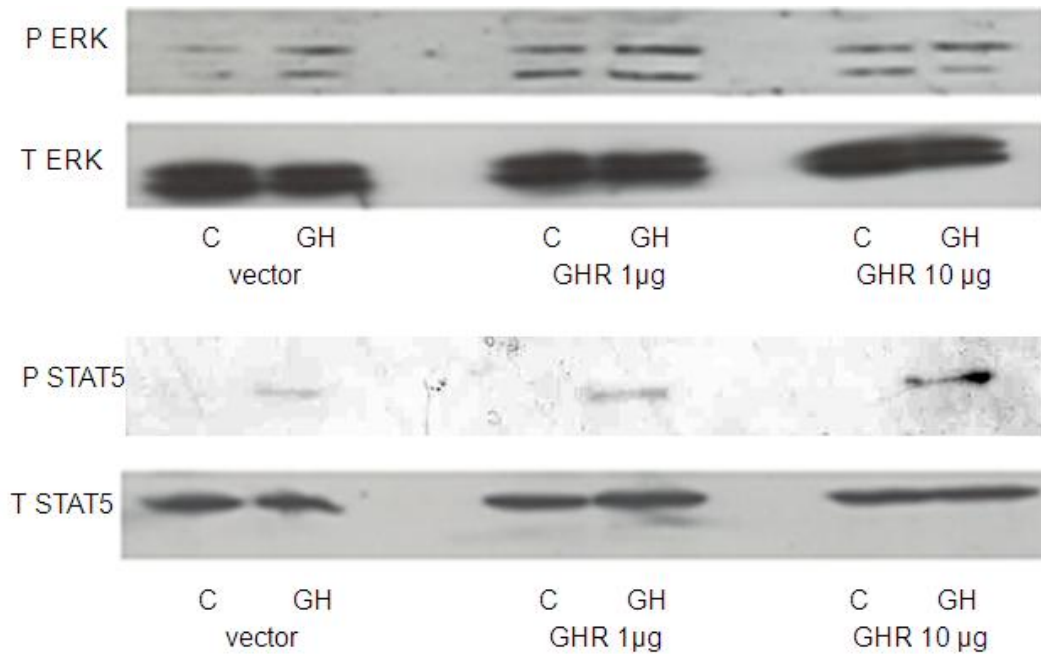


**Figure 4.12 Effect of hGHR dose on GH activation of ERK and STAT5**

Western blot which shows phosphorylation of ERK following GH treatment in cells transfected with 1  $\mu$ g empty vector (Vector) and the GHR expression vector (GHR) and 10  $\mu$ g empty vector (Vector) and the GHR expression vector (GHR). The level of GH-stimulated ERK phosphorylation is unaltered in GHR transfected cells compared 1  $\mu$ g transfected cells and 10  $\mu$ g.

The level of GHR expression in cells transfected with 1  $\mu$ g or 10  $\mu$ g of plasmid was much higher than that achieved during adipogenesis (approximately 10 fold, Chapter 3). Consequently additional experiments were performed using cells transfected with different lower doses 1  $\mu$ g, 0.1  $\mu$ g and 0.01  $\mu$ g hGHR to try to mimic the effects of adipogenesis more closely (see Figure 4.13-4.15). The results show no difference between the levels of activation of ERK in cells transfected with 1  $\mu$ g, 0.1  $\mu$ g and 0.01  $\mu$ g hGHR. Level ERK activation was detected in 1  $\mu$ g, 0.1 $\mu$ g, 0.01  $\mu$ g GHR expression vector compared with empty vector treatment 10 minutes GH (mean  $\pm$  SE, n=3, 1  $\mu$ g p=0.09, 0.1  $\mu$ g p=0.23 and 0.01  $\mu$ g p=0.06). The results show GH-stimulated STAT5 activation in transfected cells with 1  $\mu$ g, 0.1  $\mu$ g and 0.01  $\mu$ g hGHR plasmid and empty vector. The results display increased STAT5 activation in hGHR transfected cells.

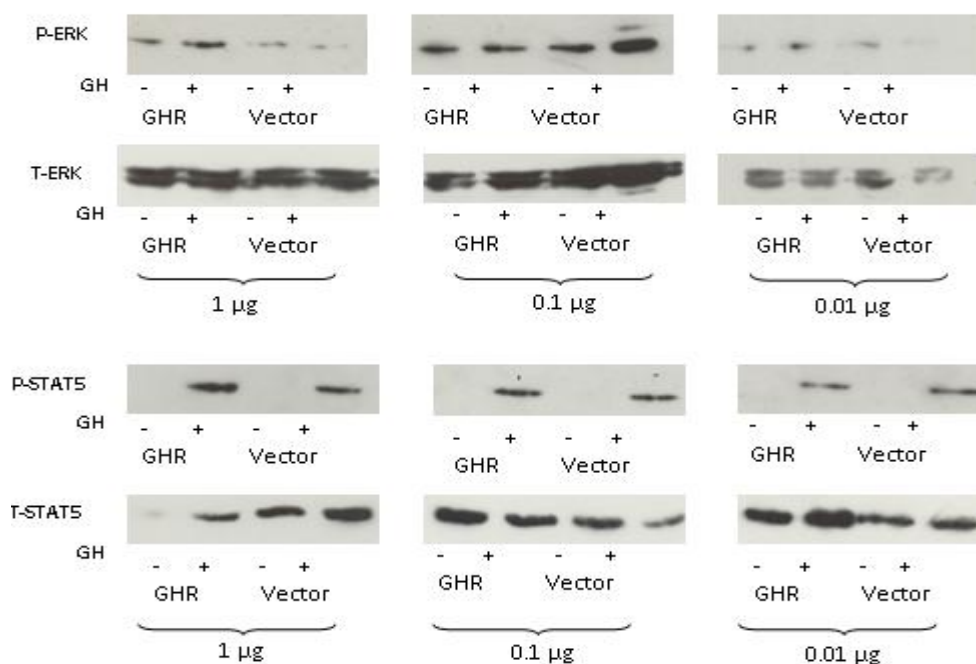


**Figure 4.13 Effect of hGHR dose on GH activation of ERK and STAT5**

Western blot shows phosphorylation of ERK/STAT5 after GH treatment/10 minute in cells transfected with 1  $\mu$ g empty vector (Vector) and 1  $\mu$ g GHR expression vector (GHR), 0.1  $\mu$ g empty vector (Vector) and 0.1  $\mu$ g GHR expression vector (GHR) and 0.01  $\mu$ g empty vector (Vector) and 0.01  $\mu$ g GHR expression vector (GHR). Level of GH-stimulated ERK phosphorylation altered in GHR transfected cells compared empty vector transfected cells (0.1  $\mu$ g GHR expression vector (GHR) and 0.01  $\mu$ g empty vector (Vector)). Level of GH stimulated STAT5 phosphorylation increased with 3T3-L1 transfected with hGHR.

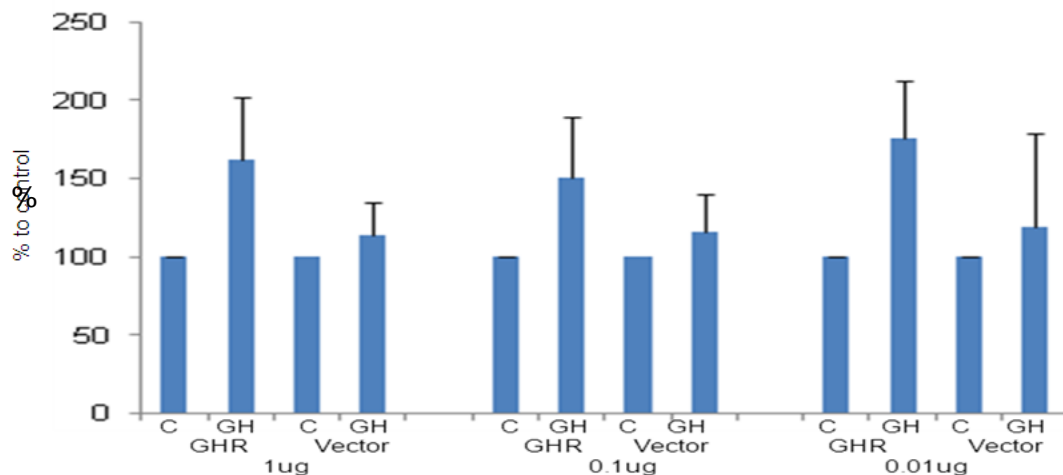


**Figure 4.14 Densitometric analysis of GH on ERK activation following transfection with hGHR.**

Densitometric analysis of western blots which look at the effect of GH on ERK activation following in cells transfected with 1  $\mu$ g, 0.1  $\mu$ g and 0.01  $\mu$ g hGHR plasmid. Each value is the % of the control for that experiments (mean  $\pm$  SE, n=3). These results show no significant difference between the vector and GHR transfected cells.

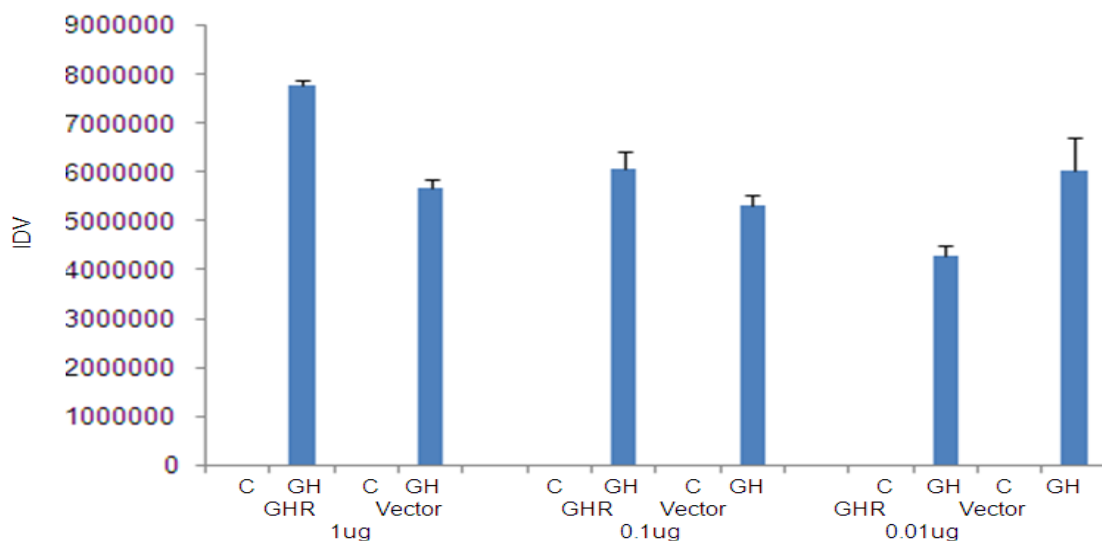


**Figure 4.15 Densitometric analysis of GH on STAT5 activation following transfection hGHR.**

Densitometric analysis of western blots shown in Figure 4.13. Phospho-STAT5 was undetectable in empty vector, but easily detectable in transfected cells with 1  $\mu$ g, 0.1  $\mu$ g and 0.01  $\mu$ g hGHR plasmid, however, since there are no bands empty vector results are expressed as IDV absolute values, (mean  $\pm$  SE, n=3), (integrated density value, IDV). The results show GH-stimulated STAT5 activation in transfected cells with 1  $\mu$ g, 0.1  $\mu$ g and 0.01  $\mu$ g hGHR plasmid and empty vector. The results display increased STAT5 activation in hGHR transfected cells.

## 4.4 Discussion

Results from Chapter 3 demonstrated increased expression of GHR in differentiated 3T3-L1 cells and that adipogenic differentiation had two distinct effects on GHR-associated cell signalling pathways. GH-induced STAT5 activation increased in differentiated cells which reflected the increase in levels of total STAT5 and GHR. In contrast, GH-induced ERK activation declined in differentiated cells while total ERK was unchanged. Elevated levels of PMA-induced ERK activation were observed in differentiated cells. This would appear to be a specific decline in GH-induced ERK activation as GH-induced STAT5 activation and PMA-induced ERK activation both increased with cell differentiation clearly indicating that ERK has the potential to be activated. As such, there seems to be a specific uncoupling of GHR activation from the ERK pathway in adipocyte differentiated 3T3-L1 cells. My second investigation tried to explain this decline in ERK activation.

As previously discussed Love *et al.*, (1998) demonstrated that the ERK pathway adapter protein p66<sup>Shc</sup> was necessary for coupling GH to ERK. The p46<sup>Shc</sup> and p52<sup>Shc</sup> isoforms are expressed in all tissues while the p66<sup>Shc</sup> form was observed to be missing in some types of cells (Almind *et al.*, 1999). Activation of the ERK pathway by GH appears to be cell type specific involving the p66<sup>Shc</sup> form of the adapter protein. p66<sup>Shc</sup> is expressed in 3T3-F442A cells where GH was able to activate both ERK and STAT5, but was found to be absent in IM-9 lymphocyte cells that lack ERK activation following GH treatment (Love *et al.*, 1998). As such, it was proposed that p66<sup>Shc</sup> was necessary to couple GHR activation to the ERK pathway. As such it was hypothesized that down regulation of p66<sup>Shc</sup> may mediate the reduction in GH stimulated ERK in 3T3-L1 cells during conversion of pre-adipocytes into adipocytes. To test whether p66<sup>Shc</sup> levels declined in 3T3-L1 cells undergoing adipocyte differentiation, Shc levels were analysed using western blotting. Contrary to the

original hypothesis p66<sup>Shc</sup> levels did not decrease as 3T3-L1 cells undergoing adipocyte differentiation, but instead were observed to be similar to cells at day 0 and day 8 despite a total lack of GH stimulation of ERK at day 8 in differentiation medium. Therefore, a reduction in p66<sup>Shc</sup> cannot explain the loss of GH-stimulated ERK in differentiation. This result eliminates the possibility that a decline of p66<sup>Shc</sup> levels prevents the activation of ERK in GH-stimulated differentiated 3T3-L1 cells.

During 3T3-L1 differentiation, expression of GHR was observed to increase (section 3.4.5) as previously described by Winston and Bertics, 1992; Jin *et al.*, 2002; Flint *et al.*, 2006; Story and Stephens, 2006 and Lewis *et al.*, 2006. Therefore, it was hypothesized that altered levels of GHR expression may modulate the signalling pathways coupled to the receptor. If this resulted in preferential coupling to JAK2-STAT5, the hypothesis may explain the reduction in GH activated observed during differentiated 3T3-L1 cells. Experiments were performed to test the hypothesis using GHR over expression in 3T3-L1 pre-adipocyte cells to mimic the differentiated state, but failed to cause a decline in GH activation of ERK. The data presented suggests that there is no relationship between the over expression of GHR in 3T3-L1 cells and the decline in ERK activation observed in adipocyte differentiated cells. Instead the level of ERK activation was the same in empty vector and GHR 3T3-L1 transfected cells, while GH-induced STAT5 activation was slightly increased in 3T3-L1 cells transfected with the hGHR vector compared to the empty vector.

The finding that high expression levels of GHR increases during 3T3-L1 differentiation into adipocytes (Zou *et al.*, 1997; Ji *et al.*, 2002; Flint *et al.*, 2006) supports the view that GH acts on adipose tissue through GHR and modulates cellular function (Zou *et al.*, 1997). GH binding to its receptor results in activation of the STAT5 pathway in many cell types including adipocytes (Story and Stephens, 2006). STAT5 levels are increased during adipocyte differentiation and are important

mediators of cell development. Expression of STAT5 proteins correlates with lipid accumulation and the expression of PPAR $\gamma$  and C/EBP $\alpha$  in BMSCs and adipocytes (Winston and Bertics, 1992; Floyd and Stephens, 2003; Lewis *et al.*, 2006).

During physiological processes the ERK pathway plays a critical role in regulating signalling pathways which mediate different cellular processes. The upstream activators of ERK kinases, phosphorylate and activate the MAPKs on regulatory threonine and tyrosine residues, thereby regulating ERK activity (Imajo *et al.*, 2006). ERK is essential in the early phase of adipocyte differentiation while the down regulation of the pathway appears to be more important for cells to progress to later stages of differentiation. Activated ERK is switched off by dephosphorylation by specific phosphatases known as MKPs (Clark, 2003; Dickinson and Keyse, 2006; Roth *et al.*, 2009). Defective activation leads to unusual ERK activity by upstream signalling pathways and/or by defective regulation of the ERK phosphatase 1 (MKP-1) (Cuevas *et al.*, 2007; Roth *et al.*, 2009). MKP-1 plays an essential physiological role in the regulation of MAPK signal transduction pathways by dephosphorylating their serine/threonine and tyrosine residues (Tanoue *et al.*, 2001; Clark, 2003).

The MKP-1 inactivates ERK1 and ERK2, p38 and c-Jun N-terminal kinase (JNK). A variety of stimuli induce MKP-1 expression such as: cellular stresses, pro-inflammatory cytokines and agonists with anti-inflammatory effects which include the transforming growth factor (TGF) cholera toxin B subunit and cAMP elevating mediators (Clark, 2003; Sakaue *et al.*, 2004). Up regulation of MKP-1 in adipocytes differentiation could be the mechanism that causes the reduction of ERK activation in adipocytes. Further studies are planned to investigate this possibility.

Coupling of the GHR to ERK pathway requires the GHR to be localized in the caveolae–lipid raft membrane fraction (Yang *et al.*, 2004). Subcellular fractionation of pre-adipocytes demonstrated a high level of GHR in the caveolae membrane fraction (CM) along with signalling proteins associated with activation of ERK, but no STAT signalling molecules (Yang *et al.*, 2004; Lanning and Carter-Su, 2006). Furthermore, disruption of the CM resulted in reduced activation of ERK by GH, but unaltered activation of STATs (Yang *et al.*, 2004). In differentiated 3T3-L1 cells, the level of GH activation of ERK declined, therefore the possibility may exist that differentiation caused the GHR to move from the CM to the plasma membrane thus explaining the reduced GH-stimulated ERK signalling in adipocyte-differentiated 3T3-L1. Further work is required involving separation of the plasma membrane and CM fraction to confirm this.

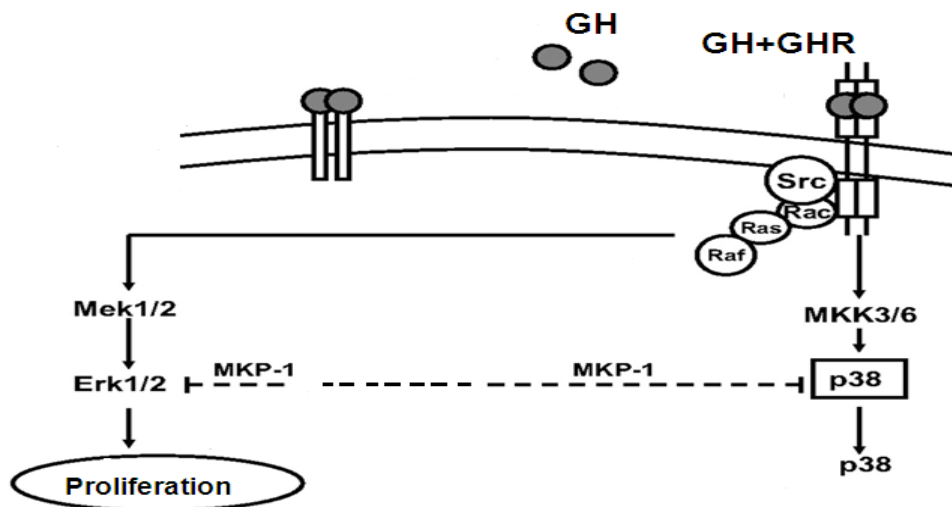


**Figure 4.16:**

MKP-1 target members of the MAP kinases and inactivate their function in both the cytosol and the nucleus.

## **Chapter Five**

**Do similar changes in GH-induced ERK and STAT5 signalling also occur in primary preadipocytes undergoing differentiation? Are there species or depot-specific differences?**

## 5. Chapter Five

### 5.1 Introduction

The studies described in Chapters 2 through 4 used the 3T3-L1 murine pre-adipocyte cell line to investigate GH signalling during adipogenesis. These results illustrated major differences in signalling as differentiation proceeded, distinct effects of GH on the cell signalling pathway which induced STAT5 activation were observed to increase in differentiated cells reflecting an increase in levels of total STAT5 as well as GHR expression. This study has also shown that GH-induced ERK activation decreased in differentiated cells whereas total ERK was unaltered during differentiation.

Characteristics specific to 3T3-L1 pre-adipocytes make them valuable for the study of cellular processes. As these cells are cloned they are homogenous and at the same stage of differentiation which allows for their response to treatment to be both measurable and repeatable. The 3T3-L1 pre-adipocytes can be passaged to provide a regular supply and are able to be maintained in culture for long periods. Also, they can be passaged frequently without affecting those processes necessary for differentiation (Green and Meuth, 1974). Pre-adipocyte cell lines have been used to study the molecular and cellular actions that regulate adipogenesis (Gregoire *et al.*, 1998). Once the cells are confluent (and hence growth arrested) exposure to adipogenic inducers stimulates the early proliferative phase known as mitotic clonal expansion (MCE) (section 1.3.1.1) which in turn is followed by a second growth arrest. The second growth arrest is required for terminal differentiation that leads to adipogenic gene expression (Qiu *et al.*, 2001; Qian *et al.*, 2010). Mature adipocytes acquire a round lipid-filled morphology as they progress through differentiation (Gregoire *et al.*, 1998). They also express adipocyte-specific genes such as PPAR $\gamma$

and C/EBPs which are themselves a product of C/EBP $\beta$  and essential for MCE (Gregoire *et al.*, 1998; Patel and Lane, 2000; Qian *et al.*, 2010; Tang and Lane, 2012). This cell line's capacity to differentiate within 6 to 8 days makes them suitable for studies which are subject to a combination of time constraints and reproducibility. In contrast cultured human primary pre-adipocytes take at least 14 to 15 days to differentiate and experiments are limited by the availability of human adipose tissue along with inconsistencies at the molecular level due to inter-donor variation. Although the 3T3-L1 cell line has been invaluable in elucidating the transcriptional cascade that regulates new fat formation, it is possible that it may behave differently from primary pre-adipocytes or in fat precursors from other species.

### **5.1.1 Human primary pre-adipocyte model**

Adipose tissue depots have different physiological profiles depending on the location of the tissue. Human adipose tissue is commonly described within the literature as residing in two general locations, subcutaneous and visceral. Pre-adipocytes from white adipose tissue (WAT) depots exhibit distinct depot-dependent characteristics. *In vitro* studies of subcutaneous pre-adipocytes have indicated regional variations in the capacity of precursors for replication of pre-adipocyte number, adipogenic differentiation and susceptibility to apoptosis (Tchkonia *et al.*, 2006). Depot-dependent distinctions in the expression level of select adipocyte differentiation marker genes have been identified. Aspects of depot-related pre-adipocyte gene expression are of an inherent and possible cell-autonomous nature. However, these recent studies have highlighted the fact that different white adipose depots should be regarded as distinct (Bjørndal *et al.*, 2011)

Advances in cell culture techniques have made it possible to isolate and culture human primary preadipocytes, which have the advantage of being more physiologically relevant for the study of adipogenesis (Gregoire *et al.*, 1998). Isolation of pre-adipocytes from different anatomical locations allows the characteristics specific to their original locations to be studied *in vitro*. However, there are some limitations when attempting to use human primary pre-adipocytes. First, while placed within culture medium human primary pre-adipocytes differentiate into adipocytes without undergoing MCE (Tang and Lane, 2012). Next, these primary cells are thought to represent a stage that is further along the adipogenic pathway (Gregoire *et al.*, 1998). Finally, primary cell models have a limited life span in culture, grow slowly and vary in their adipogenic potential according to the donor (Newell *et al.*, 2006).

### **5.1.2 Human orbital pre-adipocytes**

Orbital adipose tissue is derived from the neuroectoderm tissue located within the bony orbit cavity (Wolfram-Gabel, 2002). Various *in vitro* studies have shown that adipogenesis occurs in orbital fibroblasts in Graves' orbitopathy (GO); a condition in which overproduction of thyroid hormones by thyroid follicular cells is stimulated by TSH receptor (TSHR) autoantibodies (TRAb). Expansion of orbital adipose tissue is the process of increasing the number and size of adipose cells. This occurs by hyperplasia (the formation of new fat, i.e. adipogenesis) and hypertrophy (adipose cell enlargement). Human orbital cells are capable of undergoing differentiation when cultured in the appropriate medium (Hausman and Richardson, 1998; Valyasevi *et al.*, 1999).

### **5.1.3 Aims**

The principle aims of this chapter were to address these questions: - 1) Do similar changes in GH-induced ERK and STAT5 signalling which take place during 3T3-L1 adipogenesis also occur in primary pre-adipocytes? 2) Are there species or depot-specific differences? This was achieved by studying GH stimulated cell signalling in differentiating primary preadipocytes from murine and human sources and also by comparing the results in differing human depots, i.e. orbit and subcutaneous breast.

## 5.2 Material and methods

### 5.2.1 Isolation and culture of primary mouse pre-adipocytes

Samples of adipose tissue were obtained from mainly subcutaneous fat in the lower abdomen and groin area of male and female mice. The adipose tissue was minced with a sterile scalpel into small pieces and washed three times with HBSS to remove red blood cells. These small pieces were incubated for 40 minutes in a shaking water bath at 37°C with 10 ml HBSS containing 1.5 mg/ml collagenase type II and 1.5% BSA. The suspension was allowed to sediment for 1 minute and then large pieces and debris were removed. The suspension was then centrifuged at 1500rpm for 5 minutes, to form a preadipocytes pellet. These cells were resuspended in complete medium, counted and plated into 6 well plates at 300,000 per well. The preadipocytes were maintained in DMEM (section 2.2.1.1) modified with 20 ml 10% fetal calf serum.

#### 5.2.1.1 Differentiation of primary mouse pre-adipocytes

Although several protocols were tried, the best method used was from Gharibi *et al.*, (2011). In order to induce differentiation, primary mouse cell differentiation medium (Table 5.1) was added when the cells became confluent. The medium comprised a 1:1 mix of DMEM and Ham's F12 supplemented with 10% FCS along with a cocktail of supplements as shown (Table 5.1).

**Table 5.1:** Components of the primary mouse pre-adipocytes differentiation medium.

Components	Final concentration
Dexamethasone	1 $\mu$ M
Indomethacin	50 $\mu$ M
Insulin	500 nM

## **5.2.2 Tissue specimen and preparation**

Orbital adipose was obtained with informed consent and relevant ethical approval (06/WSE03/37) as required from patients undergoing scheduled surgery (Appendix 2). Orbital fat biopsies approximately 4-8 mm in length taken during surgery were transported to the laboratory in normal saline at room temperature. These biopsies were diced using a scalpel blade and placed in 6 well plates in complete medium DMEM/F12 10% FCS (see Chapter 2, section 2.2.1.1). Preadipocytes migrate out from the explants and were maintained in the culture plate as a monolayer at 37°C in a humidified atmosphere of 5% CO<sub>2</sub>. Cells were grown to confluence replacing media every 7 days. The cells were trypsinized and frozen in liquid nitrogen until further use. Cells were used at low passage number (less than 3).

### **5.2.2.1 Cell culture of primary human pre-adipocytes**

Human primary orbital pre-adipocytes were cultured in complete medium (section 2.2.1.1). The cells were plated in 6 well plates and once confluent the medium was changed to differentiation medium.

### **5.2.2.2 Differentiation of primary human pre-adipocytes**

In order to induce differentiation in primary human orbital pre-adipocytes the medium was changed to differentiation medium (section 2.2.1.4) when the cells became confluent. This medium comprised of a 1:1 mix of DMEM and Ham's F12 supplemented with 10% FCS along with a cocktail of supplements (Table 2.1). Adipogenesis was assessed using phase contrast microscope to detect the characteristic morphological changes of cell rounding and accumulation of lipid droplets, Oil Red O staining and transcript measurement of adipogenic markers, PPAR $\gamma$  and lipoprotein lipase (LPL), by QPCR as described previously (section 2.2.2.1).

### **5.2.3 Breast fat tissue extraction**

Preadipocytes from breast adipose tissue removed during planned surgery were also obtained with ethical approval (06/WSE03/37) and informed consent (Appendix 2). Samples of adipose tissue were collected and placed in 20 ml universal container containing 7 ml of HBSS, 1 ml 300 mg/ml collagenase type II and 2 ml 7.5% BSA. These were then incubated for 1 hour in a water bath at 37°C, shaking every 5 minutes. The resultant solution was centrifuged at 4°C for 5 minutes at 1500 rpm. Supernatant was removed leaving cell pellets that were resuspended in complete medium and placed in 75 cm<sup>2</sup> flask containing 20 ml complete medium at 37 °C. Following 24 hours the cells were washed twice with 5 ml of HBSS to remove any remaining red blood cells. The cells were trypsinized and frozen in liquid nitrogen until further use. The cells were plated in 6 well plates with complete medium (section 2.2.1.1), once confluent medium was changed to differentiation medium (section 2.2.1.4).

### **5.2.4 Oil Red O staining**

Oil Red O staining was performed as previously described (section 2.2.1.5).

#### **5.2.4.1 Cell proliferation studies**

Cell numbers were determined using a hemocytometer. The 3T3-L1 or human primary pre-adipocyte cells were cultured as described previously (see Chapter 2, section 2.2.1.1). In three independent experiments cells were grown in 6-well plates. Once confluent, medium was changed to differentiation medium (section 2.2.1.4). Media in all wells was changed every 24 hours. At each time point medium was removed and cells trypsinized as described (section 2.2.1.2). Cells were then re-suspended in 1 ml complete medium (section 2.2.1.1). The number of cells/ml of

solution was estimated using a haemocytometer. Each sample was counted three times and an average value used in the statistical analysis.

## 5.2.5 QPCR analysis of gene expression

QPCR analysis of gene expression was performed as previously described (section 2.2.2.)

### 5.2.5.1 Extraction RNA of primary mouse adipocytes cultures

RNA was isolated as previously described (section 2.2.2.1).

### 5.2.5.2 Reverse transcription

RNA was reverse transcribed to cDNA as previously described (section 2.2.2.2). The primers for the hPPAR $\gamma$ , hLPL and hAPRT QPCR assays are detailed (Table 5.2) Rice *et al.*, 2010). The mouse cultures used the same primers as 3T3-L1 cell line (Table 2.2) (Zhang *et al.*, 2006).

**Table 5.2:** QPCR primers along with amplicon size.

<b>hPPAR<math>\gamma</math></b>		
<b>Forward</b>	<b>Reverse</b>	<b>Amplicon size</b>
CAGTGGGGATGTCTCATAA Exon3 (300 nM)	CTTTTGGCATACTCTGTGAT Exon5 (500 nM)	390 bp
<b>hARPT</b>		
<b>Forward</b>	<b>Reverse</b>	<b>Amplicon size</b>
GCTGCGTGCTCATCCGAAAG Exon 3 (300 nM; using 100nM)	CCTTAAGCGAGGTCAGCTCC Exon 5 (500 nM; using 100 nM)	247 bp
<b>hLPL</b>		
<b>Forward</b>	<b>Reverse</b>	<b>Amplicon size</b>
GAGATTTCTCTGTATGGACC Exon 7 (300 nM)	CTGCAAATGAGACACTTTCTC Exon 9 (300 nM)	275 bp

### **5.2.6 Western blot analysis of protein**

Western blotting techniques were used to determine P-ERK, total ERK, P- STAT5 and total STAT5 levels during differentiation of the cells, using the same antibodies and protocol as for the 3T3-L1 cells (section 3.2.2). Western blot was also used to analyse the endogenous levels of total PPAR $\gamma$  protein. Blots were incubated in rabbit PPAR $\gamma$  monoclonal antibody overnight at 4°C (Cell Signalling, Technology, Danvers, MA, USA) at 1:1000 dilution. Secondary antibody, anti-rabbit IgG horseradish peroxidase (GE Healthcare, Little Chalfont, Bucks, UK), was used at a 1:5000 dilution for 1 hour. The blots were then visualised using ECL Plus (GE Healthcare) as described earlier (section 3.2.2.6).

### **5.2.7 Statistical analysis**

Statistical analysis was performed as described (section 2.2.3.).

## 5.3 Results

### 5.3.1 Are the changes in GH signalling during adipogenesis unique to the 3T3-L1 cell line?

During 3T3-L1 differentiation GHR levels increase. Additionally there is alteration in GHR associated cell signalling in differentiated cells. GH-induced STAT5 activation and total STAT5 increased, while GH-induced ERK activation decreased in differentiated cells, but total ERK was unchanged and high levels of PMA-induced ERK activation were also observed. This inverse relationship between the decline in GH-induced ERK activation compared to increased GH-induced STAT5 together with increased levels of GHR suggests that there is a specific uncoupling of GHR activation from the ERK pathway differentiated 3T3-L1 cells *in vitro*.

In the first part of this chapter mouse primary pre-adipocytes were studied to determine whether the effects observed in the 3T3-L1 cells were a feature unique to this cell line. The differentiation protocol developed by Zhang *et al.* (2006) which was used to differentiate the 3T3-L1 cell line was used initially but the primary mouse pre-adipocytes failed to achieve differentiation. Various parameters of this protocol were changed, again with no success. After exhausting all variations of this method (data not shown) the protocol from Gharibi *et al.*, (2011) was used which allowed robust differentiation to be achieved as described below.

### **5.3.1.1 Morphology of primary mouse cells during differentiation**

During differentiation primary mouse cells underwent morphological changes characteristic of conversion from fibroblast to adipocyte morphology. Undifferentiated primary mouse cells have the appearance of fibroblasts with an elongated shape (Figure 5.1). Whereas the cells cultured in differentiation medium (section 5.2.1.1) appear to have a morphology more typical of mature adipocyte cells at day 9 where they appear as very rounded shape and with lipid droplet accumulation in approximately 50-60% cells (Figure 5.1D), which is slightly less than in the 3T3L1 cell line. Apart from this, no differences were observed between primary mouse and 3T3-L1 mouse pre-adipocytes cell line samples at the microscopic level during routine differentiation occurring over the same time points in both cultures. However, the primary cells were obviously larger and more rounded than 3T3-L1 cell line pre-adipocytes.

### **5.3.1.2 Oil Red O of primary mouse cells during differentiation**

Primary mouse cells undergoing adipogenic differentiation were stained with Oil Red O to highlight the lipid droplets (Figure 5.1). No Oil Red O staining was detected at day 0 (Figure 5.1B). However, by day 9 in differentiation medium approximately 50-60% of the cells contained Oil Red O (Figure 5.1D). The results show that primary mouse cells differentiate well using this protocol as assessed by Oil Red O staining after 9 days.

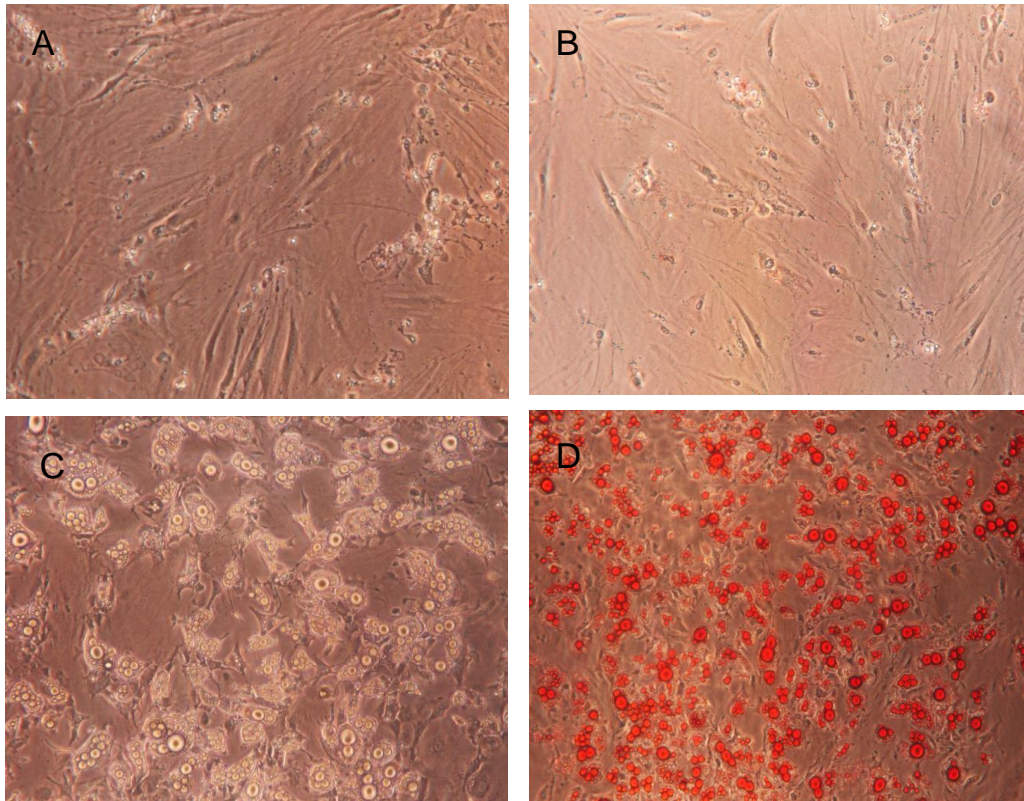


**Figure 5.1: Mouse adipocyte differentiation**

Phase contrast photomicrographs which show various stages of mouse pre-adipocyte differentiation. (A) Undifferentiated mouse pre-adipocytes at day 0 and cells (C) after 9 days in differentiation medium. (B) Undifferentiated Oil Red O stained cells at day 0, and (D) after 9 days in differentiation medium. After 9 days in differentiation medium lipid droplet accumulation in differentiated cells is clearly visible. Magnification 100x

### 5.3.1.3 PPAR $\gamma$ expression during primary mouse cells differentiation

QPCR was used to determine PPAR $\gamma$  (Table 2.2) gene expression at 0, 5 and 9 days after the start of differentiation. Mouse ARP (Table 2.2) housekeeping gene was used for studies investigating differentiation of the mouse per-adipocytes cells. ARP housekeeping gene expression showed minimal change during differentiation (Figure 5.2). Results are expressed as fold increase compared to cultures at day 0 with mean  $\pm$  SE, n=3. PPAR $\gamma$  expression increased (Figure 5.3 and Table 5.3) with high expression of PPAR $\gamma$  observed in differentiated cells at day 5 ( $5.19 \pm 1.80$  mean  $\pm$  SE, n=3 \*p < 0.046) and day 9 ( $4.90 \pm 1.11$  mean  $\pm$  SE, n=3, compared to day 0, \*p < 0.050).

This data demonstrates an overall increase in PPAR $\gamma$  transcript number following the differentiation protocol in mouse adipocytes and 3T3-L1 cells, with the magnitude of increase slightly greater in 3T3-L1 (Table 5.4).

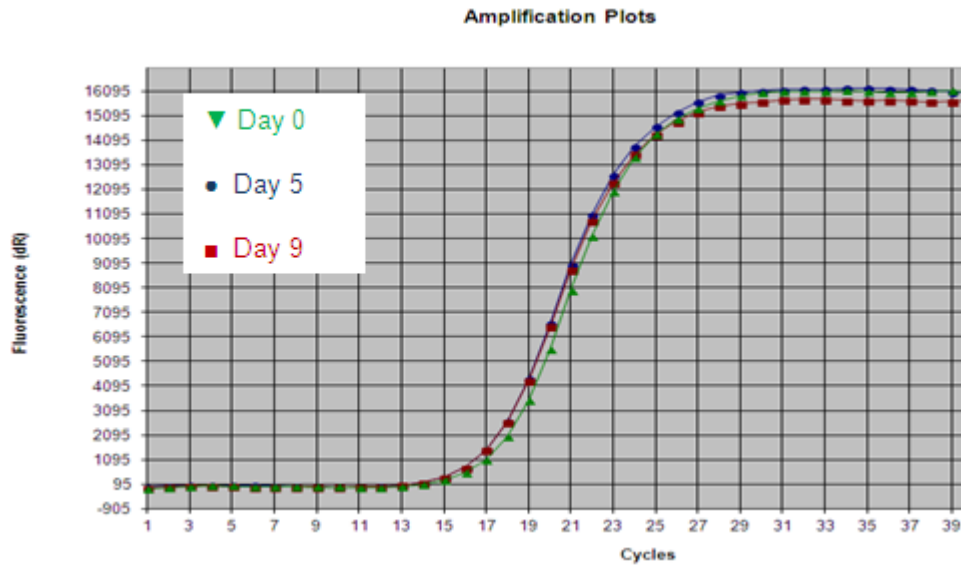


**Figure 5.2: ARP amplification plot**

Amplification plots show that ARP expression was unchanged during primary mouse pre-adipocytes differentiation. Cells were treated in differentiation medium at day 0, 5 and 9. The plots show that the Ct values were minimally altered by the length of time in differentiation medium (Table 5.3).

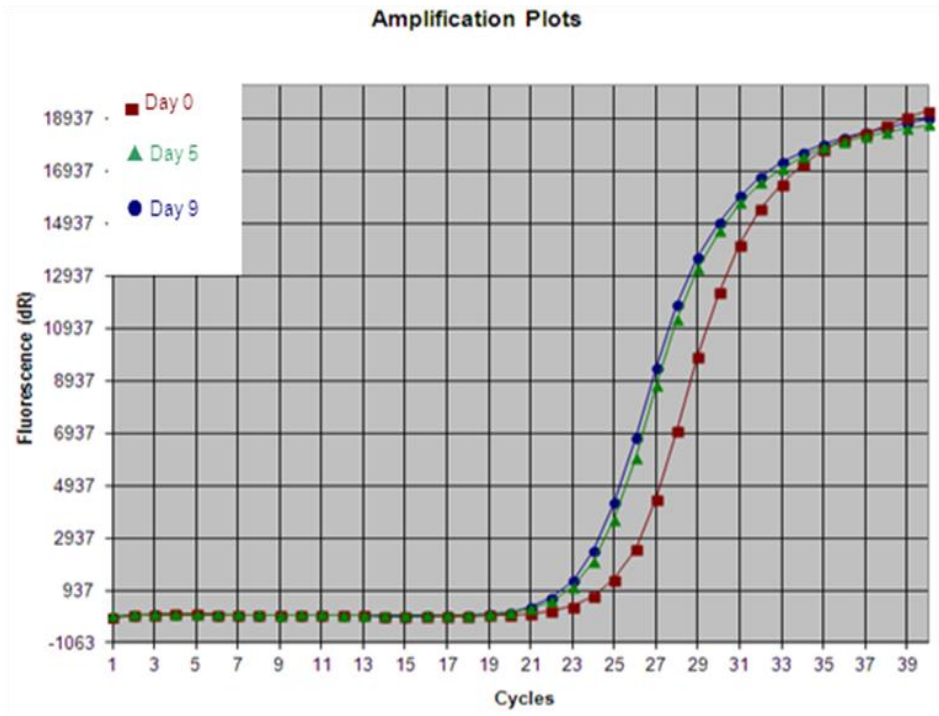


**Figure 5.3: PPAR $\gamma$  amplification curve**

PPAR $\gamma$  amplification curves at day 0, 5 and 9 after the addition of differentiation medium. PPAR $\gamma$  expression was increased during primary mouse pre-adipocytes differentiation.

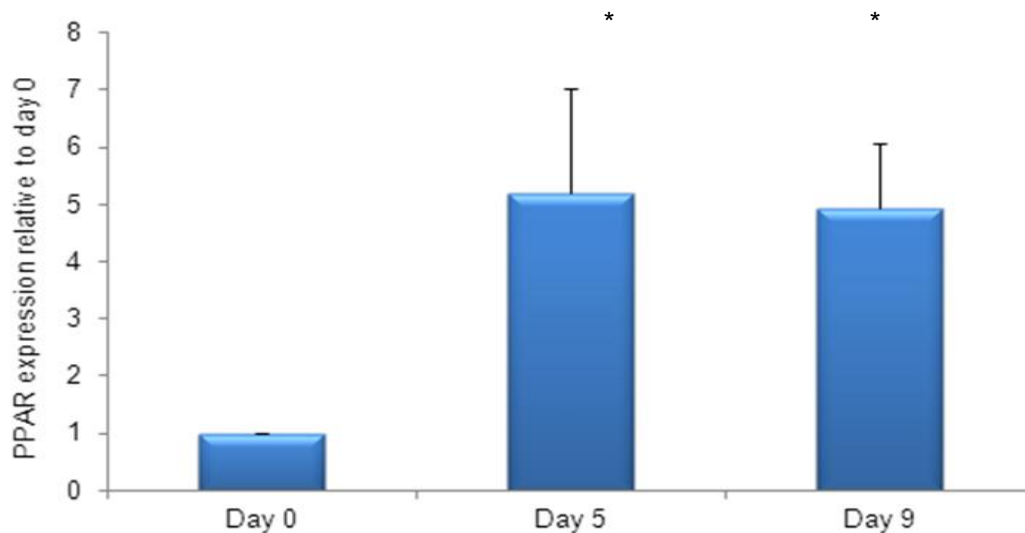


**Figure 5.4: PPAR $\gamma$  expression during primary mouse pre-adipocytes differentiation**

QPCR analysis of PPAR $\gamma$  expression during primary mouse pre-adipocytes differentiation shows increase of PPAR $\gamma$  at day 5 and day 9 with differentiation medium compared to control cultures at day 0 (n=3).

**Table 5.3: PPAR $\gamma$ /ARP Ct values**

Ct values for PPAR $\gamma$  and ARP QPCR assays during mouse adipogenic differentiation at day 0, 5 and 9 shows increased the level of PPAR $\gamma$  expression, reduced the Ct value, minimal effect on ARP.

	Ct value		
	0 days	5 days	9 days
ARP	15.45	15.45	15.89
PPAR $\gamma$	23.77	22.77	21.89

**Table 5.4: QPCR for PPAR $\gamma$**

QPCR for PPAR $\gamma$  in both 3T3-L1 cells and mouse primary adipocytes following 9 days exposure to differentiation medium. Data are presented as mean  $\pm$  SE. Mean values of the results obtained from 3 separate experiments (n=3). The PPAR $\gamma$  expression increased in both, but was slightly greater in 3T3-L1 than mouse primary adipocytes.

PPAR $\gamma$ expression relative to day 0			
Samples	Day 5	Day 8	Day 9
3T3-L1	7.68 $\pm$ 1.346	11.73 $\pm$ 3.11	
Primary adipocytes	5.19 $\pm$ 1.80		4.9 $\pm$ 1.11

### 5.3.1.4 GPDH expression during primary mouse cells differentiation

QPCR was used to determine GPDH (Table 2.2) gene expression at 0, 5 and 9 days after the start of differentiation. Mouse ARP housekeeping gene was used for studies that investigated differentiation of the mouse adipocytes cells. ARP housekeeping gene expression showed minimal change during differentiation (Figure 5.2). Results are expressed as fold increase compared to cultures at day 0 with mean  $\pm$  SE, n=3. GPDH expression increased (Figure 5.5 and 5.6, Table 5.5 and 5.6) with high levels of GPDH observed in differentiated cells at day 9 ( $16.44 \pm 4.53$ ) compared to day 0, \* p<0.05 (Figure 5.6). This data demonstrate an overall increase in GPDH transcript number following the differentiation protocol in both mouse adipocytes cells and 3T3-L1 cell line, again with the increase greater in the cell line.

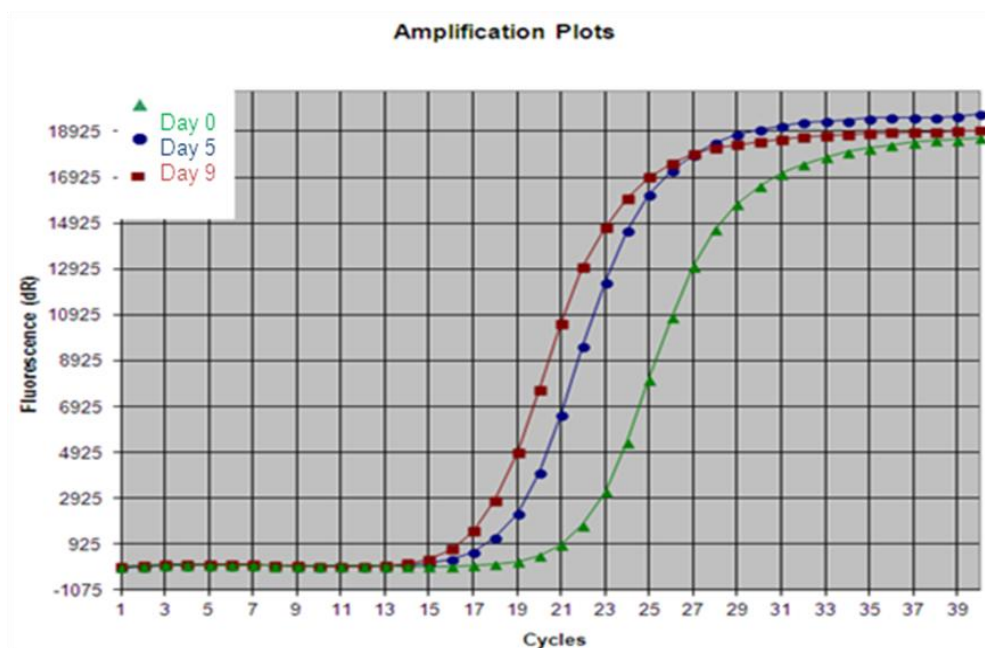


**Figure 5.5: GPDH amplification curve**

GPDH amplification curves at day 0, 5 and 9 after the addition of differentiation medium. GPDH expression was increased during primary mouse pre-adipocytes differentiation.

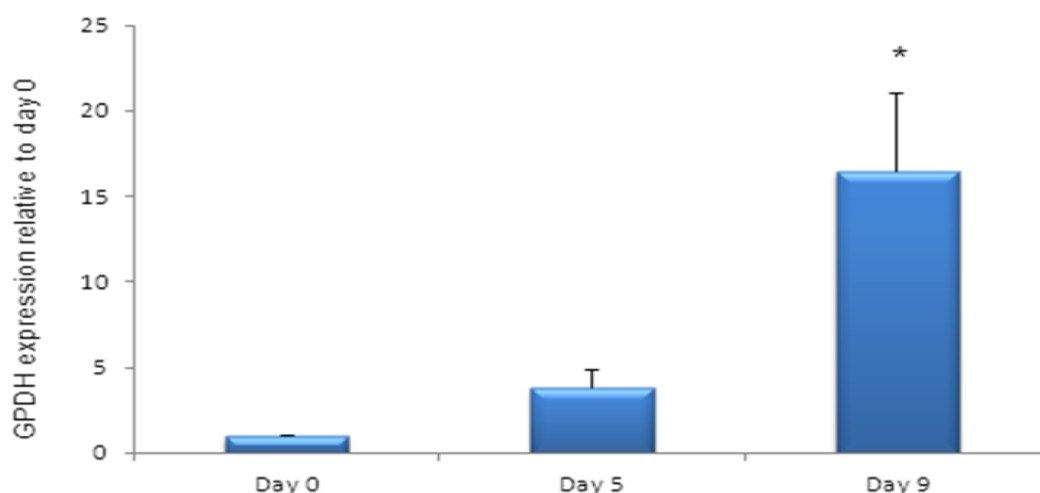


**Figure 5.6: GPDH expression during primary mouse pre-adipocytes differentiation**

QPCR analysis of GPDH expression during primary mouse pre-adipocytes differentiation shows increase of GPDH at day 9 with differentiation medium compared to control cultures at day 0. \* $p < 0.05$ , vs. control cultures,  $n=3$  separate experiments, ANOVA, post hoc analysis with Student-Newman-Keuls test.

**Table 5.5: GPDH Ct values**

Ct values for GPDH and ARP QPCR assays during mouse adipogenic differentiation at day 0, 5 and 9 shows increased the level of GPDH expression, reduced the Ct value, minimal effect on ARP.

	Ct value		
	0 days	5 days	9 days
<b>ARP</b>	15.45	15.45	15.89
<b>GPDH</b>	20.60	17.17	15.94

**Table 5.6: QPCR for GPDH**

QPCR for GPDH in both 3T3-L1 cells and mouse primary adipocytes follow 9 days exposure to differentiation medium. Data are presented as mean and SE. Mean values of the results obtained from 3 separate experiments. GPDH in both 3T3-L1 cells and mouse primary adipocytes increase during cell differentiation while slight increase in 3T3-L1 cell line.

GPDH expression relative to day 0			
Samples	Day 5	Day8	Day 9
<b>3T3-L1</b>	8.97 ± 1.20	53.76 ± 2.65	
<b>Primary adipocytes</b>	3.76 ± 1.10		16.44 ± 4.53

### 5.3.1.5 GHR expression during primary mouse pre-adipocytes differentiation

The level of GHR (Table 3.3) gene transcription during mouse pre-adipocytes differentiation was analyzed using QPCR. Results are expressed as fold increase compared to cultures at day 0 with mean  $\pm$  SD, n=3. GHR expression increased during the differentiation process (Figure 5.7 and Table 5.7) with higher expression levels being observed in differentiated cells at day 9 ( $7.033 \pm 1.86$  of day 0 \*p<0.05 vs. day 0, n=3). These data demonstrate an overall increase in GHR transcript number following the differentiation protocol in mouse adipocyte cells and 3T3-L1 cell lines. In both cases GHR expression increased with differentiation and by the same amount in 3T3-L1 and primary cells.

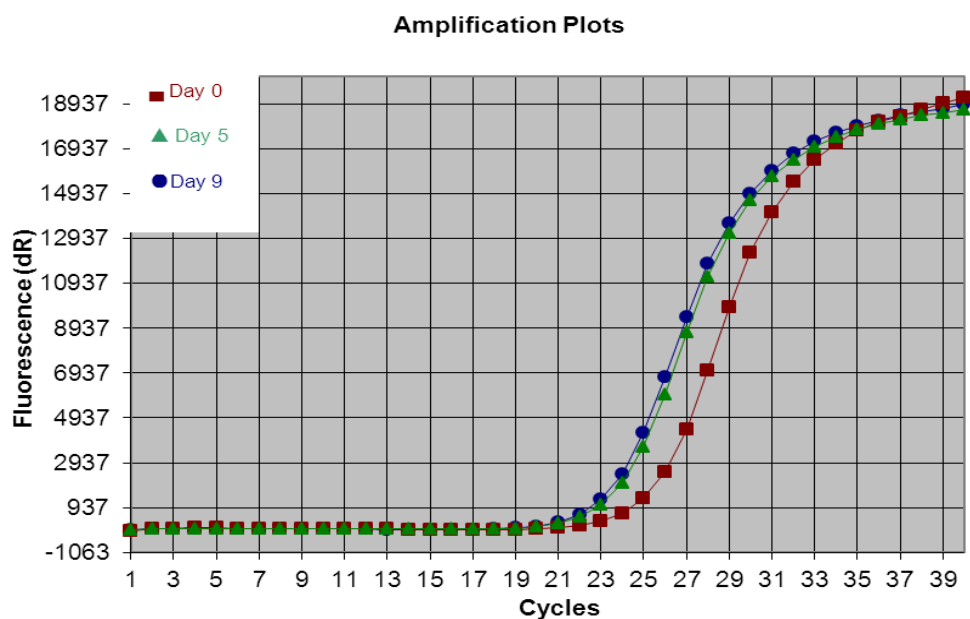


**Figure 5.7: Amplification curve of GHR**

GHR QPCR amplification curve primary mouse cells in differentiation medium at day 0, 5 and 9. GHR expression increased with the primary mouse cells differentiation.

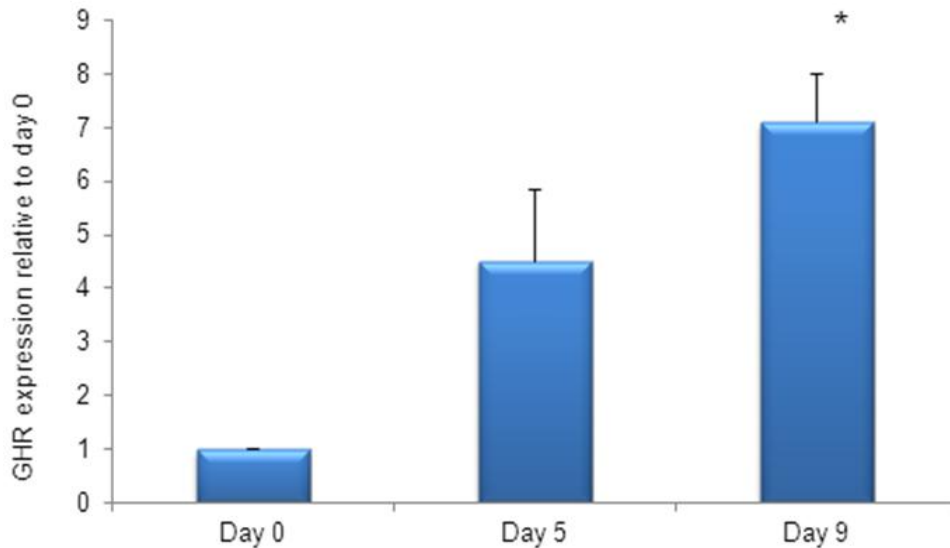


**Figure 5.8: GHR expression during mouse pre-adipocytes differentiation**

QPCR analysis of GHR expression during mouse pre-adipocytes differentiation shows a significant increase with cellular differentiation compared to control cultures, \*  $p < 0.05$  vs. day 0 cultures,  $n = 3$ .

**Table 5.7: GHR and ARP QPCR assays**

Ct values for the GHR and ARP QPCR assays during primary mouse adipogenic differentiation at day 0, 5 and 9 shows that differentiation increased GHR expression reducing Ct value, but had minimal effect on ARP.

	Ct value		
	0 days	5 days	9 days
ARP	15.45	15.45	15.89
GHR	26.13	25.43	24.61

**Table 5.8: QPCR for GHR**

QPCR for GHR in both 3T3-L1 cells and mouse primary adipocytes following a 9 day exposure to differentiation medium. Data are presented as mean and SE. Mean values of the results obtained from 3 separate experiments. The GHR expression increased was similar in 3T3-L1 and primary cells.

GHR expression relative to day 0			
Samples	Day 5	Day 8	Day 9
3T3-L1	4.5 ± 3.20	6.0 ± 2.65	
Primary adipocytes	4.0 ± 2.4		7.033 ± 1.86

### **5.3.1.6 Basal ERK activation during mouse primary pre-adipocytes differentiation**

Mouse primary pre-adipocyte were plated in 6 well plates and once confluent were incubated with differentiation medium and samples collected at day 0, 5 and 9. Medium was changed every two days. The mouse primary cells were analysed over time points when the medium was removed and cells were then washed twice with 1 ml of PBS. Cells were lysed with 250  $\mu$ l loading buffer and were rapidly frozen in liquid nitrogen before being stored at  $-20^{\circ}\text{C}$ . Basal ERK phosphorylation (activation) was detected by western blotting. The bands are phospho-ERK1 (p44) and ERK2 (p42) (Figure 5.9 below). Basal ERK activation was influenced by the length of time in differentiation medium with high activation at day 0 of both ERK1 (p44) and ERK2 (p42). The level of p42 ERK activation reduced with increased adipogenic differentiation to a level that is barely detectable by day 9 in contrast levels of p44 ERK remained unchanged. The appearance of the cells altered over the time points of experiment changing from an elongated fibroblast shape into more rounded cells which can be seen from day 9 onward. This observation was accompanied by an increase in lipid droplet accumulation, being seen in approximately 50-60% of the mouse primary cells by day 9. The data demonstrated slower reduction in p ERK in primary mouse adipocytes compared with 3T3-L1 samples (see Chapter 3 section 3.3.1).

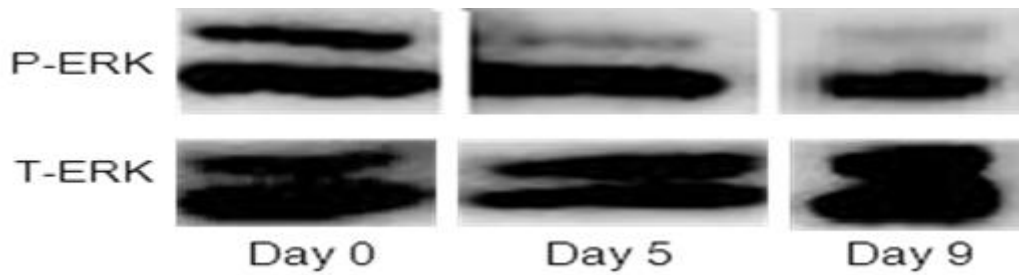


**Figure 5.9: Basal P-ERK and total ERK levels**

Basal P-ERK activation and total ERK during mouse primary pre-adipocytes differentiation.

### **5.3.1.7 GH stimulated ERK and STAT5 activation during primary mouse pre-adipocytes differentiation**

*In vitro* differentiated mouse primary adipocytes were treated with GH and PMA. GH-induced ERK and STAT5 activation was analysed by phospho-specific western blotting in cells treated for 10 minutes with GH (50nM). These experiments were performed and the combined results are summarised in a histogram shown in (Figure 5.11). The results of each experiment were somewhat different as illustrated by the large error bars, but in all cases demonstrated very little GH induced p ERK at day 0 in three separate experiments (n=3). In two experiments the highest GH-induced p ERK occurred on day 9, but in the third experiment day 5 was maximal, total ERK was unchanged in all cases indicating equal lane loading (Figure 5.10).

Following densitometry assessment, the maximum phosphorylated ERK by GH in primary mouse adipocyte cells was observed at day 5 compared to control at day 0 ( $242.30\% \pm 141.53$  of day 0, at day 5 vs. day 0,  $p > 0.05$   $n=3$ ) and at day 9 ( $230.28\% \pm 84.21$  of day 0, at day 9 vs. day 0,  $p > 0.05$   $n=3$ ). Phospho-STAT5 was undetectable at day 0, but easily detectable at days 5 and 9, however, since there are no bands at day 0 results are expressed as IDV absolute values, mean  $\pm$  SE,  $n=3$ . GH-stimulated STAT5 phosphorylation was increased with higher change being observed in differentiated cells at day 5 ( $5829084 \pm 1567543$ , absolute value IDV,  $n=3$ ) and 9 ( $10701144 \pm 3565432$ ,  $*p < 0.05$   $n=3$ ) and total STAT5 increased with significantly higher levels being observed in differentiated cells ( $228.23\% \pm 24.97$  of day 0, at day 9,  $p < 0.01$  vs. day 0,  $*p < 0.05$   $n=3$ ) (Figure 5.11).

This data demonstrated significant variations between preadipocytes from primary sources compared with a cell line during differentiation. Hence levels of ERK activation in primary mouse adipocytes and 3T3-L1 samples (see Chapter 3 section 3.3.2) were different. These results seem to indicate that the specific uncoupling of GHR activation from the ERK pathway during adipogenesis may be unique to the 3T3-L1 cell line.

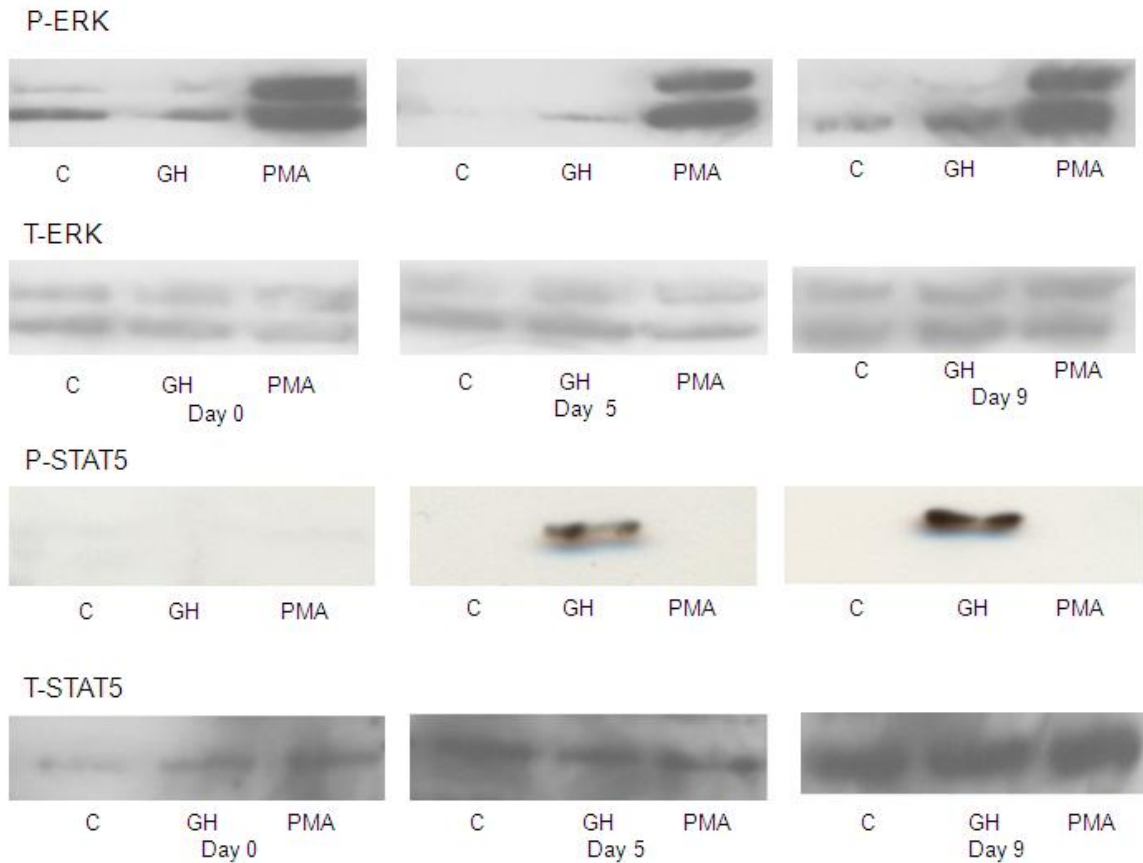


**Figure 5.10: Phosphorylation of ERK and STAT5**

A western blot which shows phosphorylation of ERK and STAT5 following GH stimulation (+) over a time points at day 0, 5 and 9 in adipocyte differentiation medium. The level of GH-stimulated ERK phosphorylation shows change with increasing time in differentiation medium. The total ERK blot has two bands; the upper is p44 and lower the p42. In contrast the level of total STAT5 and GH stimulated STAT5 phosphorylation increased with mouse primary adipocytes differentiation. PMA shows levels of ERK activation were the same during differentiated cells with no significant difference between them.

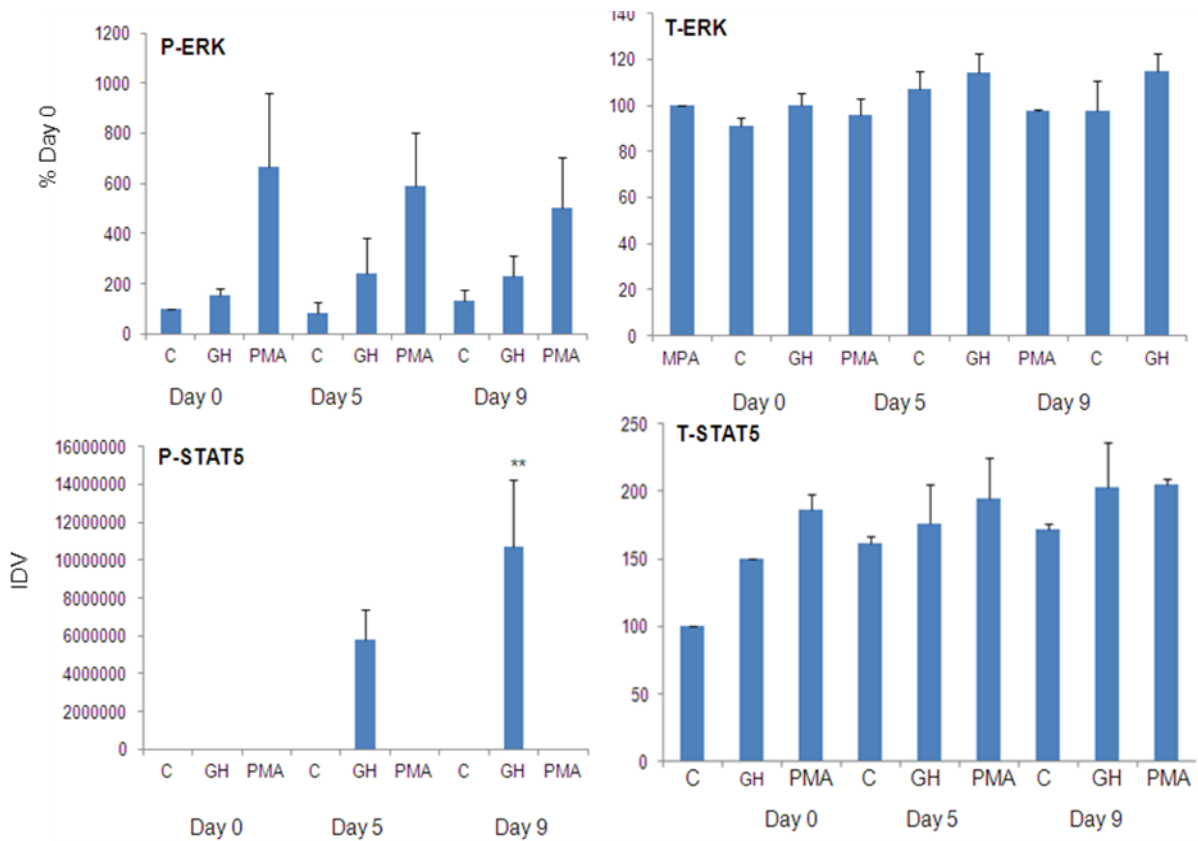


**Figure 5.11: Densitometric analysis of ERK and STAT5**

Densitometric analysis of the western blots (Figure 5.10) the results are expressed as % day 0 for P-ERK, total ERK and total STAT5 but P-STAT5 undetectable at day 0, but easily detectable at days 5 and 9, however, the result for P-STAT is expressed as IDV absolute values, mean  $\pm$  SE, n=3 and demonstrated increased total STAT5 and GH-stimulated STAT5 activation following differentiation despite no changed in ERK activation and total ERK.

### **5.3.2 Are the changes in GH signalling during adipogenesis species dependent?**

Having established the similarities and differences between mouse pre-adipocyte cell lines and primaries, this study considered whether the change in GH signalling might be dependent on donor species and fat depot. The capacity for differentiation may differ significantly depending on the species, the anatomical origin of the adipose tissue, the age and gender of the donor. Samples of human adipose tissue were collected during surgery, the research interests of another group made fat from the orbit available. This fat is not typical being derived from neural crest whereas other fat depots originate from the mesoderm, but there was sufficient supply to investigate whether there are differences in GH induced ERK activation and other aspects of adipogenesis, for comparison with the 3T3-L1 pre-adipocytes cell line.

#### **5.3.2.1 Morphology of primary human orbital cells during differentiation**

While in differentiation medium (section 5.2.2) (Zhang *et al.*, 2006) primary human orbital cells underwent morphological change characteristic of conversion from fibroblast to adipocyte morphology. Undifferentiated primary human orbital cells have the appearance of fibroblasts with an elongated shape (Figure 5.12). Whereas the cells cultured in differentiation medium for 15 days (section 5.2.2) appear to have morphology more typical of mature adipocyte cells where they appear rounded in shape and some of them eventually acquire large lipid vacuoles with lipid droplet accumulation. The amount of differentiation induced was highly variable across the plate. In some regions it was observed in approximately 40-50% of the primary human orbital cells (foci of differentiation, Figure 5.12C) but was absent in other parts of the plate. In addition, adipogenesis in the orbital requires at least 15 days in differentiation medium, thus less differentiation can be induced when compared with murine cell lines or primary preadipocytes.

### 5.3.2.2 Oil Red O of human orbital during differentiation

Primary human orbital cells undergoing adipogenic differentiation stained with Oil Red O to highlight lipid droplets (Figure 5.12). No Oil Red O staining was detected at day 0 (Figure 5.12B). However, by day 15 in differentiation medium approximately 40-50% of the cells in foci of differentiation contained Oil Red O (Figure 5.12D). The results show that primary human orbital cells differentiate well using this protocol as assessed by Oil Red O staining after 15 days.

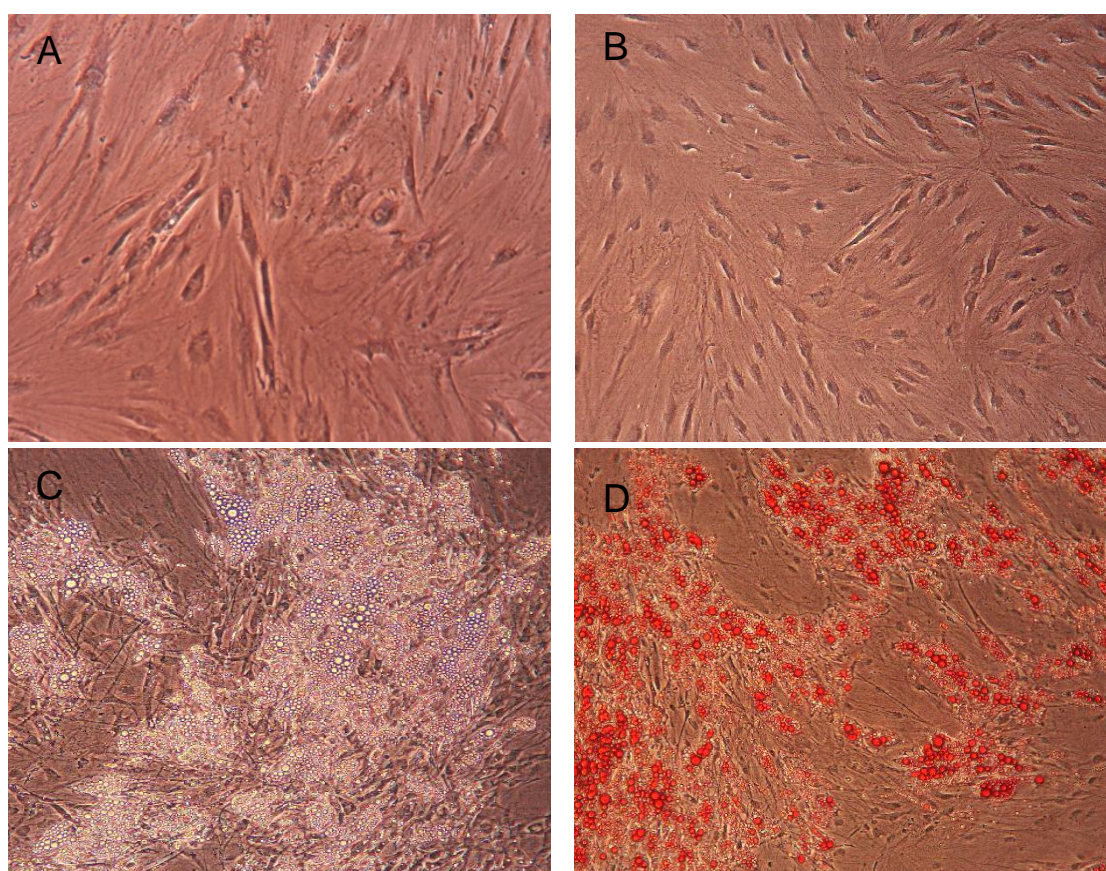


**Figure 5.12: Adipocyte differentiation**

Phase contrast photomicrographs show various stages of adipocyte differentiation. (A) Undifferentiated human orbital pre-adipocytes at day 0 and (C) cells after 15 days in differentiation medium. (B) Undifferentiated Oil Red O stained cells at day 0 and (D) after 15 days in differentiation medium stained with Oil Red O. After 15 days in differentiation medium lipid droplet accumulation in differentiated cells was clearly visible in 40-50% of the cells. Magnification 100x

### 5.3.2.3 LPL expression during primary orbital cells differentiation

QPCR was used to determine LPL (Table 5.2) gene expression in the human orbital cells at day 0, 7 and 15 after the start of differentiation. Human adenine phosphorybosyltransferase (APRT) (Table 5.2) housekeeping gene was used for studies which investigated differentiation of the orbital adipocytes cells (Rice *et al.*, 2010). APRT housekeeping gene expression showed minimal change during differentiation of the human orbital pre-adipocytes to mature adipocytes (Figure 5.13). Results are expressed as fold increase compared to cultures at day 0 and are mean  $\pm$  SE, n=3. LPL is a marker of late adipogenesis stage expression increased (Figure 5.14 and Table 5.6) with high expression of LPL observed in differentiated cells at day 15 (77.44  $\pm$ .11) compared to day 0, (mean  $\pm$  SE, n=3 separate experiments \* $p$ < 0.05, ANOVA post hoc analysis with student-Newman-Keuls test (Figure 5.15).

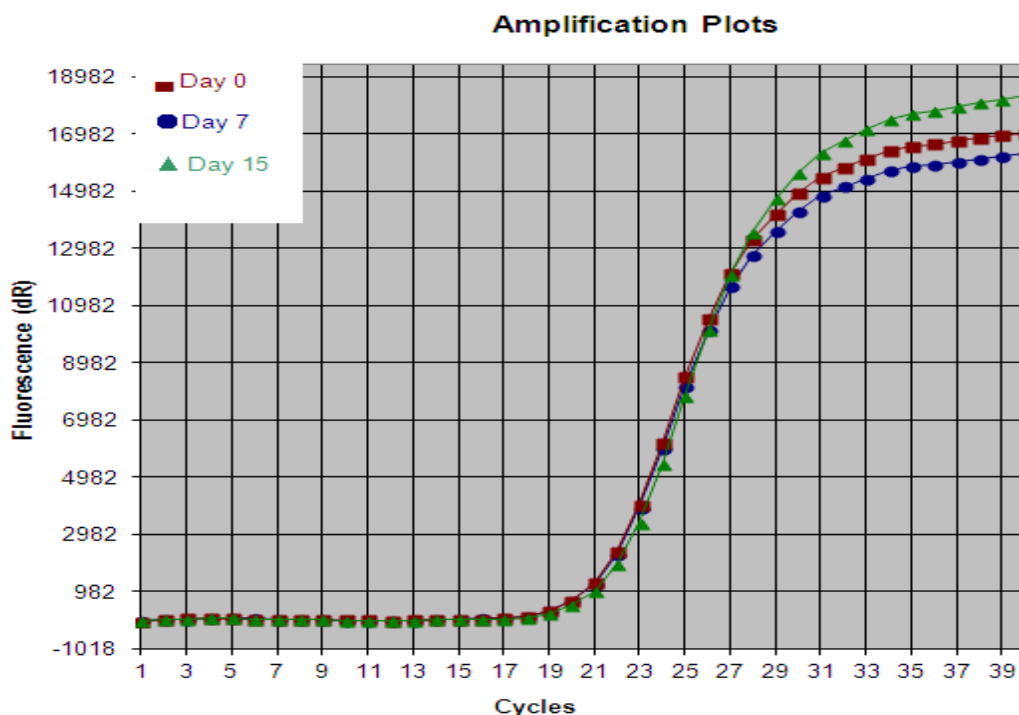


**Figure 5.13: APRT Amplification plot**

Amplification plots show that APRT expression was unchanged during primary human orbital pre-adipocytes differentiation. Cells were treated in differentiation medium at day 0, 7 and 15. The plots show the Ct values were minimally altered by the length of time in differentiation medium (Table 5.6).

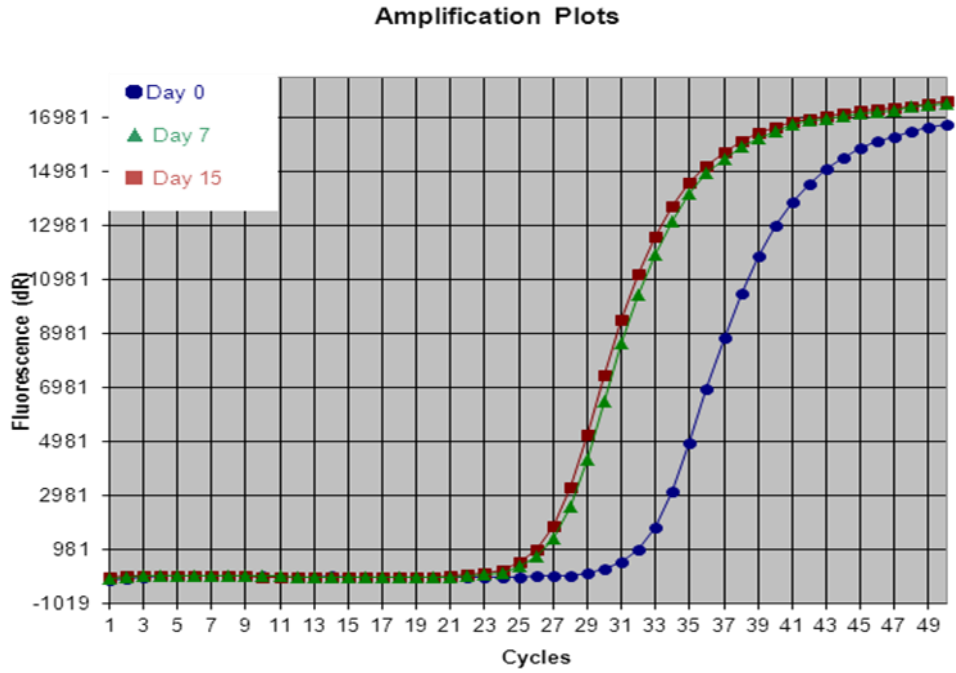


**Figure 5.14: LPL amplification curve**

LPL amplification curve of the human orbital cells shows at day 0, 7 and 15 after the addition of differentiation medium. LPL expression was increased during primary human orbital differentiation.

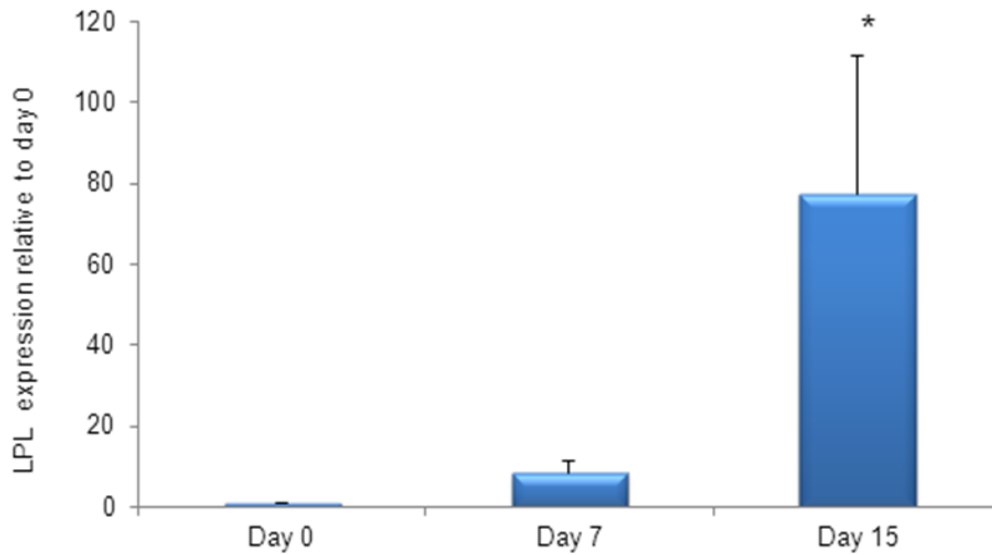


**Figure 5.15: LPL expression during primary human orbital cells differentiation**

QPCR of LPL expression during primary human orbital differentiation shows increase of LPL at day 0, 7 and 15 with differentiation medium compared to control cultures day 0. \*  $p < 0.05$ , vs control cultures,  $n=3$  separate experiments, ANOVA, post hoc analysis with student-Newman-Keuls test.

**Table 5.9: LPL CT values**

Ct values for LPL and APRT QPCR assays during human orbital adipogenic differentiation at day 0, 7 and 15 shows increased the level of LPL expression, reduced the Ct value, minimally effect on ARPT.

	Ct value		
	0 days	7 days	15 days
APRT	21.55	21.50	21.85
LPL	30.36	24.97	24.48

**Table 5.10: QPCR GPDH and LPL late marker for adipogenesis**

QPCR for GPDH in 3T3-L1 cells following 9 days exposure to differentiation medium increased and LPL in human primary orbital adipocytes following 15 days in differentiation medium that LPL and GPDH are used as markers of terminal differentiation and that both are greatly increased.

Samples	Day 5	Day 7	Day 8	Day 15
3T3-L1 GPDH	8.97 ± 1.20	-	53.76 ± 2.65	-
Human Primary adipocytes LPL	-	8.58 ± 2.90	-	77.44 ± 34.11

#### 5.3.2.4 PPAR $\gamma$ expression during human orbital pre-adipocytes differentiation.

Cells were seeded in 6 well plates and once confluent were incubated with differentiation medium until day 15. Medium was changed every two days. The cells were analysed over a time course when the medium was removed and cells were then washed twice with 1 ml of PBS. Cells were lysed with 250  $\mu$ l loading buffer and were rapidly frozen in liquid nitrogen before being stored at -20°C. Total PPAR $\gamma$  was detected by western blotting (section 3.3.2). The bands representing PPAR $\gamma$  are shown below (Figure 5.16). Levels of PPAR $\gamma$  protein were influenced by the length of time in differentiation medium. After an initial decline, amounts of the transcription factor showed an approximate doubling and peaked at day 8, the point at which elongated fibroblast shape cells had started changing into more rounded cells.

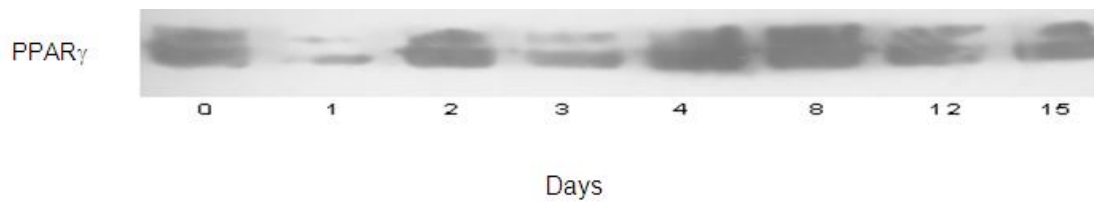


**Figure 5.16: PPAR $\gamma$  expression**

A representative western blot which shows total of PPAR $\gamma$  over a time points of 15 days was during adipocyte differentiation medium. The level of PPAR $\gamma$  level was high at day 0 and decline at day 1 then increase at day 4 with a high level can observed at day 8.

### **5.3.2.5 GHR expression during human orbital pre-adipocytes differentiation**

The level of GHR gene transcription during primary human orbital pre-adipocytes differentiation was analyzed using QPCR. GHR expression was increased during the differentiation process (Figure 5.17, 5.18 and Table 5.7) with significantly higher expression being observed in differentiated cells at day 15 ( $11.04 \pm 4.51$  of day 0  $p < 0.05$  vs. day 0,  $n=4$ ). This data demonstrated that in human orbital cells, primary mouse adipocytes cells and 3T3-L1 cell lines general there was a increase in GHR transcript number following the differentiation protocol.

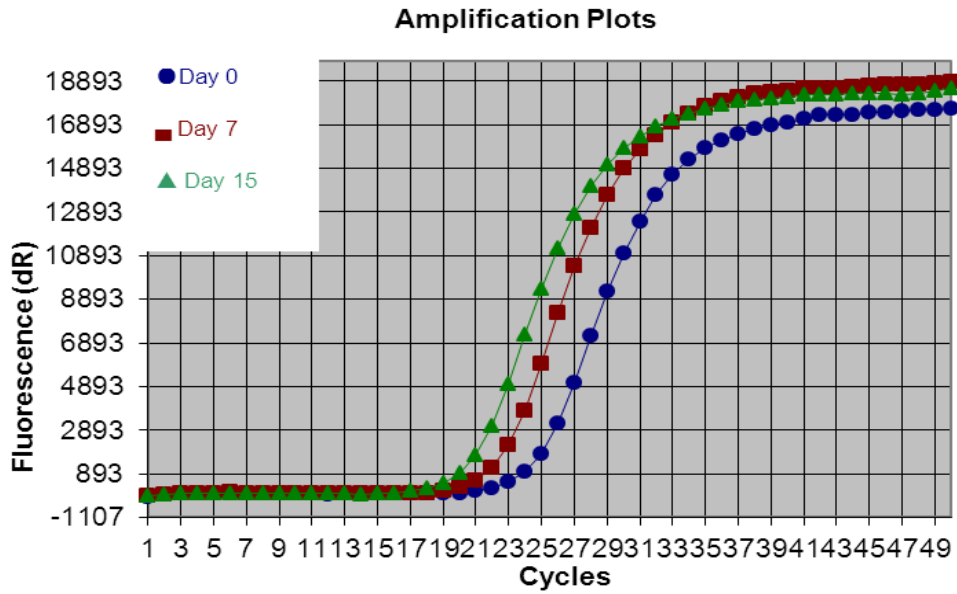


**Figure 5.17: Amplification curve of GHR**

QPCR amplification curve of GHR shows human primary orbital cells in differentiation medium at day 0, 7 and 15. GHR expression was increased with the human primary orbital cells differentiation.

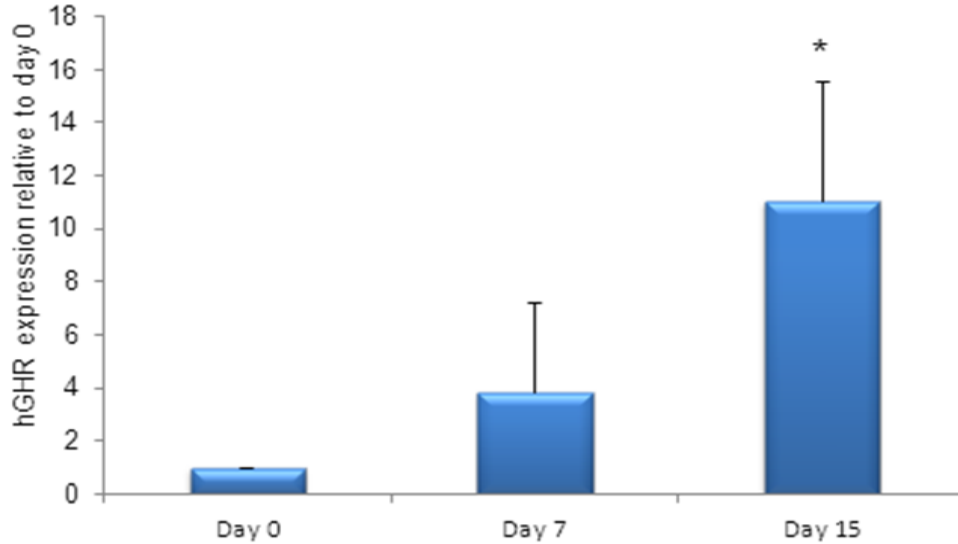


**Figure 5.18: GHR expression during human orbital pre-adipocytes differentiation**

QPCR analysis of GHR expression during human orbital adipocytes differentiation shows a significant increase with cellular differentiation compared to control cultures, \*  $p < 0.05$  vs. day 0 cultures,  $n = 4$ .

**Table 5.11: GHR and APRT QPCR assays**

Ct values for the GHR and APRT QPCR assays during primary human orbital adipogenic differentiation at days 0, 7 and 15 show that differentiation increased GHR expression reducing Ct value, but had a minimal effect on APRT.

	Ct value		
	0 days	7 days	15 days
APRT	21.55	21.5	21.85
GHR	22.69	20.42	18.80

**Table 5.12: QPCR for GHR**

QPCR for GHR in both 3T3-L1 cells follow 9 days of exposure to differentiation medium and human primary adipocytes following 15 days in differentiation medium were increased.

Samples	Day 5	Day 7	Day 8	Day 15
3T3-L1 GHR	4.5 ± 3.20		6.0 ± 2.65	-
Human primary adipocytes GHR		3.86 ± 3.38	-	11.04 ± 4.51

### 5.3.2.6 Basal ERK activation during human orbital pre-adipocyte differentiation

Human orbital pre-adipocyte were plated in 6 well plates and once confluent incubated with differentiation medium for 17 days with protein samples being collected at various time points (section 3.3.2). Basal unstimulated ERK phosphorylation was detected by western blotting. The phospho-ERK1 (p44) and ERK2 (p42) bands are shown (Figure 5.19). Basal ERK activation started high then declined following a similar pattern of expression to that seen for PPAR $\gamma$  (Figure 5.16) before rebounding then declined to levels that are barely detectable through day 8, but increasing again from day 11 onwards. This increase in basal phospho-ERK in the late stages of adipogenesis is in a marked contrast to the steady decline observed in mouse primaries and 3T3-L1 cell line. Whether it is a feature of all human precursors differentiating into fat or a particularity of the orbital requires further study.

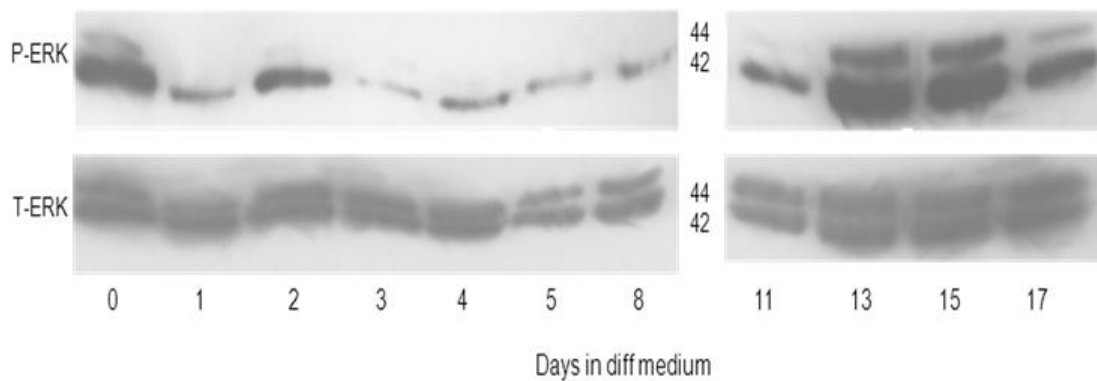


**Figure 5.19: Basal ERK levels**

Basal ERK activation during human orbital adipocytes differentiation

### 5.3.2.7 GH stimulated ERK and STAT5 activation during orbital human pre-adipocytes differentiation

Differentiating human orbital pre-adipocytes were treated with GH and PMA (10 minutes) at various time points following addition of differentiation medium. GH-induced ERK and STAT5 activation was analysed by phospho-specific western blotting in cells treated for 10 minutes with GH (50 nM). Results do not show any difference between the levels of GH-induced ERK activation in cells at day 0, 7 and 15. Analysis of the data from multiple experiments showed no significant increase of GH-induced ERK activation at day 7 ( $114.63\% \pm 22.6$  vs. day 0,  $p > 0.05$   $n=3$ ) compared with % day 0 and the total ERK was unchanged. As can be observed (Figure 5.10) GH induces ERK activation was detected in mouse primaries, but with orbital cells no activation of the ERK pathway occurs during adipogenesis. Orbital pre-adipocytes are a particular fat depot, being derived from the neural crest which may explain the differences between these results following GH induced ERK activation and those obtained using a murine pre-adipocyte cell line.

Phospho-STAT5 undetectable at day 0, but easily detectable at days 7 and 15, however, the result is expressed as IDV absolute values, mean  $\pm$  SE, n=3. GH-stimulated STAT5 phosphorylation increased with a significantly higher change being observed in differentiated cells at day 7 ( $7772112 \pm 2389451$  \*\*p < 0.01, n = 3), at day 15 ( $12655344 \pm 3123410$ , \*\*p < 0.01 n = 3) and total STAT5 increased with significantly higher levels being observed in differentiated cells at day 15 ( $225.01 \pm 11.30$  of day 0) (Figure 5.21).



**Figure 5.20: Phosphorylation of ERK and STAT5 in human orbital adipocyte differentiation** A representative western blot which shows phosphorylation of ERK and STAT5 following GH stimulation at day 0, 7 and 15 in adipocyte differentiation medium. The level of GH-stimulated ERK phosphorylation over time did not change in differentiation medium. The total ERK blot has two bands where the upper is p44 and the lower is p42. In contrast the level of total STAT5 and GH-stimulated STAT5 phosphorylation increased with human orbital adipocytes differentiation. PMA shows levels of ERK activation were the same during differentiation cells with no significant difference between the bands.

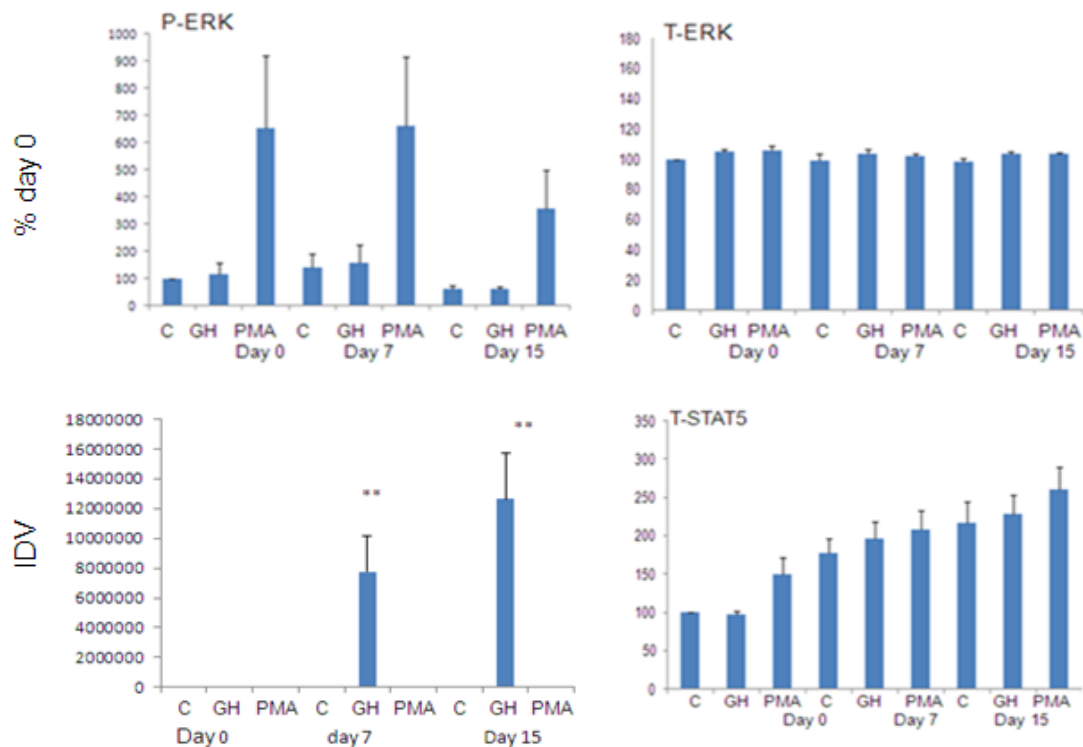


**Figure 5.21: Densitometric analysis of ERK and STAT5 in human orbital adipocyte differentiation**

Densitometric analysis of the western blots shown in (Figure 5.20) the results are expressed as % day 0 control for P-ERK, total ERK and total STAT. Phospho-STAT5 undetectable at day 0, but easily detectable at days 7 and 15, however, the result is expressed as IDV absolute values, mean  $\pm$  SE, \*\* $p < 0.01$ ,  $n = 3$ . The results demonstrate that an increase in total STAT5 and GH-stimulated STAT5 activation following differentiation; despite unchanged in the levels of total ERK also no P-ERK activation at any time point.

### 5.3.2.8 Mitotic clonal expansion (MCE)

The human primary orbital pre-adipocytes had very different GH-induced signalling with no activation of ERK by GH in orbital cells compared with the 3T3-L1 cell line. GH signalling is thought to be important in the MCE phase of differentiation which seems to occur in the cell line, but not in primary precursors. The abundance of orbital pre-adipocytes enabled this study to investigate whether MCE occurs in human primary orbital cells and then compared with 3T3-L1 cell line.

### 5.3.2.8.1 MCE of human orbital pre-adipocyte during adipogenic differentiation

Cells were grown to confluence and medium changed to either differentiation or complete medium and then cells counted at day 0 to 15 (Figure 5.23). In the human orbital cells there was no difference in number between cells in differentiation medium compared to those in complete medium. Furthermore, there was a gradual increase in cell number in both types of medium ( $p>0.05$ ,  $n=3$ ). The data presented clearly illustrates differentiation of human orbital pre-adipocytes is not accompanied by an initial MCE.

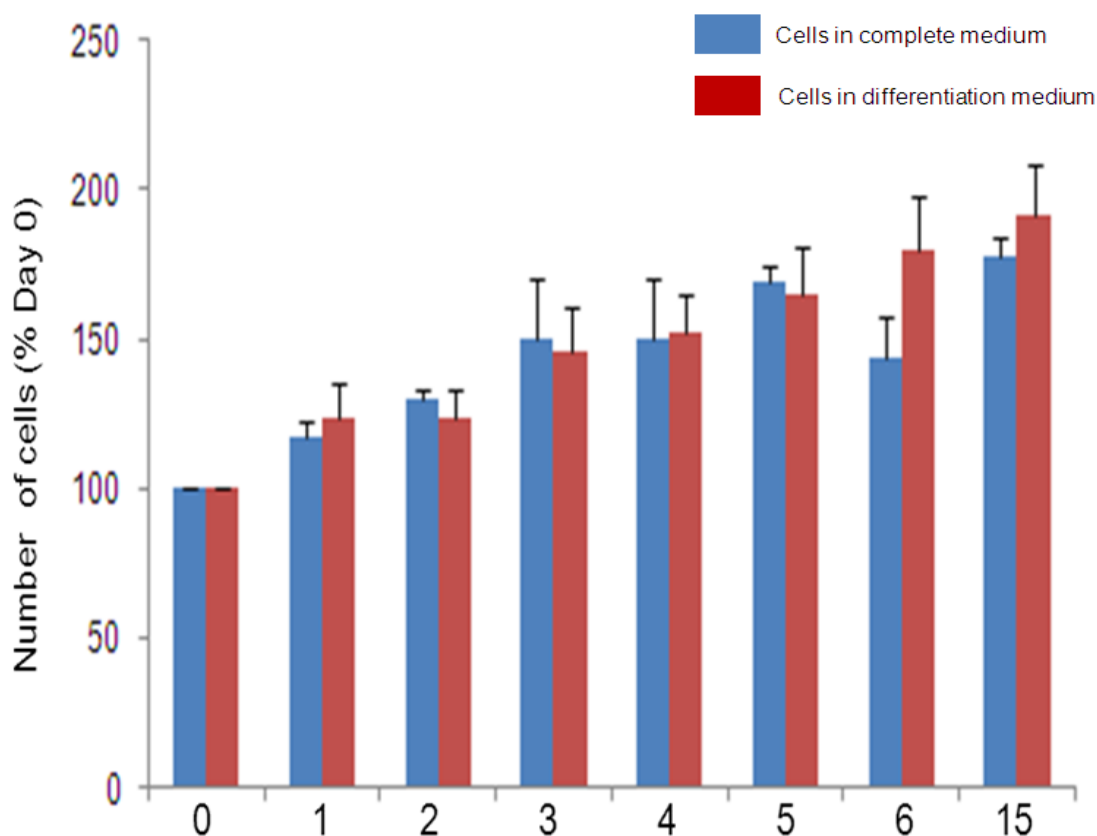


**Figure 5.22: MCE in human orbital cells**

Human orbital pre-adipocyte incubated from day 0 to 15 with differentiation medium (red) or complete medium (blue). No variations in the cell number observed indicated that orbital pre-adipocyte do not require MCE during differentiation.

### 5.3.2.8.2 MCE of the 3T3-L1 during adipogenic differentiation

Cells were grown to confluence and medium changed to either differentiation or complete medium, then counted at day 0 to day 7. In the 3T3-L1 cells samples, there was an obvious increase in the number of cells in differentiation medium compared to those in complete medium. The difference was most marked on days 2 and 3 following addition of differentiation medium compared with complete medium, ( $p < 0.01$ ,  $n = 3$ ) and indicated MCE. It is possible that the absence of GH-induced P-ERK activation in the orbital cells, which contrasts with its robust activation in 3T3-L1 before adipogenesis is underway, may provide some explanation for lack of MCE in the orbital cells.

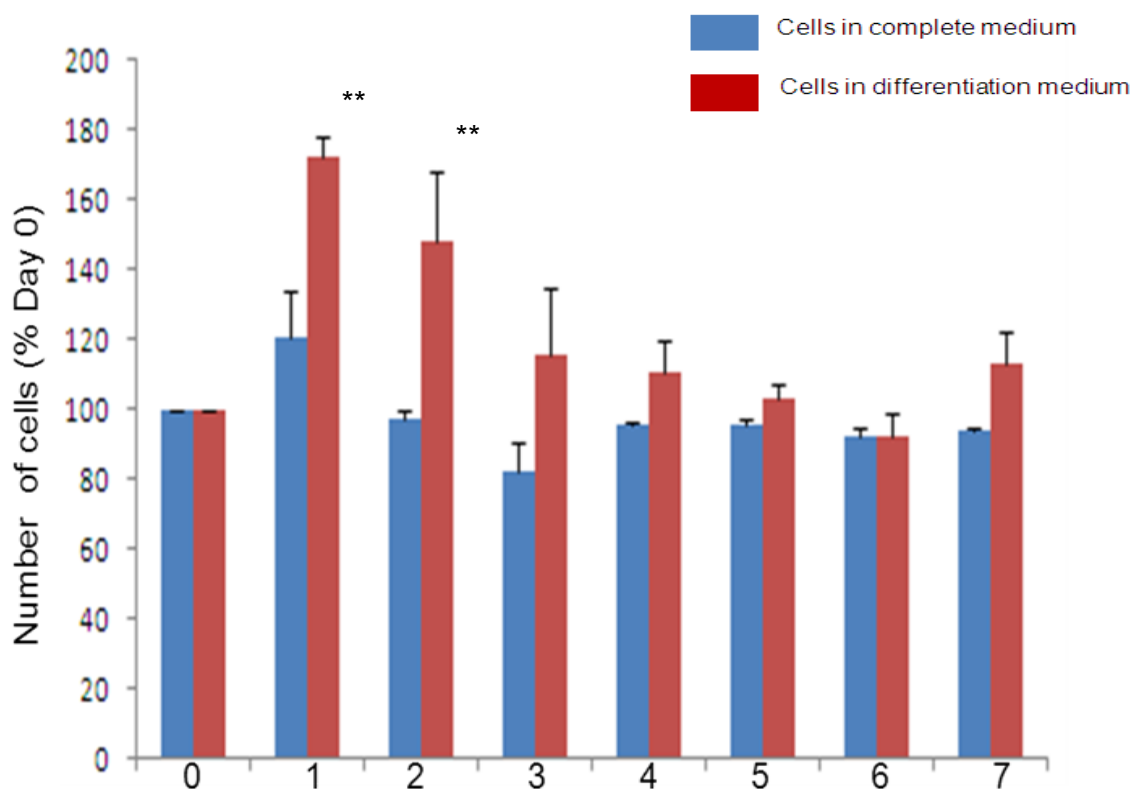


**Figure 5.23: MCE in 3T3-L1 cell line**

3T3-L1 pre-adipocyte was incubated from day 0 to day 7 with either differentiation medium (Red) or complete medium (blue). 3T3-L1 pre-adipocyte differentiation was induced with the induction protocol. Cells in complete medium remain constant, while cells in differentiation medium spiked on day 1 and 2 which is consistent with MCE.

### **5.3.3 Are there depot-specific differences in GH signalling during adipogenesis?**

Fat depots in mice are very small making it difficult to compare the responses between them. Human adipose tissue can be obtained from patients undergoing elective surgery of which breast adipose tissue has been used as a more typical human fat as its behaviour *in vitro* is very similar to subcutaneous fat. Consequently experiments were performed using subcutaneous pre-adipocytes from breast tissue for comparison with the atypical orbital.

#### **5.3.3.1 Morphology of primary human breast fat cells during differentiation**

During differentiation primary human breast fat cells underwent the characteristic conversion from fibroblast to adipocyte morphology. Undifferentiated primary human breast fat cells have the appearance of fibroblasts with an elongated shape (Figure 5.25). However, a much longer time in differentiation medium is required to achieve adipogenesis in breast precursors, up to 19 days. Furthermore, far fewer cells can be induced to differentiate *in vitro* when compared with murine cell lines, primary mouse or human orbital cells

#### **5.3.3.2 Oil Red-O of human breast fat cells during differentiation**

Human breast fat cells undergoing adipogenic differentiation were stained with Oil Red O (Figure 5.25). No Oil Red O was detected at day 0 (Figure 5.25B). However, by day 19 in differentiation medium a small number of cells contained Oil Red O (Figure 5.25D).

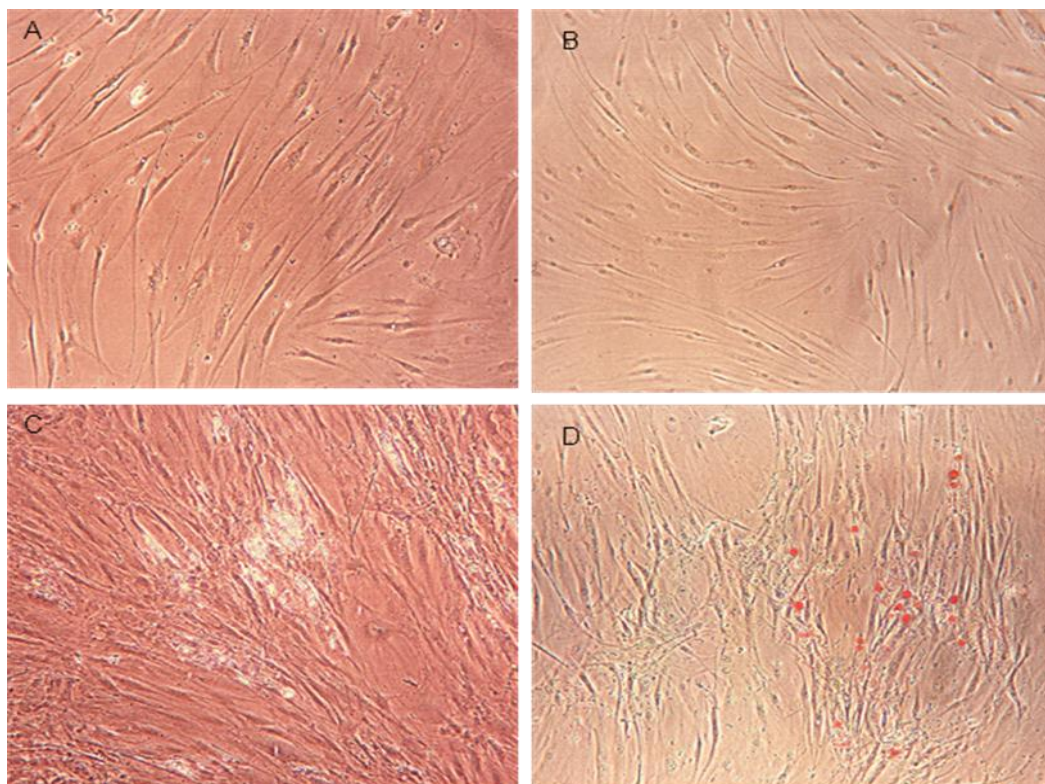


**Figure 5.24: Breast fat pre-adipocyte differentiation**

Phase contrast photomicrographs show various stages of adipocyte differentiation. (A) Undifferentiated human breast fat pre-adipocytes at day 0 and (C) cells after 19 days in differentiation medium. (B) Undifferentiated Oil Red O stained cells at day 0, and (D) after 19 days in differentiation medium stained with Oil Red O. After 19 days in differentiation medium lipid droplet accumulation in small number of differentiated cells is clearly visible. Magnification 100x.

### 5.3.3.3 hPPAR $\gamma$ expression during breast fat cells differentiation

QPCR was used to determine PPAR $\gamma$  (Table 5.2) gene expression in the human breast fat cells at day 0, 15 and 19 after the start of differentiation. APRT (Table 5.2) housekeeping gene was used for studies which look at differentiation of the breast fat cells. APRT housekeeping gene expression showed minimal change during differentiation (Table 5.13). Results are expressed as fold increase compared to cultures at day 0 with mean  $\pm$  SE,  $p > 0.05$ ,  $n=3$ . PPAR $\gamma$  expression was reduced (Figure 5.25 and Table 5.13). As can be observed from Oil Red O staining a few cells able to accumulate lipid droplets, this may explain why PPAR $\gamma$  reduced during the time of differentiation.

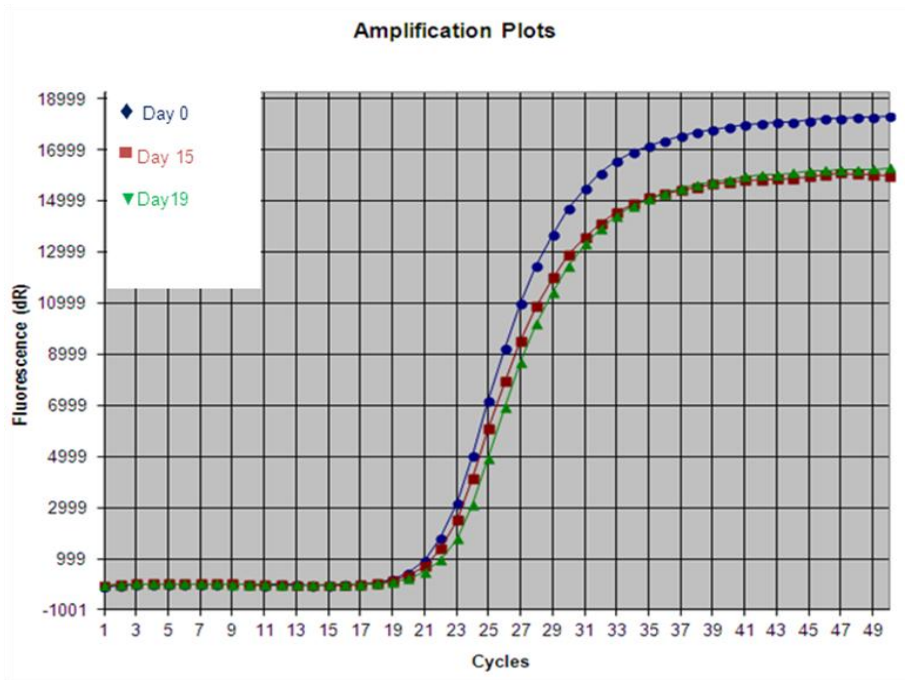


**Figure 5.25: hPPAR $\gamma$  amplification curve.** PPAR $\gamma$  amplification curve of the human breast cells shows at day 0, 15 and 19 after the addition of differentiation medium. PPAR $\gamma$  expression was decreased during breast fat cells differentiation

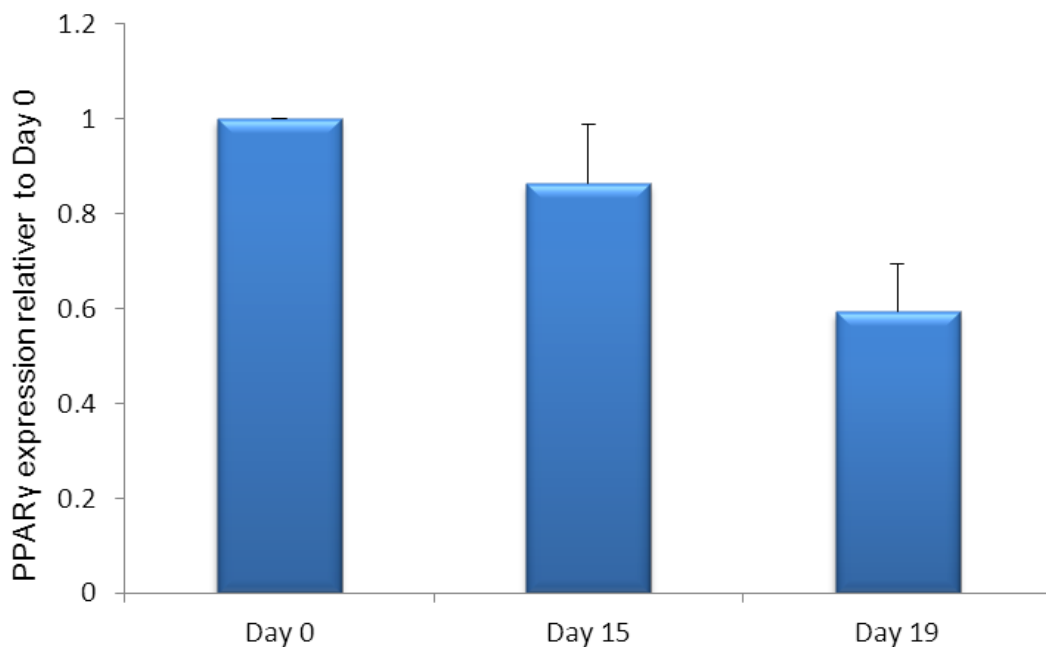


**Figure 5.26: hPPAR $\gamma$  expression during breast fat differentiation**  
 QPCR analysis of PPAR $\gamma$  expression during breast fat differentiation shows reduced of PPAR $\gamma$  at day 15 and day 19 with differentiation medium compared to control cultures at day0.

**Table 5.13: hPPAR $\gamma$  QPCR assays**

Ct values for the PPAR $\gamma$  assays during breast fat adipogenic differentiation at days 0, 15 and 19 show that differentiation down regulation of PPAR $\gamma$  with increase Ct value.

	Ct value		
	0 days	15 days	19 days
APRT	24.39	23.78	24.04
PPAR $\gamma$	19.87	20.30	20.84

### 5.3.3.4 hLPL expression during breast fat cells differentiation

QPCR was used to determine LPL (Table 5.2) gene expression in the human breast fat cells at day 0, 15 and 19 after the start of differentiation. APRT (Table 5.2) housekeeping gene was used for studies which investigated differentiation marker of the breast fat cells. APRT housekeeping gene expression showed minimal change during differentiation of the human breast fat (Table 5.13). LPL, a marker of late adipogenesis expression appeared to be down regulated and only a very low level was detected (Figure 5.26 and Table 5.14) in differentiated cells at day 19, in keeping with the very limited induction of adipogenesis in these cells. Results are expressed as fold increase compared to cultures at day 0 with (mean  $\pm$  SE,  $p = 0.13$ ,  $n=3$ ).

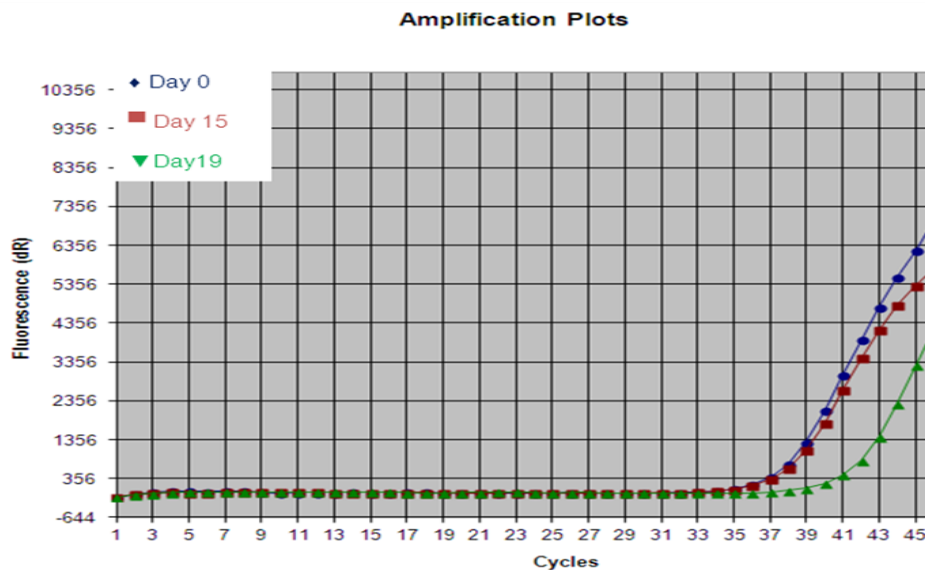


**Figure 5.27: hLPL amplification curve.** LPL amplification curve of the breast fat cells shows at day 0, 15 and 19 after the addition of differentiation medium. LPL expression was reduced during breast fat cells differentiation as can be seen Ct value at day 19 forms later.

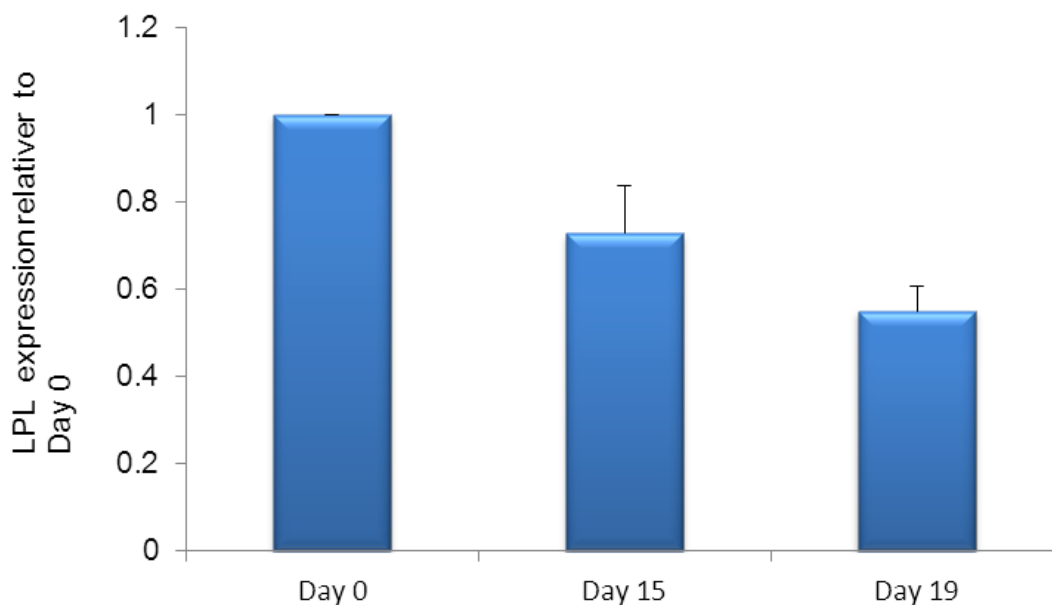


**Figure 5.28: hLPL expression during breast fat differentiation**

QPCR analysis of LPL expression during breast fat differentiation shows reduced of LPL at day 15 and day 19 with differentiation medium compared to control cultures at day 0 with mean  $\pm$  SE,  $p > 0.05$ ,  $n=3$ .

**Table 5.14: hLPLQ PCR assays**

Ct values for the LPL assays during breast fat adipogenic differentiation at days 0, 15 and 19 shows that differentiation caused down regulation of LPL with increase Ct value at day 19.

	Ct value		
	0 days	15 days	19 days
APRT	24.39	23.78	24.04
LPL	37.34	37.07	40.90

### 5.3.3.5 hGHR expression during human breast fat differentiation

Experiments to measure the transcript copy number adjusted to the quantity of RNA were performed. RNA was extracted at day 0, 15 and 19 and reverse transcribed. The levels of GHR gene transcription during human breast fat cells differentiation were analyzed using QPCR. GHR expression was unchanged by the differentiation process (Figure 5.28, 5.29). Results are expressed as fold compared to cultures at day 0 with mean  $\pm$  SE,  $p = 0.09$ ,  $n=3$ . This result is very different from all other fat depots studied, irrespective of species or source from cell lines or primaries.

Therefore, it may be possible that the very low level of adipogenesis induced masked any increase in GHR expression.

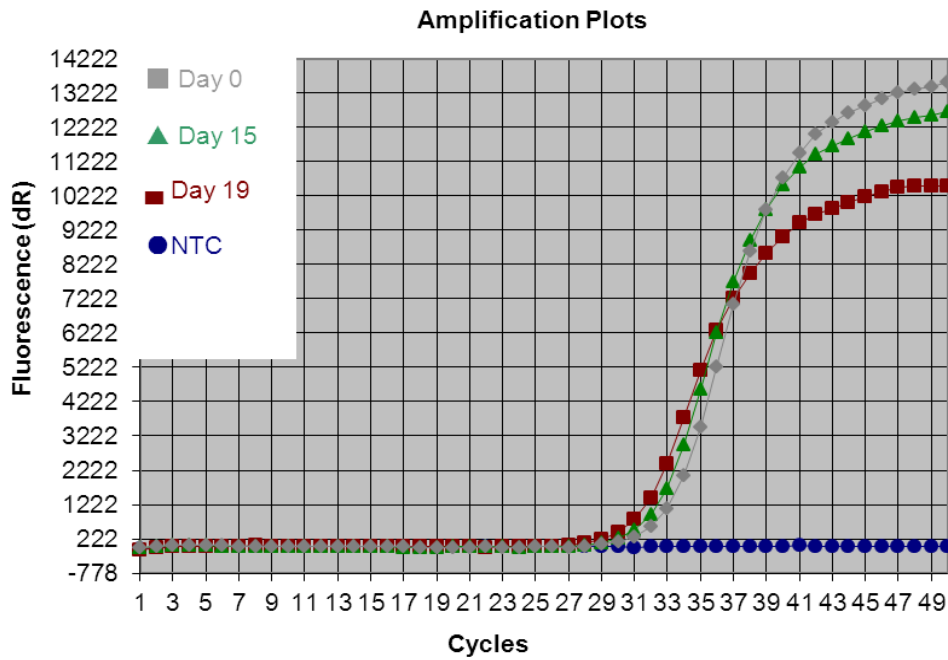


**Figure 5.29: Amplification curve of hGHR**  
 QPCR amplification curve of GHR shows human breast fat cells in differentiation medium at day 0, 15 and 19. GHR expression did not increase with the primary breast fat cells during differentiation. NTC no template control.

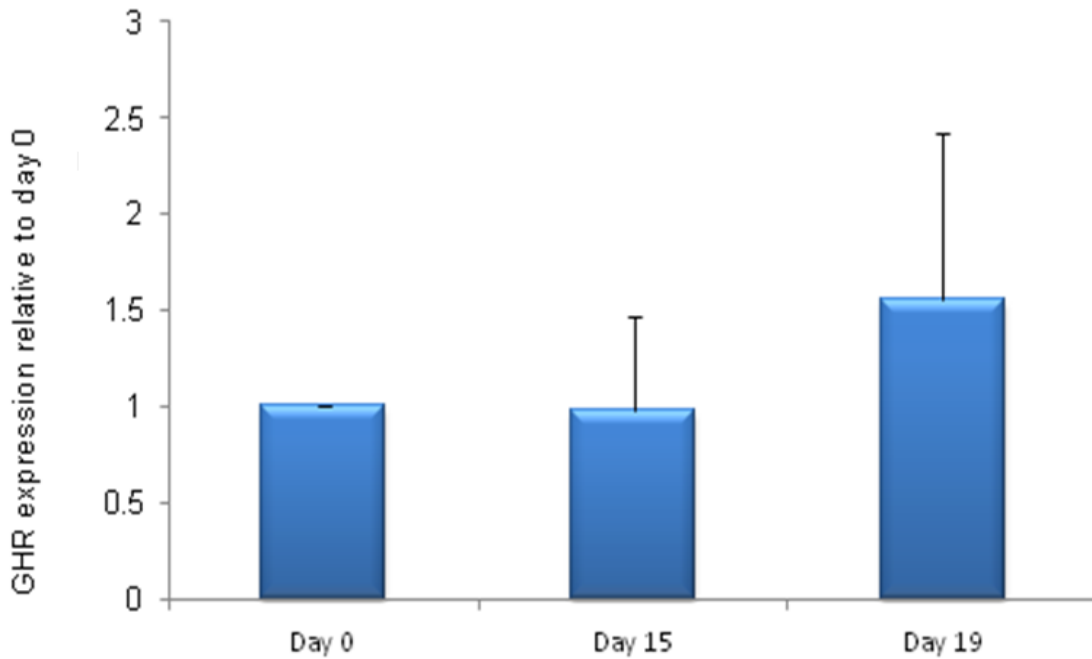


**Figure 5.30: hGHR expression during human breast fat differentiation**  
 QPCR analysis of GHR expression during human breast fat adipocytes differentiation shows no increase with cellular differentiation compared to control cultures at day 0.

**Table 5.15: hGHR Q PCR assays**

Ct values for the GHR assays during breast fat adipogenic differentiation at days 0, 15 and 19 shows that differentiation no significant increase with of GHR with increase Ct value at day 19.

	Ct value		
	0 days	15 days	19 days
APRT	24.39	23.78	24.04
hGHR	30.93	30.32	29.43

### 5.3.3.6 GH stimulated ERK and STAT5 activation during breast fat cells

Human breast fat pre-adipocytes were treated with GH and PMA (10 minutes) at various time points following addition of differentiation medium. GH-induced ERK and STAT5 activation was analysed by phosph-specific western blotting (section 3.3.2). Results show no difference between the levels of activation ERK in cells treated with GH or without treatment at day 0, 15 and after 19 days (Figure 5.31). Analysis of the data from multiple experiments showed no change of GH-induced ERK activation at day 15 ( $135 \pm 17.00$  of % day 0, n=3 compared with % day 0, p= 0.26), 19 ( $161.78 \pm 17.13$  of % day 0, n=3 compared with % day 0, p= 0.15) and that total ERK was unchanged. In contrast, GH-stimulated STAT5 phosphorylation was increased with significantly higher change being observed in differentiated cells at day 19 ( $7189829 \pm 2395456$  of day 0, \*p<0.05, vs. day 0, n=3) (Figure 5.32).

GH-stimulated ERK activation during adipogenesis behaved differently, depending on the fat depots (Figures 3.5, 5.10 and 5.20). In primary human orbital pre-adipocytes and breast fat cells there is no activation at all in GH-stimulated ERK activation during adipogenesis. In contrast, mouse primary pre-adipocyte cells show GH-stimulated ERK activation which increased, whilst 3T3-L1 cell-line GH-stimulated ERK activation declined throughout adipogenesis.

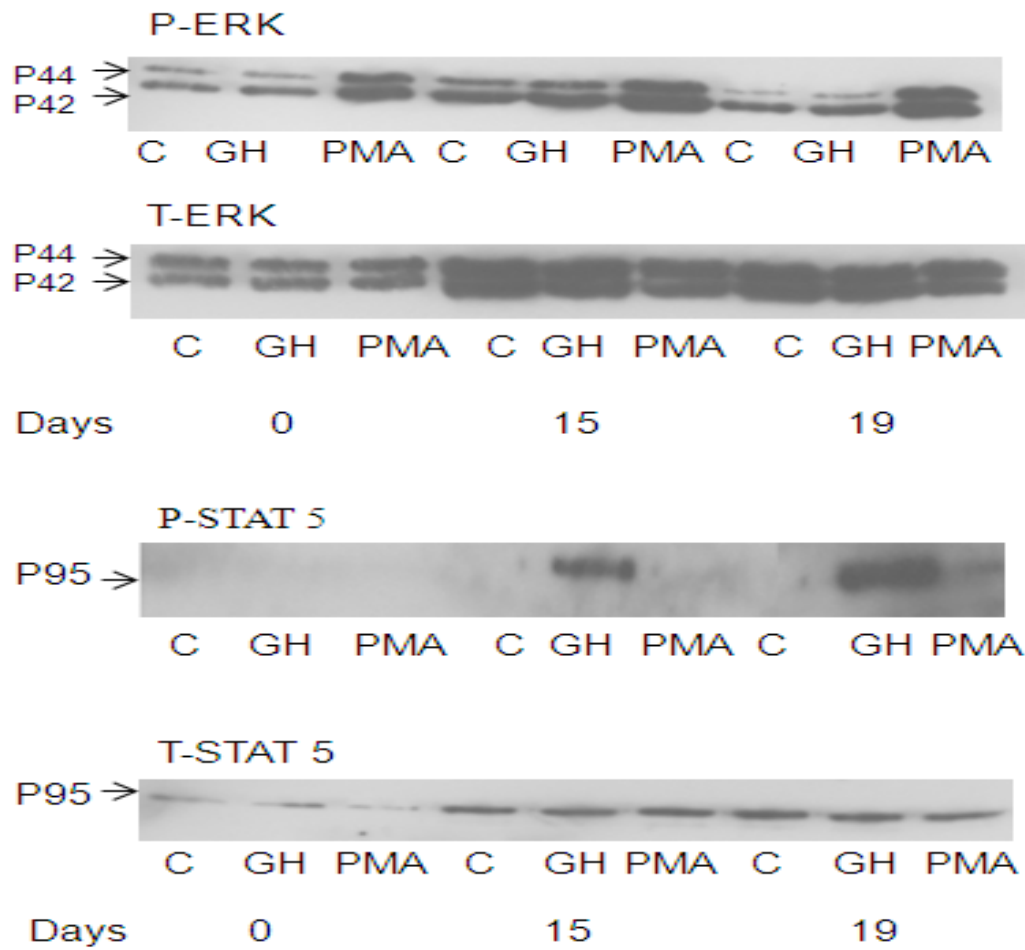


**Figure 5.31: Phosphorylation of ERK and STAT5 in breast fat cells**

A representative western blot shows phosphorylation of ERK and STAT5 following GH stimulation at day 0, 15 and 19 of the breast fat cells in adipocyte differentiation medium. The level of GH-stimulated ERK phosphorylation in differentiation medium appears with no changes. The phosphorylation and total ERK blot have two bands where the upper is p44 and the lower is p42. In contrast the level of total and GH stimulated STAT5 phosphorylation increased with breast fat adipocytes differentiation. PMA shown levels of ERK activation were the same between the bands in differentiated cells.

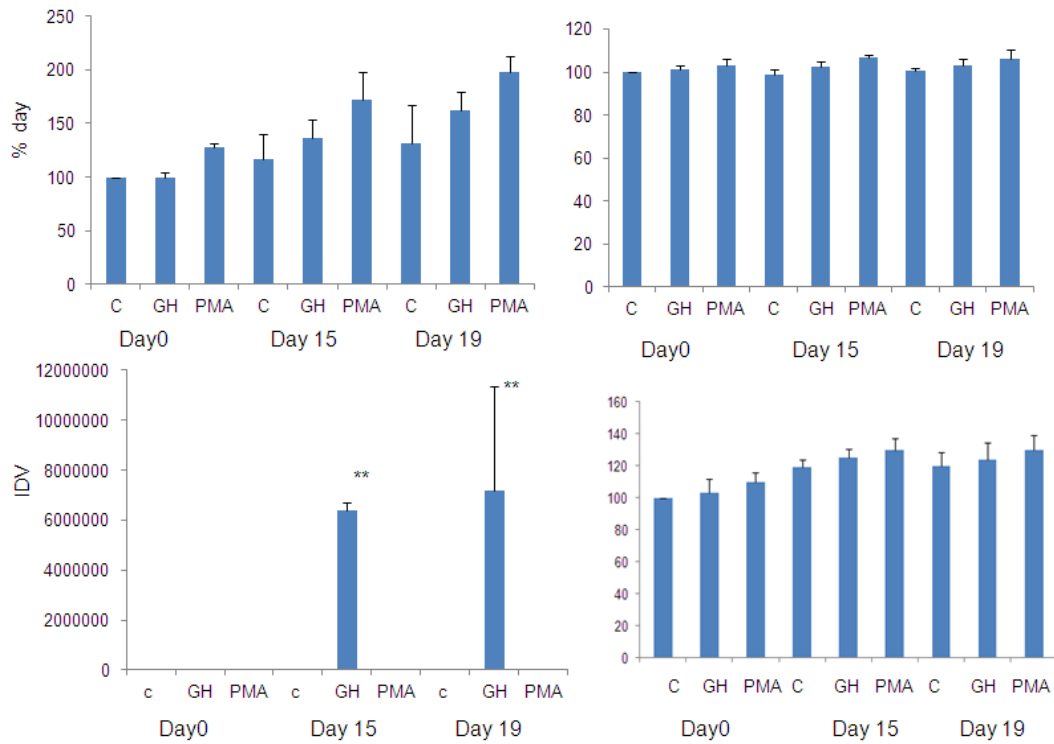


**Figure 5.32: Densitometric analysis of ERK and STAT5**

Densitometric analysis of the western blots shown in Figure 5.30 the results are expressed as % day 0 for P-ERK, total ERK and total STAT5. P-STAT5 undetectable at day 0, but easily detectable at days 15 and 19, however, the result is expressed as IDV absolute values, mean  $\pm$  SE, n=3. The results demonstrated increased total STAT5 and GH-stimulated STAT5 activation following differentiation, despite unchanged in ERK activation and total ERK, \* p<0.05, \*\*p<0.01 vs. control cultures at day 0, n=3 separate experiments.

## 5.5. Discussion

As discussed in Chapter 3 and 4 studies using the 3T3-L1 cell line showed that GH-stimulated ERK activation decreased as differentiation progressed. In this chapter I have investigated whether adipogenesis in primary pre-adipocytes from different species and fat depots results in the alterations to GH-induced signalling characterized in the 3T3L1 pre-adipocyte cell line (section 3.3.2).

The results indicate both similarities and differences. Firstly, in all fat depots in which adipogenesis can be induced *in vitro*, transcript expression levels of the GHR increased as differentiation progresses. The increase is about 10-fold compared with undifferentiated cells in primary pre-adipocytes and the cell line. This level of increase illustrates the short-comings in my attempts to mimic the increase in GHR by transfecting with an expression plasmid (section 4.3.4) and will be discussed further in chapter 6.

Secondly, GH-induced activation of P-ERK, and its reduction during adipogenesis, appears to be unique to the 3T3-L1 cell line. In all primaries studied, there was minimal GH-induced phosphorylation of ERK at all time points before and during differentiation and no depot, either murine or human, demonstrated a reduction in P-ERK when comparing pre-adipocytes with *in vitro* differentiated adipocytes.

Thirdly, in all pre-adipocytes studied, whether cell line or primary, GH-induced STAT5 activation is increased as adipogenic differentiation proceeds. Similar results were obtained using two different adipogenic cocktails (differentiation medium) supporting the conclusion that differentiation *per se* is responsible, rather than one of the components of the adipogenic medium. The only caveat is the similar pattern of reactivity obtained using human breast preadipocytes, despite very poor induction of adipogenesis. Possible methods to explore this will be discussed in chapter 6.

In contrast, the orbit is a very active depot and several of the samples were from people with Graves' Orbitopathy, a condition in which adipogenesis contributes to the tissue remodelling causing the disease. Although the depot is not typical, I was provided with sufficient cells to investigate whether the lack of ERK phosphorylation in primaries could affect mitotic clonal expansion (MCE). MCE is known to take place in the first few days after addition of adipogenic medium to confluent 3T3-L1 cells. There is some controversy as to whether MCE is necessary for differentiation to occur but if some pre-adipocyte populations undergo adipogenesis without an initial MCE it would suggest that it is not essential. I measured proliferation in 3T3-L1 and human orbital pre-adipocytes after addition of adipogenic medium to confluent cells and the two populations behaved very differently. The cell line demonstrated MCE but orbital primaries did not. This result indicates that MCE is not a requirement for adipogenic differentiation, at least in human orbital pre-adipocytes. The lack of GH-induced ERK activation by phosphorylation in all primary pre-adipocyte cells leads me to suggest that this is an explanation for the absence of MCE in primaries and that it may be the stimulus driving MCE seen in 3T3-L1.

The results obtained with fat from some special mouse strains in which adipogenesis was induced very rapidly and as efficiently as in 3T3-L1 suggests that the main difference between primaries and the cell line is that the majority of 3T3-L1 have committed to the adipogenic lineage, but in the mixed populations of primaries we use, only a small proportion are true pre-adipocytes (Pref1 positive). It seems that the genetic modification altering levels of insulin expression in the mice has increased the numbers of cells committing to being preadipocytes.

# **Chapter Six**

## **General Discussion**

## 6. Chapter Six

### 6.1 Discussion

The 3T3-L1 fibroblast cell line can differentiate into mature adipocytes under appropriate conditions and is a very well characterized *in vitro* model system for the study of adipocyte differentiation. During adipogenesis, GH progressively loses the ability to activate p42/44 ERK despite elevated GHR and unaltered total ERK levels. In contrast, GH-stimulated STAT5 activation increases as 3T3-L1 differentiation proceeds. As the role of ERK during differentiation is complex an initial framework for this study was based upon research by Lewis *et al.*, 2004 who argued that adipocyte differentiation controls the GHR to allow activation of the ERK pathway. An inverse relationship between the decline in GH-induced ERK activation and GH-induced STAT5 activation/PMA-induced ERK activation and an apparent uncoupling of GHR from the ERK pathway in adipocyte differentiated 3T3-L1 cells was observed. This study confirmed previous research by Lewis *et al.*, 2004 that GH-induced STAT5 activation increased during differentiation of BMSCs into adipocytes. However, Lewis *et al.* study also demonstrated that GH-induced ERK activation increased in differentiated adipocyte cells. Conversely, this discrepancy with my finding in 3T3-L1 cells may be due to the presence of cells other than those which differentiated along the adipocyte lineage.

In order to explain why GH-stimulated ERK activation declined as 3T3-L1 cells underwent adipogenic differentiation this study drew upon the paper by Love *et al.*, (1998) who suggested that the ERK pathway adapter protein p66<sup>Shc</sup> was necessary to couple the GHR to the ERK pathway. To test whether p66<sup>Shc</sup> levels declined in 3T3-L1 cells as they underwent adipocyte differentiation levels of Shc were measured using western blotting. Interestingly, p66<sup>Shc</sup> levels did not decline, but were similar in cells at day 0 and day 8.

Therefore, as a reduction in p66<sup>Shc</sup> cannot explain why GH-stimulated ERK activation declined this explanation could be eliminated.

Nonetheless, as expression of GHR was observed to increase (section 3.4.5) this study tested whether altered levels of GHR expression could modulate signalling pathways coupled to the GHR. To mimic the increase in GHR transcripts which take place during adipogenesis, varying levels of the receptor was introduced using an expression plasmid. Transfection efficiency was monitored using a control GFP plasmid, while GH stimulated pERK and pSTAT5 were analysed using western blotting and densitometric analysis. With this hypothesis it was expected to observe GH-induced pERK signal reduce as the amount of receptor introduced into the cells as confirmed by QPCR GHR gene expression increased. However, the data suggests that there is no relationship between the over expression of GHR in 3T3-L1 cells and the decline in ERK activation. Instead, the level of ERK activation was the same in empty vector and GHR 3T3-L1 transfected cells, while GH-induced STAT5 activation increased in 3T3-L1 cells transfected with the hGHR vector compared to the empty vector. Transfection of the cells with the GHR expression vector increased GHR transcript to much higher levels than occurs during adipogenesis as determined by QPCR analysis. Therefore, the conclusion reached using the 3T3-L1 cell line is that during adipogenesis, the decrease GH stimulated ERK activation is not related to the increase in GHR expression seen in differentiated cells. However, the finding that high expression levels of GHR increased during 3T3-L1 differentiation into adipocytes supports the argument that GH acts on adipose tissue through GHR and modulates cellular function.

Results from this study are in general agreement with other studies that show the level of GHR expression increases during adipocyte differentiation (Zou *et al.*, 1997; Ji *et al.*, 2002). GH binds to its receptor results in activation of STAT5 pathway in many cell types including adipocytes (Story and Stephens, 2006). Fleenor *et al.*, (2006) demonstrated that mouse GH stimulated increases in STAT5 activity in undifferentiated and differentiating 3T3-L1 cells.

Additionally, GH activates ERK pathway in BMSCs and adipocytes (Winston and Bertics, 1992; Bost, *et al.*, 2005; Lewis *et al.*, 2006; Wang *et al.*, 2009). The expression of STAT5 proteins correlates well with lipid accumulation and the expression of PPAR $\gamma$  and C/EBP $\alpha$ . MKP-1 inactivates ERK1 and ERK2. Therefore, up regulation of MKP-1 in adipocytes differentiation could be an alternate mechanism to explain the observed reduction of ERK activation in adipocytes, future studies are planned to investigate this possibility.

A further investigation was undertaken to test whether adipogenesis in primary pre-adipocytes from different species and fat depots results in the alterations to GH-induced signalling characterized in the 3T3-L1 pre-adipocyte cell line. In all fat depots in which adipogenesis can be induced *in vitro*, transcript expression of the GHR increase as differentiation progresses. However, in all primaries studied, there was minimal GH-induced phosphorylation of ERK at all time points before and during differentiation and no depot, either murine or human, demonstrated a reduction in P-ERK when comparing pre-adipocytes with *in vitro* differentiated adipocytes. As such it would appear that the reduction seen in GH-stimulated ERK phosphorylation during adipogenesis in 3T3-L1 cells may be unique to this type of experimental model and may not reflect what occurs *in vivo*.

In all pre-adipocytes studied, whether cell line or primary, GH-induced STAT5 activation is increased as adipogenic differentiation proceeds. The GHR increase with adipogenesis might explain this increase in STAT5, since similar results were obtained by transfecting with the GHR plasmid (section 4.3.4). Although the results add to current knowledge, they also lead to further questions and ideas. The studies included in this thesis are based on expression using QPCR and western blotting. These are powerful, reliable and reproducible methods that could be used in related future research. The coupling of the GHR to the ERK pathway requires that the GHR is localized in the caveolae–lipid raft membrane fraction. Subcellular fractionation of pre-adipocytes shows a high level of GHR in the caveolae membrane fraction (CM) along with components of the ERK pathway (Yang *et al.*, 2004;

Lanning and Carter-Su, 2006). In differentiated 3T3-L1 cells, the level of GH activation of ERK declined, therefore the possibility may exist that differentiation caused the GHR to move out of the CM thereby explaining the decrease in GH-stimulated ERK signalling in differentiated 3T3-L1 cells. Further research will be required involving the separation of the plasma membrane and CM fraction using differential detergent solubility and ultracentrifugation to confirm this possibility.

Similar results were obtained using two different adipogenic cocktails supporting the conclusion that differentiation is responsible for the observed effects rather than one of the components of the adipogenic medium. However, human breast pre-adipocyte cultures also showed increased GHR expression and GH-induced STAT5 activation following incubation in differentiation medium despite few cells showing lipid droplet accumulation. This leads to the question of whether in these cultures adipogenic differentiation actually caused the observed effects. One approach to determine whether differentiation is responsible would be to incubate parallel cultures in 'normal' complete medium and differentiation medium to see whether 'complete medium' cultures exhibit the same changes as those seen in cultures incubated in differentiation medium. This highlights one of the main problems in using primary cultures i.e. heterogeneity, meaning it is not always possible to be sure in a mixed culture which cell type is responsible for the observed effect. One approach that could improve the protocol would be to increase the proportion of pre-adipocytes at the start of the experiment using fluorescence-activated cell sorting (FACS) or magnetic beads to enrich cells positive for the pre-adipocyte marker Pref 1.

Despite the above observed difference between primary cultures, the 3T3-L1 cell line as an adipocyte model will continue. Although, it is not clear how close or how far 3T3-L1 adipocytes are from a perfect adipocytes model, some characteristics, at least the key ones, such as fat accumulation, PPAR $\gamma$  expression and GH signalling pathways are reflected well in 3T3-L1 cells. The advantage of using a cloned cell line is also of importance with regard to

convenience reproducibility and cell homogeneity. To highlight the importance of human validation, in this thesis we showed the widely observed ability of GH to stimulate ERK in 3T3-L1 cells however little to no GH-induced ERK activation was observed in primary cultures. Additionally, MCE was observed in 3T3-L1 cells, but not in primary cultures. This question is the relevance of the 3T3-L1 cell line as a model of human adipogenic differentiation.

Another important question which remains to be clarified is whether altered GHR expression is a cause or a consequence of adipogenesis. In order to clarify these issues, experiments could be performed using siRNA to inhibit GHR expression in differentiating cells to determine whether GHR expression is necessary for this process.

Ex vivo analyses of whole adipose tissue could also be performed. Since fat is comprised of different cell type (e.g. fibroblast-like pre-adipocytes, mature adipocytes, macrophages), it would be important to study these cells independently in order to account for any changes in adipose tissue composition between different donors (e.g. increased macrophage infiltration, altered adipogenesis and increased apoptosis of certain cell types). This may be of most relevance for future studies of GHR expression and function.

In summary, this study observed that GH-induced STAT5 activation increased as all pre-adipocytes from various fat depots underwent adipocyte differentiation. However, GH-stimulated ERK activation during adipogenesis behaved differently depending on the type of cells. The selection and use of an in vitro system must consider multiple levels of regulation of proliferation, differentiation and function to ensure relevant results. Further research is necessary to gain insight in the molecular processes that are involved in adipocyte differentiation.

# Appendix 1

### 30% acrylamide stock solution

Acrylamide	29g
bisacrylamide	1g

Adjusted to final volume of 100ml and stored in the dark at 4°C.

### Loading buffer

10% SDS	2ml
Glycerol	1ml
0.5M Tris (pH6.8)	1ml
Distilled water	800µl
2% Pyronin Y	100µl
β-mercaptoethanol	(20µl/ml)
*PMSF	(100mM, 10µl/ml)
*Sodium orthovanadate	(100mM, 10µl/ml)

This stock solution was then stored at 4°C.

\* added immediately prior to use.

### Running buffer

Tris	15g
Glycine	2g
SDS	5g

Make up to 1 litre distilled water.

### Blotting buffer

0.025M Tris	3.025g
0.182M glycine	13.66g
Methanol	200 ml
Distilled water	800ml

Cool to -20°C for 1 hour prior to use.

**Sodium orthovanadate**

Sodium orthovanadate	9.5g
Distilled water	~400 ml

Adjusted to pH 10.2 with hydrochloric acid.

Heat just the pH to 10.2 with 1M NaOH.

pH between 9.9 and 10.1.

**Chymostatin, Leupeptin, Antipain, Pepstatin (CLAP)**

1000X protease inhibitor (CLAP)	5mg
DMSO	500µl

5µl were stored at -20°C.

**TBS (x10)**

Tris	24.2g
Sodium chloride	80g

Adjusted to pH 7.6 with hydrochloric acid.

Make up to 1 litre with distilled water.

**TBS – T**

TBS (10x)	100ml
Distilled water	900ml
Tween 20	1ml

**Blocking buffer**

Non-fat milk powder	5g
TBS – 1x	100ml

**Stripping buffer**

Tris (0.5M, pH 6.8)	6.25ml
10% SDS	10ml
β-mercaptoethanol	0.35ml
Distilled water	3.5ml

**Phosphate buffered saline (PBS)**

NaCl	16g
Na <sub>2</sub> HPO <sub>4</sub>	2.9g
KH <sub>2</sub> PO <sub>4</sub>	0.5g
KCL	0.4g
Distilled water	2L

Adjusted to pH 7.2 using 10M sodium hydroxide.

# Appendix 2

## Molecular biology reagent

### Luria agar (ampicillin- 10µg/ml)

Luria agar	7.4g
Distilled water	200ml

Autoclave and leave to cool to approximately 50°C, then add 200µl ampicillin (100mg/ml). Mix thoroughly, pour out into sterile plates (approximately 10) and allow to set. Store at 4°C until required.

### Luria agar

LB medium	1.8g
Distilled water	490ml

Autoclaved, cooled and stored at 4°C.

### Glycerol stock (40%)

Glycerol	4ml
Distilled water	6ml

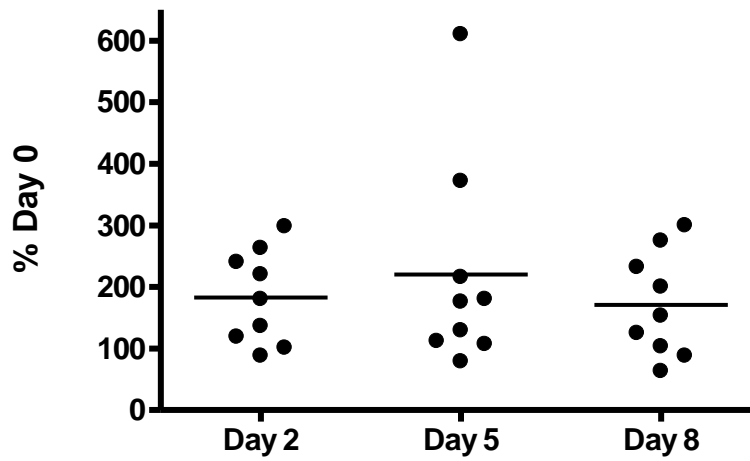
### TEA buffer x1

Tris base	40Mm pH 7.6
EDTA	1ml
Glacial acetic acid	20mM

### 1% agarose gel

Agarose	1g
TEA buffer	50ml

### 66 kDa form of Shc levels



### 66 kDa form of Shc levels

Data from Figure 4.3 66 kDa form of Shc levels were reanalysed and plotted on a scatter plot. There was no difference between groups or with respect to Day 0,  $p=0.337$ . Thus confirming that  $p66^{\text{Shc}}$  level did not decline as 3T3-L1 cells underwent adipogenic differentiation.

## Ethical approval (06/WSE03/37)



Canolfan Gwasanaethau Busnes  
Business Services Centre

### South East Wales Local Research Ethics Committee Panel C

Direct Line: 02920 376823/376822  
Facsimile: 02920 376835  
Email: Carl.phillips@bsc.wales.nhs.uk

Dr Dafydd A Rees  
Senior Lecturer in Endocrinology  
Cardiff University  
Department of Endocrinology  
University Hospital of Wales  
Heath Park, Cardiff  
**CF14 4XW**

30 May 2006

Dear Dr Rees

**Full title of study:** Physiological and pharmacological modulation of  
adipose/connective tissue remodelling  
**REC reference number:** 06/WSE03/37

Thank you for your letter of 12 May 2006, responding to the Committee's request for further information on the above research [and for submitting revised documentation].

The further information has been considered on behalf of the Committee by the Chair.

#### Confirmation of ethical opinion

On behalf of the Committee, I am pleased to confirm a favourable ethical opinion for the above research on the basis described in the application form, protocol and supporting documentation [as revised].

#### Ethical review of research sites

The favourable opinion applies to the research sites listed on the attached form.

#### Conditions of approval

The favourable opinion is given provided that you comply with the conditions set out in the attached document.

You are advised to study the conditions carefully.



Canolfan Gwasanaethau Busnes  
Ty Churchill  
17 Ffordd Churchill  
Caerdydd, CF10 2TW  
Ffôn: 029 20376820 WHTN: 6855  
Ffacs: 029 20376926

Business Services Centre  
Churchill House  
17 Churchill Way  
Cardiff, CF10 2TW  
Telephone: 029 20376820 WHTN: 6855  
Fax: 029 20376826

rhan o Bwrdd Iechyd Lleol Powys / part of Powys Local Health Board

**Approved documents**

The final list of documents reviewed and approved by the Committee is as follows:

<i>Document</i>	<i>Version</i>	<i>Date</i>
Application	5.0	13 March 2006
Investigator CV	Dr M Ludgate	01 January 2006
Investigator CV	Dr D A Rees	20 January 2006
Protocol	2	01 May 2006
Letter from Sponsor		07 February 2006
Peer Review		27 February 2006
Statistician Comments		23 January 2006
GP/Consultant Information Sheets	2	01 May 2006
Participant Information Sheet:	2	01 May 2006
Participant Consent Form	1	01 January 2006
Response to Request for Further Information		12 May 2006
Letter from Funder		07 March 2006

**Research governance approval**

The study should not commence at any NHS site until the local Principal Investigator has obtained final research governance approval from the R&D Department for the relevant NHS care organisation.

**Statement of compliance**

The Committee is constituted in accordance with the Governance Arrangements for Research Ethics Committees (July 2001) and complies fully with the Standard Operating Procedures for Research Ethics Committees in the UK.

<b>06/WSE03/37</b>	<b>Please quote this number on all correspondence</b>
--------------------	---

With the Committee's best wishes for the success of this project

Yours sincerely



Carl Phillips  
**Executive Officer**  
**South East Wales Research Ethics Committees**

Enclosures:           Standard approval conditions SL-AC2  
                                   Site approval form

Copy to:               R&D Department for Cardiff University  
                                   R&D Department for Cardiff & Vale NHS Trust

SF1 list of approved sites

## References

Abdel-Meguid, S., Sheih, H.S., Smith, W.W., Dayringer, H.E., Violand B.N. and Bentle, L.A. (1987) Three-dimensional structure of a genetically engineered variant of porcine growth hormone. *Proc Natl Acad Sci U S A.* 84: 6434–6437.

Adams, M., Reginato, M.J., Shao, D., Lazar, M.A., and Chatterjee, V.K. (1997) Transcriptional activation by peroxisome proliferator-activated receptor gamma is inhibited by phosphorylation at a consensus mitogen-activated protein kinase site. *J Biol Chem.* 272: 5128–5132.

Amselem, S., Sobrier, M.L., Dastot, F., Duquesnoy, P., Duriez, B. and Goossens. M. (1996) Molecular basis of inherited growth hormone resistance in childhood. *Baillieres Clin Endocrinol Metab* 10: 353–359.

Asada, N., Takahashi, Y., Wada, M., Naito, N., Uchida, H., Ikeda, M. and Honjo, M. (2000) GH induced lipolysis stimulation in 3T3-L1 adipocytes stably expression hGHR: analysis on signalling pathway and activity of 20 K hGH. *Mol Cell Endocrol.* 162: 121-129.

Almind, K., Ahlgren, M.G., Hansen, T., Urhammer, S.A., Clausen, J.O. and Pedersen, O. (1999) Discovery of a Met300Val variant in Shc and studies of its relationship to birth weight and length, impaired insulin secretion, insulin resistance, and type 2 diabetes mellitus. *J Clin Endocrinol Metab.* 84: 2241-4.

Altiok, N., Altiok, S. and Changeux, J.P. (1997) Heregulin-stimulated acetylcholine receptor gene expression in muscle: requirement for MAP kinase and evidence for a parallel inhibitory pathway independent of electrical activity. *EMBO J.* 16: 717–725.

Anderson, L.L., Jeftinija, S. and Scanes, C.G. (2004) Growth hormone secretion: Molecular and cellular mechanisms and in vivo approaches. *Exp Biol Med.* 229: 291-302.

Argetsinger, L., Kouadio, J.L., Steen, H., Stensballe, A., Jensen, O.N. and Carter-Su, C. (2004) Autophosphorylation of JAK2 on Tyrosines 221 and 570 Regulates Its Activity. *Mol Cell Biol.* 24: 4955–4967.

Argetsinger, L.S., Campbell, G.S., Yang, X., Witthuhn, B.A., Silvennoinen, O., Ihle, J.N. and Carter-Su, C. (1993) *Cell.* 74: 237-44.

Armengol, J., Villena, J.A., Hondares, E., Carmona, M.C., Sul, H.S., Iglesias, R., Giralt, M. and Villarroya, F., (2012) Pref-1 in brown adipose tissue: specific involvement in brown adipocyte differentiation and regulatory role of C/EBP $\delta$ . *Biochem J.* 443: 799-810.

Aubert, J., Belmonte, N. and Dani, C. (1999) Role of pathways for signal transducers and activators of transcription, and mitogen-activated protein kinase in adipocyte differentiation. *Cell Mol Life Sci.* 56: 538–542.

Banerjee, S.S., Feinberg, M.W., Watanabe, M., Gray, S., Haspel, R.L., Denking, D.J., Kawahara, R., Hauner, H., Jain, M.K.. (2003) The Kruppel-like factor KLF2 inhibits peroxisome proliferator-activated receptor-gamma expression and adipogenesis. *J Biol Chem* 278: 2581–2584.

Barclay, J.L., Kerr, L.M., Arthur, L., Rowland, J.E., Nelson, C.N., Ishikawa, M., d'Aniello, E.M., White, M., Noakes, P.G., and Waters, M.J. (2010) In Vivo Targeting of the Growth Hormone Receptor (GHR) Box1 Sequence Demonstrates that the GHR Does Not Signal Exclusively through JAK2. *Mol Endocrn.* 24: 204-217.

Barsh, G., Seeburg, P. and Gelinias, R., (1983) The human growth hormone gene family: structure and evolution of the chromosomal locus. *Nucleic Acid Res.* 11:3939-3958.

Bartlett, J. M. S and Stirling, D. (2003). A Short History of the Polymerase Chain Reaction. *PCR Protocols.* 226: 3–6.

Behncken, S. and Waters, M., (1999) Molecular recognition events involved in the activation of the growth hormone receptor by growth hormone. *J Mol Recognit.* 12: 355-362.

Benekli, M., Baer, M.R., Baumann, H. and Wetzler, M., (2003) Signal transducer and activator of transcription proteins in leukemias. *Blood.* 101: 2940-54.

Bengtsson, B.A., Brummer, R.J., Eden, S., Rosen, T. and Sjostrom, L., (2002). Effects of growth hormone on fat mass and fat distribution. *Acta Paediatrica.* 38362-65.

Berneis, K. and Keller, U. (1996) Metabolic actions of growth hormone: Direct and indirect. *Bailliere's Clin Endocrinol Metab.* 10: 337-352.

Birsoy, K., Chen, Z. and Friedman, J. (2008) Transcriptional regulation of adipogenesis by KLF4. *Cell Metab.* 7: 339-347.

Bjørndal, B., Burri, L., Staalesen, V., Skorve, J., Berge, R.K., (2011) Different adipose depots: their role in the development of metabolic syndrome and mitochondrial response to hypolipidemic agents. *J Obes.* 2011: 1-15.

Blum, W., Machinis, K., Shavrikova, E., Keller, A., Stobbe, H., Pfaeffle, R. and Ameslem, S. (2006) The growth response to growth hormone (GH) treatment in children with isolated GH

deficiency is independent of the presence of the exon 3-minus isoform of the GHR receptor. *J Clin Endocrinol Metab.* 91: 4171-4179.

Bonilla, E. and Prella, A. (1987) Application of Nile blue and Nile red, two fluorescent probes, for detection of lipid droplets in human skeletal muscle. *J Histochem Cytochem.* 35: 619–621.

Bost, F., Aouadi, M., Caron, L. and Binétruy, B. (2005) The role of MAPKs in adipocyte differentiation and obesity. *Biochimie.* 87: 51-6.

Bost F, Caron, L., Marchetti, I., Dani, C., Le Marchand-Brustel, Y. and Binetruy, B. (2002) Retinoic acid activation of the ERK pathway is required for embryonic stem cell commitment into the adipocyte lineage. *Biochem J.* 361: 621–627.

Bouloumié, A., Curat, C.A., Sengenès, C., Lolmède, K., Miranville, A. and Busse, R. (2005) Role of macrophage tissue infiltration in metabolic diseases. *Curr Opin Clin Nutr Metab Care.* 8: 347-54.

Breed, D.R., Margraf, L.R., Alcorn, J.L. and Mendelson, C.R. (1997) Transcription Factor C/EBP  $\gamma$  in Fetal Lung: Developmental Regulation and Effects of Cyclic Adenosine 3',5'-Monophosphate and Glucocorticoids. *Endocrinol.* 138: 5527-5534.

Brey CW, Nelder MP, Hailemariam T, Gaugler R and Hashmi S. 2009. Kruppel-like family of transcription factors: an emerging new frontier in fat biology. *Int J Biol Sci.* 5: 622–636.

Brown, R.J., Adams, J.J., Pelekanos, R.A., Wan, Y., McKinstry, W.J., Palethorpe, K., Seeber, R.M., Monks, T.A., Eidne, K.A., Parker, M.W. and Waters, M.J. (2005) Model for

growth hormone receptor activation based on subunit rotation within a receptor dimer. *Nat Struct Mol Biol.* 12: 814-21.

Brunori, A., Bruni, P., Delitala, A. and Chiappetta, F. (1995) Acromegaly and pituitary tumors, early anatomoclinical observations. *Surg Neurol.* 44: 83-88.

Butler, A.A. and Le Roith, D. (2001) Control of growth by somatotrophic axis: Growth hormone and the insulin-like growth factors have related and independent roles. *Annu Rev Physiol.* 65: 141–146.

Cao, Z., Umek, R.M. and McKnight, S.L. (1991) Regulated expression of three C/EBP isoforms during adipose conversion of 3T3-L1 cells. *Genes Dev.* 5: 1538–1552.

Caprio, S., Hyman, L.D., Limb, C., McCarthy, S., Lange, R., Sherwin, R.S., Shulman, G. and Tamborlane, W.V. (1995) Central adiposity and its metabolic correlates in obese adolescent girls. *J Am Physiol.* 269: E118-E126.

Carter-Su, C., Schwartz, J. and Simt, L.S. (1996) Molecular mechanism of growth hormone action. *Annu Rev Physiol.* 58: 187-207.

Chawla, P., John, S., Parks, J. and Rudman, D. (1983) Structural Variants of Human Growth hormone. *Ann Rev Med.* 34: 519-47.

Chen, H., Jackson, S., Doro, M. and McGowan, S. (1998) Perinatal expression of genes that may participate in lipid metabolism by lipid-laden lung fibroblasts. *J Lipid Res.* 39: 2483-2492.

Chen, S., Chen, J., Johnson, P.F., Muppala, V. and Lee, Y. (2000) When Expressed from the C/EBP $\beta$  Gene Locus, Can Functionally Replace C/EBP $\alpha$  in Liver but Not in Adipose Tissue. *Mol Cell Biol.* 20: 7292–7299.

Chen, Z., Torrens, J.I., Anand, A., Spiegelman, B.M. and Friedman, J.M. (2005) Krox20 stimulates adipogenesis via C/EBP $\beta$ -dependent and independent mechanisms. *Cell Metab.* 1: 93-106.

Chu, G., Hayakawa, H. and Berg, P. (1987) Electroporation for the Efficient Transfection of Mammalian Cells with DNA. *Nuc Acids Res.* 15: 1311-1326.

Chuderland, D. and Seger, R. (2005) Protein-protein interactions in the regulation of the extracellular signal-regulated kinase. *Mol Biotechnol.* 29: 57-74.

Cipolletta, D., Feuerer, M., Li, A., Kamei, N., Lee, J., Shoelson, S.E., Benoist, C., Mathis, D. (2012) PPAR- $\gamma$  is a major driver of the accumulation and phenotype of adipose tissue Treg cells. *Nature.* 486: 549-53.

Clark, A.R. (2003) MAP kinase phosphatase 1: a novel mediator of biological effects of glucocorticoids? *J Endocrinol.* 178: 5-12.

Clemmons, D.R. (2007) Modifying IGF1 activity: an approach to treat endocrine disorders, atherosclerosis and cancer. *Nat Rev Drug Discov.* 2007: 821-833.

Cole, H. (1938) The endocrine control of growth. *J Anim Sci.* 20-26.

Colonna, V.G., Cella, S.G., Locatelli, V., Loche, S., Ghigo, E., Cocchi, and Muller, E.E. (1989) Neuroendocrine Control of Growth Hormone Secretion. *Acta Pdiatr Scand.* 349: 87-92.

Corbacho, M., Martinez de la Escalera, G. and Clapp, C. (2002) Roles of prolactin and related members of the prolactin/growth hormone/placental lactogen family in angiogenesis. *J Endocrinol.* 173: 219–238.

Corin, R.E., Guller, S., Wu, K.Y. and Sonenberg, M. (1990) Growth hormone and adipose differentiation: growth hormone-induced antimitogenic state in 3T3-F442A preadipose cells. *Proc Natl Acad Sci U S A.* 87: 7507-11.

Darlington, G.J., Ross, S.E. and MacDougald, O.A. (1998) The role of C/EBP genes in adipocyte differentiation. *J Biol Chem.* 273: 30057-30060.

Daughaday, W.H. and Rotwein, P. (1989) Insulin-like growth factors I and II. Peptide, messenger ribonucleic acid and gene structures, serum, and tissue concentrations. *Endocr Rev.* 10: 68-91.

Davidson, M.B. (1987) Effect of growth hormone on carbohydrate and lipid metabolism. *Endocr Rev.* 8: 115-131.

Debs, R.J., Fuchs, H.J., Philip, R., Brunette, E.N, Düzgüneş, N., Shellito, J.E., Liggitt, D. and Patton, J.R. (1990) Immunomodulatory and toxic effects of free and liposome-encapsulated tumor necrosis factor alpha in rats. *Cancer Res.* 50: 375-80.

Del Rincon, J.P., Iida, K., Gaylinn, B.D., McCurdy, C.E., Leitner, J.W., Barbour, L.A., Kopcgick, J.J., Friedman, J.E., Draznin, B. and Thomer, M.O. (2007) Growth hormone regulation of p85 $\alpha$  expression and phosphoinositide 3-kinase activity in adipose tissue mechanism for growth hormone-mediated insulin resistance. *Diabetes*. 56: 1638-1646.

Deng, L., He, K., Wang, X., Yang, N., Thangavel, C., Jiang, J., Fuchs, S.Y. and Frank, S. (2007) Determinants of growth hormone receptor down-regulation. *Mol Endocrinol*. 21: 1537-1551.

De Vos., A.M., Ultsch, M. and Kossiakoff, A.A. (1992) Human growth hormone and extracellular domain of its receptor: Crystal structure of the complex. *Sci*. 255: 306-312.

Dickinson, R.J. and Keyse, S.M. (2006) Diverse physiological functions for dual-specificity MAP kinase phosphatases. *J Cell Sci*. 119: 4607-15.

Dietz, J. and Schwartz, J. (1991) Growth hormone alters lipolysis and hormone-sensitive lipase activity in 3T3-F442A adipocytes. *Metabolism*. 40: 800-806.

Du L, Frick, G.P., Tai, L.R., Yoshimura, A. and Goodman, H.M. (2003) Interaction of the growth hormone receptor with cytokine-induced Src homology domain 2 protein in rat adipocytes. *Endocrinol*. 144: 868–876.

Edens, A. and Talamantes, F. (1998) Alternative processing of growth hormone receptor transcripts. *Endocrine Soci*. 19: 559-582.

Escher, P. and Wahli, W. (2000) Peroxisome proliferator-activated receptors: insight into multiple cellular functions. *Mutat. Res*. 448:121-138.

Evans, H.M. and Long, J.A. (1922) Characteristic effects upon growth, oestrus, and ovulation induced by the intraperitoneal administration of fresh anterior hypophyseal substance. *Proc Natl Acad Sci* 8:38–39.

Fajas, L., Debril, M. and Auwerx, J. (2001) Peroxisome proliferator-activated receptor  $\gamma$ : from adipogenesis to carcinogenesis. *J Mol Endocrinol.* 27: 1–9.

Farmer, S.R. (2006) Transcriptional control of adipocyte formation. *Cell Metab* 4: 263-273.

Felgner, P.L., Gadek, T.R., Holm, M., Roman, R., Chan, H.W., Wenz, M., Northrop, J.P., Ringold, G.M. and Danielsen, M. (1987) Lipofection: a highly efficient, lipid-mediated DNA-transfection procedure. *Proc Natl Acad Sci U S A.*84: 7413-7.

Felgner, P.L., Tsai, Y.J., Sukhu, L., Wheeler, C.J., Manthorpe, M., Marshall, J. and Cheng, S.H. (1995) Improved cationic lipid formulations for in vivo gene therapy. *Ann N Y Acad Sci.* 27; 772:126-39.

Fernyhough, M.E., Okine, E., Hausman, G., Vierck, J.L. and Dodson, M.V. (2007) PPAR $\gamma$  and GLUT-4 expression as developmental regulators/markers for preadipocyte differentiation into an adipocyte. *Domist Anim Endocrin.* 33: 367-378.

Flint, D.J., Binart, N., Boumard, S., Kopchick, J.J. and Kelly, P. (2006) Developmental aspects of adipose tissue in GH receptor and prolactin receptor gene disrupted mice: site-specific effects upon proliferation, differentiation and hormone sensitivity. *J Endocrinol.* 191: 101-111.

Floyd, Z.E. and Stephens, J.M. (2003) STAT5A promotes adipogenesis in nonprecursor cells and associates with the glucocorticoid receptor during adipocyte differentiation. *Diabetes*. 52: 308-14.

Floyd, Z.E., Segura, B.M., He, F. and Stephens, J.M. (2007) Degradation of STAT5 proteins in 3T3-L1 adipocytes is induced by TNF- $\alpha$  and cycloheximide in a manner independent of STAT5a activation. *J Physiol Endocrinol Metab*. 292: 461-468.

Forsyth, I.A. (1986) Variation among species in the endocrine control of mammary growth and function: the role of prolactin, growth hormone, and placental lactogen. *J Dairy Sci*. 69: 886-903.

Frank, S.J. (2002) receptor dimerization in GH and erythropoietin action-it takes two to Tango, but how? *Endocrinol*. 143:2-10.

Francia P, Cosentino F, Schiavoni M, Huang Y, Perna E, Camici GG, Lüscher TF and Volpe M.(2009). p66(Shc) protein, oxidative stress, and cardiovascular complications of diabetes: the missing link. *J Mol Med (Berl)*. 87: 885-91.

Freda, P.U. (2003) Current concepts in the biochemical assessment of the patient with acromegaly. *Growth Horm IGF Res*. 13: 171-84.

Freytag, S.O., Paielli, D.L. and Gilbert, J.D. (1994) Ectopic expression of the CCAAT/enhancer-binding protein alpha promotes the adipogenic program in a variety of mouse fibroblastic cells. *Genes Dev*. 8: 654-1663.

Frick, P., Baumbach, W. and Goodman, H. (1998) Tissue distribution, turnover and glycosylation of the long and short growth hormone receptor isoforms in rat tissues. *Endocrinology*. 30: 2824-2830.

Fruhbeck, G., Aguado, M. and Martinez, J.A . (1997) In vitro lipolytic effect of leptin on mouse adipocytes: evidence for a possible autocrine/paracrine role of leptin. *Biochem Biophys Res Commun*. 240: 590 –594.

Fu, Y., Luo, N., Klein, R.L. and Garvey, W.T. (2005) Adiponectin promotes adipocyte differentiation, insulin sensitivity, and lipid accumulation. *J Lipid Res*. 46: 1369-1379.

Fuentes, E.N., Einarsdottir, I.E., Valdes, J.A., Alvarez, M., Molina, A., Björnsson, B.T. (2012) Inherent growth hormone resistance in the skeletal muscle of the fine flounder is modulated by nutritional status and is characterized by high contents of truncated GHR, impairment in the JAK2/STAT5 signalling pathway, and low IGF-I expression. *Endocrinol*. 53: 283-94.

Galic, S., Oakhill, J.S. and Steinberg, G. (2009) Adipose tissue as an endocrine organ. *Mol and Cell Endocrinol*. 316: 129-139.

Gerfault, V., Louveau, I. and Mouro, J. (1999) The effect of GH and IGF-I on preadipocytes from Large White and Meishan pigs in primary culture. *Gen Comp Endocrinol*. 114: 396-404.

Gharibi, B., Abraham, A.A., Ham, J., Evans, B.A. (2011) Adenosine receptor subtype expression and activation influence the differentiation of mesenchymal stem cells to osteoblasts and adipocytes. *J Bone Miner Res*. 26: 2112-2124.

Gent, J., Kerkhof, P., Roza, M., Bu, G. and Strous, G.J. (2002) Ligand-independent growth hormone receptor dimerization occurs in the endoplasmic reticulum and is required for ubiquitin system-dependent endocytosis. *Proc Natl Acad Sci.* 99: 858-9863.

Gerin, I., Dolinsky, V.W., Shackman, J.G., Kennedy, R.T., Chiang, S.H., Buran, C.F., Steffensen, K.R., Gustafsson, J.A. and MacDougald, O.A. (2005) LXRbeta is required for adipocyte growth, glucose homeostasis, and beta cell function. *J Biol Chem.* 280: 23024-31.

Goralski, K. and Sinal, C. (2007) Type 2 diabetes and cardiovascular disease: getting to the fat of the matter. *Can J Physiol Pharmacol.* 85: 113-32.

Green, H. and Kehinde, O. (1974) Sublines of mouse 3T3 cells that accumulate lipid. *Cell.* 1:113-117.

Green, H. and Kehinde, O. (1975) An established preadipose cell line and its differentiation in culture. II. Factors affecting the adipose conversion. *Cell.* 5:19–27.

Green, H. and Meuth, M. (1974) An established pre-adipose cell line and its differentiation in culture. *Cell.* 3:127-133.

Gregoire, F.M. (2001) Adipocyte differentiation: from fibroblast to endocrine cell. *Exp Biol Med (Maywood).* 226: 997-1002.

Gregoire, F.M., Smas, C.M. and Sul, H.S. (1998) Understanding adipocyte differentiation. *Physiol Rev.* 8: 83–809.

Grimaldi, P.A. (2001) The roles of PPARs in adipocyte differentiation. *Prog Lipid Res.* 40: 269-281.

Grimaldi, P., Negrel, R. and Ailhaud, G. (1978) Induction of the triglyceride pathway enzymes and of lipolytic enzyme during differentiation in a preadipocyte cell line. *Eur J Biochem.* 84: 369-376.

Gude, M.F., Frystyk, J., Flyvbjerg, A., Bruun, J.M., Richelsen, B. and Pedersen, S.B. (2012) The production and regulation of IGF and IGFBNs in human adipose tissue cultures. *Growth Horm IGF Res.* 6: 200-5.

Guller, S., Sonenberg, M., Wu, K.Y., Szabo, P. and Corin, R.E. (1989) Growth hormone-dependent events in the adipose differentiation of 3T3-F442A fibroblasts: modulation of macromolecular synthesis. *Endocrin.* 125: 2360-7.

Harp, J.B., Franklin, D., Vanderpuije, A.A. and Gimble, J.M. (2001) Differential expression of signal transducers and activators of transcription during human adipogenesis. *Biochem Biophys Res Commun.* 281: 907-912.

Hausman, G.J. and Richardson, R.L. (1998) Newly recruited and pre-existing preadipocytes in cultures of porcine stromal-vascular cells: morphology, expression of extracellular matrix components, and lipid accretion. *J Anim Sci.* 76: 48-60.

He, W., Barak, Y., Hevener, A., Olson, P., Liao, D., Le, J., Nelson, M., Ong, E., Olefsky, J.M. and Evans, R.M. (2003) Adipose-specific peroxisome proliferator-activated receptor  $\gamma$  knockout causes insulin resistance in fat and liver but not in muscle. *PNAS.* 100: 15712-15717.

Herrera, R., Ro, H.S., Robinson, G.S., Xanthopoulos, K.G. and Spiegelman, B.M. (1989) A direct role for C/EBP and the AP-1-binding site in gene expression linked to adipocyte differentiation. *Mol Cell Biol.* 9: 5331-5339.

Higuchi, R., Fockler, C., Dollinger, G. and Watson, R. (1993) Kinetic PCR analysis: Real-time monitoring of DNA amplification reactions. *Biotechnol.* 11: 1026–1030.

Horbinski, C. and Chu, CT. (2005) Kinase signaling cascades in the mitochondrion: a matter of life or death. *Free Radic Biol Med.* 38: 2–11.

Horie, Y., Suzuki, A., Kataoka, E., Sasaki, T., Hamada, K., Sasaki, J., Mizuno, K., Hasegawa, G., Kishimoto, H., Iizuka, M., Naito, M., Enomoto, K., Watanabe, S., Mak, T.W. and Nakano, T. (2004) Hepatocyte-specific Pten deficiency results in steatohepatitis and hepatocellular carcinomas *J Clin Invest.* 113: 1774–1783.

Hossain, P., Kavar, B. and El Nahas, M. (2007) Obesity and Diabetes in the Developing World – A Growing Challenge. *N Engl J Med.* 356: 213-215.

Ihle, J.N., Witthuhn, B.A., Quelle, F.W., Yamamoto, K. and Silvennonine, O. (1995) Signalling through the hematopoietic cytokine receptors. *Annu Rev Immunol.* 13: 369-398.

Iida, K., Takahashi, Y., Kaji, H., Yoshioka, S., Murata, M., Iguchi, G., Okimura, Y. and Chihara, K. (2003) Diverse regulation of full-length and truncated growth hormone receptor expression in 3T3-L1 adipocytes. *Mol Cell Endocrinol.* 210: 21-29.

Imai, T., Takakuwa, R., Marchand, S., Dentz, E., Bornert, J.M, Messaddeq, N., Wendling, O., Mark, M., Desvergne, B., Wahli, W., Chambon, P. and Metzger, D. (2004) Peroxisome proliferator-activated receptor gamma is required in mature white and brown adipocytes for their survival in the mouse. *Proc Natl Acad Sci U S A.* 101: 4543-4547.

Jeay, S., Sonenshein, G.E., Postel-Vinay, M.C., Kelly, P.A. and Baixeras, E. (2002) Growth hormone can act as a cytokine controlling survival and proliferation of immune cells: new insights into signaling pathways. *Mol Cell Endocrinol.* 1: 88:1–7.

Ji, S., Frank, S.J. and Messina, J.L. (2002) Growth hormone-induced differential desensitization of STAT5, ERK, and Akt Phosphorylation. *J Biol Chem.* 277: 28384–28393.

Johnson, G.L. and Lapadat, R. (2002) Mitogen-activated protein kinase pathways mediated by ERK, JNK, and p38 protein kinases. *Sci.* 298: 1911-1912.

Kahn, B.B. and Flier, J.S. (2000) Obesity and insulin resistance. *J Clin Invest.* 106: 473-81.

Kamel, A., Norgren, S., Elimam, A., Danielsson, P. and Marcus, C. (2000) Effects of growth hormone treatment in obese prepubertal boys. *J. Clin. Endocrinol. Metab.* 85: 1412-1419.

Kamai, Y., Mikawa, S., Endo, K., Sakai, H., Komano, T. (1996) Regulation of insulin-like growth factor-I expression in mouse preadipocytes Ob1771 cells. *J Biol Chem.* 271: 9883-6.

Kanazawa, A., Kawamura, Y., Sekine, A., Iida, A., Tsunoda, T., Kashiwagi, A., Tanaka, Y., Babazono, T., Matsuda, M., Kawai, K., Iizumi, T., Fujioka, T., Imanishi, M., Kaku, K., Iwamoto, Y., Kawamori, R., Kikkawa, R., Nakamura, Y., Maeda, S. (2005) Single nucleotide polymorphisms in the gene encoding Kruppel-like factor 7 are associated with type 2 diabetes. *Diabetologia.* 48:1315-1322.

Kawai, M., Namba, N., Mushiake, S., Etani, Y., Nishimura, R., Makishima, M. and Ozono, K. (2007) Growth hormone stimulates adipogenesis of 3T3-L1 cells through activation of the Stat5A/5B-PPAR $\gamma$  pathway. *J Mol Endocrinol.* 38: 19-34.

Khanna-Gupta, A. (2008) Sumoylation and the function of CCAAT enhancer binding protein alpha (C/EBP $\alpha$ ). *Blood Cell Mol Dis.* 41: 7-81.

Kim, K.A., Kim, J.H., Wang, Y., Sul, H.S. (2007) Pref-1 (preadipocyte factor 1) activates the MEK/extracellular signal-regulated kinase pathway to inhibit adipocyte differentiation. *Mol Cell Biol.* 27: 2294–2308.

Kim, Y.C and Ntambi J.M. (1999) Regulation of stearyl-CoA desaturase genes: role in cellular metabolism and preadipocyte differentiation. *Biochem Biophys Res Commun.* 266: 1-4.

Kim, J.B. and Spiegelman, B.M. (1996) ADD1/SREBP1 promotes adipocyte differentiation and gene expression linked to fatty acid metabolism. *Genes Dev.* 10: 1096–1107.

Kim, J.B., Sarraf, P., Wright, M., Yao, K.M., Mueller, E., Solanes, G., Lowell, B.B. and Spiegelman, B.M. (1998) Nutritional and insulin regulation of fatty acid synthetase and leptin gene expression through ADD1/SREBP1. *J Clin Invest.* 101: 1–9.

Kim, J.E. and Chen, J. (2004) Regulation of peroxisome proliferator-activated receptor $\gamma$  activity by mammalian target of rapamycin and amino acids in adipogenesis. *Diabetes.* 53: 2748-2756.

Kim, S.H., Kwon, H.B., Kim, Y.S., Ryu, J.H., Kim, K.S., Ahn, Y., Lee, W.J. and Choi, K.Y. (2002) Isolation and characterization of a *Drosophila* homologue of mitogen-activated protein kinase phosphatase-3 which has a high substrate specificity towards extracellular-signal-regulated kinase. *Biochem. J.* 361: 143-151.

Kim, S.W., Muise, A.M., Lyons, P.J. and Ro, H.S. (2001) Regulation of adipogenesis by a transcriptional repressor that modulates MAPK activation. *J Biol Chem.* 276: 10199-10206.

Klaus, S. (2004) Adipose tissue as a regulator of energy balance. *Curr Drug Targets*. 5: 241-250.

Kletzien, R.F., Foellmi, L.A., Harris, P.K., Wyse, B.M. and Clarke, S.D. (1992) Adipocyte fatty acid-binding protein: regulation of gene expression in vivo and in vitro by an insulinsensitizing agent. *Mol Pharmacol*. 42: 558-562.

Klötting, N., Koch, L., Wunderlich, T., Kern, M., Ruschke, K., Krone, W., Brüning, J.C. and Blüher, M. (2008) Autocrine IGF-1 action in adipocytes controls systemic IGF-1 concentrations and growth. *Diabetes* 57: 2074 –2082.

Knai, C., Suhrcke, M. and Lobstein, T. (2007) Obesity in Eastern Europe: an overview of its health and economic implications. *Econ Hum Biol*. 5: 392-408.

Koeffler, H.P. (2003) Peroxisome proliferator-activated receptor gamma and cancers. *Clin. Cancer Res*. 9:1 – 9.

Kolch, W. (2000) Meaningful relationships: the regulation of the Ras/Raf/MEK/ERK pathway by protein interactions. *Biochem J*. 351: 289-305.

Kopchick, J. and Andry, J. (2000) Growth hormone (GH), GH receptor, and signal transduction. *Mol Genet Metab*. 71: 293-314.

Kopchick, J., Parkinson, C., Stevens, E. and Trainer, J. (2002) Growth hormone receptor Antagonists: discovery, development, and use in patients with acromegaly. *Endocr Rev*. 23: 623-646.

Kozak, L.P., Britton, J.H., Kozak, U.C. and Wells, J.M. (1988) The mitochondrial uncoupling protein gene. Correlation of exon structure to transmembrane domains. *J Biol Chem.* 263: 12274-12277.

Kricka, L.J. (1991) Chemiluminescent and bioluminescent techniques. *Clin Chem.* 37: 1472-81.

Langin, D. (2006) Adipose tissue lipolysis as a metabolic pathway to define pharmacological strategies against obesity and the metabolic syndrome. *Pharmacol Res.* 53: 482-491.

Lanning, N.J. and Carter-Su, C. (2006) Recent advances in growth hormone signalling. *Rev Endocr Metab Disord.* 7: 225-235.

Large, V., Peroni, O., Letexier, D., Ray, H. and Beylot, M. (2004) Metabolism of lipids in human white adipocyte. *Diabetes Metab.* 30: 294-309.

Lazar MA. (2002) Becoming fat. *Genes Dev.* 16:1–5

Lefterova, M.I., Zhang, Y., Steger, D.J., Schupp, M., Schug, J., Cristancho, A., Feng, D., Zhuo, D., Stoeckert, C.J., Liu, X.S. and Lazar, M.A. (2008) PPAR $\gamma$  and C/EBP factors orchestrate adipocyte biology via adjacent binding on a genome-wide scale. *Gene Dev.* 22: 2941–2952.

Lehmann, J.M., Moore, L.B., Smith-Oliver, T.A., Wilkison, W.O., Willson, T.M., Sandouk, T., Reda, D. and Hofmann, C. (1993) Antidiabetic agent pioglitazone enhances adipocyte differentiation of 3T3-F442A cells. *Am J Physiol Cell Physiol.* 264: 1600-1608.

Leonardsson, G., Steel, J.H., Christian, M., Pocock, V., Milligan, S., Bell, J., So, P.W., Medina-Gomez, G., Vidal-Puig, A., White, R. and Parker, M.G. (2004) Nuclear receptor corepressor RIP140 regulates fat accumulation. *Proc. Natl. Acad. Sci.* 101: 8437–8442.

Le Roith D, Bondy C, Yakar S, Liu JL and Butler A. (2001). The somatomedin hypothesis: 2001. *Endocrin.* 22: 53-74.

Le Tissier, P.R., Hodson, D.J., Lafont, C., Fontanaud, P., Schaeffer, M. and Mollard, P. (2012) Anterior pituitary cell networks. *Front Neuroendocrinol.* 33:252-66.

Lewis, M.D., Horan, M., Millar, D.S., Newsway, V., Easter, T.E., Fryklund, L., Gregory, J.W., Norin, M., Del Valle, C.J., Lopez-Siguero, J.P., Canete, R., Lopez-Canti, L.F., Diaz-Torrado, N., Espino, R., Ulied, A., Scanlon, M.F., Procter, A.M. and Cooper, D.N. (2004) A novel dysfunctional growth hormone variant (Ile179Met) exhibits a decreased ability to activate the extracellular signal-regulated kinase pathway. *J Clin Endocrinol Metab.* 89: 1068-1075.

Lewis, M.D., Easter, T.E., Elford, C., Ludgate, M.E., Evans, B.J., Rees, D.A. and Scanlon, M.F. (2006) The effect of bone marrow stem cell (BMSC) differentiation on growth hormone receptor (GHR)-associated signalling pathways. *Endocrine Abstracts* 11:OC7.

Li, C.H., Dixon, J.S. and Liu, W.K. (1969) Human pituitary growth hormone: XIX. The primary structure of the hormone. *Arch Biochem Biophys.* 133:70-91.

Li, C.H., Evans, H.M. and Simpson, M.E. (1945) Isolation and properties of the anterior hypophyseal growth hormone. *J. Biol. Chem.* 159:353–366.

Li, D., Yea, S., Li, S., Chen, Z., Narla, G., Banck, M., Laborda, J., Tan, S., Friedman, J.M., Friedman, S.L. and Walsh, M.J. (2005) Kruppel-like factor-6 promotes preadipocyte

differentiation through histone deacetylase 3-dependent repression of DLK1. J Biol Chem. 280: 26941-26952.

Li, L., Xie, X., Qin, J., Jeha, G. S., Saha, P.K., Yan, J., Haueter, C.M., Chan, L., Tsai, S.Y. and Tsai, M.J. (2009) The nuclear orphan receptor COUP-TFII plays an essential role in adipogenesis, glucose homeostasis, and energy metabolism. Cell Metab. 9: 77-87.

Liao, Z.Y. and Zhu, S.Q. (2004) Identification and characterization of GH receptor and serum GH-binding protein in Chinese Sturgeon (*Acipenser sinensis*). Acta Bioch Bioph Sin, 36: 811-816.

Lichanska, A.M. and Waters, M.J. (2008) New Insights into Growth Hormone Receptor Function and Clinical Implications. Horm Res. 69: 138-145.

Liongue, C. and Ward, A.C. (2007) Evolution of class 1 cytokine receptors. BMC Evol Biol. 7:120.

Listenberger, L.L. and Brown, D.A. (2007) Fluorescent detection of lipid droplets and associated proteins. Current Protocols in Cell Biology, chapter 24, unit 24 22.

Lloyd, R. (2004) Endocrine pathology: differential diagnosis and molecular advances. New Jersey, Humana Press, Inc.

Louveau, I. and Gondret, F. (2004) Growth hormone and insulin affect fatty acid synthase activity in isolated porcine adipocytes in culture without any modifications of sterol regulatory element binding protein-1 expression. J Endocrinol. 181: 271-280.

Love, D., Whatmore, A., Clayton, P. and Silva, C. (1998) Growth hormone stimulation of the mitogen-activated protein kinase pathway is cell type specific. *Endocrinology*. 139: 1965-1971.

Ma, F., Wei, Z., Shi, C., Gan, Y., Lu, J., Frank, S.J., Balducci, J. and Huang, Y. (2011) Signaling cross talk between growth hormone (GH) and insulin-like growth factor-I (IGF-I) in pancreatic islet  $\beta$ -cells. *Mol Endocrinol*. 25: 2119-33.

Maeda, N., Shimomura, I., Kishida, K., Nishizawa, H., Matsuda, M., Nagaretani, H., Furuyama, N., Kondo, H., Takahashi, M., Arita, Y., Komuro, R., Ouchi, N., Kihara, S., Tochino, Y., Okutomi, K., Horie, M., Takeda, S., Aoyama, T., Funahashi, T., Matsuzawa, Y. (2002) Diet-induced insulin resistance in mice lacking adiponectin/ACRP30. *Nat Med*. 8: 731-7.

Maharajan, P. and Maharajan, V. (1993) Growth hormone signal transduction. *Experientia*. 49: 980-987.

Malone, R.W., Felgner, P.L. and Verma, I.M. (1989) Cationic liposome-mediated RNA transfection. *Proc Natl Acad Sci U S A*. 86: 6077-6081.

Mandell, J.W. (2003) Phosphorylation state-specific antibodies: applications in investigative and diagnostic pathology. *Am J Pathol*. 163: 1687-1698.

Marie, P., (1886) Sur deux cas d'acromegalie; hypertrophie singliere non congenitale des extremités superieures, inferieures et cephalique. *Rev de Med*. 6: 297-333.

Marr, E., Tardie, M., Carty, M., Brown Phillips, T., Wang, I.K., Soeller, W., Qiu, X. and Karam, G. (2006) Expression, purification, crystallization and structure of human adipocyte lipid binding protein (aP2). *Acta Crystallogr Sect F Struct Biol Cryst Commun*. 1: 1058-60.

Marx, N. (2002) Peroxisome proliferator-activated receptor gamma and atherosclerosis. *Curr Hypertens Rep.* 4: 71-77.

Matsuaue, K., Peters, J.M. and Gonzalez, F.J. (2004) PPAR $\beta/\alpha$  potentiates PPAR $\gamma$ -stimulated adipocyte differentiation. *FASEB J* 18:1477-1479.

Matsushita, T., Chan, Y.Y., Kawanami, A., Balmes, G., Landret, G.E and Murakami, S. (2009) Extracellular Signal-Regulated Kinase 1 (ERK1) and ERK2 play essential roles in osteoblast differentiation and in supporting osteoclastogenesis. *Mol Cell Biol.* 29: 5843-5857.

Miard, S. and Fajas, L. (2005) Atypical transcriptional regulators and cofactors of PPAR[ $\gamma$ ]. *Int J Obes Relat Metab Disord.* 29: 10-12.

Miyoshi, H., Perfield, J.W., Obin, M.S. and Greenberg, A.S. (2008) Adipose triglyceride lipase regulates basal lipolysis and lipid droplet size in adipocytes. *J Cell Biochem.* 105: 1430-1436.

Moffat, J.G., Edens, A. and Talamantes, F. (1999) Structure and expression of the mouse growth hormone receptor/growth hormone binding protein gene. *J Mol Endocrinol.* 23: 33-44.

Moller, J., Nielsen, S. and Hansen, T.K. (1999) Growth hormone and fluid retention. *Horm Res.* 51 Suppl 3: 116–120.

Moller, N. and Jorgensen, J.L. (2009) Effects of growth hormone on glucose, lipid, and protein metabolism in human subjects. *Endocr Rev.* 30: 152-177.

Mori, T., Sakaue, H., Iguchi, H., Gomi, H., Okada, Y., Takashima, Y., Nakamura, K., Nakamura, T., Yamauchi, T., Kubota, N., Kadowaki, T., Matsuki, Y., Ogawa, W., Hiramatsu,

R. and Kasuga, M. (2005) Role of Kruppel-like Factor 15 (KLF15) in Transcriptional Regulation of lipogenesis. *J Biol Chem.* 280: 12867–12875.

Morikawa, M., Green, H. and Lewis, U. (1984) Activity of human growth hormone and related polypeptides on the adipose conversion of 3T3 cells. *Mol Cell Biol.* 4: 228-231.

Morrison, R.F and Farmer, S.R. (2000) Hormonal signaling and transcriptional control of adipocyte differentiation. *J Nutr.* 130: 3116S-3121S.

Morrison, R.F. and Farmer, S.R. (1999) Insights into the transcriptional control of adipocyte differentiation. *J Cell Biochem.* 33: 59-67.

Moutoussamy, S., Kelly, P.A. and Finidori, J. (1998) Growth hormone-receptor and cytokine-receptor-family signalling. *Eur J Biochem* 5: 1-11.

Muller, E.E. (1987) Neural control of somatotrophic function. *Physiol Rev.* 67: 962-1053.

Mullis, K., Faloona, F., Scharf, S., Saiki, R., Horn, G. and Erlich, H. (1986) Specific enzymatic amplification of DNA in vitro: the polymerase chain reaction. *Quant Biol.* 51: 263–273.

Murakami, M., Narazaki, M., Hibi, M., Yawata, H., Yasukaea, K., Hamaguchi, M., Taga, T. and Kishimoto, T. (1991) Critical cytoplasmic region of the interleukin 6 signal transducer gp 130 is conserved in the cytoplasmic receptor family. *Proc Natl Acad Sci USA.* 88: 11349-11353.

Moya-Camarena, S.Y., Vanden Huevel, J.P., Blanchard, S.G., Leesnitzer, L.A. and Belury, M.A. (1999) Conjugated linoleic acid is a potent naturally occurring ligand and activator of PPAR $\alpha$ . *J. Lipid Res.* 40: 1426-1433.

Nam, S.Y. and Marcus, C. (2000) Growth hormone and adipocyte function in obesity. *Horm Res.* 53: 87-97.

Nam, S.Y. and Lobie, P.E. (2000) The mechanism of effect of growth hormone on preadipocyte and adipocyte function. *Obesity Rev.* 1: 73-86.

Nanbu-Wakao, R., Morikawa, Y., Matsumura, I., Masuho, Y., Muramatsu, M.A., Senba, E. and Wakao, H. (2002) Stimulation of 3T3-L1 adipogenesis by signal transducer and activator of transcription 5. *Mol Endocrinol.* 16: 1565–1576.

Niall, H.D., Hogan, M.L., Sauer, R., Rosenblum, I.Y. and Greenwood, F.C. (1971) Sequences of pituitary and placental lactogenic and growth hormones: Evolution from a primordial peptide by gene reduplication. *Proc nat Acad Sci USA.* 68: 866-870.

Nam, S.Y. and Lobie, P.E. (2000) The mechanism of effect of growth hormone on preadipocyte and adipocyte function. *Obesity.* 1: 73-86.

Newell, F.S., Su, H., Tornqvist, H., Whitehead, J.P., Prins, J.B. and Hutley, L.J. (2006) Characterization of the transcriptional and functional effects of fibroblast growth factor-1 on human preadipocyte differentiation. *FASEB J.* 20: 2615-7.

Ntambi, J.M. and Young-Cheul, K. (2000) Adipocyte differentiation and gene expression. *J Nutr.* 130: 3122S-3126S.

Obregon, M.J. (2008) Thyroid Hormone and Adipocyte Differentiation. *Thyroid* 18: 185-195.

Ohta, T. (1993) Pattern of nucleotide substitutions in growth hormone-prolactin gene family: A paradigm for evolution by gene duplication. *Genetics* 134:1271–1276.

Ohta, T., Tokishita, S. and Yamagata, H. (2001) Ethidium bromide and SYBR Green I enhance the genotoxicity of UV-irradiation and chemical mutagens in *E. coli*. *Mutat Res.* 492: 91-7.

Oishi, Y., Manabe, I., Tobe, K., Tsushima, K., Shindo, T., Fujii, K., Nishimura, G., Maemura K., Yamauchi, T., Kubota, N., Suzuki, R., Kitamura, T., Akira, S., Kadowaki, T., Nagai, R. (2005) KLF5 is a key regulator of adipocyte differentiation. *Cell Metab.* 1:27-39.

Otto, T.C. and Lane, M.D. (2005) Adipose development: from stem cell to adipocyte. *Crit Rev Biochem Mol Bio.* 40: 229-42.

Patel, Y. M and Lane, M.D. (2000) Mitotic clonal expansion during preadipocyte differentiation: calpain-mediated turnover of p27. *J Biol Chem.* 275: 17653-60.

Perret-Vivancos, C., Abbate, A., Ardail, D., Raccurt, M., Usson, Y., Lobie, P.E. and Morel, G. (2006) Growth hormone activity in mitochondria depends on GH receptor Box 1 and involves caveolar pathway targeting. *Exp Cell Res.* 312: 215-232.

Postel-Vinay, M-C. and Kelly, P.A. (1996) Growth hormone receptor signalling. *Clin Endocrinol Metab.* 10: 323-336.

Procter, A.M., Phillips, J.A. and Cooper, D.N. (1998) The molecular genetics of growth hormone deficiency. *Hum Genet.* 103: 255-272.

Prusty, D., Park, B.H., Davis, K.E. and Farmer, S.R. (2002) Activation of MEK/ERK signaling promotes adipogenesis by enhancing peroxisome proliferator-activated receptor  $\alpha$  (PPAR $\alpha$ ) and C/EBP $\alpha$  gene expression during the differentiation of 3T3-L1 preadipocytes. *J Biol Chem.* 277: 46226-4623.

Qian, S.W., Li, X., Zhang, Y.Y., Huang, H.Y., Liu, Y., Sun, X. and Tang, Q.Q. (2010) Characterization of adipocyte differentiation from human mesenchymal stem cells in bone marrow. *BMC Dev Biol.* 10: 47.

Qian, X., Riccio, A., Zhang, Y. and Ginty, D.D. (1998) Identification and characterization of novel substrates of Trk receptors in developing neurons. *Neuron.* 21: 1017-1029.

Qiu, Z., Wei, Y., Chen, N., Jiang, M., Wu, J. and Liao K. (2001) DNA synthesis and mitotic clonal expansion is not a required step for 3T3-L1 preadipocyte differentiation into dipocytes. *J Biol Chem.* 276: 11988-95.

Raben, M.S. (1958) Treatment of a pituitary dwarf with human growth hormone. *J Clin Endo and metab.* 18: 901-3.

Rahman, S.M., Janssen, R.C., Choudhury, M., Baquero, K.C., Aikens, R.M., de la Houssaye, B.A., Friedman, J.E. (2012) CCAAT/enhancer-binding protein  $\beta$  (C/EBP $\beta$ )

expression regulates dietary-induced inflammation in macrophages and adipose tissue in mice. *J Biol Chem.* 287: 34349-60.

Ramsay, T.G. (2003) Porcine leptin inhibits lipogenesis in porcine adipocytes. *J Anim Sci.* 81: 3008-3017.

Rasumussen, R., Morrison, T., Herrmann, M., Wittwer, C. (1998) Quantitative PCR by continuous fluorescent monitoring of a double stranded DNA specific binding dye. *Biochemica.* 2: 8-11.

Richelsen, B., Pedersen, S.B., Borglum, J.D., Moller-Pedersen, T., Jorgensen, J. and Orgensen, J.J. (1994) Growth hormone treatment of obese women for 5 wk: effect on body composition and adipose tissue LPL activity. *Am J Physiol Endoc.* 266: E211.

Rice SPL., Zhang L., Grennan-Jones F., Agarwal N., Lewis MD., Rees DA., Ludgate M. (2010) Dehydroepiandrosterone (DHEA) treatment in vitro inhibits adipogenesis in human omental but not subcutaneous adipose tissue. *Mol Cell Endocrinol.* 14: 51-7.

Richter, H.E., Albrekten, T. and Billestrup. (2003) The role of signal transducer and activator of transcription 5 in the inhibitory effects of GH on adipocyte differentiation. *Mol Endocrinol.* 30:130-150.

Ricote M and Glass CK (2007) PPARs and molecular mechanisms of transrepression. *Biochim Biophys Acta.* 2007 August; 1771: 926–935.

Roemmich, J.N. and Rogol, A.D. (1997) Exercise and growth hormone: does one affect the other? *J Pediatr.* 131: S75-80.

Rosen, E.D., Hsu, C.H., Wang, X., Sakai, S., Freeman, M.W., Gonzalez, F.J. and Spiegelman, B.M. (2002) C/EBPalpha induces adipogenesis through PPARgamma: a unified pathway. *Genes Dev.* 16: 22–26.

Rosenbaum, M., Gertner, J.M., Leibel, R.L. (1989) Effects of systemic growth hormone (GH) administration on regional adipose tissue distribution and metabolism in GH-deficient children. *J Clin Endocrinol Metab.* 69: 1274-1281.

Ross, S.E., Erickson, R.L., Gerin, I., DeRose, P.M., Bajnok, L., Longo, K.A., Misek, D.E., Kuick, R., Hanash, S.M., Atkins, K.B., Andresen, S.M., Nebb, H.I., Madsen, L., Kristiansen, K., and MacDougald, O.A. (2002) Microarray analyses during adipogenesis: understanding the effects of Wnt signaling on adipogenesis and the roles of liver X receptor alpha in adipocyte metabolism. *Mol Cell Biol.* 22: 5989-5999.

Roux, P.P. and Blenis, J. (2004) ERK and p38 MAPK-activated protein kinases: a family of protein kinases with diverse biological functions. *Microbiol Mol Biol. Rev.* 68: 320–344.

Sakaue, H., Ogawa, W., Nakamura, T., Mori, T., Nakamura, K. and Kasuga, M. (2004) Role of MAPK phosphatase-1 (MKP-1) in adipocyte differentiation. *J Biol Chem.* 279: 39951-7.

Sakharova, A.A., Horowitz, J.F., Surya, S., Goldenberg, N., Harber, M.P., Symons, K. and Barkan, A. (2008) Role of growth hormone in regulating lipolysis, proteolysis, and hepatic glucose production during fasting. *J Clin Endocrinol Metab* 93: 2755–2759.

Saladin, R., Fajas, L., Dana, S., Halvorsen, Y., Auwerx, J. and Briggs, M. (1999) Differential regulation of Peroxisome Proliferator Activated Receptor  $\alpha$ 1 (PPAR $\alpha$ 1) and PPAR $\alpha$ 2 messenger RNA expression in early stages of adipogenesis. *Cell Growth Differ.* 10: 43-48.

Salazar-Olivo, L.A., Castro-Munozledo, F. and Kuri-Harcuch, W. (1995) A preadipose 3T3 cell variant highly sensitive to adipogenic factors and to human growth hormone. *J cell Sci.* 108: 2101-2107.

Sale, E.M., Atkinson, P.G. and Sale, G.J. (1995) Requirement of MAP kinase for differentiation of fibroblasts to adipocytes, for insulin activation of p90 S6 kinase and for insulin or serum stimulation of DNA synthesis. *EMBO J.* 14: 674–684.

Sandouk, T., Reda, D. and Hofmann, C. (1993) Antidiabetic agent pioglitazone enhances adipocyte differentiation of 3T3-F442A cells. *Am J Physiol Cell Physiol.* 264: 1600-1608.

Scherer, P.E. (2006) Adipose tissue: from lipid storage compartment to endocrine organ. *Diabetes.* 55: 1537-1545.

Schwartzbauer, G. and Menon, R.K. (1998) Regulation of growth hormone receptor gene expression. *Mol Genet Metab.* 63: 243-253.

Seo, J.B., Moon, H.M., Kim, W.S., Lee, Y.S., Jeong, H.W., Yoo, E.J., Ham, J., Kang, H., Park, M.G., Steffensen, K.R., Stulnig, T.M., Gustafsson, J.A., Park, S.D., Kim, J.B. (2004) Activated liver X receptors stimulate adipocyte differentiation through induction of peroxisome proliferator-activated receptor - expression. *Mol Cell Biol.* 24: 3430–3444.

Shang, C.A. and Waters, M.J. (2003) Constitutively active signal transducer and activator of transcription 5 can replace the requirement for growth hormone in adipogenesis of 3T3-F442A preadipocytes. *Mol Endocrinol.* 17: 2494–2508.

Shen, B., Chu, E.H., Zhao, G., Man, K., Wu, C.W., Cheng, J.Y., Li, G., Nie, Y., Lo, C.M., Teoh, N., Farrell, G.C., Sung, J.Y. and Yu, J. (2012) PPARgamma inhibits hepatocellular carcinoma metastases in vitro and in mice. *Br J Cancer.* 106: 1486–1494.

Shimano, H., Horton, J.D., Shimomura, I., Hammer, R.E., Brown, M.S. and Goldstein, J.L. (1997) Isoform 1c of sterol regulatory element binding protein is less active than isoform 1a in livers of transgenic mice and in cultured cells. *J Clin Invest.* 99: 846-854.

Shimomura, I., Hammer, R.E., Richardson, J.A., Ikemoto, S., Bashmakov, Y., Goldstein, J.L. and Brown, M.S. (1998) Insulin resistance and diabetes mellitus in transgenic mice expressing nuclear SREBP-1c adipose tissue: model for congenital generalized lipodystrophy. *Genes Dev.* 12: 3182–3194.

Smas, C.M., Chen, L., Sul, H.S. (1997) Cleavage of membrane-associated pref-1 generates a soluble inhibitor of adipocyte differentiation. *Mol Cell Biol.* 17: 977–987.

Smas, C.M., Kachinskas, D., Liu, C.M., Xie, X., Dircks, L.K. and Sul, H.S. (1998) Transcriptional control of the pref-1 gene in 3T3-L1 adipocyte differentiation. Sequence requirement for differentiation-dependent suppression. *J Biol Chem.* 273: 31751–31758.

Smith, P.E., Greenwood, C.F., Foster, G.L. (1927) A Comparison in Normal, Thyroidectomized and Hypophysectomized Rats of the Effects upon Metabolism and Growth Resulting from Daily Injections of Small Amounts of Thyroid Extract. *Am J Pathol.* 3: 669-87.

Smith, P.J., Wise, L., Berkowitz, R., Wan, C. and Rubin, C.S. (1988) Insulin-like growth factor-I is an essential regulator of the differentiation of 3T3-L1 adipocytes. *J Biol Chem.* 263: 9402-9408.

Sottile, V. and Seuwen, K. (2001) High-capacity screen for adipogenic differentiation. *Anal Biochem.* 293: 124–128.

Stephens, J.M., and Pekala, P.H. (1992) Transcriptional repression of the C/EBP-alpha and GLUT4 genes in 3T3-L1 adipocytes by tumor necrosis factor-alpha. A regulation is coordinate and independent of protein synthesis. *J Biol Chem.* 267: 13580-13584.

Stephens, J.M., Morrison, R.F. and Pilch, P.F. (1996) The expression and regulation of STATs during 3T3-L1 adipocyte differentiation. *J Biol Chem.* 271: 10441-41044.

Story, D.J. and Stephens, J.M. (2006) Modulation and lack of cross-talk between signal transducer and activator of transcription 5 and Suppressor of cytokine signaling-3 in insulin and growth hormone signaling in 3T3-L1 adipocytes. *Obesity (Silver Spring).* 14: 1303-11.

Su, H.S., Smas, C., Mei, B. and Zhou, L. (2000) Function of pref-1 as an inhibitor of adipocyte Differentiation. *Internat J Obesity.* 24: S15-S19.

Sul, H.S. (2009) Pref-1: Role in Adipogenesis and Mesenchymal Cell Fate. *Mol Endocrin.* 23: 1717-1725.

Sul, H.S., Smas, C., Mei, B, and Zhou, L. (2000) Function of pref-1 as an inhibitor of adipocyte differentiation. *Int J Obes Relat Metab Disord .* 24: S15-S19.

Sundstrom, M., Lundqvist, T., Rodin, L., Giebel, L.B., Milligan, D. and Norstedt, G. (1996) Crystal structure of an antagonist mutant of human growth hormone, G120R, in complex with its receptor at 2.9 Å resolution. *J Biol Chem.* 271: 32197-32203.

Stewart, P.M. (2000) Current therapy for acromegaly. *Trends Endocrin Met.* 11: 128-132.

Stewart, W.C., Percy, L.A., Floyd, Z.E. and Stephens, J.M. (2011) STAT5A expression in Swiss 3T3 cells promotes adipogenesis in vivo in an athymic mice model system. *Obesity (Silver Spring).* 19: 1731-4.

Talamantes, F. and Ortiz, R. (2002) Structure and regulation of expression of the mouse GH receptor. *J Endocrinol.* 175: 55-59.

Tamori, Y., Masugi, J., Nishino, N. and Kasuga, M. (2002) Role of Peroxisome Proliferator-Activated Receptor- $\gamma$  in Maintenance of the Characteristics of Mature 3T3-L1 Adipocytes. *Diabetes.* 51: 2045-2055.

Tanaka, T., Yoshida, N., Kishimoto, T. and Akira, S. (1997) Defective adipocyte differentiation in mice lacking the C/EBP-and/or C/EBP-gene. *EMBO J.* 16: 7432– 7443.

Tang, Q.Q. and Lane, M.D. (2012) Adipogenesis: From Stem Cell to Adipocyte. *Annu Rev Biochem.* 81:715-36.

Tanoue, T., Yamamoto, T., Maeda, R. and Nishida, E. (2001) A Novel MAPK phosphatase MKP-7 acts preferentially on JNK/SAPK and p38 alpha and beta MAPKs. *J Biol Chem.* 276: 26629-39.

Tchkonia T., Giorgadze N., Pirtskhalava T., Thomou T., DePonte M., Ada Koo A., Forse RA., Chinnappan D., Martin-Ruiz C., Zglinicki TV. and Kirkland JL. (2006) Fat Depot–

Specific Characteristics Are Retained in Strains Derived From Single Human Preadipocytes. *Diabetes*. 55: 2571-2578.

Tiraby, C. and Langin, D. (2003) Conversion from white to brown adipocyte: A strategy for the control of fat mass. *Trends Endocrin Met*. 14: 439-441.

Todaró, G.J. and Green, H. (1963) Quantitative studies of the growth of mouse embryo cells in culture and their development into established lines. *J Cell Biol*. 17: 299-313.

Tong, Q., Tsai, J., Tan, G., Dalgin, G. and Hotamisligil, G.S. (2005) Interaction between GATA and the C/EBP family of transcription factors is critical in GATA-mediated suppression of adipocyte differentiation. *Mol Cell Biol*. 25: 706–715.

Toneguzzo, F., Keating, A., Glynn, S. and McDonald, K. (1988) Electric field-mediated gene transfer: characterization of DNA transfer and patterns of integration in lymphoid cells. *Nucleic Acids Res*. 16: 5515-32.

Tontonoz, P., Hu, E. and Spiegelman, B.M. (1994) Stimulation of adipogenesis in fibroblasts by PPAR[gamma]2, a lipid-activated transcription factor. *Cell*. 79: 47-1156.

Touyz, R.M. and Schiffrin, E.L. (2006) Peroxisome proliferators-activated receptors in vascular biology-molecular mechanisms and clinical implications. *Vascul Pharmacol* 45: 19-28.

Trayhurn, P., Bing, C. and Woods, I.S. (2006) Adipose tissue and adipokines-energy regulation from the human perspective. *J Nutrition*. 136: 1935-1939.

Trobec, K., von Haehling, S., Anker, S.D. and Lainscak, M. (2011) Growth hormone, insulin-like growth factor 1, and insulin signaling-a pharmacological target in body wasting and cachexia. *J Cachexia Sarcopenia Muscle*. 2: 191-200.

Uyttendaele, I., Lemmens, I., Verhee, A., De Smet, A.S., Vandekerckhove, J., Lavens, D., Peelman, F. and Tavernier, J. (2007) Mammalian protein-protein interaction trap (MAPPIT) analysis of STAT5, CIS, and SOCS2 interactions with the growth hormone receptor. *Mol Endocrinol*. 21: 2821-2831.

Valyasevi, R.W., Erickson, D.Z., Harteneck, D.A., Dutton, C.M., Heufelder, A.E., Jyonouchi, S.C. and Bahn, R.S. (1999) Differentiation of human orbital preadipocyte fibroblasts induces expression of functional thyrotropin receptor. *J Clin Endocrinol Metab*. 84: 2557-62.

Vanderkuur, J.A., Butch, E.R., Waters, S.B., Pessin, J.E., Guan, K.L. and Carter-Su, C. (1997) Signalling molecules involved in coupling growth hormone receptor to mitogen-activated protein kinase activation. *Endocrinology*. 138: 4301-4307.

Vantaggiato, C., Formentini, I., Bondanza, A., Bonini, C., Naldini, L., Brambilla, R. (2006) ERK1 and ERK2 mitogen-activated protein kinases affect Ras-dependent cell signaling differentially. *J Biol*. 4: 1-15.

Vernon, R.G., Piperova, L., Watt, P.W., Finley, E. and Lindsay-Watt, S. (1993) Mechanisms involved in the adaptations of the adipocyte adrenergic signal-transduction system and their modulation by growth hormone during the lactation cycle in the rat. *Biochem J*. 289: 845-851.

Vishwakarma, S.L., Sonawane, R.D., Rajani, M. and Goyal, R.K. (2010) Evaluation of effect of aqueous extract of *Encicostemma littorale* Blume in streptozotocin-induced type 1 diabetic rats. *J Exp Biol.* 48: 26–30.

Wabitsch, M., Hauner, H., Heinze, E. and Teller, W.M. (1995) The role of growth hormone/insulin-like growth factors in adipocyte differentiation. *Metabolism.* 44: 45-9.

Walker, J.M. and Rapley, R. (2008) *Molecular Biomethods Handbook*. Humana Press. 978-1-60327-374-9.

Wang, Y. and Sul, H.S. (2009) Pref-1 regulates mesenchymal cell commitment and differentiation through Sox9. *Cell Metab* 9: 287–30.

Wang, Y., Kim, K.A., Kim, J.H. and Sul, H.S. (2006) Pref-1, a preadipocyte secreted factor that inhibits adipogenesis. *J Nutr.* 136: 2953–295.

Wang, x., Yang, N., Deng, L., Li, x., Jing, J., Gan, Y. and Frank, S.J. (2008) Interruption of growth hormone signalling via SHC and ERK in 3T3-F442A preadipocytes upon knockdown of insulin receptor substrate-1. *J Mol Endocrinol.* 23: 486-496.

Ward, A.C., Touw, I. and Yoshimura, A. (2000) The Jak-Stat pathway in normal and perturbed hematopoiesis. *Blood.* 95: 19-29.

Watahiki, M., Yamamoto, M., Yamakawa, M., Tanaka, M. and Nakashima, K. (1989) Conserved and unique amino acid residues in the domains of the growth hormones. Flounder growth hormone deduced from the cDNA sequence has the minimal size in the growth hormone prolactin gene family. *J Biol Chem.* 264: 312-316.

Waters, M.J., Hoang, H.N., Fairlie, D.P., Pelekanos, R.A. and Brown, R.J. (2006) New insights into growth hormone action. *J Mol Endocrinol.* 36: 1-7.

Watt, F.W. (1991) Cell culture model of differentiation. *FASEB J.* 5: 287-294.

Waxman, D.J. and O'Connor, C. (2006) Growth Hormone Regulation of Sex-Dependent Liver Gene Expression. *Mol Endocr.* 20: 2613-2629.

Wei, Y., Puzhko, S., Wabitsch, M. and Goodyer, C.G. (2009) Structure and activity of the human growth hormone receptor (hGHR) Gene V2 Promoter. *Mol Endocrinol.* 23: 360-372.

Well, T. (2009) Ghrelin–Defender of fat. *Prog Lipid Res.* 48: 257-274.

Weltman, A., Weltman, J.Y., Roy, C.P., Wideman, L., Patrie, J., Evans, W.S. and Veldhuis, J.D. (2006) Growth hormone response to graded exercise intensities is attenuated and the gender difference abolished in older adults. *J Appl Physiol.* 100: 1623-1629.

Willson, T.M., Brown, P.J., Sternbach, D.D. and Henke, B.R. (2000) The PPARs from orphan receptors to drug discovery. *J Med Chem.* 43: 527–550.

Winston, L.A. and Bertics, P.J. (1992) Growth hormone stimulates the tyrosine phosphorylation of 42- and 45-kDa ERK-related proteins. *J Biol Chem.* 267: 4747-51.

Wise, L.S. and Green, H. (1979) Participation of one isozyme of cytosolic glycerophosphate dehydrogenase in the adipose conversion of 3T3 cells. *J Biol Chem.* 254: 273-275.

Yang, N., Huang, Y., Jiang, J., Frank, S.J. (2004) Caveolar and lipid raft localization of GH receptor and its signaling elements: impact on GH signalling. *J Biol Chem.* 279: 20898–20905.

Yawood, S.J., Sale, E.M., Sale, G.J., Houslay, M.D., Kilgour, E. and Anderson, N.G. (1999) Growth hormone-dependent differentiation of 3T3-F442A preadipocytes requires janus kinase/signal transducer and activator of transcription but not mitogen-activated protein kinase or p70 S6 kinase signalling. *J Biol Chem.* 274: 8662-8668.

Yu, J.H. (2000) Expression of growth hormone receptor gene during 3T3-L1 differentiation. *J Korean Soc Pediatr Endocrinol.* 5: 45-51.

Zhang, L., Baker, G., Janus, D., Paddon, C.A., Fuhrer, D., Ludgate, M. (2006) Biological effects of thyrotropin receptor activation on human orbital preadipocytes. *Invest Ophthalmol Vis Sci.* 47: 5197-5203.

Zhang, L., Paddon, C., Lewis, M.D., Grennan-Jones, F., Ludgate, M. (2009) G $\alpha$  signalling suppresses PPAR $\gamma$ 2 generation and inhibits 3T3-L1 adipogenesis. *J Endocrinol.* 202: 207-15.

Zhang, J.W., Klemm, D.J., Vinson, C. and Lane, M.D. (2004) Role of CREB in transcriptional regulation of CCAAT/enhancer-binding protein  $\beta$  gene during adipogenesis. *J Biol Chem* 279: 4471–4478.

Zhou, Y., He, L., Baumann, G. and Kopchick, J.J. (1997) Deletion of the mouse GH-binding protein (mGHBP) mRNA polyadenylation and splicing sites does not abolish production of mGHBP. *J Mol Endocrinol.* 19: 1–13.

Zhu, T., Goh, E.L., LeRoith, D., Lobie, P.E., (1998) Growth hormone stimulates the formation of a multiprotein signaling complex involving p130(Cas) and CrkII. Resultant activation of c-Jun N-terminal kinase/stress-activated protein kinase (JNK/SAPK). *J Biol Chem.* 273: 33864-33875.

Zhu, T., Goh, E.K., Graichen, R., Ling, L. and Lobie, P.E. (2001) Signal transduction via the growth hormone receptor. *Cell signal*. 13: 599-616.

Zhu, T., Ling, L. and Lobie, P.E. (2002) Identification of a JAK2-independent pathway regulating growth hormone (GH)-stimulated p44/42 mitogenactivated protein kinase activity. GH activation of Ral and phospholipase D is Src-dependent. *J Biol Chem*. 277: 45592-45603.

Zou, L., Menon, R.K. and Sperling, A. (1997) Induction of mRNA for the growth hormone receptor gene during mouse 3T3-L1 preadipocyte differentiation. *Metabolism*. 46: 114-118.